UFBA

UNIVERSIDADE FEDERAL DA BAHIA
ESCOLA POLITÉCNICA
PROGRAMA DE PÓS-GRADUAÇÃO EM
ENGENHARIA INDUSTRIAL - PEI

DOUTORADO EM ENGENHARIA INDUSTRIAL

FELIPE ANDRADE TORRES

SYNERGETIC EFFECTS OF ALTERNATIVE FUELS ON COMPRESSION-IGNITION ENGINES: POTENTIAL OF ETHANOL AND FISCHER-TROPSCH DIESEL BLENDS

PEI

PROGRAMA DE PÓS-GRADUAÇÃO EM
ENGENHARIA INDUSTRIAL - PEI

SALVADOR
2021

UNIVERSIDADE FEDERAL DA BAHIA

ESCOLA POLITÉCNICA

PROGRAMA DE PÓS-GRADUAÇÃO EM ENGENHARIA INDUSTRIAL

FELIPE ANDRADE TORRES

SYNERGETIC EFFECTS OF ALTERNATIVE FUELS ON COMPRESSION-IGNITION ENGINES: POTENTIAL OF ETHANOL AND FISCHER-TROPSCH DIESEL BLENDS

Salvador

2021

FELIPE ANDRADE TORRES

SYNERGETIC EFFECTS OF ALTERNATIVE FUELS ON COMPRESSION-IGNITION ENGINES: POTENTIAL OF ETHANOL AND FISCHER-TROPSCH DIESEL BLENDS

Thesis presented to the Graduate Program in Industrial Engineering of the Federal University of Bahia in partial fulfillment of the requirements for the degree of Doctor of Science in Industrial Engineering.

Supervisor:

Prof. Dr. Silvio Alexandre Beisl Vieira de Melo

External co-supervisors:

Prof. Dr. Jorge José Gomes Martins

Prof. Dr. Athanasios Tsolakis

Salvador

2021

SYNERGETIC EFFECTS OF ALTERNATIVE FUELS ON COMPRESSION-IGNITION ENGINES: POTENTIAL OF BIOETHANOL AND FISCHER-TROPSCH DIESEL BLENDS

FELIPE ANDRADE TORRES

Thesis submitted to the Industrial Program at the Federal University of Bahia as partial fulfillment of the requirements for the degree of Doctor of Science in Industrial Engineering.

Examining Committee:

Prof. Dr. Silvio A. B. Vieira de Melo – Supervisor
Doctor in Chemical Engineering at the Federal University of Rio de Janeiro, Brazil, 1997
Federal University of Bahia, Brazil
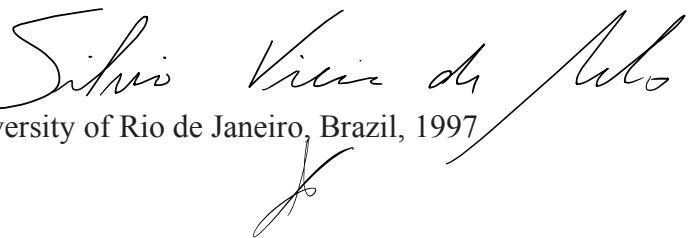
Prof. Dr. Athanasios Tsolakis – Co-supervisor
Doctor in Mechanical Engineering at the University of Birmingham, UK, 2004
University of Birmingham, United Kingdom

Prof. Dr. Jorge José Gomes Martins – Co-supervisor
Doctor in Engineering at the University of Birmingham, UK, 1989
University of Minho, Portugal

Prof. Dr. Khamid Mahkamov
Doctor in Mechanical Engineering at Bauman Moscow Technical University, Russia, 1992
Northumbria University, United Kingdom

Prof. Dr. José Ricardo Sodré
Doctor in Mechanical Engineering at the University of Manchester, UK, 1995
Aston University, United Kingdom
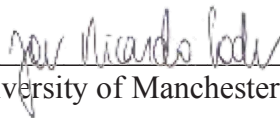
Prof. Dr. Magín Lapuerta Amigo
Doctor in Mechanical Engineering at the University of Valencia, Spain, 1989
University of Castilla-La Mancha, Spain

Prof. Dr. Julio Augusto Mendes da Silva
Doctor in Mechanical Engineering at University of São Paulo, Brazil, 2013
Federal University of Bahia, Brazil

Salvador, BA - BRAZIL
August, 2021

This work is dedicated to my beloved wife, Rose, and our two sons, João Felipe and Caio.

ACKNOWLEDGEMENTS

"Life is and will ever remain an equation incapable of solution, but it contains certain known factors."

(Nikola Tesla)

ABSTRACT

Nowadays, research interest related to the application of alternative fuels, such as ethanol, to mitigate the utilization of fossil diesel fuel is increasing. Furthermore, another potential non-conventional fuel is the Fischer-Tropsch (F-T) diesel, which is a synthesized fuel that may also be produced from biomass. However, as the miscibility between these two biofuels is limited, thus, another biofuel was considered to promote the blend stability, the biodiesel. The present work aimed to propose a blend of alternative fuels and investigate the effects of the mixture on a diesel engine's combustion, exhaust emissions, particulate matter characteristics, the performance of an aftertreatment system, as well as an exergetic analysis. Ethanol, F-T diesel, and biodiesel were blended in the volumetric fractions of 15, 50, and 35%, respectively (FTD50E15B35). A single-cylinder diesel engine equipped with a common-rail injection system was used to test this blend and compare the results with diesel and a blend of ethanol, diesel, and biodiesel in these same volumetric fractions (D50E15B35). It was shown that F-T diesel and ethanol could be combined to conform with the current fuel standards provided that biodiesel is added to the mixture. FTD50E15B35 reduced the regulated emissions of THC, NO, and PM, however, with a penalty in CO emissions in comparison with diesel fuel. The heavy-hydrocarbons decreased, whilst the light-hydrocarbons increased in comparison with diesel. The unregulated emissions, N_2O, NH_3, and HNCO, decreased for the blends, although CH_2O slightly increased. Besides, the diesel oxidation catalyst (DOC) has effectively reduced the levels of CO, THC, and NO in the exhaust. However, the DOC light-off temperatures of the blends were shifted to higher values. Further, the total particle number and mass concentrations of FTD50E15B35 were lower than for D50E15B35 and diesel. Further, the energy and the exergy efficiencies were found to be similar, around 26% and 24%, respectively. Both energy and exergy efficiencies of FTD50E15B35 were slightly lower than for diesel fuel. It was concluded that ethanol, F–T diesel, and biodiesel have individual properties that, when combined, have a potential for particulate emission-reducing along with aftertreatment systems and injection strategies promoting benefits for the engine combustion, as future emissions legislation standards are foreseen to be more stringent.

Keywords: Biofuels, Ethanol, Fischer-Tropsch, Emissions, Aftertreatment system, Diesel engines

RESUMO

Atualmente, o interesse de pesquisas relacionadas à aplicação de combustíveis alternativos, como o etanol, para mitigar o uso do diesel fóssil é crescente. Além disso, outro potencial combustível, embora não convencional, é o Fischer-Tropsch (F-T) diesel, que é um combustível sintetizado que também pode ser produzido a partir de biomassa. Porém, como a miscibilidade entre esses dois combustíveis é limitada, outro biocombustível foi considerado para promover a estabilidade da mistura, o biodiesel. O presente trabalho objetivou propor uma mistura de combustíveis alternativos e investigar os efeitos desta mistura na combustão, caracterização das emissões e do material particulado, desempenho de um sistema de pós-tratamento de gases e análise exergética de um motor diesel. Etanol, F-T diesel e biodiesel foram misturados nas respectivas frações volumétricas de 15, 50 e 35% (FTD50E15B35). Um motor diesel monocilíndrico equipado com sistema de injeção *common-rail* foi utilizado para testar essa mistura e comparar os resultados com o diesel e uma mistura de etanol, diesel e biodiesel, nessas mesmas frações volumétricas (D50E15B35). Foi demonstrado que o F-T diesel e o etanol podem ser combinados para atender aos padrões atuais de combustível, desde que o biodiesel seja adicionado à mistura. O FTD50E15B35 reduziu as emissões regulamentadas de HC, NO e MP, porém, com uma penalidade nas emissões de CO em comparação com o óleo diesel. Os hidrocarbonetos pesados diminuíram, enquanto os hidrocarbonetos de cadeia leve aumentaram em relação ao diesel. As emissões não regulamentadas, N_2O, NH_3 e HNCO, diminuíram, embora o CH_2O tenha aumentado para as misturas. Além disso, o catalisador de oxidação do diesel reduziu efetivamente os níveis de CO, HC e NO, entretanto, as temperaturas de *light-off* tiverem seus valores aumentados. Além disso, o número total de partículas e a concentração de massa de FTD50E15B35 foram menores que para o D50E15B35 e o diesel. Além disso, as eficiências, energética e exergética, foram semelhantes, em torno de 26% e 24%, respectivamente. A eficiência energética e a exergética do FTD50E15B35 foram inferiores às do diesel. Concluiu-se que o etanol, o F-T diesel e o biodiesel possuem propriedades individuais que, quando combinadas, apresentam potencial de redução da emissão de particulados juntamente com sistemas de pós-tratamento e estratégias de injeção, promovendo benefícios para a combustão do motor, conforme previsão para futuras normas regulamentárias de controle de emissões.

Palavras-chave: Biocombustíveis, Etanol, Fischer-Tropsch, Emissões, Motores diesel

LIST OF FIGURES

LIST OF TABLES

NOMENCLATURE

Abbreviations

BTL	Biomass-to-liquid
bTDC	Before the top dead center
C2H2	Acetylene
C2H4	Ethylene
C2H6	Ethane
C3H6	Propylene
C3H8	Propane
CH2O	Formaldehyde
CH4	Methane
CI	Compression ignition
CO	Carbon monoxide
CO2	Carbon dioxide
D50E15B35	15% ethanol, 35% biodiesel, 50% diesel
FTD50E15B35	15% ethanol, 35% biodiesel, 50% Fischer-Tropsch diesel
FID	Flame ionization detector
F-T	Fischer-Tropsch
FTD	Fischer-Tropsch diesel
FTIR	Fourier transform infrared
GTL	Gas-to-liquid
HC	Hydrocarbons
HEV	Hybrid electric vehicles

ICE	Internal combustion engines
IMEP	Indicated mean effective pressure
LHV	Lower heating value
N2O	Nitrous oxide
NH3	Ammonia
NO	Nitrogen oxige
NO2	Nitrogen dioxide
NOx	Nitrogen oxides
PCIS	Pre-chamber ignition system
PM	Particulate matter
RCCI	Reactivity-controlled compression ignition
TDC	Top dead center
THC	Total hydrocarbons

Symbols

$\dot{En}$	energy rate, W
$\dot{Ex}$	exergy rate, W
ex	specific exergy, J/kg or J/mol
h	enthalpy, J/kg or J/mol
$\dot{m}$	mass flow rate, kg/s
$\dot{n}$	molar flow rate, mol/s
N	engine speed, rpm
n_R	number of crank revolutions for each power stroke per cylinder, -
P	absolute pressure, Pa
T	temperature, °C or K
V_d	displaced volume, m3
R	universal gas constant, J/kg.K or J/mol.K
s	entropy, J/kg.K or J/mol.K
$\dot{S}$	Entropy rate, W
x	molar fraction, -

Subscripts

0	reference state
ch	chemical
cool	coolant
dest	destruction
exh	exhaust
gen	generation
i	individual gaseous species
in	inlet
out	outlet
ph	physical
W	work

Greek symbols

γ	activity coefficiency, -
ε	standard chemical exergy, J/mol
η	energy efficiency, -
φ	chemical exergy factor, -
ψ	exergy efficiency, -

TABLE OF CONTENTS

1 INTRODUCTION

Energy represents an important aspect of human society in general, being directly related to social and economic aspects. Consumption of energy has been increasing over the past decades due to population growth and associated demands to produce more food, supply goods, and improve lifestyle. As the world's population is expected to grow from an estimated 7.7 billion in 2019 to 8.5 billion in 2030 and 9.7 billion in 2050, based on United Nations projections (UNITED NATIONS, 2019), this increase in population is expected to rise the global energy demand in 20% from 2017 to 2040 (EXXONMOBIL, 2019). Among energy consumption, the transport sector performs a major contribution, in which the internal combustion engines (ICE) are the worldwide primary powertrain system that enables road transportation.

Road transportation is a significant energy consumption sector and should significantly reduce fossil fuel dependency and environmental pollution. The world energy consumption based on liquid fossil fuel sources shows that, in 2018, road transport corresponded to roughly half of the total oil consumption, while other transport (e.g., aviation, rail, and others) represented approximately 15% (INTERNATIONAL ENERGY AGENCY (IEA), 2020d). In this scenario, biofuels and electrification are among the alternatives to fossil fuel use in internal combustion engines (ICE).

Although electric vehicles are gradually gaining inroads in the automotive market, ICE continues to be widely used worldwide (CORREA; MUÑOZ; RODRIGUEZ, 2019; SERRANO; NOVELLA; PIQUERAS, 2019) both in ICE vehicles as well as in hybrid electric vehicles (HEV). Electrification has been increasing in light-duty vehicles over the late years and, in a long-term scenario, is expected to partially replace liquid hydrocarbons in transport (KALGHATGI, 2018). However, fully electrification is still in the early stages of development in most countries. For example, in Brazil, hybrid and flexible-fuel vehicles are projected for the future with 52% and 32% contribution by 2050, respectively. Therefore, biofuels are still one of the most likely alternatives in decarbonizing and cleaning road transport in the short term.

Current legislation is forcing the reduction of exhaust emissions, mainly nitrogen oxides (NO_x) and particulate matter (PM), for compression ignition (CI) engines. The European Union (EU) directive 2009/30/EC promotes the use of biofuels from 2020 while countries such as the

USA, China, and Brazil also mandate the utilization of biofuels blended with conventional fuels (UNGLERT *et al.*, 2020). In Brazil, one of the alternatives to reduce engine exhaust emissions towards emissions decrease is alternative fuels (BEATRICE *et al.*, 2020; PAREDES ROJAS *et al.*, 2020). Moreover, vehicle emissions, including gaseous and particulate emissions, are regulated, while future legislation like the "Euro 7" standard is expected to be even more stringent (PUŠKÁR; KOPAS, 2018). Also, the Brazilian government has controlled the vehicle emissions through the Air Pollution Control Program for Motor Vehicles (*Programa de Controle da Poluição do Ar por Veículos Automotores* - PROCONVE, in Portuguese), and the PROCONVE P-8 is expected to be implemented by 2022-23.

Biofuels can effectively contribute to mitigating the dependence on fossil fuels and the greenhouse gases and air quality issues associated with their emissions. Those synergies are applicable to the utilization of the fuel in the vehicle and a well-to-wheel system evaluation. This scenario reinforces the renewable energy proposal, especially in countries in which the electrical matrix is primarily renewable, such as the case of Brazil. In this scenario, investigations for alternative and sustainable fuels to meet transportation demand continuously receive special attention. In this case, biofuels application is considered one of the most crucial research efforts for reducing diesel engine emissions.

Many countries have diversified the research, development and production of alternative fuel to fossil diesel, such as the USA, China and Brazil. Since the 1970s, Brazil has already adopted biofuels addition on gasoline and in early 2000s on diesel fuels (AGÊNCIA NACIONAL DO PETRÓLEO GÁS NATURAL E BIOCOMBUSTÍVEIS (ANP), 2016). In a global scale scenario, Brazil is the second-largest producer of biofuels, whereas the country represented 22.4% of biofuels production in 2018 in the world (BP, 2019).

In this scenario, this work answers for the increasing interest in the utilization of alternative renewable fuels in compression ignition engines, widely used in Brazil and worldwide in the road, marine, and railroad transport sector. Figure 1 shows the total share of final energy consumption by sector in 2015 and the projection for 2050 in Brazil. It is highlighted that road transport accounted for approximately 90% of the share in either year. This share emphasizes the impact of road transportation on the energy matrix of the transport sector.
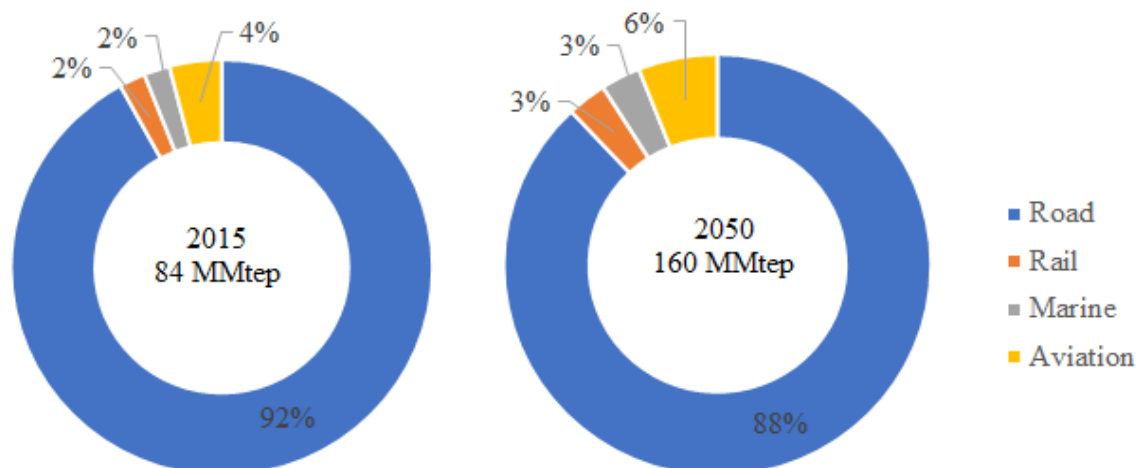
Figure 1. Share of final energy consumption in the transport sector, in 2015 and 2050, in Brazil (EMPRESA DE PESQUISA ENERGÉTICA (EPE), 2020a).

Figure 2 shows that Brazil has significant participation of renewable sources in the energetic matrix, 48.4% in 2020 (EMPRESA DE PESQUISA ENERGÉTICA (EPE), 2020a). Moreover, regarding the transport sector, renewable contributes to 25% of energy consumption due to the ethanol and biodiesel share in the matrix (EMPRESA DE PESQUISA ENERGÉTICA (EPE), 2020a). In this scenario, Brazil has considerable potential for biofuels production. The country is the second larger producer of both ethanol and biodiesel and has a large consumption of biofuels. The ethanol consumption increased 11%, while biodiesel consumption increased 9% in 2019 (EMPRESA DE PESQUISA ENERGÉTICA (EPE), 2020a).

Among biofuels such as biogas, alcohol, and biodiesel, ethanol seems to be the most feasible and attractive due to its cost, availability, storage, and handling. Although not commonly used in diesel engines, ethanol is the most produced biofuel at a global scale and can be used as a fuel component in CI engines (ÇELEBI; AYDIN, 2019; OECD/FAO, 2019). Biodiesel is a diesel-like fuel that can partially substitute the diesel fuel in a diesel engine. These alternative fuels can form binary and ternary fuel blends in CI engines without requiring major powertrain modifications (MENDES GUEDES; LEAL BRAGA; PRADELLE, 2018).

Fischer-Tropsch (F-T) fuels, as one of the common biofuels, are synthetic fuels that can be produced from catalytic conversion processes. This process can occur using biomass (biomass-to-liquid or BTL) as raw materials that can be used to synthesize diesel-like fuels (SHI *et al.*, 2019), among others. Therefore, the F-T diesel might be considered a renewable fuel

depending on the type of raw material used to convert it into synthetic diesel-like fuel (MAHMOUDI *et al.*, 2020).
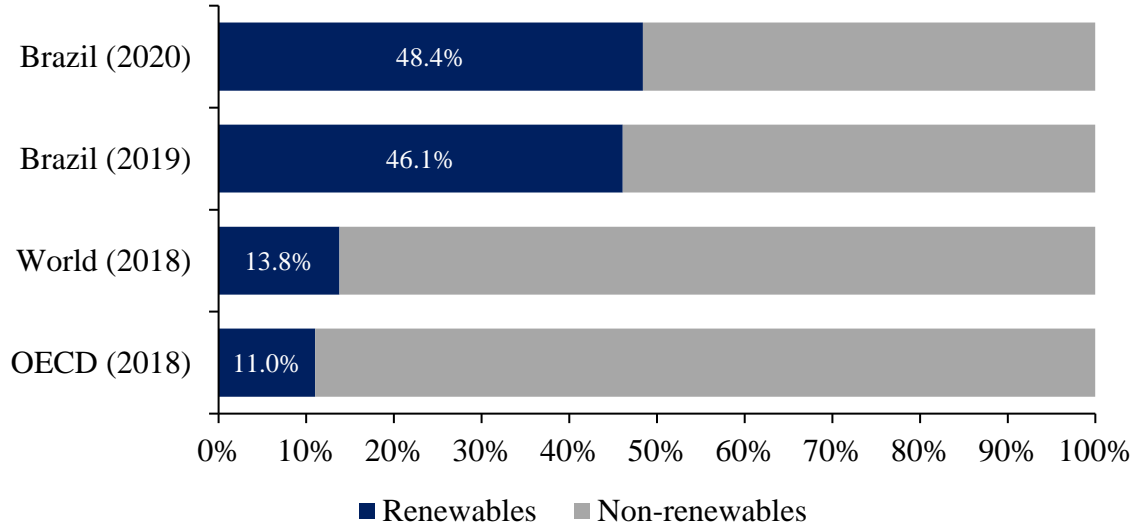
Figure 2. Contribution of renewable sources of energy to the energetic matrix of Brazil in comparison with the rest of the world (EMPRESA DE PESQUISA ENERGÉTICA (EPE), 2021).

Complex energy scenarios using sustainably CO_2 emissions in "green" energy production, storage, and distribution have been seen as a way to combat climate change. This scenario can be promoted by utilizing renewable energy in the production of alcohols, ethers, esters, and clean synthetic fuels (MARTINS; BRITO, 2020) using novel and energy-efficient catalytic systems. Apart from demonstrating that industrial production levels of these new fuels can be achieved, their efficient utilization will contribute to improving their design and contributing to the additional tank-to-wheel CO_2 emissions reduction.

1.1 Research aims and objectives

The overall aim of this research is to investigation the effect of alternative fuels on engine performance, combustion, exhaust emissions, and particulate matter (PM) characteristics, the performance of an aftertreatment system, as well as an energetic and exergetic analysis. The specifics objectives of this thesis are to:

a) Propose a fuel blend composed of renewable fuels that fulfill fuel regulation requirements, finding a way to enhance the miscibility of ethanol in Fischer-Tropsch diesel fuel and stabilize the mixture by adding biodiesel to the composition

b) Comparison of the engine performance and combustion when fueled with alternative fuels and with diesel fuel;

c) Investigate the effect of renewable fuels (e.g., ethanol, Fischer-Tropsch diesel, and biodiesel) on the regulated (CO, HC, NO_x, PM) and unregulated (N_2O, NH_3, CH_2O, HNCO, heavy- and light- hydrocarbons) exhaust emissions;

d) Assess the effect of the exhaust gas from the combustion of these alternative fuels on the performance of an aftertreatment system;

e) Evaluate the PM characteristics (particle number, size, mass) resulted from the combustion of the proposed blend on a modern non-modified diesel engine;

f) Examine the effects of F-T diesel and ethanol properties on energetic and exergetic efficiencies of the engine performance.

1.2   Motivation

According to the global status report by REN21 (REN21, 2020), the energy demand for the transport sector accounted for nearly one-third of the total energy consumption of the world in 2017. Nevertheless, the transport sector still has a minor share of the renewable energy demand. In contrast, oil products depict 96.7% of the world`s transport energy, biofuels account for 3%, and 0.3% is represented by electricity. In this scenario, the share of road transport (light- and heavy-duty) was 75% of the world`s transport energy demand in 2017, with passenger vehicles representing more than two-thirds of this share (EXXONMOBIL, 2019). In 2017, biofuels comprised nearly the entire renewable energy share in road transport demand (91%) (REN21, 2020).

In the Brazilian transport sector, the demand for biofuels is expected to increase progressively due to implementing the National Biofuels Policy (*Política Nacional de Biocombustíveis*, in Portuguese - *RenovaBio*), which was established by legislation nº 13.576/2017 and was implemented in early 2020. The biofuels considered by *RenovaBio* policy are anhydrous and hydrated ethanol (first and second generation); biodiesel; biomethane, biojet; and alternative biofuels (AGÊNCIA NACIONAL DO PETRÓLEO GÁS NATURAL E BIOCOMBUSTÍVEIS (ANP), 2021). Among the goals of this policy are the following.

- To provide an important contribution to the fulfillment of the commitments determined by Brazil under the Paris Agreement;

- To promote the adequate expansion of biofuels in the energy matrix, with emphasis on the regularity of fuel supply;

- To ensure predictability for the fuel market, promoting increases in energy efficiency and reducing greenhouse gas emissions (GHG) in the production, sale, and utilization of biofuels.

The potential include ethanol in diesel stimulates the research effort over this biofuel, mainly because it may be produced from renewable feedstock (i.e., biomass). Ethanol has the potential to reduce exhaust gas emissions (CO, HC, and PM). Moreover, it could enhance the reduction of carbon deposits at the fuel injector and in the combustion chamber, as ethanol has a lower viscosity than biodiesel, for example. As depicted in Figure 3, the share of ethanol in the Brazilian transport sector energy consumption stands for 19.3% in 2020. In Brazil, passenger vehicles are not allowed to use diesel. Therefore, the utilization is restricted to gasoline or ethanol, or blends of both, fueled in flex-fuel vehicles. Also, the share of ethanol utilization in the light-duty passenger's vehicles was 45% against 55% of gasoline (type A) (EMPRESA DE PESQUISA ENERGÉTICA (EPE), 2020a).
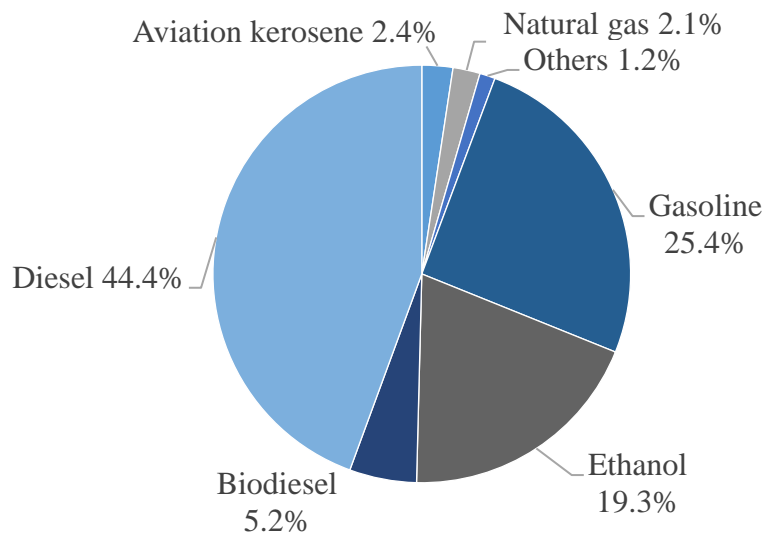
Figure 3. Share of renewable sources in the transport sector in Brazil (EMPRESA DE PESQUISA ENERGÉTICA (EPE), 2021).

The utilization of diesel is regulated for passengers' vehicles in many countries, such as in the European Union, the USA, and Argentina. However, in the case of the USA, diesel fuel is more popular for medium and heavy trucks than passenger cars. Nevertheless, in Brazil, diesel fuel is still restricted to light-duty commercial and heavy-duty vehicles, although

discussions related to the utilization of diesel fuel in passenger vehicles are recurrent. Despite that, over the last decade, the country had increasing participation in renewables being added to diesel (i.e., biodiesel). The addition of biodiesel to diesel fuel yields to reduce the importation cost of diesel fuel as well as comply with sustainable policies without compromising with current fuel standards. The share of biodiesel in the Brazilian transport sector energy consumption was 5.2% in 2020 (Figure 3). Also, in the case heavy-duty of road transportation, biodiesel increased by 8.4% in its consumption, driven by the entry addition policy of biodiesel to diesel fuel in Brazil, which was composed of 12% biodiesel and 88% diesel in all commercial transport diesel, in 2020 (EMPRESA DE PESQUISA ENERGÉTICA (EPE), 2021).

The consumption of diesel fuel is increasing worldwide, mainly due to the heavy-duty transport sector demand for this fuel. Passenger vehicles and heavy-duty engines fleet has significant growth in the last decades and thus the health and environmental attention related to this subject. Further, the concern over oil reserves depletion has stimulated the research for partial or complete replacement of fossil fuels, particularly diesel fuel. Besides the considerations regarding the limited future oil resources and also policies that regulate CO_2 emissions, the interest in renewable and alternative fuel increased.

The concept of fuel selection was established wherein different fuels are mixed in order to achieve a combination of fuel properties that may be beneficial to the application in diesel engines. New diesel fuels are necessary not only to aim to improve the engine's performance and reduce emissions but also to ensure the sustainability of the fuel supplies. An alternative such as the case of Fischer-Tropsch diesel fuels can contribute to the partial substitution of diesel fuel (LAPUERTA, Magín et al., 2015; SOLOIU et al., 2019). This synthesized fuel is considered free of aromatics and can potentially reduce engine-out emissions (NO_x and PM) (JIAO; LIU; ZHANG; DONG; et al., 2019). The F-T fuels can also be considered as renewable fuel, depending on the raw material to produce the gas that this fuel is synthesized. In the case that the base fuel to produce the syngas is biomass, it is named BTL (biomass to liquid) and is considered second-generation biofuel (MARTINS; BRITO, 2020).

In this scenario, the potential of Brazil to intensify biomass production is already quite significant, and the country could be able to increase the share of biofuels in the domestic and international market in a sustainable manner (EMPRESA DE PESQUISA ENERGÉTICA (EPE), 2020b). As an alternative, the investment in Fischer-Tropsch fuel plants could be seen as an effort towards the mitigation of fossil fuels. This could be effectively implemented, mainly

due to the recent policies such as *RenovaBio* and the *Rota2030*. The *Rota2030* is an initiative of the Brazilian government, which was established by legislation nº 13.755/2018, to stimulate investment and to strengthen the Brazilian companies in the automotive sector through the development and application of new technologies, as well as to promote the use of biofuels and alternative fuels to improve the Brazilian energy matrix (MINISTÉRIO DA ECONOMIA, 2021).

Some research effort has already been made to evaluate the utilization of F-T and biofuels. Considering the blending of F-T diesel and alcohols, even though there are studies that have been previously conducted, most have considered long-chain alcohols, such as butanol (MUINOS *et al.*, 2017; YE, Lihua *et al.*, 2020), although others have considered methanol blended with diesel and also biodiesel (YANG *et al.*, 2017). However, these works were focused mainly on engine performance and regulated emissions. As summarized in the review papers (CAO *et al.*, 2016; JIAO; LIU; ZHANG; YANG; *et al.*, 2019; SUN, Dandan *et al.*, 2017), an increase in the specific fuel consumption was registered when using the alternative fuels blended in comparison with diesel fuel, despite none of these works evaluated the specific energy consumption. Also, it was reported that the exhaust emissions have either increased or decreased when using conventional diesel injection systems, but limited studies considered a modern injection system such as common-rail direct injection. Moreover, a minimal number of works have considered the utilization of F-T diesel and ethanol. This can be explained due to these two fuels have low miscibility due to limited temperature as reviewed in the literature (LAPUERTA, Magín *et al.*, 2015). However, the central focus of these works (MAGAND *et al.*, 2011; PIDOL *et al.*, 2012) was in the engine optimization for utilization of alternative fuels such as biodiesel/ethanol/diesel and F-T diesel. They reported CO, NO_x, HC, and smoke emissions; however, according to the literature review, there is a lack of investigation conducted to evaluate the impact of the blended fuels on the performance of an aftertreatment system, neither evaluated the PM characteristics (including size, distribution, and total mass), or the unregulated emissions (NO_2, NH_3, N_2O, HNCO, CH_4, and CH_2O), and none included the light hydrocarbons speciation.

Technology can provide an increase in biofuels production efficiency, both in the agricultural and industrial areas, increasing the global productivity of this segment in terms of economic aspects. On the other hand, current alternatives to produce advanced biofuels are still not very competitive in comparison with conventional diesel; however, in the middle- or long

term, it is expected that the simultaneous utilization of different biomasses will be feasible thus, minimizing the residues of this process.

Besides, the share of energy consumption in the industry sector is roughly one-third based on biomass, which can be considered a low-cost non-edible feedstock that can be used in the F-T process to produce diesel-like fuels (Figure 4). Also, it is depicted that 63% of the share is from renewable sources, whilst the share of natural gas and coal are respectively 8.8% and 12.4%, which can also be raw materials for the F-T process. Moreover, according to the report, the energy consumption in Brazil increased by nearly 4% from 2019 to 2020, which shows an increase in the energy demand and also an expansion in the industry sector.
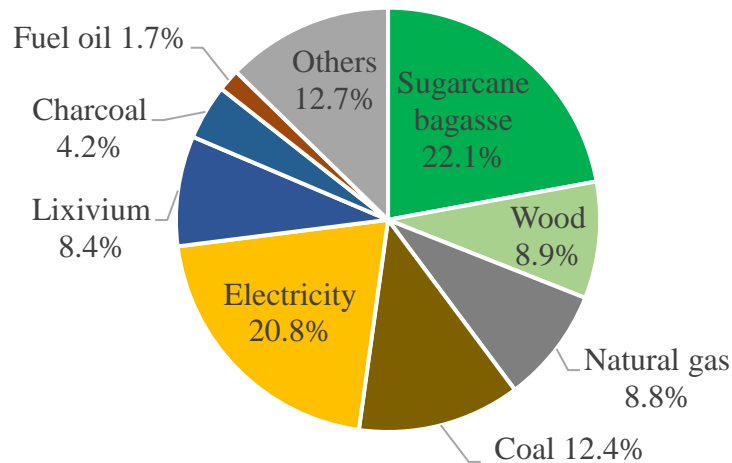
Figure 4. Share of energy consumption by industry sector in 2020, in Brazil (EMPRESA DE PESQUISA ENERGÉTICA (EPE), 2021).

There are still actions to be taken for the dissemination and development of these new biofuels, such as new policies, technological development, and price competitiveness against fossil fuels. Especially in the case of F-T diesel, the production cost has been pointed as a significant drawback to the large-scale production (GILL *et al.*, 2011a; JIAO; LIU; ZHANG; YANG; *et al.*, 2019; YANG *et al.*, 2017). Therefore, to minimize the final associated cost of the F-T diesel-like fuel, it could be blended with another renewable fuel, such as biodiesel and ethanol, which are likely more competitive against diesel fuel. In summary, some of the main challenges that must be considered to expand the use of biofuels in the transport energy matrix are:

- Decentralization of biofuel production

Two countries, Brazil and the USA are responsible for almost two-thirds of the total biofuels production in the world. These countries account for more than 80% of ethanol production and are the two largest producers of biodiesel (~35%) (OECD/FAO, 2019). It is necessary to increase and diversify the number of countries with significant production and consumption of biofuels to boost the biofuels trade market.

- Utilization of different types of biomasses

Extend the use of other sources and even the development of the biomass that is already used for the production of biofuels, such as non-edible biomass, could support large-scale production (EMPRESA DE PESQUISA ENERGÉTICA (EPE), 2020b)

- Biofuels policies for the transport sector

Some legislation policies are currently implemented with the objective of promoting the increase of the transport sector in a more efficient, cleaner, reliable, and economically sustainable way. As an example, only in Brazil, there are the *RenovaBio*, *Rota2030*, *Proconve*, National Program for the Production and Use of Biodiesel (*Programa Nacional de Produção e Uso do Biodiesel*, in Potuguese - PNPB), and the National Urban Mobility Policy (*Política Nacional de Mobilidade Urbana*, in Portuguese - PNMU). An effort could be made to manage these policies to delineate strategies to achieve common and practical goals.

In this investigation, two blends were selected to contain multicomponent alternatives and renewable to be used in CI engines. The considered blends had a fixed volumetric share of 15% ethanol and 35% biodiesel, whereas the remaining 50% was F-T diesel in one and diesel fuel in the second blend, aiming to improve the combustion and reduce exhaust emissions when compared to diesel fuel. Therefore, at the same time that it was possible to investigate the effect of the oxygen content to the fossil fuel, it could be compared the potential benefits of the alternative synthetic fuel, F-T diesel.

Moreover, this research intends to contribute to the utilization of alternative renewable fuels that have the potential to reduce the dependence on diesel fuel. Also, it aims to gain a deeper understanding of the effect of alternative fuels on the engine's performance, regulated and unregulated exhaust emissions, light hydrocarbons speciation, particulate matter (PM) characteristics, impact on the aftertreatment system, and energy and exergy analysis. It is expected, as the novelty of this work, that this investigation can effectively demonstrate

favorable synergistic effects in terms of individual fuel properties towards the selection of a blend of F-T diesel and ethanol aiming to obtain improvements in combustion characteristics and exhaust emissions when ethanol and biodiesel are blended with F-T diesel.

1.3   Thesis outline

This thesis is divided into six chapters in which the research overview, justification, and objectives have been presented in this Chapter. Chapter 2 is an overview of the related literature to show the methods, operating conditions, and results of previous investigations which are related to this work. Chapter 3 presents the fundamentals of the diesel engine, emissions formation, and legislations that are pertinent to the present conjecture. Chapter 4 presents the experimental setup and procedures for performing the tests and analyzing the results. Chapter 5 presents the results of the performance and combustion characteristics, exhaust emissions and PM characteristics, impact on aftertreatment system, and thermodynamic analysis. The conclusions and suggestions for future research are presented in Chapter 6.

1.4   Investigation constraints

The primary limitations during this current investigation have been listed below. Some of these have been restricted because of technical issues or due to the impact of the COVID-19 pandemic. Only two blends were considered to be tested during the experiments. Despite that this work was intended to investigate different formulations, a practical solution was to reduce the number of tested fuels and blend ratios. Also, the engine operation condition (speed and load) was decided to remain constant during the tests as this investigation was focused on evaluating the aspects of the fuels and not the engine. In addition, only one aftertreatment system (diesel oxidation catalyst - DOC) had the performance tested. A diesel particulate filter (DPF) and a selectivity reaction catalyst (SCR) were also considered, as well as a different configuration was proposed to be tested its efficiency, but some technical issues have limited the application to the DOC catalyst. Besides, the experimental plan was intended to include some physical (morphology and nano-structure) properties of PM emitted from the combustion of the proposed blend. However, the collected samples could not be sent to analysis due to the COVID-19 pandemic that has forced most research facilities to remain closed during the entire 2020. Further, the thermodynamic analysis, especially the exergy analysis, had some boundaries listed in the respective section. However, the sources of irreversibilities were not calculated individually, especially those related to the combustion process. Also, it must be noticed that this work used the indicated power and not the brake power to calculate the engine

efficiency. Also, the thermoeconomic, exergoeconomic, environmental, and enviroeconomic analyses were not included in the thermodynamic section.

2 LITERATURE REVIEW

This chapter presents a concise overview of some experimental findings on the use of biofuels in conventional diesel engines conducted by former studies. Several biofuels such as alcohols (methanol, ethanol, butanol, pentanol) and diesel-type fuels (diesel, biodiesel, F-T diesel) are investigated to find the impacts of these biofuels on the engine's performance, exhaust emissions, particulate matter, and aftertreatment systems. Special attention is drawn to ethanol and Fischer-Tropsch diesel as both fuels can mitigate the overall exhaust emissions from diesel engines, particularly NO_x and PM. At the end of this chapter, a summary of the knowledge gaps to be filled up by this work is presented.

2.1 Ethanol as a fuel in diesel engines

Emissions benefits have increased interest for alcohols addition in diesel engines, especially ethanol, caused by high oxygen content in its fuel structure. In addition, the benefits of using ethanol in a diesel engine are the potential to reduce engine exhaust emissions such as particulate matter (PM), hydrocarbons (HC), and carbon monoxide (CO), as widely reported in the literature (AGARWAL, 2007; ÇELEBI; AYDIN, 2019; GHADIKOLAEI, 2016).

Different techniques are available to promote ethanol utilization in CI engines, some of which require minor engine modifications or dedicated solutions. The more common methods, which can be divided into four main categories such as fumigation, blends, emulsion, or dual injection, as shown in Table 1. Ethanol can also be used in diesel engines after the conversion from diesel to spark ignition, which allows the use of 100% ethanol fuel (DE MORAIS *et al.*, 2019).

Table 1. Classification of ethanol utilization as a fuel in CI engines.

Injection technique	Description	Refs.
Ethanol fumigation	In this case, ethanol is introduced into the intake air upstream of the manifold by fumigation (i.e., using carbureting, vaporizing, or injecting via spraying), which leads to a premixing of the injected fuel with the intake air.	(ABU-QUDAIS; HADDAD; QUDAISAT, 2000; HANSDAH; MURUGAN, 2014; JAMUWA; SHARMA; SONI, 2017)
Blends of ethanol and diesel	Both fuels are premixed uniformly and injected into the cylinder of the engine through a fuel injector. Blending is applicable in the case that both fuels are miscible. In addition to the phase separation, there is a concern regarding the cetane number.	(JAMROZIK, 2017; LAPUERTA, Magín; ARMAS; HERREROS, 2008; TUTAK et al., 2017)
Addition of an emulsifier or co-solvent	In the cases that ethanol and diesel fuels are immiscible, an emulsifier or co-solvent is utilized to avoid phase separation of the alcohol with diesel.	(DE CARVALHO, Márcio A. S. et al., 2020; GUARIEIRO et al., 2009; LEI et al., 2012)
Dual injection system	An external injection system operating (i.e.) with high pressure is required for the port-fuel injection of the alcohol fuel upstream of the cylinder. In this case, either the diesel or the ethanol may be port-fuel injected, whereas the other is directly injected into the cylinder.	(HAN et al., 2020; NOUR et al., 2017; PEDROZO et al., 2018)

2.1.1 Ethanol fumigation and port-fuel injection in diesel engines

Among these techniques, the most used for ethanol in diesel engines are fumigation or port-fuel injection and blends with diesel-type fuels. In the first case, the fuel is injected into the air intake by a carburetor, vaporizer, or sprayed, which leads to premixing the intake air with ethanol fuel. The main disadvantage of this mode is that it requires some modifications, such as the additional fuel tank and a fueling system control to supply ethanol. However, this mode avoids problems related to miscibility between ethanol and diesel fuel.

Furthermore, it has been widely reported (HANSDAH; MURUGAN, 2014; TELLI *et al.*, 2018) that this strategy may decrease particle matter and NO_x emissions, although the reduction is related to the replacement of diesel energy by ethanol, which could be up to 50%. Also, some researchers reported a reduction in CO_2 and NO emissions using up to 30% of ethanol port-injection (DE OLIVEIRA *et al.*, 2017), whilst others researchers reported a reduction in simultaneous CO and NO_x (ROSA *et al.*, 2021). On the other hand, the effect on thermal efficiency may are reported to either increase (JAMUWA; SHARMA; SONI, 2016) or decrease (GHADIKOLAEI; CHEUNG; YUNG, 2019), which may be dependent on engine operation conditions. Moreover, fumigation and port-fuel injection of ethanol in CI engines has been extensively reviewed by (IMRAN *et al.*, 2013), is further covered by Kumar et al. (KUMAR, Satish *et al.*, 2013), and more recently by Ghadikolaei (GHADIKOLAEI, 2016) and No (NO, 2019). Hence, this review will only cover the blending mode, as it is the main interest of this investigation.

2.1.2 Blending ethanol with diesel fuel in CI engines

Blending ethanol with diesel consists of ethyl alcohol and diesel fuel being uniformly premixed and later injected through the engine fuel injector to the cylinders. Blends of ethanol with diesel fuel are often referred to as "e-diesel." In this mode, the supply of ethanol is limited due to the poor miscibility of ethanol and diesel fuel. The blends are not stable, and phase separation is observed in the presence of water. In order to overcome the phase separation of an ethanol-diesel blend, the introduction of additives is commonly used (LAPUERTA, Magín; ARMAS; GARCÍA-CONTRERAS, 2009). Moreover, the addition of fractions of ethanol into diesel fuel promotes alterations in the properties of diesel fuel, such as decreasing the values of density, viscosity, the cetane number, and the heating value. On the other hand, ethanol has nearly 35% of oxygen content in its molecule, which contributes to complete combustion. In

comparison with fumigation or port-fuel injection modes, this strategy may be used in diesel engines without significant modifications.

Previous investigations have been conducted in order to evaluate the effect of the fuel blend on engine performance, durability, and emissions (DHARMA *et al.*, 2016; MOFIJUR *et al.*, 2016; SARAVANAN *et al.*, 2020). Furthermore, blend properties such as miscibility and viscosity (GERDES; SUPPES, 2001; LAPUERTA, Magín; ARMAS; GARCÍA-CONTRERAS, 2009; SHAHIR *et al.*, 2014), and effect of the blended fuel on engine performance, emissions, and durability (DE OLIVEIRA *et al.*, 2015; LAPUERTA, Magín; ARMAS; HERREROS, 2008; PAUL; PANUA; DEBROY, 2017) have been widely researched.

2.1.2.1 *Studies on ethanol and diesel blends*

Abu-Qudais et al. (ABU-QUDAIS; HADDAD; QUDAISAT, 2000) evaluated the effect of both fumigation and blend modes on a single-cylinder, four strokes, direct injection, naturally aspirated and water-cooled diesel engine with a swept volume of 582 cm3 and variable compression ratio. The research was conducted with a fixed 20° of injection timing and an 18:1 compression ratio. The results have indicated that both injection methods had similar behavior in relation to engine performance and emissions. The researchers have concluded that the optimum percentage for ethanol-diesel fuel blends was 15%, whilst for fumigation, the percentage was 20%. The fumigation method resulted in an increase of 7.5% in BTE, 55% in CO, 36% in HC, and a reduction of 51% in soot mass concentration. As for the blended mode, an increase of 3.6% in BTE, 43.3% in CO, and 34% in HC were observed, whereas a decrease of 32% in soot mass concentration has been noted.

Li et al. (LI *et al.*, 2005) have assessed the effects of different ethanol-diesel, aiming to find the optimum percentage of ethanol which simultaneously provides better performance and lower emissions. The work has considered four blends (E5, E10, E15, and E20) and diesel as a reference fuel, which were evaluated in a single-cylinder, water-cooled, DI diesel engine with 903 cm³ of cylinder volume and 17.5:1 of CR, under four loads and two engine speeds. The results have indicated that BSFC and BTE increased with blends for all conditions, smoke opacity decreased for high loads, however, increased for low and medium loads. As for gaseous emissions, CO and NO_x reduced, but THC increased significantly for the ethanol-diesel blends.

Sayin et al. (SAYIN, Cenk; USLU; CANAKCI, 2008) analyzed the effects of engine performance using ethanol-diesel blends in a single-cylinder, four-stroke, DI, naturally aspirated diesel engine with 700 cm³ of swept volume and 17:1 of CR under five speeds, two

loads and five different injection timings. The ratios of the blends were 5%, 10%, and 15%. Results have shown that EGT, NO_x, and CO_2 increased, whereas CO and HC decreased with increasing the amount of ethanol fraction in the blends under different speeds. On the other hand, NO_x and CO_2 increased, and HC and CO diminished for all test conditions under different injection timings.

Gnanamoorthi and Devaradjane (GNANAMOORTHI; DEVARADJANE, 2015) have investigated the influence of different compression ratios on a diesel engine. The investigation has considered four ethanol-diesel blends (E10, E20, E30, and E40) and used 1% of ethyl acetate plus 1% diethyl carbonate to prevent phase separation. The tests were conducted on a single-cylinder, water-cooled, DI diesel engine with 661 cm³, 17.5:1 of CR, and 5.9 kW, under three compression ratios (17.5, 18.5, and 19.5) and six loads (from 0.7 to 4.7 kW). They have reported that BTE, in-cylinder pressure, and peak HRR increased with ethanol addition. As for the exhaust emissions, CO increased under low and medium loads. HC increased for all conditions, whereas NO_x decreased for CR 17.5 and 18.5 and increased for CR 19.5. They also reported that smoke increased for high ethanol fractions for CR 17.5 and 18.5.

Praptijanto et al. (PRAPTIJANTO *et al.*, 2015) have studied the effects of ethanol on a simulated diesel engine using AVL Boost. Different blends of ethanol-biodiesel were simulated (E0, E2.5, E5, E7.5, and E 10), under a range of speed of 1000-1500 rpm and seven engine loads (0, 10, 20, 30, 40, 50, and 60 Nm). By using the virtual engine simulation tool, the researchers have reported that the direct blending of ethanol and diesel fuel has advantages in reducing exhaust emissions CO, soot, and NO_x percentages. The engine brake power of pure diesel was slightly lower than those of E2.5-E10, especially for speeds above 1400 rpm. As for the emissions, they reported that CO decreased at full load, as well as soot emissions and NO_x increased.

Tutak et al. (TUTAK *et al.*, 2017) have conducted a comparative analysis of the combustion of diesel-ethanol with biodiesel-ethanol blends. A single-cylinder, 4-stroke, naturally aspirated, 573 cm³, 17:1 CR, and the tests were conducted under a constant angle of diesel fuel injection, full load, and constant speed. The ethanol fraction of both blends was variated up to 45% with an increment of 5%. Results were compared with pure diesel and pure biodiesel as reference fuels under the same operating conditions. They have reported that diesel-ethanol blends have increase ITE and HRR, whereas EGT has decreased. Regarding the engine-

out emissions, THC and NO$_x$ have increased, whilst CO and CO2 decreased in comparison with reference fuels.

Lee et al. (LEE; LEE; LEE, 2018) have evaluated the performance and emissions of ethanol-diesel dual-fuel combustion on a diesel engine. The tested engine was a heavy-duty single-cylinder diesel engine with two direct injectors. The engine had 1.8 L displacement, four-stroke, with 17.1 of CR, naturally aspirated, and with a common-rail DI. Each fuel was injected separately from the two fuel injectors. Various ethanol substitution ratios were investigated with the engine kept fixed at 1000 rpm and variating the IMEP range from 0.2 to 0.8 MPa. They have reported that the NO$_x$ and PM emissions decreased, as well as the particulate mean diameter size.

Emiroğlu and Şen (EMIROĞLU; ŞEN, 2018a) have used methanol, ethanol, and butanol to investigate the influence of alcohol addition in diesel fuel on combustion, performance and exhaust emission of a single-cylinder, naturally aspirated, AC, DI diesel engine with 349 cm³ displacements and 20.3:1 of CR. The alcohols were mixed with the diesel fuel in a 10% (m/m) proportion, and the fuel was injected at 207 bar at 20 BTDC under fixed speed and four different loads. The researchers have reported that the alcohols increased the peak cylinder pressure, maximum heat release rate, and BSFC whilst reduced BTE for all loads. Regarding the exhaust emissions, they have reported that the alcohols have slightly increased NO$_x$ while reduced smoke and CO.

Also, studies showed a remarkable emission reduction with hybrid electric vehicles running with biofuels (GLENSOR; MUÑOZ B., 2019). García et al. (GARCÍA *et al.*, 2020) investigated two advanced dual-fuel combustion modes using ethanol as the primary fuel for hybrid passenger vehicles, a pre-chamber ignition system (PCIS) using ethanol and hydrogen, and reactivity-controlled compression ignition (RCCI) combustion mode fueled with ethanol/diesel. As a result, the RCCI mode has shown the highest potential to decrease the NO$_x$ emissions while presented the highest benefits in energy consumption; however, it had penalties in terms of CO$_2$ emissions. García and Monsalve-Serrano (GARCÍA; MONSALVE-SERRANO, 2019) also studied dual-fuel diesel and E85 (85% ethanol and 15% gasoline) in a series hybrid vehicle concept and concluded that ultra-low engine-out emissions could be achieved for NO$_x$.

A summary of studies conducted with ethanol and diesel blends in compression ignition engines is shown in Table 2. Most studies have considered multiple engine operating conditions

and different ratios of ethanol addition to diesel fuel. Generally, ethanol-diesel blends resulted in an increase in engine thermal efficiency, HRR, and fuel consumption. As for the exhaust emissions, it increases CO, HC, and NO_x emissions, although it reduces PM.

Table 2. Summary of studies with ethanol and diesel blends compared to reference fuel.

Authors	Year	Alcohol	Blends	Reference fuel	Engine parameters	Operating conditions	BTE	SFC	SEC	HRR	EGT	CO	CO₂	HC	NOₓ	PM
Abu-Qudais et al. (ABU-QUDAIS; HADDAD; QUDAISAT, 2000)	2000	Et	E15, E20	D100	1-cylinder, 4 strokes, DI, NA WC, 582 cm³, 18:1 CR	Different speeds, fixed CR and injection angle	↑	n.a.	n.a.	n.a.	n.a.	↑	n.a.	↑	n.a.	→
Li et al. (LI *et al.*, 2005)	2005	Et	E0, E5, E10, E15, E20	Diesel	1-cylinder, DI, WC, 903cm³, 17.5:1 CR, 12.1 kW	Different speeds and loads	↑	↑	n.a.	n.a	n.a.	→	n.a.	↑	↑	↑
Sayın et al. (SAYIN, Cenk; USLU; CANAKCI, 2008)	2008	Et	E5, E10, E15	Pure diesel	1-cylinder, 4 stroke, DI, NA, 700cm³, 17:1 CR	Variable speeds, loads and injection timings	n.a.	n.a.	n.a.	n.a.	↑	↑	↑	→	↑	n.a.
Gnanamoorthi and Devaradjane (GNANAMOORTHI; DEVARADJANE, 2015)	2015	Et	E10, E20, E30, E40	Diesel	1-cylinder, WC, DI, 661 cm³, 17.5:1 CR, 5.9 kW	Different loads and compression ratios	↑	n.a.	n.a.	↑	n.a.	↑	n.a.	↑	→	↑
Praptijanto et al. (PRAPTIJANTO *et al.*, 2015)	2015	Et	E0, E2.5, E5, E7.5, E10	Diesel	2-cylinder, 4 stroke, DI, NA, WC, 1.63 L, 19:1 CR, 13.5 kW	Variable speeds and loads (simulated conditions)	n.a.	↑	n.a.	↑	n.a.	→	n.a.	→	↑	n.a.
Tutak et al. (TUTAK *et al.*, 2017)	2017	Et	Blends with diesel and with biodiesel (E0, E5, E10, E15, E20, E25, E30, E35, E40, E45)	D100, B100	1-cylinder, 4-stroke, DI, NA, 573 cm³, 17:1 CR, 7 kW	Constant angle of diesel fuel injection, full load, and constant speed	↑	n.a.	n.a.	↑	→	→	→	↑	↑	n.a.
Lee et al. (LEE; LEE, 2018)	2018	Et	various ethanol fractions	Diesel	1-cylinder, 4-stroke, common rail DI, NA, 1.8 L, 17:1 CR	Fixed speed, variable IMEP, and fuel injection timings	→	n.a.	n.a.	↑	n.a.	↑	n.a.	↑	→	→
Emiroğlu and Şen (EMIROĞLU; ŞEN, 2018a)	2018	M, Et, Bu	10 wt%	D100	1-cylinder, AC, NA, DI, 349 cm³, 20.3:1 CR, 7.5 kW	Constant engine speed and variable load	→	↑	n.a.	↑	n.a.	→	n.a.	n.a.	↑	→

1

2

2.1.2.2 *Miscibility of ethanol and diesel blends*

The miscibility of the blends of ethanol and diesel is mainly related to the purity of the ethanol and the temperature. Moreover, it has been reported that aromatic contents and intermediate distillate temperatures had a significant impact on diesel-ethanol blend miscibility limits (GERDES; SUPPES, 2001). Kwanchareon et al. (KWANCHAREON; LUENGNARUEMITCHAI; JAI-IN, 2007) reported that in the case of diesel and hydrous ethanol (ethanol with 95% purity and 5% water in its mixture), they are not miscible at room temperature due to the high polarity of water that enhances the polar part in ethanol molecule, thus affecting the mixture, since diesel is a non-polar molecule. Moreover, Liu et al. (LIU; HU; JIN, 2016) recommended that n-hexanol and n-octanol may be used as a co-solvent additive for hydrous ethanol/diesel blends due to the acceptable fuel properties and soluble performance.

On the other hand, high purity ethanol (i.e., 99.5% and 99.9% ethanol in volume) can be mixed into a homogenous solution at any ratio at room temperature, at 10ºC, or between the range of 30º to 40ºC. Nevertheless, at 20ºC, the ratios of ethanol between 30% to 70%, forming a liquid 2 phases in which are immiscible (KWANCHAREON; LUENGNARUEMITCHAI; JAI-IN, 2007). For temperatures above 40ºC, all blends are stable, as reported by Lapuerta et al. (LAPUERTA, Magín *et al.*, 2010). Additionally, (LAPUERTA, Magín *et al.*, 2010) recommend that blends with ethanol concentration lower than 12% or higher than 78% should be used with temperatures above 10ºC.

The separation between diesel-ethanol blends may be prevented by adding an emulsifier or co-solvent. The former acts to suspend small droplets of ethanol within the diesel fuel whilst the latter acts as a bridging agent through molecular compatibility and bonding to produce a homogeneous blend (HANSEN; ZHANG; LYNE, 2005), such as the biodiesel (GUARIEIRO *et al.*, 2009). Emulsification usually requires heating and blending steps to generate the final blend, whereas co-solvents allow fuels to be "splash-blended," thus simplifying the blending process.

Biodiesel is considered a biodegradable fuel derived from renewable sources, which may be produced from vegetable oils (e.g., plant species such as soy, rapeseed, castor, palm, jatropha, sunflower, peanuts, among others) and or animal fats. In Brazil, soybeans are the primary raw material used (MARTINS *et al.*, 2013; PINTO *et al.*, 2005). The major producers of biodiesel in the world are the USA, Brazil, and the EU.

Regarding the Brazilian scenario, it has also been announced plans to progressively scale up its biodiesel mandate from 2%, in 2008, to 15%, by 2023, as shown in Table 3.

Currently, since March 2021, the biodiesel content is 13%, as established by the Resolução nº 16/2018 by the National Energy Policy Council (Conselho Nacional de Política Energética - CNPE, in Portuguese). However, only a month later, in April 2021, the biodiesel content that is added to commercial diesel in Brazil has been reduced from 13% to 10% (Resolução nº 4/2021 CNPE). This change happened due to the recent effects of the appreciation of the cost of soybean oil in the Brazilian and international markets, combined with the exchange devaluation of the Brazilian currency (Real, R$) against the US dollar (US$), which has boosted the soybean exports and also increased the value of biodiesel.

Table 3. Evolution of the biodiesel content added to the commercialized diesel fuel in Brazil.

Year	Biodiesel content (%)	Year	Biodiesel content (%)
2003	Optional	Nov/2014	7
Jan/2008	2	Mar/2017	8
Jul/2008	3	Mar/2018	10
Jul/2009	4	Mar/2019	11
Jan/2010	5	Mar/2020	12
Ago/2014	6	Mar/2021	13
Nov/2014	7	Apr2021	10

As for Brazilian biodiesel production, the country's raw material is mainly comprised of soybean oil (69.3%), bovine tallow (16.9%), and others (10.7%) (DA SILVA CÉSAR *et al.*, 2019; DE SOUZA *et al.*, 2019).

2.1.2.3 *Studies on ethanol, diesel, and biodiesel blends*

Yilmaz et al. (YILMAZ, Nadir; VIGIL; BURL DONALDSON; *et al.*, 2014) have investigated the effect of different ethanol ratios on a fixed biodiesel-diesel mixture on a CI engine. Four blends (BDE3, BDE5, BDE15, BDE25) were evaluated and compared with diesel fuel. The research has assessed a two-cylinder, four-stroke, water-cooled, naturally aspirated, indirect injection diesel engine with 479 cm³, 23.5:1 CR, and 6.5 kW and have reported that EGT increased for all conditions, CO increased with ethanol addition although decreased with increasing engine load, NO decreased for all conditions, but HC increased under low load and decreased for medium and high loads.

Roy et al. (ROY *et al.*, 2016) have studied the effects of ethanol and DEE as additives to biodiesel and biodiesel blends during the engine warm-up period of multiple speed idle conditions. A modern (Tier 4) 4-cylinder, turbocharged, DI diesel engine with 4.5 L, 17.3:1 CR, and 97 kW at three idling speeds (800, 1000, and 1200 rpm) with no load conditions was tested with a DPF catalyst. Two additives (5% and 15% by volume), ethanol and diethyl ether (DEE), were mixed with biodiesel-diesel blends B20, B50, and B100. The results have shown that CO decreased except for B20E15 under all speeds, NOx increased with increased load, although HC decreased. Also, they have reported that formaldehyde and acetaldehyde emissions had no significant increase after the warm-up period.

Khoobbakht et al. (KHOOBBAKHT; NAJAFI; *et al.*, 2016) investigated the effect of blending biodiesel-ethanol with diesel fuel to a Euro II four-cylinder, water-cooled, direct injection diesel engine with 4.81 L, 17:1 CR, and 81 kW. The engine was evaluated under five engine speeds (1000, 1450, 1900, 2350, 2800 rpm) and loads (20%, 40%, 60%, 80%, 100%). The research has used the Design of Experiments (DoE) based on the central composite rotatable design (CCRD) of response surface methodology (RSM) and considered various blends of diesel (56%-84%) biodiesel (13%-40%), and ethanol (0%-22%). The researchers have reported that biofuels may reduce CO, HC, and smoke opacity; however, their addition to diesel fuel provokes detrimental impacts to be dominant over advantages. They have concluded that an engine load of 80%, speed of 2800 rpm, and a blend of B26E11D63 the most suitable.

Emiroğlu and Şen (EMIROĞLU; ŞEN, 2018b) investigated the effect of the biodiesel and various alcohols additions to petroleum-based diesel fuel. 20% cottonseed biodiesel was mixed with DF (B20), and different alcohols (10% butanol, 10% ethanol, or 10% methanol) were blended (B20Bu10, B20E10, and B20M10). A single-cylinder, naturally aspirated, air-cooled DI diesel engine with 349 cm³, 20.3:1 CR, and 5.6 kW was tested under four different loads (0.09, 0.18, 0.27, and 0.36 MPa) and fixed engine speed. They have reported that all alcohols increased ID, peak in-cylinder pressure, and peak HRR for all conditions. The BTE was very similar to diesel fuel, and BSFC increased. As for the exhaust emissions, CO, HC, and NOx increase whilst smoke opacity decreased.

Pradelle et al. (PRADELLE *et al.*, 2019) experimentally assessed diesel engine performance and combustion characteristics. The research has considered different blends of diesel, biodiesel, and ethanol (DB15 + E0, E5, E10, E15, E20), which were compared with diesel B7 as reference fuel. A Euro III four-cylinder, four-stroke, turbocharged and with air

aftercooler DI diesel engine with 4.3 L, 15.8:1 of CR, and 107 kW has been rested under different torques (25, 50, 75% and full) and engine speeds (1500, 1800, 2100 rpm). The researchers have reported that the specific fuel consumption, specific energy consumption, ID, and ITE have increased with DBE blends in comparison with diesel B7 fuel.

Ma et al. (MA *et al.*, 2021) tested blends of diesel-biodiesel-alcohol (ethanol and pentanol) in a modified single-cylinder diesel engine, four-stroke, water-cooled, 1.081 L, with 16:1 compression ratio, and with a common rail fuel injection system under three different engine speeds (1000, 1500, and 1800 rpm). The performance and emissions characteristics of the engine fueled with the ternary blends were compared with a blend of diesel-biodiesel and diesel fuel. The researchers reported that the peak in-cylinder pressure and peak-HRR were higher for the engine fueled with 20% ethanol, 10% biodiesel, and 80% diesel (in vol.). As for the emissions results, the NO_x, soot, THC, and CO emissions had decreased when the engine was fueled with 10% ethanol, 10% biodiesel, and 80% diesel (in vol.).

Srikanth et al. (SRIKANTH *et al.*, 2021) evaluated the utilization of biodiesel in diesel-ethanol blends at different volumetric concentrations (D85E5B10, D80E10B10, D75E15B10, D75E5B20, D70E10B20, and D65E15B20). The researchers tested a single-cylinder direct injection diesel engine, four-stroke, water-cooled, with 625 cm³, 5.5 kW, and a compression ratio of 17.5:1. The results of the performance and emissions of the engine were compared to biodiesel fuel and diesel fuel as a baseline. The tests were conducted at a fixed speed (1500 rpm), constant injection pressure (220 bar), and injection timing (23°CA bTDC) at four different loads (25, 50, 75%, full load). They reported that the BTE, BSFC, and BSEC increased for the blends in comparison with diesel. Also, the blends have increased the CO2 and NO_x emissions, whilst HC decreased. The CO decreased in comparison to diesel for 25% and 50% loads. The smoke results decreased for all blends except D85E5B10 and D80E10B10.

Table 4 summarizes the main results of ethanol, diesel, and biodiesel blends fueled on diesel engines. Overall, the researches using ethanol-biodiesel-diesel blends have shown that the ternary fuel can be employed as an alternative fuel for existing unmodified diesel engines due to its improved emission and performance characteristics. It is possible to observe that generally, the engine-specific fuel consumption increased, HRR, NO_x, whilst CO, PM, and HC decreased.

Table 4. Summary of studies with ethanol, diesel, and biodiesel compared to reference fuel.

Authors	Year	Alcohol	Biodiesel	Additive	Blends	Reference fuel	Engine parameters	Operating conditions	BTE	SFC	SEC	HRR	EGT	CO	CO₂	HC	NOₓ	PM
Yilmaz et al. (YILMAZ, Nadir; VIGIL, BURL DONALDSON; et al., 2014)	2014	Et	used cooking oil	-	BDE3, BDE5, BDE15, BDE25	diesel	2-cylinder, 4-stroke, NA, WC, IDI, 479 cm³, 23.5:1 CR, 6.5 kW	Variable loads	n.a.	n.a.	n.a.	n.a.	↑	↑	n.a.	↓	n.a.	n.a.
Roy et al. (ROY et al., 2016)	2016	Et	canola oil	Et and DEE	DB20, DB50, DB100+ (E5, E15 or DEE5, DEE15)	Neat diesel	(Tier 4) 4-cylinder, TC, DI, 4.5 L, 17.3:1 CR, 97 kW	no load and multiple idle speed during engine war-up	n.a.	n.a.	n.a.	n.a.	=	↓	n.a.	↑	↑	n.a.
Khoobbakht et al. (KHOOBBAKHT; NAJAFI; et al., 2016)	2016	Et	waste cooking oil	-	Various blends D(56%-84%), B(13%-40%), E(0%-22%)	diesel	4-cylinder, WC, DI, 3.81 L, 17:1 CR, 81 kW	Different engine speeds and loads	n.a.	n.a.	n.a.	n.a.	n.a.	↑	↑	↑	↑	↑
Emiroğlu and Şen (EMIROĞLU; ŞEN, 2018b)	2018	M, Et, Bu	cottonseed biodiesel	-	10 wt% (B20Bu10, B20E10, B20M10)	petroleum-based diesel fuel	1-cylinder, NA, AC, DI, 349 cm³, 20.3:1 CR, 5.6 kW	Fixed speed and various loads	=	↑	n.a.	↑	n.a.	↑	n.a.	↑	↑	↑
Pradelle et al. (PRADELLE et al., 2019)	2019	Et	80% soybean + 20% beef tallow	72.5% castor oil, 17.5% soybean biodiesel, 10 vol% n-butanol	DB15 + E0, E5, E10, E15, E20	diesel S10 B7	Euro III 4-cylinder, 4-stroke, TC, AC, DI, 4.3 L, 15.8:1 CR, 107 kW	Variable speeds and loads (simulated conditions)	n.a.	↑	n.a.	↑	n.a.	↓	n.a.	↑	↑	n.a.
Ma et al. (MA et al., 2021)	2021	Et, P	n.a.	-	D80B10P10, D80B10E10, D70B10E20	D90B10, diesel	1-cylinder, WC, DI, 1.081 1, 16;1 CR, common-rail	3 speeds (1000, 1500, 1800 rpm)	n.a.	n.a.	n.a.	↑	n.a.	↓	↓	↓	↓	↓

Reference	Year	Alcohol	Oil/biodiesel	Fuel	Engine	Test conditions	Blends											
Srikanth et al. (SRIKANTH et al., 2021)	2021	Et	Niger seed oil biodiesel	diesel, biodiesel	1-cylinder, four-stroke, DI, WC, 625 cm³, 5.5 kW, CR 17.5:1	Fixed speed, injection pressure and injection timing, 4 loads	D85E5B10, D80E10B10, D75E15B10, D75E5B20, D70E10B20, and D65E15B20	↑	↑	↑	n.a.	n.a.	↓↑	↓↑	→	↑	↓↑

n.a.: not available, Turbo: Turbocharged, IC: Intercooled, CRDI: common-rail direct injection, DI: direct injection, WC: water-cooled, AC: air-cooled, EGR: exhaust gas recirculation, Et: Ethanol, M: Methanol, Bu: Butanol, P: Pentanol

2.2 Fischer-Tropsch diesel as a fuel in diesel engines

Other alternative second-generation biofuels are the Fischer-Tropsch diesel type fuels, which are synthesized alternative fuels to diesel. Fischer-Tropsch diesel has been proved feasible for direct application on diesel engines without any engine hardware modification (WANG *et al.*, 2017). Furthermore, Fischer-Tropsch diesel type fuels have been pointed as one of the most promising fuels to reduce fossil diesel dependence (RODRÍGUEZ-FERNÁNDEZ, José; HERNÁNDEZ; SÁNCHEZ-VALDEPEÑAS, 2016). Although Fischer-Tropsch technology is not new, many recent studies have been conducted in order to evaluate production, life-cycle assessment, and economic aspects related to Fischer-Tropsch diesel (BORUGADDA; KAMATH; DALAI, 2020; OKEKE *et al.*, 2020; SANTOS, Ronaldo Gonçalves dos; ALENCAR, 2020). Overall, these works concluded that the Fischer-Tropsch synthesis of liquid fuels is an environmentally friendly alternative, the technology is deemed to be economically feasible and could compete with fossil-based liquid fuels, and the Fischer-Tropsch biofuels are aiming to industrial and automotive application.

However, Fischer-Tropsch diesel has a high cost, low production and poor lubricity as limiting factors for wide application (GILL *et al.*, 2011a; JIAO; LIU; ZHANG; YANG; *et al.*, 2019). Hence, it is unreasonable to use solely Fischer-Tropsch diesel in diesel engines (JIAO; LIU; ZHANG; YANG; *et al.*, 2019; YANG *et al.*, 2017). Nevertheless, Fischer-Tropsch diesel may be blended with different fuels to reduce its cost at the same that promote the use of blends of alternative fuels that may contribute to mitigate the fossil fuel dependence as well as promote significant impact over the engine combustion, performance, and exhaust emissions.

2.2.1 Studies on Fischer-Tropsch diesel and diesel type fuels

Previous studies have evaluated the impact of blends of Fischer-Tropsch diesel with pure diesel (HOSSAIN *et al.*, 2015; SAJJAD *et al.*, 2014), biodiesel (LAPUERTA, Magín *et al.*, 2010; MOON *et al.*, 2009) and diesel-biodiesel (ROUNCE *et al.*, 2009; SAJJAD *et al.*, 2015). In general, the F-T diesel decreases CO, THC, and NOx. PM emissions are improved when using F-T diesel fuel or F-T diesel blended with diesel or biodiesel. Also, PM reduction by using F-T diesel is higher than that by using biodiesel.

Moon et al. (MOON *et al.*, 2010) investigated the engine-out emission characteristics of a diesel engine fueled by diesel, GTL fuel, diesel–biodiesel blends, and GTL–biodiesel blends. The tests were conducted on a 4-cylinder Intercooled and VGT turbocharger (Variable-Geometry Turbocharger) diesel engine with 1.996 L of displacement, 17.7:1 of compression

ratio, and equipped with a common rail direct injection operated under three speeds (1500, 2000, and 2500 rpm), three loads (0.4, 0.8, and 1.2 BMEP), and different EGR rates. The blends of D80B20, GTL80B80, and GTL60B40 (v/v) were compared with diesel as baseline fuel. The researchers reported a decrease in THC (22-56%) and CO (16-52%) emissions, whilst NOx emissions increased (by a maximum of 12%) for GTL–biodiesel blends compared to diesel. Regarding the PM size distribution (PSD), the GTL-biodiesel blends reduced the PM concentration in the accumulation mode as a result of the oxygen content in biodiesel. However, the opposite result occurred in the nucleation mode, when the engine was operated with EGR. Also, the total PM concentration of the blends of GTL-biodiesel decreased in comparison with those for diesel, achieving a reduction of 46% for the blend GTL60B40.

Du et al. (DU *et al.*, 2014) studied the effect of F-T diesel (GTL) and diesel blends on combustion and particle size distribution. A total of four blends were tested (10, 20, 30, and 60%GTL in volume blended to diesel) and compared to both 100% diesel and 100% GTL fuel in a 3.168L turbocharged intercooler common-rail direct injection (CRDI), with 17:1 of compression ratio engine under steady-state and transient-state operating conditions, both without EGR. The results have shown that the blends of GTL and diesel fuel presented a shorter ignition delay and reduced the proportion of premixed burning compared to diesel. By increasing the ratio of GTL fuel in the blends, the HRR and pressure-rise rate of premixed burning dropped. The researchers also reported that increasing the blend ratio was found to reduce the nucleation mode particle number and favor the accumulation mode particles formation, whilst the total particle number concentration increased. They concluded that the PM number emission could be improved by using the blends under a transient-state operating condition.

Choi et al. (CHOI *et al.*, 2019) investigated the effects of using blends of F-T diesel (GTL) and biodiesel (GTL80B60 and GTL60B40, v/v) on the fuel properties, heat release, and emission characteristics under various fuel injection timing and blending ratios. The tested engine was a single-cylinder, direct injection diesel engine with 0.37 L of displacement and a compression ratio of 17.3:1, equipped with a common rail injection system. The engine experiment was conducted at an engine speed of 1200 rpm and an injection pressure of 160 MPa. The researchers reported that the blends of GTL-biodiesel resulted in reduced NOx and soot emissions when compared to GTL fuel. Also, as the injection timing was advanced, the NOx emissions were significantly increased, while the effect of the injection timing on the soot emission was small compared to the NO_x emissions. Moreover, the CO emissions, the blends

resulted in similar (GTL80B20) or significantly higher emissions (GTL60B40), especially with the advance of the injection timing. As for the HC, the blends increased the emissions for advanced injection timings when compared to GTL fuel.

Sadeq et al. (SADEQ *et al.*, 2019) evaluated three different intake manifolds designs (named 1D, 2D, 3D, in which D was the internal diameter of the manifold inside the engine cylinder. The single-cylinder, 4-stroke, water-cooled, direct injection diesel with 360 cm³, 18:1 of compression ratio, and 4.85 kW of rated power was operated using alternative fuels, including blends of diesel, F-T diesel, and two types of biodiesels (waste cooking oil and corn oil). The tests were conducted at a fixed speed and five loads. The results have shown that the blend of diesel, GTL, biodiesel (waste cooking oil and corn oil) exhibited the highest peak pressure and BSFC among the tested fuel for the same type of manifold at different loads. Regarding the exhaust gas temperature, the diesel, GTL, and both biodiesel (waste and corn) were higher than diesel fuel. Also, the exhaust emissions, the lowest levels of CO, HC, and PM were for the blend of diesel, GTL, and biodiesel (waste cooking oil); however, they had higher NO emissions for the same manifold at different loads. Overall, the researchers concluded that the 1D manifold had better results at the same time that the engine was fueled with GTL.

Nabi et al. (NABI; HUSTAD; AREFIN, 2020) investigated the influence of Fischer-Tropsch diesel and biodiesel blends under three volumetric ratios (25, 50, and 75% biodiesel blended with F-T diesel). The engine was a six-cylinder, four-stroke, turbocharged, direct-injection diesel engine with 1.773 L, 18:1 of compression ratio, and 280 kW of rated power. The experiments were conducted at a constant engine speed (1450 rpm), whilst the fuel injection timing was set at 20 ∘CA BTDC, and the engine was run at five different loads (3, 25, 50, 75, and 92% of full load). The researchers have measured the gaseous emissions (CO, O2, CO2, HC, and NO) and also conducted both energy and exergy analysis of the engine with these blends. All parameters of the engine fueled with the three blends were compared to pure F-T diesel fuel (100% F-T diesel). They reported that there were no significant variations in the different parameters with the three oxygenated blends when compared to those of the FT100.

Parravicini et al. (PARRAVICINI; BARRO; BOULOUCHOS, 2021) tested blends of alternative fuels under different EGR rates in a single-cylinder heavy-duty 4-stroke diesel with 3.96 L of displacement, 13.77:1 of compression ratio, and equipped with a common rail. The researchers compared blends of GTL, HVO (Hydrotreated Vegetable Oil), and OME (Polyoxymethylene Dimethyl Ether) with diesel fuel as a baseline under different EGR rates. Regarding the GTL20D80, they reported that the combustion analyses showed that GTL20D80

had shorter premixed combustion because of the shorter ignition delay of the blend. However, the reduction in ignition delay of the blends compared to diesel is depending on the operating condition of the engine and does not represent the blending ratio. Also, the exhaust gas temperature and the ISEC of GTL20D80 were lower than those for diesel. Regarding the NOx-soot trade-off, the researchers observed that the GTL20D80 blend emitted less soot than diesel but minorly more NOx at comparable EGR rates.

Table **5** summarizes the main results of Fischer-Tropsch diesel and diesel-type fuels blends fueled on diesel engines. Overall, the researches using Fischer-Tropsch diesel and diesel-type fuels blends has shown that blending F-T diesel with diesel, biodiesel, or another fuel is suitable for being used in compression ignition diesel engines without any modification. Also, it is possible to observe that overall, the specific fuel consumption increases, although the specific energy consumption decreases, whilst CO, HC, and PM decrease, however, NOx emissions increase.

Table 5. Summary of studies with Fischer-Tropsch diesel and diesel type fuels compared to reference fuel.

Authors	Year	Fuels	Biodiesel	Blends	Reference fuel	Engine parameters	Operating conditions	BTE	SFC	SEC	HRR	EGT	CO	CO₂	HC	NOₓ	PM
Moon et al. (MOON et al., 2010)	2010	Diesel / GTL / Biodiesel	waste cooking oil, soybean oil at	D80B20 / GTL80B80 / GTL60B40	Diesel / GTL	4-cyl, IC, Turboand, 1.996 L, 17.7:1, CRDI	3 speeds (1500, 2000, 2500 rpm), 3 loads (0.4, 0.8, 1.2 BMEP), variable EGR	n.a.	↑	↓	↑	n.a.	↓	n.a.	↓	↑	↓
Du et al. (DU et al., 2014)	2014	GTL / Diesel	-	GTL10D90, GTL20D80 / GTL30D70, GTL60D40	Diesel / GTL	4-cyl, 4-str, 3.168 L, Turbo, IC, 17:1	steady-state and transient-state, no EGR	n.a.	n.a.	n.a.	↓	n.a.	n.a.	n.a.	n.a.	n.a.	↑
Choi et al. (CHOI et al., 2019)	2019	GTL / Biodiesel	soybean oil	GTL80B60, GTL60B40	GTL	1-cyl, DI, 0.37 L, 17.3:1, CRDI	1200 rpm, 160 MPa, variable injection timing	n.a.	n.a.	n.a.	↑	n.a.	↑/=	n.a.	↑	↓	↓
Sadeq et al. (SADEQ et al., 2019)	2019	Diesel / GTL / Biodiesel	waste cooking oil, corn oil	D50GTL50, D50WB50 / D33GTL33WB33 / D25GTL25CB25	Diesel / GTL	1-cyli, 4-str, WC, DI, 360 cm³, 18:1, 4.85 kW	fixed speed, 5 loads, 3 intake manifold designs	n.a.	↑	n.a.	n.a.	↑	↓	n.a.	↓	↑	↓
Nabi et al. (NABI; HUSTAD; AREFIN, 2020)	2020	F-T diesel / Biodiesel	Jatropha curcas	FT75B25, FT50B50 / FT25B75	F-T diesel	6-cyl, 4-str, Turbo, DI, 1.773 L, 18:1, 280 kW	1450 rpm	↑	↑	n.a.	n.a.	n.a.	n.a.	=	n.a.	n.a.	n.a.
Parravicini et al. (PARRAVICINI; BARRO; BOULOUCHOS, 2021)	2021	Diesel / GTL / HVO / OME	-	GTL20D80, OME15D85 / OME7D93, HVO20D80 / HVO77OME18A5HEX	Diesel	1-cyl, 4-str, 3.96 L, 13.77:1, CRDI	variable pressure and EGR	n.a.	n.a.	↓	=	↓	n.a.	n.a.	n.a.	↑	↓

n.a.: not available, Turbo: Turbocharged, IC: Intercooled, DI: direct injection, WC: water-cooled, AC: air-cooled, CRDI: common-rail direct injection, WC: water-cooled, AC: air-cooled, EGR: exhaust gas recirculation, HEX: hexanol

2.2.2   Studies on Fischer-Tropsch diesel and alcohols

Light chain alcohols such as methanol and especially ethanol have very significant availability, lower cost, and can be effectively used in compression ignition engines. Some studies have investigated the effect of blends of alcohols with Fischer-Tropsch diesel with butanol (HERREROS; GEORGE; *et al.*, 2014). Moreover, the addition of methanol, pentanol, and hexanol with Fischer-Tropsch diesel has also been studied to investigate the combustion characteristics, engine performance, and emissions at different operational conditions.

Rodríguez-Fernández et al. (RODRÍGUEZ-FERNÁNDEZ, J. *et al.*, 2009) have studied ethanol addition to diesel engine fueled with Fischer-Tropsch diesel and fossil diesel, although the researchers have introduced the ethanol through port-fuel injection (PFI) mode. They used a single-cylinder, 4-stroke, naturally aspirated direct injection diesel engine with 773 cm³, 15.5:1 of compression ratio, and 8.6 kW of rated power. The fuels tested were diesel/GTL and diesel/GTL + ethanol PFI (50 ml/h and 100ml/h) under fixed speed (1500 rpm), 2 and 4 bar IMEP, EGR (no EGR, 10%, 20%, and 30%). The researchers reported that the in-cylinder pressure that the GTL + ethanol PFI was lower than diesel for all EGR ratios at 4 bar IMEP. Also, the BSFC was lower for GTL and GTL + ethanol PFI for both 2 and 4 bar IMEP; however, the thermal efficiency was higher for GTL and for GTL + ethanol PFI (2 and 4IMEP). Regarding the exhaust emissions, the NOx was lower for GTL and also for GTL + ethanol PFI (at 4IMEP); however, the opposite occurred at 2 IMEP for all EGR ratios. Also, both CO and THC were lower for GTL and GTL + ethanol PFI (at 4IMEP), opposite at 2 IMEP GTL + ethanol ratio for all EGR ratios.

The following researches were conducted using the same engine, a 4-cylinder, four-stroke, turbocharged, intercooler diesel engine with 3.298 L, 17.5:1 of compression ratio, and 70 kW or rated power. Sun et al. (SUN, Dandan *et al.*, 2017) have evaluated Fischer-Tropsch diesel/methanol blends (5%, 10%, and 15% methanol v/v) on a fixed speed (2000 rpm) and five different loads. They reported CO, NOx, and soot were reduced as compared with diesel fuel; however, HC increased, and the in-cylinder pressure and HRR of the blends were lower than for diesel fuel. Moreover, Cao et al. (CAO *et al.*, 2016) used methanol/Fischer-Tropsch diesel/biodiesel blends (5, 10, and 15% methanol v/v; 10% biodiesel v/v) under five engine speeds (1200, 1600, 2000, 2400, and 2800 rpm) and a fixed load. They reported that in comparison with diesel fuel, methanol, the engine had lower output power although improved fuel consumption up to 11.3%. Also, the NO_x and soot emissions decreased when using the

blends in comparison with diesel fuel. The researchers concluded that blending methanol and biodiesel to F-T diesel improved the NO_x-soot trade-off emission. Also, considered different blends of methanol/biodiesel/Fischer Tropsch diesel with n-decanol as co-solvent (5%, 10%, and 15% methanol v/v; 10% biodiesel v/v; 0%, 4%, 7%, 10% n-decanol v/v) under a fixed engine speed (2000 rpm) and two loads (0.19 and 0.57 MPa BMEP) and reported that methanol addition to the blend prolonged the ignition delay, normal and post-combustion duration of combustion were shortened, increased peak heat release and peak in-cylinder pressure. Also, the peak value phase and peak value of pressure rise were delayed, whilst the combustion pressure oscillation amplitude increase, although the peak value phase of pressure oscillation was delayed.

Muinos et al. (MUINOS *et al.*, 2017) assessed the combustion and emissions characteristics of GTL/n-butanol (25% and 50% m/m n-butanol) and diesel/ n-butanol (25% and 50% m/m n-butanol) blends in a single-cylinder, 4-stroke, naturally-aspirated, direct injection diesel engine with 1.13 L, 16:1 of compression ratio, and 17 kW of rated power. The tests were conducted at a fixed speed (1500 rpm), 3 IMEP conditions (2.75, 4.75, and 6.75 bar IMEP), and up to 15% EGR ratio along with a supercharger to increase the intake pressure to 1.2 bar. The researchers reported that the combustion of GTL and n-butanol (50% m/m) resulted in the highest peak-pressures than neat GTL and GTL/n-butanol (75% m/m), however lower than diesel fuel for all loads. Also, the blends of GTL/n-butanol had lower ignition delay than diesel fuel at all loads, although they had a similar combustion duration to diesel fuel. The in-cylinder temperature of diesel was higher than GTL or GTL/n-butanol blends. NO_x and soot of GTL/n-butanol blends were lower than diesel. The GTL/n-butanol blends reduced soot by nearly 90% and produced 20% less NOx compared to diesel. Total unburned HC emissions were higher for GTL blends for all IMEP conditions. The CO emissions were lower for GTL/n-butanol (75% m/m/) than diesel for 2.75 and 4.75 IMEP. At last, the highest indicated thermal efficiencies were obtained for neat GTL, GTL/n-butanol (75% m/m), and the higher mechanical efficiency was obtained for GTL/n-butanol (50% m/m). The researchers concluded that GTL/n-butanol blends had an advantage over diesel/n-butanol blends in terms of emissions.

Jiao et al. (JIAO; LIU; ZHANG; YANG; *et al.*, 2019) have conducted a comparative analysis of combustion characteristics, performance, and emissions using an in-line 6-cylinder turbocharged, intercooler diesel engine with 17.5:1 of compression ratio and 258 kW of rated power. The engine was fueled with quaternary blends of methanol/Fischer-Tropsch diesel/biodiesel/diesel blend (15.2% methanol, 15.6% F-T diesel, 65% diesel, and 4.2%

biodiesel) at simulated altitudes (sea level, 3500 m, and 5500 m), three engine speeds (1000, 1400, and 2100 rpm) and full load. The researchers have reported lower values of in-cylinder pressure and heat release rate at lower altitudes although opposite result at higher altitudes, improved both engine power and specific fuel consumption and concerning emissions, the tested blends had lower PM although slightly increased NO_x at different altitudes.

Soloiu et al. (SOLOIU *et al.*, 2019) investigated diesel20/n-butanol80 (m/m) and GTL20/n-butanol 80 (m/m) as the high reactivity component in comparison to diesel40/n-butanol60 (m/m) for operation in RCCI mode, along with a constant 60% (m/m) PFI (port fuel injected) rate of n-butanol. The effects of the alternative fuels on combustion were investigated in RCCI mode compared to CDC (conventional diesel combustion). The engine was a single-cylinder, turbocharged medium-duty diesel engine, with 1.132 L, 16:1 of compression ratio, and 17 kW of rated power, which was tested under 3 IMEP conditions (4, 5, and 6 IMEP) and constant 1500 rpm. The researchers reported lower NO_x, soot, and CO, however with penalties in HC and aldehydes emissions for the blends GTL20Bu80, ULSD40Bu60, and ULSD20Bu80 blends in comparison with CDC. Also, the indicated thermal efficiency of GTL20Bu80 was higher than the other fuels; however, BSFC was higher for the blends in comparison with CDC mode.

Ye et al. (YE, Lihua *et al.*, 2020) studied the exhaust emissions and PM characteristics of n-pentanol (5%, 10%, 20% n-pentanol v/v) and F-T diesel blends in a single-cylinder, 4-stroke, air-cooled, direct injection diesel engine with 0.418 L of displacement, a compression ratio of 19:1, and 6.3 kW of rated power. The tests were conducted at different load ratios (10, 25, 50, 75%, full load) and two engine speeds (2700 rpm and 3600 rpm), and the results were compared with the engine fueled with diesel and F-T diesel as baseline fuels. The researchers reported that CO, HC, NO_x, and soot of F–T diesel blends decreased in comparison with diesel. The particle size of the blends was reduced; however, the degree of agglomeration was found to be higher than that for diesel. It was found that the arrangement between the soot particles was more compact, especially with the addition of n-pentanol to F-T diesel.

Table 6 summarizes the main results of different alcohols and Fischer-Tropsch diesel blends fueled on diesel engines. Overall, the researchers considered methanol, ethanol, butanol, and pentanol as alcohols, Fischer-Tropsch diesel synthesized from natural gas and coal, and also biodiesel. Based on the reviewed literature, it was possible to conclude that the addition of alcohols to F-T diesel promoted an increase in thermal efficiency, specific fuel consumption,

and HRR. Also, regarding the exhaust emissions, the CO, HC increased, whilst NO_x and PM decreased.

Table 6. Summary of studies with alcohols and Fischer-Tropsch diesel compared to reference fuel.

Authors	Year	Fuels	F-T diesel	Blends	Reference fuel	Engine parameters	Operating conditions	BTE	SFC	SEC	HRR	EGT	CO	CO₂	HC	NOₓ	PM
Rodríguez-Fernández et al. (RODRÍGUEZ-FERNÁNDEZ, J. et al., 2009)	2009	Ethanol (PFI)					1500 rp	↑	↑↓	n.a.	→	n.a.	↑↓	n.a.	↑↓	↑↓	n.a.
		Diesel	Natural gas	diesel/GTL	Diesel	1-cyl, 4-str, NA, DI, 773 cm³, 15.5:1, 8.6 kW	2, 4 bar IMEP, EGR (10%, 20%, 30%)										
		F-T diesel		diesel/GTL + ethanol	GTL		PFI (50 ml/h and 100ml/h)										
Cao et al. (CAO et al., 2016)	2016	F-T diesel		FT85B10M5			5 speeds (1200, 1600, 2000, 2400, 2800 rpm)	→	↑	n.a.	→	n.a.	n.a.	n.a.	n.a.	→	→
		Biodiesel	Coal	FT80B10M10		4-cyl, 4-str, DI, Turbo, IC, 3.298 L, 17.5:1, 70 kW											
		Methanol		FT75B10M15			Fixed load										
Sun et al. (SUN, Dandan et al., 2017)	2017	F-T diesel		FT95M5, FT90M10	Diesel	4-cyl, 4-str, DI, Turbo, IC, 3.298 L, 17.5:1, 70 kW	2000 rpm	n.a.	n.a.	n.a.	→	n.a.	→	n.a.	↑	→	→
		Methanol	Coal	FT85M15	F-T diesel		5 loads										
Yang et al. (YANG et al., 2017)	2017	F-T diesel		B10FT90,			2000 rpm	n.a.	n.a.	n.a.	↑	n.a.	n.a.	n.a.	n.a.	n.a.	n.a.
		Biodiesel	Coal	M5B10FT81Dec4	B10FT90	4-cyl, 4-str, DI, Turbo, IC, 3.298 L, 17.5:1, 70 kW	0.19, 0.57 MPa BMEP										
		Methanol		M10B10FT73Dec7													
		n-decanol		M15B10FT65Dec10													
Muinos et al. (MUINOS et al., 2017)	2017	Diesel		GTL75But25			1500 rpm	↑	n.a.	n.a.	↑	n.a.	↑/=	n.a.	↑	→	→
		F-T diesel	Natural gas	GTL50But50	Diesel	1-cyl, 4-str, NA, DI, 1.13 L, 16:1, 17 kW	2.75, 4.75, 6.75 bar IMEP										
		n-butanol		D75But25z	GTL		≤15% EGR										
				D50But50			1.2 bar										

Reference	Year	Fuel source	Blends	Engine specifications	Operating conditions							
Jiao et al. (JIAO; LIU; ZHANG; YANG; et al., 2019)	2019	Methanol; F-T diesel; Coal; Biodiesel (soybean); Diesel	M15.2FT15.6D65B4.2	in-line 6-cyl, Turbo, IC, 17.5:1, 258 kW	3 speeds (1000, 1400, 2100 rpm); Full load; Variable altitudes (sea level, 3500 m, 5500 m)	n.a.	↑/=	n.a.	n.a.	n.a.	↑	→
Soloiu et al. (SOLOIU et al., 2019)	2019	Diesel; Natural gas; F-T diesel; n-butanol	D20But80; D40But60; GTL20But80	1-cyl, Turbo, 1.132 L, 16:1, CRDI, 17 kW	1500 rpm; 3 IMEP (4, 5, 6 IMEP); 60% (m/m) n-butanol PFI; 20%, 30% EGR	↑	↑	n.a.	↑	↑	↑	↓
Ye et al. (YE, Lihua et al., 2020)	2020	Diesel; F-T diesel; Not specified; n-pentanol	FT95Pen5; FT90Pen10; FT80Pen20	1-cyl, 4-str AC, DI, 0.418 L, 19:1, 6.3 kW	2 speeds (2700, 3600 rpm); 3 loads (10%, 25%, 50%, 75%, full load)	n.a.	↑	n.a.	n.a.	↓	→	→

Nevertheless, it has been previously reported that blends of Fischer-Tropsch diesel with alcohol have miscibility limitations (JIAO; LIU; ZHANG; DONG; *et al.*, 2019), especially for the case of short-chain alcohol such as ethanol. Lapuerta et al. (LAPUERTA, Magín *et al.*, 2015) reported that blends of 5% ethanol/95% F T diesel are stable for temperatures between 15–38 °C, although increasing the ethanol ratio diminished the blend stability, and the 10% ethanol/90% F T diesel blend is only stable at high temperatures (>30 °C). Hence, biodiesel has the benefits of helping to produce a stable blend and enhancing the lower lubricity of F-T diesel.

As a result, very limited or no literature was found related to the utilization of ethanol blended with Fischer-Tropsch diesel in the CI engine. Hence, in order to overcome this matter, biodiesel may be introduced to form a stable blend and enhancing the lower lubricity property of Fischer-Tropsch diesel as well as maintain an alternative fuel characteristic to the final blend. Nonetheless, literature presents limited reports of ethanol/Fischer-Tropsch diesel/biodiesel.

May-Carle et al. (MAY-CARLE *et al.*, 2012) assessed this ternary blend using a jet-stirred reactor and not on an engine. Also, they considered a mixture of 68% n-decane and 32% iso-octane (in moles) to represent the F-T diesel fuel. Despite that, the focus of their work was on the numerical and experimental research of the kinetics of oxidation and concluded that further validation on an actual engine would be required.

Pidol et al. (PIDOL *et al.*, 2008) studied the potential of ethanol/biodiesel/diesel blend in CDC and Homogeneous Charge Compression Ignition (HCCI) modes. The researchers tested a Euro IV, 4-cylinders direct injection diesel engine with 1.6 L, 18:1 of compression ratio, 66 kW of rated power and equipped with a common rail injection system under three distinct operating conditions (1500 rpm and 3 bar IMEP; 2500 rpm and 6 bar IMEP; 400 rpm and full load). The focus was on comparing the standard engine calibration with optimization settings (injection timings, EGR ratio, and rail pressure). Also, a single-cylinder, four-stroke, direct injection diesel engine with 416 cm³, 15:1 of compression ratio, and equipped with a common rail injection system, running under both early injection HCCI and Diesel combustion modes. In addition to a blend of diesel/biodiesel/ethanol (ethanol 20% vol.) it was also tested a synthetic like Fischer-Tropsch fuel/biodiesel/ethanol blend (ethanol 20% vol.) and compared with two conventional diesel fuels (50 ppm and 10 ppm sulfur levels). Also, 1000 ppm Butylated hydroxytoluene was added to the biodiesel. As a result, they reported that on the multi-cylinder engine, it was achieved low levels of PM and NO_x emissions, with a penalty in fuel consumption and an acceptable engine noise level. However, these results were achievable when the diesel-

ethanol blends were used in combination with an optimized combustion control. Furthermore, regarding the single-cylinder engine, they reported that compared to diesel fuel, the blends enable to increase the range of HCCI mode whilst increased the power output in CDC mode.

Pidol et al. (PIDOL; LECOINTE; JEULAND, 2009) performed a complementary work with a focus on the improvement of the formulation of ethanol blends to avoid flashpoint drawbacks. They used the same multi-cylinder engine as in (PIDOL *et al.*, 2008) and the same blend of Fischer-Tropsch fuel/biodiesel/ethanol blend (ethanol 20% vol.), however adding iso-pentane to the blend. The engine tests were also conducted under the same operational mode as in (PIDOL *et al.*, 2008). As a result, they reported that the blend without the flashpoint improver resulted in unstable and incomplete combustion, leading to higher CO, HC emissions, and fuel consumption. Also, the blend with flash point improver and optimized engine calibration led to low levels of PM and NO_x emissions, however, with a penalty in fuel consumption.

Magand et al. (MAGAND *et al.*, 2011) evaluated the engine compatibility and optimization of the same engine in (PIDOL *et al.*, 2008; PIDOL; LECOINTE; JEULAND, 2009), however using other calibration methods (design of experiments and new maps of calibration). The engine was run with different injection schemes (main injection alone, one pilot and main injections, two pilot and one main injection), under three operational conditions (2000 rpm and 4 bar BMEP; 1500 rpm and 3 bar BMEP; 2750 rpm and 8 bar BMEP), and EGR. Also, they used the same blend as but added iso-hexane in replacement to iso-pentane, such as in (PIDOL; LECOINTE; JEULAND, 2009). As a result, the researchers reported a decrease in NO_x and PM, with a slight decrease in CO2 emissions. However, the HC and CO emissions have increased. In addition, they have tested a Citroën C4 without any hardware modification and with a similar engine on a chassis dynamometer under the New European Driving Cycle (NEDC) based on the Euro 4 standards to validate the optimized engine calibration and to perform tunings in the cold correction maps and reported that this blend could potentially achieve the compliances of the Euro 5 standards with the Euro 4 diesel vehicle.

Later, Pidol et al. (PIDOL *et al.*, 2012) had considered ethanol/biodiesel/Fischer–Tropsch diesel blend and a blend of those with the addition of iso-pentane on the aforementioned two engines. The researchers have reported that on the multi-cylinder engine, both CO and NO_x decreased, although HC increased for the blend. Regarding the single-cylinder engine, all emissions increased for the tested blend.

2.3   Energy and exergy analysis studies on alcohols and diesel type fuels

Many works in the literature have evaluated the thermodynamic analysis of alternative fuels in CI engines. Usually, the basis of those analyses is the First Law of Thermodynamics. Among the most fuels that area considered, different alcohols and biodiesel have been considered. Generally, the outcome is related to the concentration of the components in the fuel blend.

Santos et al. (SANTOS, Tito B. *et al.*, 2017) tested different concentrations of diesel/biodiesel blends under variable loads on a six-cylinder, four-stroke, naturally aspirated, direct injection diesel engine with 5.658 L, 17:1 of compression ratio, and 95.61 kW of rated power. The researchers reported a reduction in PM due to the increase in the biodiesel content in the blends. Also, the CO and NO_x increased in comparison to commercial diesel fuel in Brazil (5% biodiesel and 95% diesel). Moreover, no significant variation in energy efficiency was revealed by increasing the percentage of biodiesel in the blend.

Emiroğlu and Şen (EMIROĞLU; ŞEN, 2018b) evaluated diesel/biodiesel/alcohol fuel blends on a single-cylinder diesel engine. They reported increases in NO_x and HC emissions, decrease in smoke, and carbon monoxide (CO) were obtained compared to diesel fuel combustion. They also reported that the thermal (or energy) efficiencies of the engine were very similar when using bio-diesel/alcohols or when using diesel fuel.

Valencia Ochoa et al. (VALENCIA OCHOA; ACEVEDO PEÑALOZA; DUARTE FORERO, 2020) investigated two types of biodiesel blended with diesel fuel on a single-cylinder diesel engine. The researchers reported that the blends had lower CO, HC, smoke, and CO_2, but the NOx emissions increased compared to diesel fuel engine operation. Additionally, the results showed that diesel fuel had the highest energy efficiency among the tested fuels.

Venu et al. (VENU *et al.*, 2021) evaluated a ternary blend of diesel/biodiesel/ethanol with and without alumina (Al_2O_3) nanoparticles on a single-cylinder diesel engine. It was reported that the ternary blend decreased the CO, HC, smoke, and PM, although the NO_x increased and the engine thermal efficiency was lower for the blend than for diesel fuel.

Typically, the analysis of the First Law is the most frequently employed method, but as argued in Yesilyurt and Arslan (YESILYURT; ARSLAN, 2019) solely, this approach is not sufficient to establish the losses and the efficiency of a system. Exergy analysis is a method that combines both the First and the Second Laws of Thermodynamics to determine the losses (or

irreversibilities) of a system (DA SILVA *et al.*, 2018). It helps in assessing the source of these losses and allows more detailed information regarding the efficiency of the engine. Besides, as discussed by Sun and Liu (SUN, Wenxu; LIU, 2020), it is an important tool to provide the exergy destruction analysis of a system.

Table 7 shows a brief summary of the results of both energy and exergy analysis of previously conducted investigations. It becomes clear that the exergy efficiency is of great interest to the scientific community, as it directly identifies the existing exergy destructions during the engine operation process. It is well established by the literature that increasing the engine load leads to an increase in energy and exergy efficiencies (DOGAN *et al.*, 2020; KARAGOZ *et al.*, 2021), whilst increasing the engine speed causes the opposite effect (SARIKOÇ; ÖRS; ÜNALAN, 2020; SAYIN KUL; KAHRAMAN, 2016). Therefore, a detailed analysis of the effects of a specific fuel or blend on the energetic and exergetic efficiencies could be performed by comparing the efficiencies and the losses of the engine.

Table 7. Summary of the energy and exergy results using alcohols and diesel-type fuels.

Authors	Year	Fuels	Engine parameters	Operating conditions	Energy efficiency (%)	Exergy efficiency (%)	Outcomes
Kul and Kahraman (SAYIN KUL; KAHRAMAN, 2016)	2016	Diesel D75-92/B10-20/E5	1-cylinder 4 stroke Antor 3LD510	12 speeds (1000-3000 rpm) Full load	27.18-31.42 @ 1400 rpm 24.13-27.62 @ 2800 rpm	25.37-29.34 @ 1400 rpm 22.53-25.82 @ 2800 rpm	↑ speed ↓ efficiency $\eta_{diesel} > \eta_{blends}$ $\psi_{diesel} > \psi_{blends}$
Khoobbakht et al. (KHOOBBAKHT; AKRAM; *et al.*, 2016)	2016	Diesel D50-78/B0-40/E0-16	4-cylinders 4 stroke OM 314 Euro II	5 speeds 5 loads	n/a	25.21-32.88 @ 40% load 31.68-24.20 @ 80% load	↑ speed ↓ efficiency ↑ load ↑ efficiency
Paul et al. (PAUL; PANUA; DEBROY, 2017)	2017	Diesel D30-45/B50/E5-20	1-cylinder 4 stroke Kirloskar TV-1	1500 rpm 6 loads (20-120%)	23.49-27.05 @ 80% load 25.33-32.19 @ 100% load	20.91-24.49 @ 80% load 23.29-29.32 @ 100% load	↑ load ↑ efficiency $\eta_{D35/E15/B50} > \eta_{diesel}$ $\psi_{D35/E15/B50} > \psi_{diesel}$
Krishna et al. (KRISHNA *et al.*, 2019)	2019	Diesel D41-78/B17-49/E5-10	4-cylinders 4 stroke Yangdong Y85	1600 rpm Full load	25.82-27.08	n/a	$\eta_{diesel} > \eta_{blends}$
Kavitha et al. (KAVITHA; JAYAPRABAKAR; PRABHU, 2019)	2019	Diesel D90-98/B1.5-7.5/E0.5-2.5	1-cylinder 4 stroke Kirloskar TAF1	1500 rpm 5 loads	19.25-21.24 @ 40% load 22.73-32.77 @ full load	21.45-28.21 @ full load	↑ load ↑ efficiency $\eta_{D90/B7.5/E2.5} > \eta_{diesel}$ $\psi_{D90/B7.5/E2.5} > \psi_{diesel}$
Nabi et al. (NABI; HUSTAD; AREFIN, 2020)	2020	GTL GTL25-75/B25-75	6-cylinders 4 stroke Scania DC 1102	1450 rpm 5 loads (3-92%)	14.65-15.05 @ 3% load 43.93-45.27 @ 92% load	13.70-14.08 @ 3% load 41.12-41.65 @ 92% load	↑ load ↑ efficiency $\eta_{GTL25/B75} > \eta_{GTL}$ $\psi_{GTL25/B75} > \psi_{GTL}$
Ferreira et al. (FERREIRA *et al.*, 2020)	2020	Diesel D82/B10/E8	1-cylinder 4 stroke NSB-8.18	1900 rpm 2 loads	21.9-22.0 @ 5.71 kW 22.6-22.9 @ 7.43 kW	n.a.	↑ load ↑ efficiency $\eta_{diesel} > \eta_{D82/B10/E8}$
Sarikoç et al. (SARIKOÇ; ÖRS; ÜNALAN, 2020)	2020	Diesel D60-75/B20/But5-20	1-cylinder 4 stroke	2 speeds Full load	30.17-31.92 @ 1400 rpm 26.91-27.83 @ 2800 rpm	28.13-29.77 @ 1400 rpm 25.03-25.96 @ 2800 rpm	↑ speed ↓ efficiency $\eta_{diesel} > \eta_{blends}$ $\psi_{diesel} > \psi_{blends}$

n.a.: not available, D: diesel fuel, B: biodiesel fuel, E: ethanol fuel, GTL: GTL fuel, But: butanol fuel, FTD: Fischer-Tropsch diesel fuel

2.4   Summary

The previously mentioned literature has shown the advantages of utilizing biofuels in diesel engines. Among the reports, the major tested biofuels are biodiesel and ethanol. However, it can be found in the literature that some researchers have considered using fumigation or port-fuel injection, which requires proper engine modifications. Regarding the utilization of alcohols, especially ethanol, the application of these biofuels in diesel engines has been largely shown to have the potential to reduce carbonaceous and PM emissions. Despite that, some reports have shown opposite results, depending on the operational conditions of the engine, percentage of water in the ethanol fuel, the fraction of alcohol added to the diesel fuel, among other factors.

Also, as it has been seen in the literature, the Fischer-Tropsch diesel fuels have been assessed in CI engines, and evidence shows that this synthetic fuel can be used as a surrogate fuel to diesel (partially or totally) without engine modifications. Also, it has been pointed that F-T diesel emissions, overall, resulted in lower levels of NO_x and PM in comparison with diesel fuel. However, it has been previously discussed that there are factors that constrain a more extensive application of F-T diesel fuels in diesel engines, especially the fuel's final cost. Hence, blending F-T diesel with others fuels has been shown a practical option.

Therefore, as shown in the literature, only a limited number of works investigated the blends of ethanol and F-T diesel. This could be explained by the temperature limit that is required to allow proper phase stability for this fuel's mixture. However, the reported studies focus on engine performance and exhaust emissions, primarily associated with a series of calibrations and optimizations, but not on particulate matter (PM) characteristics, nor the interactions with the aftertreatment systems. Thus, the utilization of another biofuel, such as biodiesel, could effectively increase the miscibility range. The blend of ethanol, biodiesel, and F-T diesel could be considered as a potential substitute in a short and medium scenario, to be used in both conventional or hybrid diesel engines.

Thus, according to the above literature review, it can be concluded that despite there are studies that have considered using blends of F-T diesel and ethanol, the following knowledge gaps still exist.

- There is still a lack of investigation regarding the combustion and performance, as well as exhaust emissions, especially heavy- and light- hydrocarbons and unregulated emissions using F-T diesel, ethanol, and biodiesel blends;

- There is a lack of investigation regarding the characterization of PM for F-T diesel, ethanol, and biodiesel blends, including the particulate number, size distribution, and total mass concentration;

- There is a lack of investigation regarding evaluating the effects of F-T diesel, ethanol, and biodiesel on the aftertreatment system performance;

- There is a lack of investigation on the use of F-T diesel, ethanol, and biodiesel blends as fuel;

Therefore, this investigation is addressed to the above topics, with a significant contribution to the use of biofuels and their derivatives in diesel engines, in order to promote the mitigation of harmful effects on the environment, as well as to contribute to the advancement of engine analyzes. Particularly within an energy transition pathway that the world is facing.

3 FUNDAMENTALS

This chapter covers the main fundamentals which are related to the main topic addressed by this thesis. A brief overview of the emissions standards and engine-out emissions, aftertreatment control system, biofuels and fuels specification, as well as the main data processing equations, are covered at the end of this chapter. The respective aspects and processes of biofuels are detailed.

3.1 Emissions standards

The primary emissions standards were introduced during the 1970s, and since then, are constantly being revised throughout the world, aiming to promote cleaner engines and to reduce potentially harmful emissions for combustion engines. Although each government has particular standards, the significant legislations are moving to stricter engine output emissions. Newer and more stringent emissions regulations have imposed diesel engine developments for new technologies to control exhaust emissions.

Emission standards for light- and heavy-duty diesel vehicles have been initiated in the 1990s, based on the USA and the EU emission regulations. As an example, the European Union emissions standards regulate most vehicle types, and since Euro I was approved in 1992, a progression of the stringency of emission regulations is depicted in Figure 5, with a difference for both passenger cars and heavy-duty diesel engines for NOx and PM.
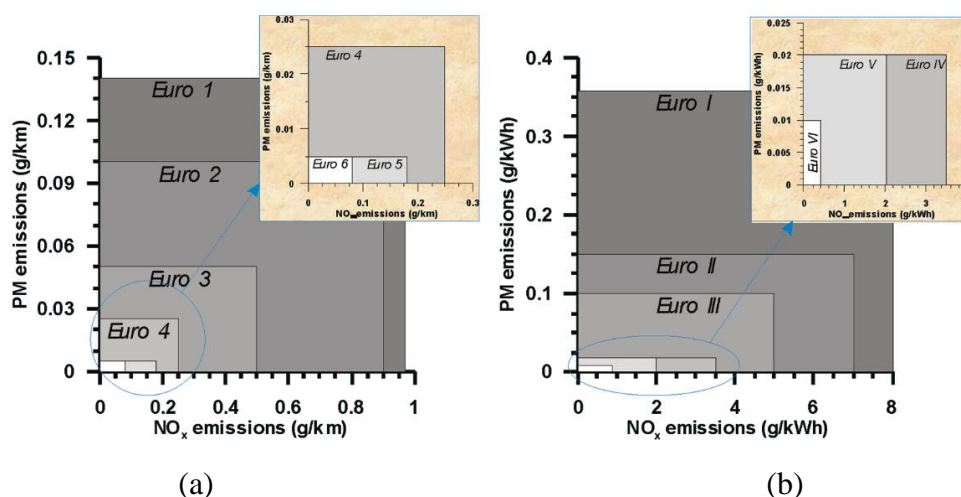
Figure 5. European Union (EU) emissions standards for (a) passenger cars and (b) heavy-duty diesel engines (RODRÍGUEZ-FERNÁNDEZ, J. *et al.*, 2010).

It must be commented that the standards units of light commercial vehicles (g/km) and heavy-duty engines (g/kWh) are not directly comparable. As it is shown below, the legislation has become more stringent from Euro I to Euro VI, and currently, there are discussions that the following Euro VII emissions standards will be even stricter (PUŠKÁR; KOPAS, 2018).

3.2 Diesel engine emissions

The combustion processes of a diesel engine operation produce substances such as CO_2, H_2O, and H_2. However, other products are resulted from the combustion due to different engine conditions such as non-stoichiometric fuel-air ratios and heterogeneous mixtures. The engine-out emissions are directly dependent on the engine operating conditions during the combustion, expansion, and exhaust processes. Additionally, other parameters (e.g., the fuel quality and the air-fuel ratio) also contribute to diesel emissions formation. Among the exhaust emissions from diesel engines, carbon monoxide (CO), total hydrocarbons (THC), nitrogen oxides (NO_x), and particulate matter (PM) are included (HEYWOOD, 2018). Some of the CI engine emissions result from incomplete combustion.

3.2.1 Carbon monoxide (CO)

Carbon monoxide (CO) emissions are an odorless, colorless, and noncorrosive gas that may be poisonous to humans. CO emissions are the result of the low oxidation of hydrocarbon-based fuels and are most prominent in the fuel-rich combustion regions. The formation of CO may be increased due to the lack of oxidants (e.g., O_2 contained in the air), temperature, and residence time during the combustion process. Further, CO formation is formed from the combustion of a hydrocarbon radical, R, is as shown in Equation (1).

$$RH \rightarrow R \rightarrow RO_2 \rightarrow RCHO \rightarrow RCO \rightarrow CO \tag{1}$$
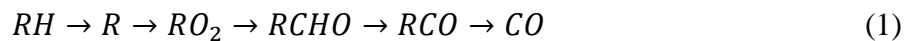
Usually, the formation of CO emissions is either low or negligible during lean combustion due to abundant amounts of air. Hence, CO is oxidized to CO_2 by the reaction mechanism shown in Equation (2).

$$CO + O_2 \rightarrow CO2 + O \tag{2}$$

The CO that is emitted from the diesel engine-out exhaust may be oxidized with the utilization of a diesel oxidation catalyst (DOC) due to the low temperature of the diesel exhaust

gas. CO emissions are generally associated with human health problems and environmental pollution. Payus et al. (PAYUS; VASU THEVAN; SENTIAN, 2019) recently mentioned that when a person is exposed to CO, the health effects might vary from acute to chronic health problems such as asthma, sensory irritation, and dysfunctional nervous system. Moreover, regarding environmental aspects, CO can affect stratospheric ozone directly (GARDNER; MANLEY; PEARSON, 1993).

3.2.2 Hydrocarbons (HC)

Hydrocarbon's species are formed from the incomplete combustion of hydrocarbon fuel, which leads to unburned and partially decomposed fuel molecules. The case of fuels that contain high proportions of aromatics and olefins produce relatively higher concentrations of reactive hydrocarbons (HEYWOOD, 2018) Furthermore, the engine's lubricating oil on the cylinder walls may also contribute to HCs formation, although this issue usually does not affect engines in good condition.

Alkidas (ALKIDAS, 1999) has listed other HC sources, which are combustion-chamber crevices and deposits, single-wall flame quenching, and exhaust valve leakage. However, the author has reported that the combustion chamber crevices are the most influential factor for HC source, contributing with 38% to 50% (ALKIDAS, 1999). This is due to the small space available in the combustion chamber, which causes flame quenching. The largest crevices are the volumes between the piston, piston rings, and cylinder walls (HEYWOOD, 2018).

Overall, the diesel engine featured lean-burn combustion has a tendency to produce low levels of hydrocarbons. Nevertheless, some adverse environmental effects are associated with HC emission, whereas the major is that they are precursors of photochemical smog and ozone level when reacted with the NO_x (MAJEWSKI; KHAIR, 2006).

3.2.3 Nitrogen oxides (NO_x)

Nitrogen oxides emitted from the combustion process mainly consist of nitric oxide (NO) and nitrogen dioxide (NO_2) (WEBB; HUNTER, 1998). NO constitutes 85-95 % of NO_x and is a colorless and odorless gas, whilst NO_2 is a reddish-brown gas with a pungent odor (REŞITOĞLU; ALTINIŞIK; KESKIN, 2015).

Factors that contribute to the formation of NO_x in diesel engines include high in-cylinder combustion temperatures and pressures, flame conditions, residence time, and concentration of species. NO formation generally consists of three primary reaction mechanics: a reaction of

atmospheric nitrogen (N_2) and oxygen at high temperature, a reaction of N_2 contained in the fuel molecule and a reaction of nitrogen with radical from the fuel. The first is considered as the primary source of NO formation, which might be further detailed by the extended Zeldovich mechanism, as shown in Equations (3)-(5), as described in the literature (HEYWOOD, 2018).

$$O + N_2 \leftrightarrow NO + N \tag{3}$$

$$N + O_2 \leftrightarrow NO + O \tag{4}$$

$$N + OH \leftrightarrow NO + H \tag{5}$$

Even though NO emissions are the main component of nitrogen oxides in diesel combustion, NO_2 can be formed by the reaction of NO and hydroperoxyl radicals (HO_2) at low temperature, as shown in the formation reaction in Equation (6).

$$NO + HO_2 \rightarrow NO_2 + OH \tag{6}$$

However, after the formation of NO2, it can be converted back (i.e., destruction) to NO at high temperature by the following destruction reactions shown in Equations (7) and (8).

$$NO_2 + O \rightarrow NO + O_2 \tag{7}$$

$$NO_2 + H \rightarrow NO + OH \tag{8}$$

Bowman (BOWMAN, 1975) has described that the formation of NO_2 takes place at lower peak combustion temperature, whilst the destruction of NO_2 occurs at high combustion temperature. The reaction of NO with excess oxygen in the engine-out exhaust using a diesel oxidation catalyst may promote the formation of NO_2.

3.2.4 Particulate matter (PM)

Particulate matter (PM) emissions from diesel engines are a result of incomplete hydrocarbon fuel combustion because part of the fuel droplets not burn and are vaporized inside of the cylinder. The PM, or suspended particulate matter, can be defined as fine solid particles (particulates) or liquid droplets suspended in a gas. The PM can be either naturally available in the atmosphere or can be resulted from an artificial process (OKUBO; KUWAHARA, 2020).

In particular, this definition may comprise the soluble organic fraction (SOF), soot particles, dust or inorganic material, trace metals from engine wear, and sulfate particles.

The particle size distribution in the engine-out exhaust gas may be divided into three main groups, as shown in Figure 6. The 'nuclei mode' particles are typically formed out of volatile precursors, as exhaust gas is diluted and then and cools down, having a diameter range from 5 nm to 50 nm. The 'accumulation mode' particles typically consist of carbonaceous agglomerates and adsorbed material, and their diameter ranges from 30 nm to 500 nm. The last is the 'coarse mode' particles, which consist of accumulation mode particles that have been deposited on the cylinder and exhaust system surfaces, with particles usually larger than 1 µm (KITTELSON, 1998).
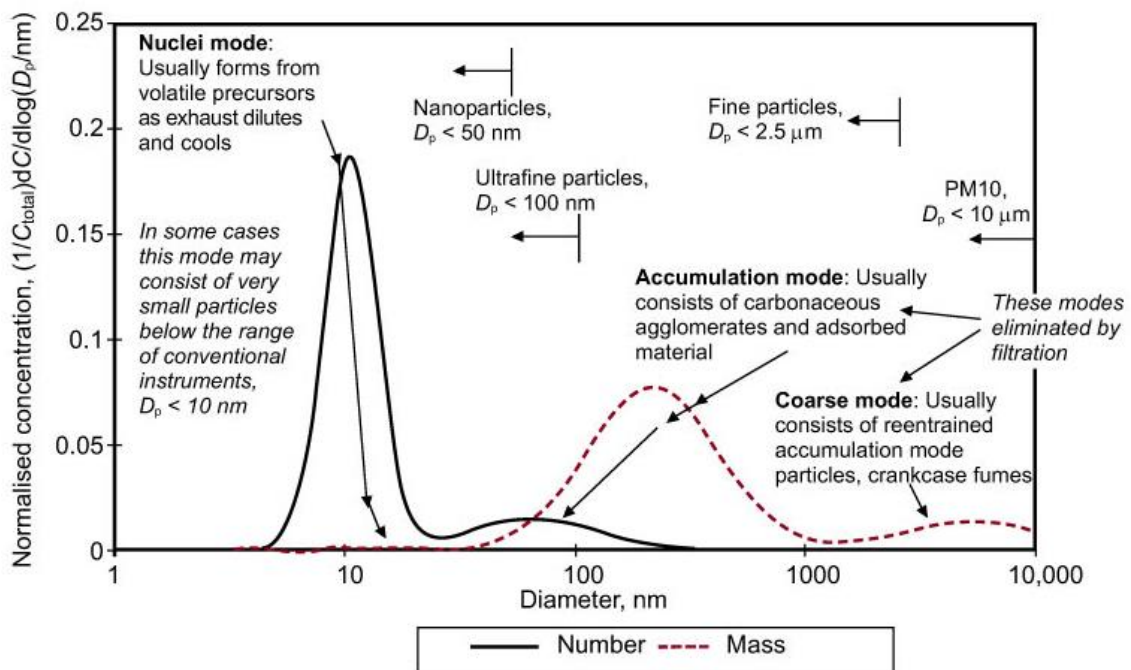
Figure 6. Typical engine-out exhaust particle size distribution for the diesel engine used in this work (TWIGG; PHILLIPS, 2009).

Further, in Figure 6 are the definitions of atmospheric particle size distributions that range from PM_{10} particles (particles smaller than 10 µm) to nanoparticles (defined as the diameter of the particles, $D_p \leq 50$ nm). Overall, over 90 % of all PM is classified as fine particles ($D_p > 100$ nm), which are in the respirable size range, which is commonly referred to as $PM_{2.5}$ (i.e., particles less than 2.5 µm in aerodynamic diameter). The upper respiratory tract is affected by PM_{10}, while lung alveoli are affected by ultrafine particles (50 nm $< D_p \leq 100$ nm) (EL MORABET, 2018).

3.3   Exhaust gas emission control (aftertreatment system)

As emission legislation has become even more stringent in the last three decades, aftertreatment system technologies are rapidly advancing with a focus on retaining the engine-out exhaust gases and PM emissions from diesel engines. In order to meet these regulations, improvements in fuel properties and the incorporation of aftertreatment systems are required. Modern engine aftertreatment systems consist of different components, such as Diesel Oxidation Catalyst (DOC), Diesel Particulate Filter (DPF), Selective Catalytic Reduction (SCR), and Exhaust Gas Recirculation (EGR). In this section, the aspects of DOC technology utilized in diesel engines will be explained.

3.3.1   Diesel oxidation catalyst (DOC)

In order to restrain the exhaust gases from a CI engine, a diesel oxidation catalyst (DOC) is utilized. The diesel oxidation catalyst (DOC) has been designed with a primary function of oxidizing CO, HC, and the organic fraction of PM to CO_2 and water. The main oxidation reactions inside are listed in Equations (9) to (10).

$$CO + \frac{1}{2}O_2 \rightarrow CO_2 \tag{9}$$

$$C_nH_mO_z + \left(\frac{2n + \frac{m}{2} - z}{2}\right)O_2 \rightarrow nCO_2 + \frac{m}{2}H_2O \tag{10}$$
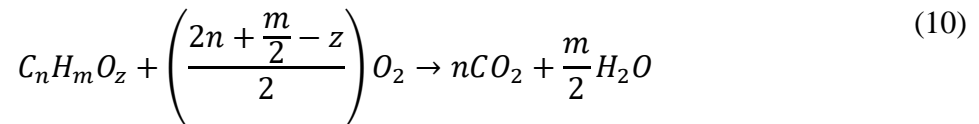
Furthermore, the DOC promotes the oxidation reaction of NO to NO_2, as shown in Equation (11). NO_2 is usually preferred to aid the soot removal in the passive regeneration of the diesel particulate filter (DPF) or to enhance the performance of some selective catalytic reduction (SCR) catalysts (AL-HARBI *et al.*, 2012; RUSSELL; EPLING, 2011).

$$NO + \frac{1}{2}O_2 \rightarrow NO_2 \tag{11}$$

The exhaust gas species may be oxidized in the DOC catalytic active sites on its channel walls. Figure 7 depicts the exhaust gas species upstream and downstream of the DOC. As the DOC reactions are highly exothermic, slight increases in NO_x are not abnormal. On the other hand, it is observed a reduction in PM in the diesel engine-out exhaust because of the oxidative atmosphere that aids in some soot oxidation. In diesel exhaust applications, total PM reductions

over a DOC (i.e., number and mass reduction) depend on the engine operating conditions, as this influences the exhaust gas temperature and composition, the exhaust gas residence time within the catalyst, the oxygen availability, the as well as the size and structure of inherent PM or organic compounds (LEFORT; HERREROS; TSOLAKIS, 2014).
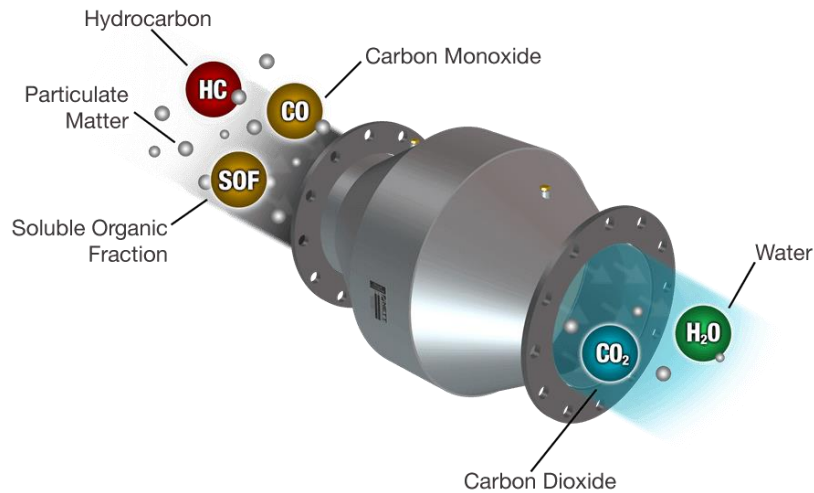
Figure 7. Representation of a typical diesel oxidation catalyst (NETT TECHNOLOGIES, 2019).

The oxidation rate of a DOC catalyst is directly governed by the diesel engine-out exhaust temperatures. When the exhaust temperature is low (< 200 °C), some of the exhaust gas are reduced but passes through the catalysts without oxidation. At higher temperatures (250 - 300°C), the catalyst may achieve maximum value of conversion efficiency; hence the CO and HC conversion occurs.

The light-off may be defined as the range of temperatures in which the reaction process starts to occur, and the species conversion rate increases exponentially with the temperature. The parameter generally used to describe this process is known as DOC light-off temperature. It may be defined as the catalyst's inlet temperature that 50% of conversion is achieved (SUTJIONO *et al.*, 2013).

3.4 Alternative fuels

Among the alternative fuels, the biofuels may be defined as renewable transportation fuels produced from biomass (ROBERTS; PATTERSON, 2014). The biomass may be converted into liquid, gaseous, or even solid biofuels; however, this review focus on the first category. Biofuels are considered as an alternative and cleaner fuel for applying in internal combustion engines, and that contributes to the reduction of fossil fuel dependence. In 2016, biofuels used in the transportation sector accounted for 4% of the world's road transport fuel

71

(INTERNATIONAL ENERGY AGENCY (IEA), 2017). In the scenario of road transportation, two major types of biofuels are notable: diesel substitutes (biodiesel) and gasoline substitutes (ethanol).

Further, biofuels have a significant role as a result of their physical and chemical properties and significant potential to reduce CO_2 emission based on the life-cycle greenhouse gas, which significantly contributes to the global climate changes (IMRAN *et al.*, 2013; MOFIJUR *et al.*, 2016). The world transport emissions growth rate was approximately 1.9% per year since the year 2000. However, in 2019, it increased at a rate lower than 0.5%, as a result of efficiency improvements, propagation of electrics and hybrids, and increased use of biofuels (INTERNATIONAL ENERGY AGENCY (IEA), 2020c). It has been reported that the transport sector represented approximately 24.5% of CO_2 emissions from fuel combustion, whereas road transport vehicles accounted for nearly 74% of this share (INTERNATIONAL ENERGY AGENCY (IEA), 2019).

Many countries have diversified the research, development and production of alternative fuels to fossil diesel, such as the case of the USA, Brazil, the European Union and Indonesia. Table 8 depicts the world biofuels production scenario since 2009. In 2019, 12 countries shared nearly 89% of the global amount of biofuels produced. The USA leaded the global biofuels production with a share of 37.8% in 2019, whilst the European Union represented 15.8% of the global share in the same year. Also, the BRICS (Brazil, Russia, China, India, and South Africa) represented around 56%, despite that Russia and South Africa have no significant contribution to the biofuels production yet. Moreover, the global production of biofuels is forecasted to grow 3% per year until 2025, increasing nearly 21% from 2019 to 2025 (INTERNATIONAL ENERGY AGENCY (IEA), 2020b; OECD/FAO, 2019).

Regarding the Brazilian biofuels scenario, the country is the second largest producer of biofuels in the world, whereas the country represented 24.1% of the total amount of biofuels produced in 2019 in the world. Additionally, since the 1970s, Brazil has already adopted biofuels addition on gasoline and in early 2000s on diesel fuels (AGÊNCIA NACIONAL DO PETRÓLEO GÁS NATURAL E BIOCOMBUSTÍVEIS (ANP), 2016; GOLDEMBERG; MACEDO, 1994). Currently, in Brazil, the National Agency of Petroleum, Natural Gas and Biofuels (ANP) resolutions n° 40/2013 and n° 621/2019 regulate the values of the ethanol addition to regular gasoline type C (27.0 ± 1.0% v/v) and biodiesel addition to diesel fuel (13.0 ± 0.5% v/v), respectively.

Table 8. Share of the world biofuels production (2008 - 2019) (BP, 2020)

Region	2008	2009	2010	2011	2012	2013	2014	2015	2016	2017	2018	2019	Growth rate per annum 2019	Growth rate per annum 2008-18
USA	42.3%	43.4%	44.5%	46.8%	43.9%	42.1%	41.0%	42.0%	43.1%	42.7%	40.1%	37.8%	-2.8%	6.2%
Brazil	31.3%	27.9%	26.7%	21.6%	21.8%	23.2%	22.4%	24.0%	21.8%	21.0%	23.1%	24.1%	7.5%	3.6%
Indonesia	0.9%	0.3%	0.3%	2.2%	2.6%	3.0%	3.9%	1.6%	3.5%	3.1%	5.1%	6.7%	35.2%	27.1%
Germany	5.1%	4.6%	5.0%	4.6%	4.3%	4.2%	4.3%	4.0%	3.8%	3.8%	3.6%	3.5%	0.0%	3.1%
France	4.2%	4.3%	3.6%	3.4%	3.9%	3.5%	3.4%	3.5%	3.1%	3.2%	3.2%	2.8%	-12.1%	4.1%
China	3.0%	3.0%	2.5%	3.0%	3.1%	3.2%	3.3%	2.8%	2.6%	3.0%	2.6%	2.7%	6.4%	5.3%
Argentina	1.2%	1.9%	2.7%	3.4%	3.4%	2.8%	3.3%	2.5%	3.4%	3.6%	2.9%	2.5%	-9.8%	16.1%
Thailand	1.1%	1.2%	1.4%	1.4%	1.9%	2.2%	2.3%	2.4%	2.0%	2.3%	2.2%	2.3%	7.5%	15.0%
Netherlands	0.2%	0.5%	0.6%	1.0%	1.9%	2.0%	2.3%	2.4%	1.9%	2.3%	2.0%	1.9%	-2.8%	37.8%
Canada	1.1%	1.4%	1.4%	1.5%	1.6%	1.4%	1.4%	1.5%	1.5%	1.5%	1.4%	1.6%	16.0%	9.4%
Spain	0.8%	1.7%	1.6%	1.3%	0.9%	1.0%	1.3%	1.4%	1.4%	1.8%	1.9%	1.6%	-11.8%	16.8%
India	0.3%	0.2%	0.3%	0.4%	0.4%	0.4%	0.3%	0.7%	0.8%	0.7%	1.1%	1.3%	26.3%	20.7%
Other countries	8.5%	9.8%	9.4%	9.5%	10.4%	11.1%	11.0%	11.4%	11.2%	11.2%	10.7%	11.2%	-	-
of which:														
OECD	59.5%	63.0%	63.8%	64.9%	63.3%	61.3%	60.3%	61.5%	61.6%	62.3%	58.9%	55.8%	-2.4%	6.7%
Non-OECD	40.5%	36.9%	36.2%	35.1%	36.7%	38.7%	39.7%	38.5%	38.4%	37.7%	41.2%	44.2%	10.6%	7.0%
European Union	15.7%	17.5%	17.2%	15.9%	17.0%	17.0%	17.3%	17.3%	16.3%	17.5%	16.7%	15.8%	-2.7%	7.5%
BRICS	34.7%	34.4%	37.8%	33.7%	34.5%	39.9%	42.2%	44.7%	42.3%	43.4%	51.7%	55.9%	8.1%	4.1%

The available feedstocks for biofuel production can be grouped into four types, as shown in Figure 8. The first-generation biofuel is mainly obtained from edible feedstocks, based on food crops such as sugars-based (sugarcane, sugar beet, and others), starch-based (corn, wheat, rice, and others), and vegetable oil (soybean, sunflower, palm, rapeseed, and others) (AZAD *et al.*, 2015; ÇELEBI; AYDIN, 2019). Currently, the majority of biofuels production is from first-generation technology (RULLI *et al.*, 2016) and the conventional processes for its production are fermentation and transesterification Figure 9). Still, first-generation biofuel production has been extensively discussed for being a plant-based production, which has a direct impact on land and the environment and thus influences land use, water usage, livestock feed, human food, and export markets (FILIP *et al.*, 2019).
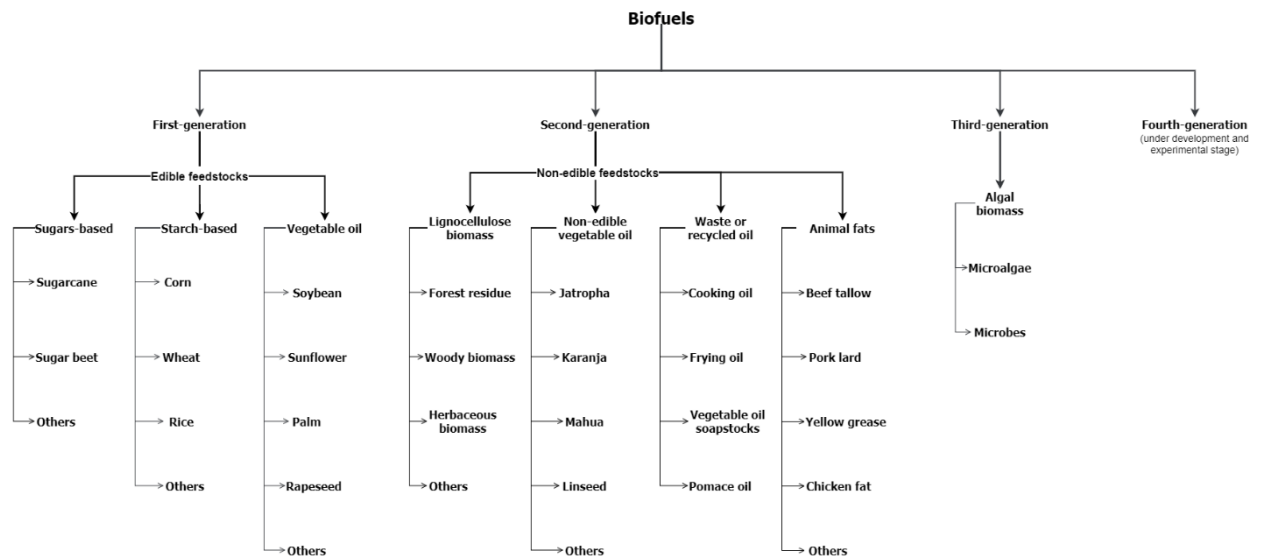
Figure 8. Technological generations and available feedstocks for biofuels production.
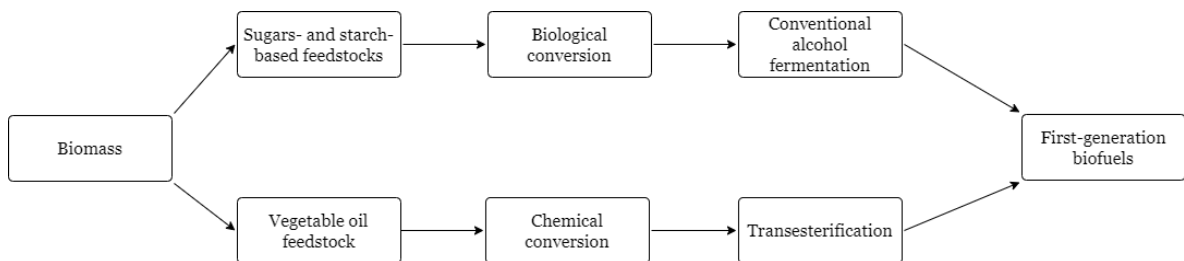
Figure 9. Synthesis of the conventional production of first-generation biofuels.

The second-generation biofuel production employs non-edible feedstock sourced from lignocellulose biomass (forest residue, woody biomass, herbaceous biomass, and others), non-edible vegetable oil (Jatropha, Karanja, Mahua, linseed, cottonseed, and others), waste or

recycled oil (cooking oil, frying oil, vegetable oil soapstocks, and pomace oil) and animal fats (beef tallow, pork lard, yellow grease, chicken fat, and others) (ADITIYA *et al.*, 2016; BHUIYA *et al.*, 2014). However, second-generation biofuel still has concerns with harvesting, collecting, and delivering cellulosic feedstocks to be overcome in order to establish an effective and affordable solution (AYODELE; ALSAFFAR; MUSTAPA, 2020; RASUL *et al.*, 2017).

The third-generation biofuel production is based on algal biomass (i.e., microalgae, microbes) feedstock. The production uses seawater, freshwater, or wastewater for the cultivation and either hydrolysis, fermentation, or distillation as conversion technologies for biofuels production. However, the third-generation production of biofuels has a high growth rate, it has a high production cost, which limits the investments (JAMBO *et al.*, 2016).

As for the fourth-generation biofuel production, it is currently under development and experimental stages. This future generation of biofuels production combines a diversity of potential applications on all levels (feedstock, technological, and processing) (ZIOLKOWSKA, 2020). Fourth-generation includes photobiological solar fuels and electrofuels (RASTOGI; SHRIVASTAVA, 2017). Other definitions for the fourth-generation biofuel are available in the literature (AZAD *et al.*, 2015).

Table 9. Annual world ethanol production (2015 - 2019)

Region	2015	2016	2017	2018	2019	Main feedstocks
USA	57%	59%	60%	56%	54%	Corn
Brazil	28%	26%	25%	28%	30%	Sugarcane
European Union	5%	5%	5%	5%	5%	Corn, wheat, sugar beet
China	3%	3%	3%	4%	3%	Corn
Canada	2%	2%	2%	2%	2%	Corn
India	1%	1%	1%	1%	2%	Sugarcane
Thailand	1%	1%	1%	1%	1%	Sugarcane, cassava
Argentina	1%	1%	1%	1%	1%	Corn, sugarcane
Others	2%	2%	2%	2%	2%	

* Data obtained from (OECD/FAO, 2019; RENEWABLE FUELS ASSOCIATION (RFA), 2020).

3.4.1 Ethanol

Ethanol is also known as ethylic alcohol or ethanol, which has the same molecular formula (C_2H_5OH) regardless of whether it is produced from starch-based, sugar-based, or cellulosic feedstocks. Ethanol is a volatile, flammable, colorless liquid with a slight characteristic odor. Ethanol may be produced from the fermentation of different types of feedstocks that contain mainly fermentable sugars or carbohydrates. The world's major ethanol producers in 2019 were the USA and Brazil, with respectively 54% and 30% of the total share of production (Table 9). These two countries stand for a total of 84% of the world's total production of ethanol, whereas the major feedstocks are corn, in the USA and sugarcane, in Brazil.

3.4.1.1 Ethanol application as a fuel

Ethanol may be used as an alternative fuel in IC engines in pure form or in blends with conventional fuels. The use of ethanol as an alternative fuel in IC engines is not new and dates from the pre-Industrial Revolution period. Figure 10 illustrates a brief history of ethanol as a fuel in IC engines. Ethanol was primarily utilized in an internal combustion engine by Samuel Morey (1762 - 1843) in 1826, and Nikolaus Otto (1832 - 1891) in 1876 was powered with ethanol, among other biofuels (MUSSATTO *et al.*, 2010). In 1896 Henry Ford (1863 - 1947) produced the first car fueled with pure ethanol, and later in 1908, the Ford Model-T car was manufactured in series, fueled with either gasoline or ethanol (SOLOMON; BARNES; HALVORSEN, 2007).

Brazil has pioneering tested using ethanol in cars in 1925 (BALAT; BALAT, 2009). Later in the 1930s, although the number of vehicles in the country was limited, the Brazilian government has introduced 5% ethanol blended with gasoline (RAELE *et al.*, 2014). In a global scenario, after World War II, the interest in ethanol has been overshadowed by gasoline due to the lower price as well as it was simpler to produce. Ethanol mainly remained ignored until the 1970s oil crisis, in 1973 and 1973 (BALAT; BALAT, 2009). Additionally, in 1975, the Brazilian government introduced the National Alcohol Program ("*Pro-Álcool*" in Portuguese) as an incentive for large-scale ethanol production in substitute for gasoline (AUGUSTO HORTA NOGUEIRA; SILVA CAPAZ, 2013). Later, in 1979, Fiat 147 was the first production car fueled entirely on ethanol, E100 (100% ethanol) launched in Brazil (KYRIAKIDES *et al.*, 2013).

During the 1980s, Scania has developed the first commercial diesel buses fueled with ethanol additives (ODZIEMKOWSKA; MATUSZEWSKA; CZARNOCKA, 2016). Since 2003, Brazil has introduced flex-fuel engines, which may be fueled with pure gasoline, pure ethanol, or blends of those(GOMEZ; LEGEY, 2015). Later, in 2007, Brazil has put into operation the first diesel bus fleet blended with 5% ethanol (JANSSEN *et al.*, 2010). Currently, in Brazil, there is a mandatory policy that targets that up to $27 \pm 1\%$ v/v ethanol must be blended with regular gasoline type C (ANP resolution n° 40/2013), although most of the gasoline that is sold uses 27% (by volume) since ethanol is less expensive than gasoline.
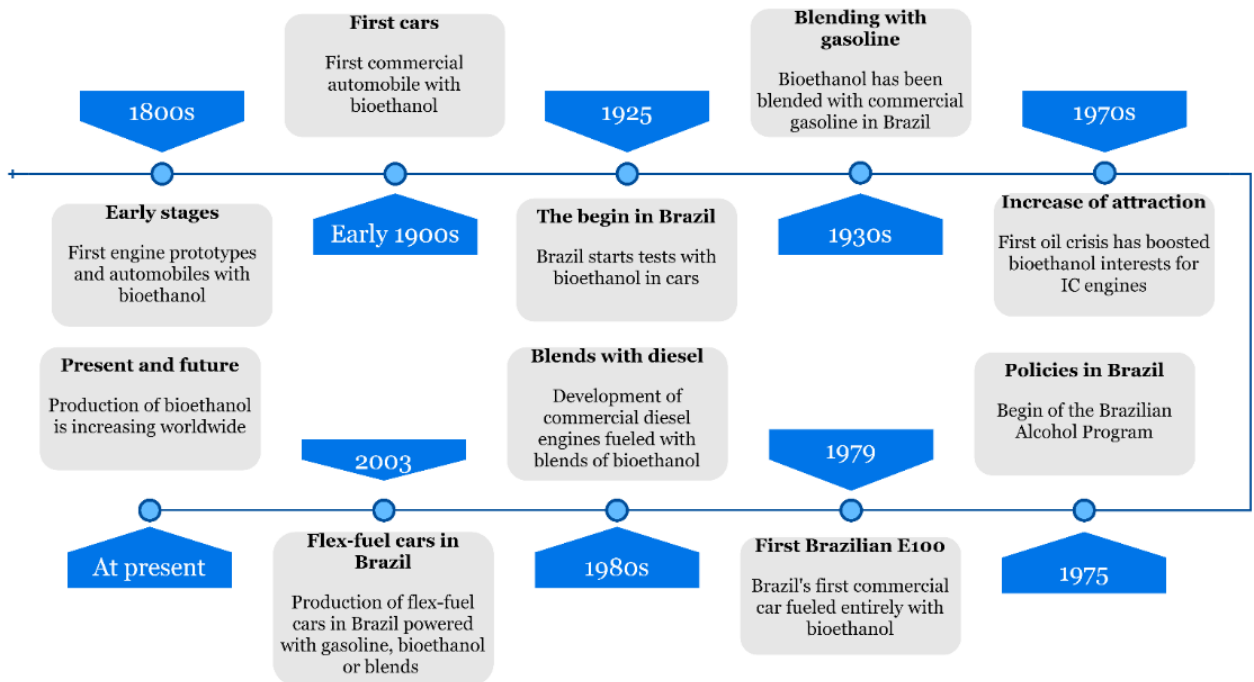
Figure 10. Brief of historical utilization of ethanol in internal combustion engines.

There are several reports in the literature related to ethanol utilization in spark ignition (SI) engines as either blended with gasoline (AWAD *et al.*, 2018; CHANSAURIA; MANDLOI, 2018; THAKUR *et al.*, 2017) or as pure fuel in flex-fuel engines (MALAQUIAS *et al.*, 2020; POLICARPO *et al.*, 2018; ROSO *et al.*, 2019). However, the focus of this review is on ethanol application in CI engines.

3.4.2   Fischer-Tropsch diesel

Fischer-Tropsch diesel is a synthetic fuel manufactured via Fischer-Tropsch conversion of syngas yielding liquid straight-chain paraffins, and alternatively, after further processing, branched paraffins and cyclic hydrocarbon mixtures (MAY-CARLE *et al.*, 2012). The final liquid fuel may be obtained from renewable sources, which can be preferably obtained from biomass,

thus the final liquid fuel being known as biomass-to-liquid (BtL). Moreover, natural gas (GtL) and coal (CtL) are also possible raw materials for Fischer-Tropsch diesel synthesis. Fischer-Tropsch diesel is often referred to in the literature as ultra-clean fuels because they have virtually no sulfur emissions compounds and aromatic hydrocarbons (GILL *et al.*, 2011a; ROSLI *et al.*, 2021). However, Fischer-Tropsch diesel has a lower density, lower boiling or distillation temperatures, and lower kinematic viscosity when compared to conventional fuels obtained from crude oil, such as diesel (GÓMEZ; SORIANO; ARMAS, 2016).

3.4.2.1 A brief history of Fischer-Tropsch synthesis

During the early 20th century, oil was fundamental to the European industrialized countries, and especially in the post-World War I (WWI). Based on recent reports, Germany has virtually no oil or natural gas reserves (INTERNATIONAL ENERGY AGENCY (IEA), 2020a), although, in 1913, the country was the first country to synthesize oil with Friedrich Karl Rudolf Bergius (1884-1949), through the hydrogenation of high-volatile bituminous coal at high temperature and pressure. Eventually, in 1931, Friedrich Bergius (1884 - 1949) and Carl Bosch (1874 - 1940) were awarded the Nobel Prize in Chemistry for the invention and development of the high-pressure chemical method. Later, in the early-1920s, Franz Fischer (1877 - 1947) and Hans Tropsch (1889 - 1935) developed the "Fischer–Tropsch process" at the Kaiser Wilhelm Institute for Coal Research in Mülheim an der Ruhr, a pioneering method that promotes the transformation of carbon monoxide and hydrogen into liquid hydrocarbons using series of chemical reactions. The researchers published several publications (FISCHER, 1925; FISCHER; TROPSCH, 1926a, b, 1927, 1926c) and fielded some patents (e.g., U.S. patent US1746464A applied in 1926, publication in 1930). These breakthroughs allowed that some German companies such as IG Farben and Ruhrchemie to develop a technologically successful synthetic fuel industry that grew from a single commercial-size coal liquefaction plant in 1927 to twelve coal liquefaction and nine Fischer-Tropsch commercial-size plants by the time World War II ended in 1945 (STRANGES, 2007).

Other nations, such as Britain, also had started synthetic fuel programs in 1920 on Fischer-Tropsch synthesis and in 1923 on coal liquefaction. Both countries, Germany and Britain, had led the synthetic fuels programs. Further, France, Canada, Japan, and Italy also had similar programs in either demonstration-, pilot- or operational plants using bitumen or coal. During World War II years, Germany and Japan started to produce synthetic oil fuel by utilizing coal resources from occupied nations. The USA started researching synthetic fuels in 1927 and

coal liquefaction in 1936 (STRANGES, 2007). Later, in 1955, the first Fischer-Tropsch plant was built in South Africa.

3.4.2.2 Fischer–Tropsch fuels project development

Several companies have taken part in research and development programs to develop their own technology with different technological solutions. A limited number have already invested in building large-scale GTL or CTL plants.

Figure 11 shows some commercially established Fischer-Tropsch plants around the world. Shell opened the first commercial GTL plant in 1993, in Malaysia, and later in 2011, in Qatar, the second and world's largest GTL plant (SHELL, 2021). Sasol, the former South African Synthetic Oil Limited, has two operational GTL plants outside of the country (Qatar and Nigeria) (SASOL, 2021). Sasol also had two planned plants (the USA and Canada) to use shale gas; however, both projects were canceled in 2017. A joint venture between Uzbekneftegaz, Petronas, and Sasol is under final steps of construction in Uzbekistan, and Since 1992, PetroSA, another South African company, has one operational plant in South Africa, the world's first GTL refinery (PETROSA, 2021). Recently, in 2019, a gas-to-liquid plant has started operation in Turkmenistan by Türkmengaz, and the company has another plant under development (TÜRKMENGAZ, 2021).

Although some large projects are under construction, other large-scale GTL projects have been abandoned. On the other hand, small-scale projects may also be used as an alternative to flaring natural gas or also to capture emissions from landfills (U.S. ENERGY INFORMATION ADMINISTRATION (EIA), 2017). Several small-scale facilities, pilot, and demonstration plants were announced and built during the last decade, including in the USA. Companies such as G2X, CompactGTL, Siluria, Primus Green Emergy, INFRA Technology, Juniper GTL, and ENVIA Energy have invested in gas-to-liquid smaller scale projects during the 2010s (GAS PROCESSING & LNG, 2017)owever, some projects were canceled, whereas some plants had their operations suspended, such as the case of ENVIA Energy, in 2018. Nevertheless, the Canadian company named Rocky Mountain GTL has an under-construction plant in Canada, expected to produce 470 bpd of synthetic fuels (ROCKY MOUNTAIN GTL, 2021).

Figure 11. Major commercial-scale gas-to-liquid plants in operation around the world in 2017 (GAS PROCESSING & LNG, 2017).

There are also several Fischer-Tropsch plants using coal-to-liquid technology around the world. Sasol has two plants that are under operation, since the 1970s, in South Africa. Also, there are many Chinese plants under operation in different regions and from different developers. Coal-to-liquids projects have become very important for energy security in China, and the country represented more than 13% of the world's proved coal reserves, being the fourth major reserve (after the USA, Russia, and Australia, respectively) and the more prominent coal producer, with more than 47% of the global production (BP, 2020). However, the CTL projects usually face the pressure of carbon reduction, especially after the Paris Agreement. Thus, China's CTL projects encounter both opportunities and challenges, mainly due to water constraints (GUO; XU, 2018).

Regarding biomass-to-liquid, in which biomass is pretreated and converted to synthesis gas via gasification and then Fischer-Tropsch synthesis into naphtha, gasoline, kerosene, or diesel, the first BTL process was developed in 1996 by CHOREN Industries, in Germany, with a plant of 350 bpd of rated capacity (AIL; DASAPPA, 2016). Velocys had success with two BTL demonstration plants in the USA, commissioned in 2018, and in Japan, commissioned in 2020 (VELOCYS, 2021b). Also, Velocys has two ongoing commercial plants projects, a BTL plant of 1,600 bpd (barrels per day) of rated capacity in the USA, and a WTL (waste-to-liquid) of 1,300 bpd of rated capacity, in the UK (VELOCYS, 2021a). Moreover, the Bioliq pilot plant at the Karlsruhe Institute of Technology (KIT) is running successfully along the complete process chain, since 2005, as a demonstration plant in cooperation with several participating

institutes (KARLSRUHE INSTITUTE OF TECHNOLOGY, 2020). The Total Group and five other partners are targeting the BioTfuel BTL demonstration project to be launched in 2021 in France (TOTAL GROUP, 2021a). Also, the company has another project that started operations in 2019 that produces HVO biodiesel, biojet, Avgas, and AdBlue, being the first biorefinery in France (TOTAL GROUP, 2021b). However, some BTL projects have been discontinued, as in the case of NSE Biofuels, a joint venture between Stora Enso and Neste Oil operated a demonstration plant from 2009 to 2012 in Finland (ETIP BIOENERGY, 2021).

There is some literature regarding the price and economic aspects of Fischer-Tropsch diesel synthetic fuel (WOOD; NWAOHA; TOWLER, 2012). Overall, it has been pointed that the competitiveness of crude oil is the central aspect to be analyzed, as well as the operational costs of the F-T plants (SAMAVATI *et al.*, 2018). Smaller-scale plants are sometimes referred to as options to larger production units. They provide a lower risk to producers. Also, the associated construction costs are lower. Moreover, the plants can be modular and may be expanded, as required, to increase production, which reduced the starting investment costs.

3.4.2.3 Fischer–Tropsch synthesis in Brazil

In Brazil, the Petrobras operated two pilot plants, as shown in Table 10. The company invested in GTL technology as an alternative for gas flaring during offshore extraction. Petrobras owned a GTL demonstration plant in the city of Aracaju, being known as the world's first fully-integrated small-scale GTL facility (Figure 12). The pilot plant had a rated production of 20 bpd, and the project was a US$45 million contract between Petrobras and CompactGTL.
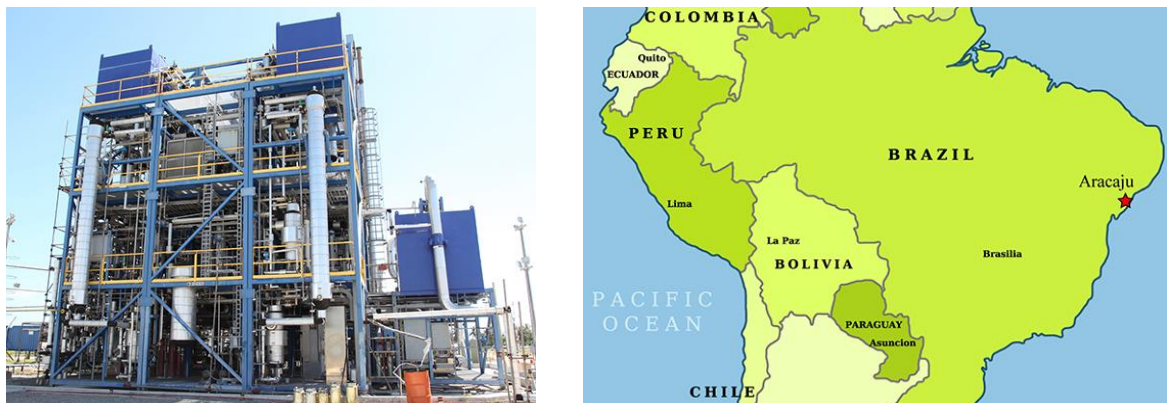
Figure 12. The pilot micro-reactor GTL plant of Petrobras (left) and the location of the plant in Aracaju, Brazil (right) (COMPACTGTL, 2021).

The pilot plant was successfully commissioned at the former Petrobras' Experimentation Nucleus (NUEx), located in the Aracaju plant, and the synthetic crude product has been effectively blended with crude oil and delivered to the company's refinery for processing (COMPACTGTL, 2021). Additionally, according to Ramos et al. (RAMOS *et al.*, 2011), the Petrobras also had another project to develop a second plant in collaboration with Velocys, Toyo Engineering, and Modec. The GTL pilot plant had a 6 bpd of rated capacity and an estimated cost of US\$ 10 million.

Table 10. Fischer-Tropsch synthesis pilot plants in Brazil by Petrobras.

Location	Technology	Period	Rated capacity (bpd)
Gas Processing Unit TECARMO (Aracaju/SE)	CompactGTL	2010-2012	20
Oil Refinery LUBNOR (Fortaleza/CE)	Velocys	2010-2013	6

Although both pilot plants demonstrated that the feasibility of the technology, both projects were shut down, the project demanded more investments, and at the same period, the Petrobras was starting an FPSO (Floating production storage and offloading) unit to perform gas reinjection (PETROBRAS, 2017).

The potential of Brazil to produce Fischer-Tropsch synthetic fuels also includes biomass as raw material. Some works have evaluated the technical and economic aspects of producing synthetic diesel fuel in the country (BRESSANIN *et al.*, 2020; NEVES *et al.*, 2020). Furtado Júnior et al. (FURTADO JÚNIOR *et al.*, 2020) performed a technical, economic, and environmental analysis of different biorefinery configurations, considering the integration of different biomass technologies with sugar and ethanol plants in Brazil. The researchers have considered syngas for electricity generation and also for synthetic diesel fuel production through the Fischer-Tropsch synthesis process. They reported that regarding global efficiency, it is interesting to give priority to Fischer-Tropsch fuel production. Also, the researchers found that from an energy point of view, the thermochemical route (gasification) had better performance than the biochemical route (fermentation). However, they concluded that from an economic point of view, the thermochemical processes demand high investments that make the projects economically unfeasible.

Tagomori et al. (TAGOMORI; ROCHEDO; SZKLO, 2019) conducted a technical and economic analysis to identify the potential of synthetic diesel production through BTL synthesis

in Brazil. In their work, the researchers considered using eucalyptus and pine residues from 21 production areas that were identified, mainly in the South, Midwest, and Southeast regions of the country, which would enable a total of 27 BTL facilities around Brazil. Despite that the results have shown that both biomasses would result in similar synthetic diesel production yields, the availability of eucalyptus residues is more significant than for pine, as shown in Figure 13.
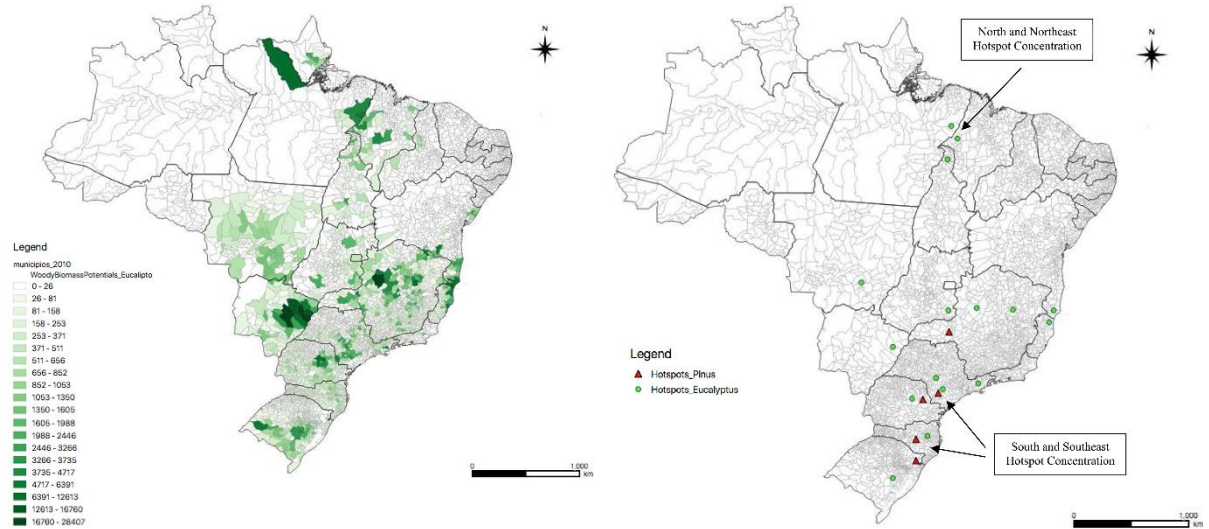
Figure 13. Potential of the eucalyptus feedstock from forestry residues (left) and the distribution of the BTL facilities (right) (TAGOMORI; ROCHEDO; SZKLO, 2019).

Tagomori et al. also reported that the capital cost of the BTL plant was estimated to be around US$ 650 million. Regarding the BTL diesel price, the results indicated that the synthetic diesel would not be competitive when compared to conventional fossil-derived diesel oil unless the oil price range was over 146 US$/barrel or with adequate climate and energy policies to stimulate the deployment of this technological route. Despite that the synthetic diesel derived from the BTL process was not cost-competitive without ambitious climate and energetic policies, the researchers concluded that the diesel from forestry residue could mitigate the reduction of diesel importation in Brazil.

Hence, biomass-to-liquid synthesis also seems to be a very interesting alternative for Brazil. The Fischer-Tropsch synthesis plants may take advantage of the integration with the currently installed sugarcane refineries or forestry residues production, although it is clear that based on the literature, new policies to mitigate the associated risks that are related to the application of this alternative fuel technology are required. In addition, the GTL technology in

Brazil may demand more testing and investments. However, it might be considered for avoiding the flaring of natural gas resources during the exploitation.

3.4.2.4 Production of Fischer-Tropsch diesel

The process of production of Fischer-Tropsch diesel involves a three-step procedure (ALLEMAN; MCCORMICK, 2003), schematically presented in Figure 14.

a. *Synthesis gas (syngas) generation*

Synthesis gas may be produced from any carbonaceous raw material such as biomass, natural gas, or coal. Solid raw materials (i.e., biomass or coal) are gasified with the presence of steam and oxygen (O_2), producing syngas that typically contains carbon monoxide (CO) and hydrogen (H_2). Moreover, in the case of natural gas, the syngas is reformed with air or pure oxygen. Different reforming processes are possible during the production of synthetic gas from natural gas, comprising steam reforming, auto thermal reforming, or partial oxidation (ALLEMAN; MCCORMICK, 2003; GILL *et al.*, 2011a). However, the differences between these processes are not the focus of this section.

b. *Fischer-Tropsch synthesis*

Based on the selection of a catalyst and the reaction conditions, this step promotes the phase change process from syngas to HC liquid fuels. These definitions determine the length or weight of the final HC chain which is produced. Thus, two processes may be defined: the high-temperature Fischer-Tropsch (HTFT) and the low-temperature Fischer-Tropsch (LTFT). While HTFT operating temperature is between a range of 310 - 340 °C and is composed of aromatics and olefins, the LTFT range is between 210 - 260 °C and composed of paraffin. Hence, HTFT is more suitable for gasoline fuel whilst LTFT is used to produce synthetic diesel fuel (DRY, 2002; LECKEL, 2009)

c. *Post-processing*

Involves hydrocracking, hydrotreating, or distillation of the synthesized fuels to meet standard specifications (e.g., lubricity and cetane number).
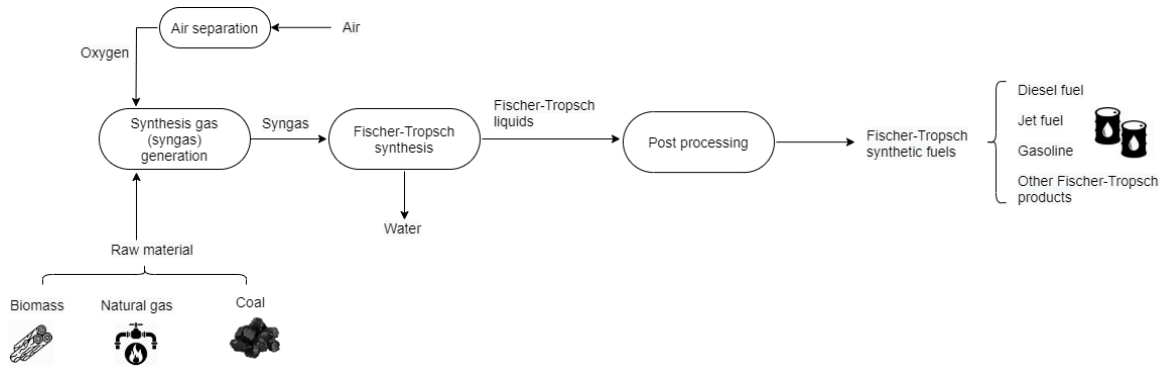
Figure 14. Simplified diagram of Fischer-Tropsch diesel fuel production. Based on (FOREST; MUZZELL, 2005; GLOBAL SYNGAS TECHNOLOGIES COUNCIL (GSTC), 2020)

The basic equation of the Bergius process involves the requirement of the gaseous stage during the conversion, as shown in Equation (12) (HÖÖK; ALEKLETT, 2010). Within the chemical reactions involved during Fischer-Tropsch diesel production, some are presented below for the syngas formation, as shown in Equation (13) and products: Paraffin's, Equation (14), and Olefins, Equation (15) (GILL *et al.*, 2011a).

- Bergius process

$$nC + (n + 1)H_2 \rightarrow C_nH_{2n+2} \tag{12}$$

- Synthesis gas (syngas) generation

$$CH_n + O_2 \rightarrow \frac{1}{2}nH_2 + CO \tag{13}$$

- Fischer-Tropsch synthesis process

$$nCO + (2n + 1)H_2 \rightarrow C_nH_{2n+2} + nH_2O \tag{14}$$

$$nCO + 2nH_2 \rightarrow C_nH_{2n} + nH_2O \tag{15}$$
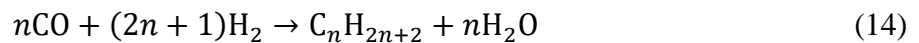
3.5   Fuel specification requirements

The generally applicable standards *Resolução* ANP n° 50/2013 and the EN 590 are in accordance to the National Agency of Petroleum, Natural Gas and Biofuels (*Agência Nacional do Petróleo, Gás Natural e Biocombustíveis* – ANP, in Portuguese) and the European Committee for Standardization (*Comité Européen de Normalisation* CEN, in French). These

statutes describe the physical and chemical properties that the road transportation diesel fuel must meet to be commercialized in Brazil and in the European Union (EU), respectively.

A brief summary of the requirements is listed in Table 11. The EN 590 was instituted along with the European emission standards, in 1993, whilst the *Resolução* ANP nº 50/2013 is a revision of the diesel fuel specification to meet the guidelines of the Air Pollution Control Program for Motor Vehicles (*Programa de Controle da Poluição do Ar por Veículos Automotores* - PROCONVE, in Portuguese), which are in accordance to the National Council for the Environment (*Conselho Nacional do Meio Ambiente* - CONAMA, in Portuguese). In Brazil, among the target objectives established by the *Resolução* CONAMA 18/1986, which instituted the PROCONVE, were to reduce the pollutants emission from vehicles, promote national technological development, establish inspection programs for vehicles, and to promote the improvement of the technical characteristics of liquid fuels.

Overall, the revisions of these two standards were adapted to the sulfur content in the diesel fuel and its cetane number. Since Euro 5 emissions standard, in 2009, the upper limit of the sulfur content in diesel is 10 mg/kg (or ppm) for EN 590, and also the Brazilian government agency, ANP, regulated the same maximum content of sulfur (10 ppm) by the *Resolução* ANP nº 40/2008. As for the cetane number, the lower limit in the *Resolução* ANP nº 50/2013 is 48, whilst in the EN 590, it is 51.

Table 11. Diesel fuel specification for EN 590(EU) and Resolução ANP n°50/2013 (Brazil)

Property	Unit	EN 590		Resolução ANP n°50/2013	
		lower limit	upper limit	lower limit	upper limit
Cetane number		51	-	48	-
Density at 15°C	kg/m³	820	845		
Density at 20°C				815	850
Polycyclic aromatic hydrocarbons	%(m/m)	-	11	-	11
Sulfur content	mg/kg	-	10[a]	-	10[b]
Flashpoint	°C	55	-	38	-
Carbon residue (on 10% distillation residue)	%m/m	-	0.30	-	0.25
Ash content	% (m/m)	-	0.01	0.01	-
Water content	mg/kg	-	200	-	200
Total contamination	mg/kg	-	24	-	24
Copper strip corrosion (3 hours at 50 °C)	rating	Class 1	Class 1	1	25
Oxidation Stability	g/m³	-	25	-	25
Lubricity corrected wear scar diameter at 60 °C	μm	-	460	-	460
Viscosity at 40 °C	mm²/s	2.0	4.5	2.0	4.5
Distillation (vol. % recovered)					
10% point	°C		report	180	report
50% point	°C		report	245	295
85% point	°C	-	350	-	360
95% point	°C	-	370	-	370
Fatty acid methyl ester content	% (V/V)	-	7	13	-
Cold Filter Plugging Point (winter)	°C	-	-15	variate for each region[c]	
Cold Filter Plugging Point (summer)	°C	-	-5	variate for each region[c]	

[a] since Euro 5, in 2009; [b] since Resolução ANP n° 40/2008, in 2008; [c] the upper limit is different for some Brazilian regions (South, Southeast, Center-West), however, it is not defined for the Northeast and North regions

3.6 Data processing

This section presents the equations used to calculate the different combustion and performance parameters.

Indicated mean effective pressure (IMEP) is calculated only from the cylinder pressure to represent the average output pressure over a cycle of the engine, being determined using the following equation (16)

$$IMEP = \frac{indicated\ work\ per\ cycle}{displaced\ volume} = \frac{W_i}{V_d} = \frac{\oint pdV}{V_d} \tag{16}$$

in which p and V represent the in-cylinder pressure and corresponding cylinder volume, respectively. V_d (m³) represents the displaced volume, which is used to measure the volume swept by the pistons inside the cylinders and can be calculated by equation (17) as follows

$$V_d(m^3) = A \times L \times n \tag{17}$$

in which A (m²) is the piston area, L (m) is the stroke length, and n is the number of cylinders.

Indicated specific fuel consumption (ISFC) is the mass fuel flow rate per unit power output and can be calculated using the following equation (18)

$$ISFC\ (g/kWh) = \frac{\dot{m}_{fuel}}{P_i} \tag{18}$$

in which $\dot{m}_{fuel}$ (kg/s) is the mass flow rate and P_i (kW) is the indicated power. The indicated power, P_i (kW), is based on IMEP and expressed by the equation (19) below

$$P_i\ (kW) = \frac{IMEP \times V_d \times N}{n_R \times 60 \times 1000} \tag{19}$$

in which N (rpm) is the engine speed and n_R is the number of crank revolutions for each power stroke per cylinder (e.g., n_R is 2 for a four-stroke engine).

Indicated specific energy consumption (ISEC) indicates the amount of total fuel energy that is consumed to produce one unit of output power in one hour (YILMAZ, I. T.; GUMUS, 2018) and it can be defined by the following equation (20).

$$ISEC \ (kJ/kWh) = \frac{\dot{m}_{fuel} \times LHV_{fuel}}{P_i} \qquad (20)$$

Indicated thermal efficiency (ITE) measures how much heat energy released from the fuel is converted into mechanical work and, being determined using the following equation (21).

$$ITE = \frac{P_i}{\left(\dot{m}_{fuel} \times LHV_{fuel}\right)} \qquad (21)$$

The measured pressure in the combustion chamber was processed for the heat release rate by combining the first law of thermodynamics, the perfect gas equation of state, and the ideal gas assumption. The model used to calculate heat release rate in this research is expressed by the following equation (22) (HEYWOOD, 2018)

$$\frac{dQ}{d\theta} = \frac{\gamma}{\gamma - 1} p \frac{dV}{d\theta} + \frac{1}{\gamma + 1} V \frac{dp}{d\theta} \qquad (22)$$

in which γ is the ratio of specific heats (Cp/Cv), p is the instantaneous in-cylinder pressure, and V is the instantaneous engine cylinder volume at crank angle θ. The values of γ are calculated by interpolation based on the actual p-V diagrams.

4 EXPERIMENTAL SETUP AND METHODOLOGY

The present chapter describes the experimental setup and procedures, as well as the facilities (instrumentation and equipment) that have been used within this work. It covers information about the diesel engine specifications, instruments, emissions analyzers, and also fuel properties. The measurement and analysis of combustion and performance parameters, the exhaust emissions, and the methodologies for the analysis of the PM characterization are also explained. Also, the details of the test bench and the respective instruments, test parameters, diesel catalyst, thermodynamic analysis are explained.

4.1 Experimental setup

The investigation was carried in a modern single-cylinder diesel engine, four-stroke, water-cooled, and equipped with a high-pressure common-rail fuel injection system. The engine used in this research is a single-cylinder research engine that was designed by the research group of the Future Engines and Fuels Laboratory at the University of Birmingham (UK) and incorporates one of the cylinder heads of a V6 Jaguar Land Rover engine (Figure 15). Table 12 presents the main specifications of the engine. The engine test rig consists of an electric dynamometer coupled into a load cell to load and motor the engine. A schematic diagram of the experimental setup is shown in Figure 16.
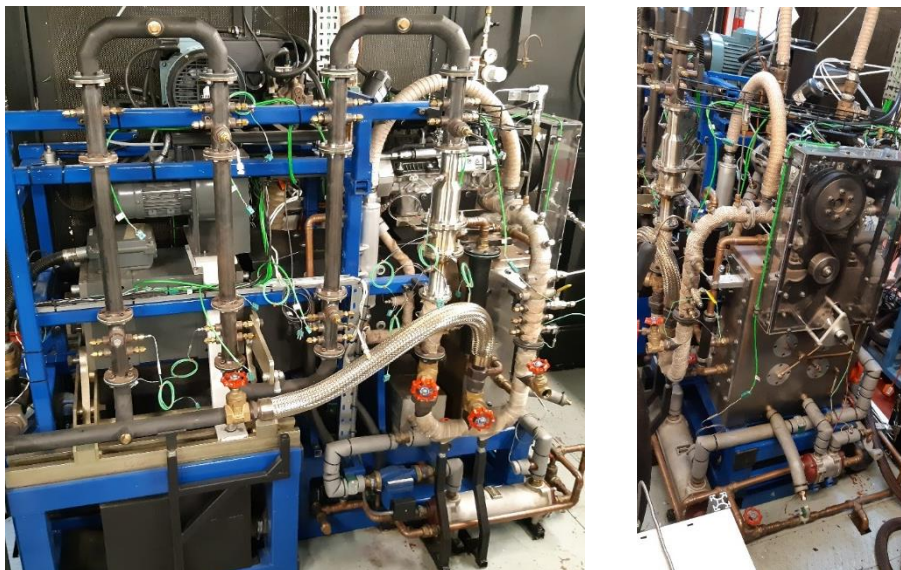
Figure 15. Single-cylinder diesel engine side view (left) and front view (right).

The in-cylinder pressure was recorded over 200 cycles using an AVL GH13P pressure sensor (AVL, 2011) mounted in the cylinder head, and the signal was amplified by an AVL

FlexIFEM 2P2 piezoelectric amplifier (AVL, 2013) as well as monitored and stored on a PC for processing. A digital shaft encoder producing 360 pulses per revolution was used to measure the crankshaft position. The data from the crankshaft position and pressure were combined to create an in-cylinder pressure trace. A LabVIEW-based code was previously developed by the research group to control, collect, and monitor the data acquisition and combustion analysis. In addition, the other engine operating parameters, including multiple fuel injection strategies, was controlled by using an in-house developed LabVIEW program (FAYAD, M. A. *et al.*, 2018). The heat release rate (HRR) was analyzed using the measured pressure data, the HRR was calculated based on the first law of thermodynamics, as shown in Equation (22) (HEYWOOD, 2018).

Table 12. Test engine specifications.

Engine parameters	Specifications
Engine type	Diesel single-cylinder
Stroke type	Four-stroke
Number of cylinders	1
Cylinder bore x stroke (mm)	84 x 90
Connecting rod length (mm)	160
Compression ratio	16:1
Displacement (cm³)	499
Engine speed range (rpm)	900 - 2000
IMEP range (bar)	<7
Fuel pressure range (bar)	500 - 1500
Injection system	Common rail
EGR	No
Turbocharged	No

The common rail fuel system enables the control of multiple injection events. The installed system allows up to three injections events per cycle (pre, main, and post fuel injection) and provides 1,200 bar of maximum pressure. However, in this work, only the pilot and main injections were utilized. While the main injection event provides the bulk of the fuel injected to the engine cylinder, the so-called pre-injections (i.e., one or more injections before the main injection) provides a small amount of fuel before the main injection event.
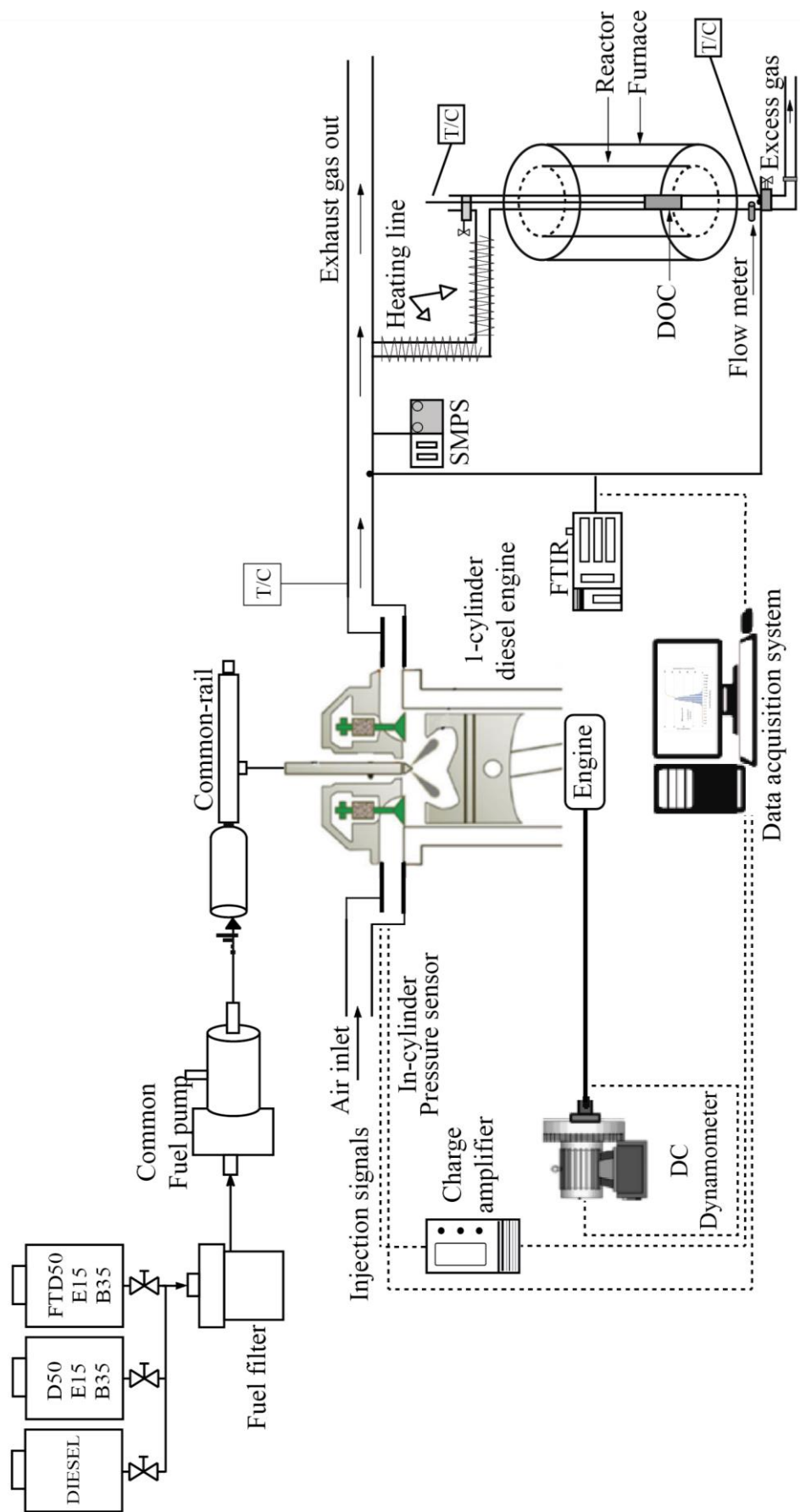
Figure 16. Schematic of the experimental facility.

In this work, the injection parameters were controlled by the engine's ECU (electronic control unit) and were monitored on a PC. The high-pressure fuel rail is measured by a sensor through the signal, which is measured by the ECU. The amount of injected fuel in the combustion chamber by the common rail system can be regulated via a solenoid valve. The ECU can control the amount of fuel injection, which can reduce the engine noise by injecting a small amount of fuel before the main injection event. This can reduce the engine block vibration; optimize the injection timing and fuel quantity. It has been reported that fluctuations of pressure inside the cylinder may be associated with engine block vibration (TAGHIZADEH-ALISARAEI; REZAEI-ASL, 2016).

Fuel was injected into the cylinder with a constant pressure of 550 bar, divided into the pilot (15 CAD BTDC) and main injection (5 CAD BTDC). Throughout the experiments, the indicated mean effective pressure (IMEP) was constantly measured during changing fuels by updating the main fuel injection duration. In order to maintain the same engine IMEP condition performed by the engine running with diesel fuel, a slightly longer fuel main injection was necessary for E15 and E15FTD, as shown in Table 13. The selection of the injection parameters in Table 13 was based on previous works of the research group of the University of Birmingham.

The tests were carried with the engine running with a fixed speed of 1500 rpm and load set at 2 bar IMEP. This condition represents a frequent engine speed-load window in real driving cycles within a vehicle, nonetheless provides a representative and stable condition of both gaseous emissions and exhaust temperature of the engine (FAYAD, M. A. *et al.*, 2018). The selection of this condition is due to the investigation focus relies on the fuel and not on the engine; therefore, one engine condition was selected. The volumetric fuel consumption has been obtained and later converted into mass fuel consumption using each fuel density value. Furthermore, the engine was warmed up in order to reduce the effects of emission variation during the engine cold-start. In addition, to minimize the influence from previously used fuels in the injection system, both fuel tanks and lines were cleaned, and the engine was kept on operation for half an hour with the newly tested fuel. The fuel consumption was measured in triplicate to obtain an average value.

Table 13. Fuel injection parameters and exhaust temperature

Fuel	Injection pressure (bar)	Pilot injection timing (CAD BTDC)	Injection duration (ms)	Main injection timing (CAD BTDC)	Injection duration (ms)	Engine-out exhaust temperature (°C)
Diesel	550	15	0.150	5	0.499	236 ± 2
D50E15B35	550	15	0.150	5	0.529	232 ± 2
FTD50E15B35	550	15	0.150	5	0.546	235 ± 2

4.2   Fuels and blends

The ultra-low sulfur diesel fuel (ULSD), with a maximum of 10 ppm of sulfur, and the Fischer-Tropsch diesel (GTL) were supplied by Shell Global Solutions UK. The biodiesel was from Egogas Ltd, and the ethanol was purchased from Fisher Scientific Company. In order to evaluate the effect of the oxygen content in the combustion process of the blends, both ULSD and Fischer-Tropsch diesel have been selected due to having zero oxygen content. The diesel was selected as reference fuel during this investigation. Ethanol fuel has high purity of 99.8%. The biodiesel fuel was composed of a blend of vegetable oils, mainly rapeseed methyl ester (~90%) blended with palm oil (~10%), as informed by the supplier. The blends were prepared at the Future Engine & Fuels Lab at the University of Birmingham, and the physical and chemical properties of all fuels were calculated or obtained from the respective suppliers or publications (FAYAD, Mohammed A. *et al.*, 2015; FAYAD, Mohammed A.; TSOLAKIS; MARTOS, 2020), as shown in

Table **15**. Before the final selection, the blends have been chosen to aim the achievement of four established targets.

1. To obtain a density based on the range for diesel fuel established in EN 590 and the *Resolução* ANP nº 50/2013, with a value below biodiesel density and higher than F-T diesel;

2. To obtain a lower heating value (LHV) resembling the value for diesel fuel, with a value between that of the biodiesel and the F-T diesel. This would possibly prevent substantial variation in injection duration in comparison with pump diesel and therefore maintain the injection pattern of the engine (LAPUERTA, Magín *et al.*, 2010);

3. To obtain a potential benefit related to the engine emissions by increasing oxygen content (both alternative fuels have the same oxygen content) and decreasing aromatic content;

4. The biodiesel fraction that was introduced has been chosen to balance the lower lubricity of ethanol that could influence the final blend value.

In order to verify the phase separation between F-T diesel and ethanol and to determine the most suitable blends that would fit the aforementioned requirements, 18 samples of 100 ml were prepared in glass bottles in such a way that a minimum excess air was left in them. These samples were kept in the absence of light for they not to be affected by sunlight (Figure 17). The miscibility test was conducted at 23 °C and 50% of relativity humidity.

(a)   (b)

(c)
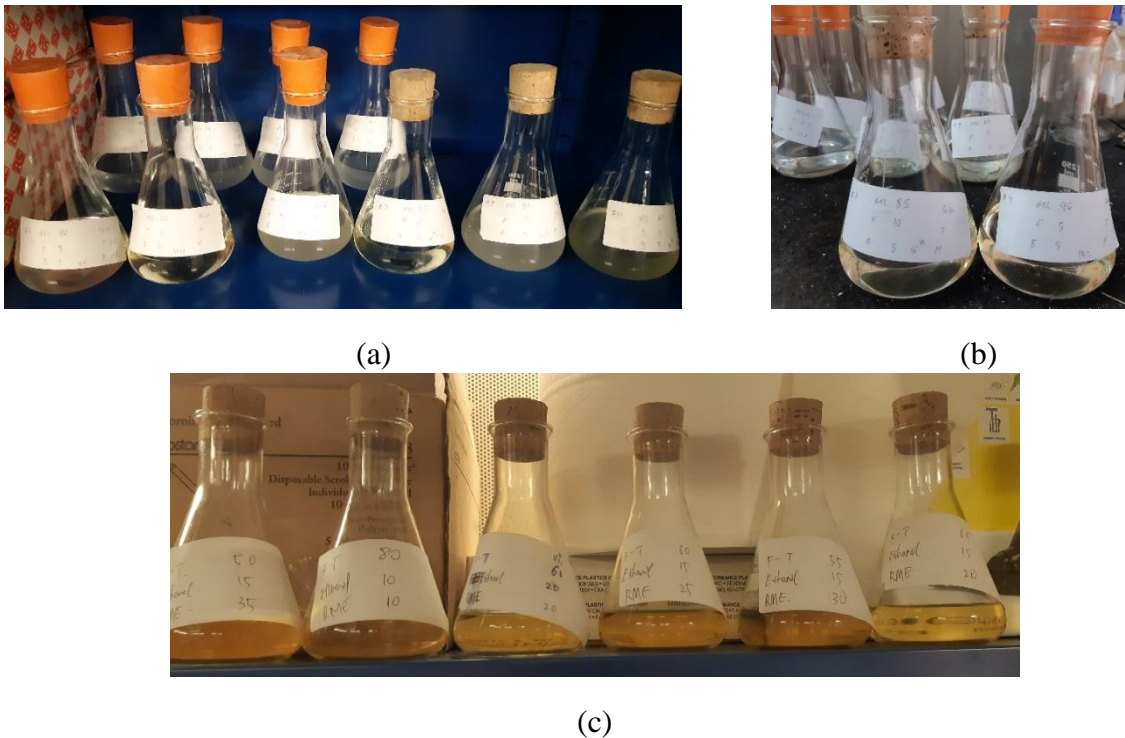
Figure 17. Part of the samples of F-T diesel, ethanol, and biodiesel blends, (a) samples prepared and stored, (b) blends that presented phase separation, and (c) blends that did not have shown phase separation.

The volumetric fractions of the proposed blends are listed in Table 14. Just a few minutes after blending, 8 of the samples were observed to present phase separation, those with zero or up to 5% of biodiesel (vol%). The remaining samples were observed for phase separation for one day, one week, two weeks, and one month period. Within a week, two other samples presented phase separation: those with the same 10% biodiesel but 15% and 20% ethanol, respectively. All remaining samples remained without phase separation for one month.

Table 14. Volumetric ratios of the samples for phase separation verification.

#	F-T Diesel	Ethanol	Biodiesel	Status
1	95	5	0	x
2	90	10	0	x
3	90	8	2	x
4	90	5	5	✓
5	85	15	0	x
6	85	13	2	x
7	85	10	5	✓
8	80	20	0	x
9	80	18	2	x
10	80	15	5	x
11	80	10	10	✓
12	75	15	10	x
13	70	20	10	x
14	65	15	20	✓
15	60	20	20	✓
16	60	15	25	✓
17	55	15	30	✓
18	50	15	35	✓

x: presented phase separation, ✓: no phase separation was observed

Thus, a sample with the volumetric fractions of 50% F-T diesel, 15% ethanol, and 35% biodiesel (FTD50E15B35) was selected based on the targets that were established. Also, a second blend with 50% diesel, 15% ethanol, and 35% biodiesel (D50E15B35) was selected. Both fuel blends had the same oxygen content, and hence the influence of the oxygen when F-T diesel was blended with ethanol and biodiesel could be investigated. The volumetric fractions of the blends are represented in the ternary diagrams, as shown in Figure 18.
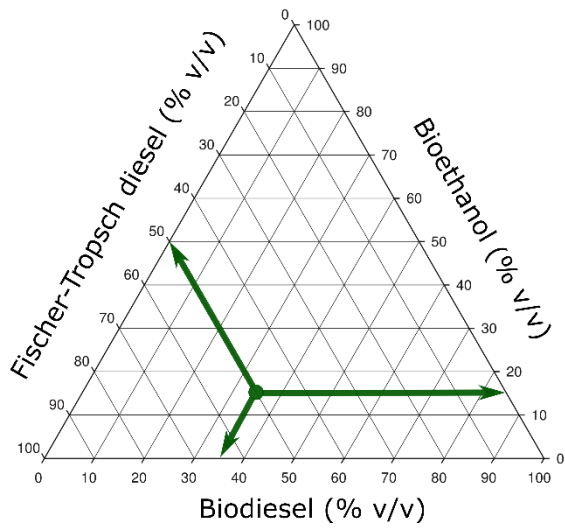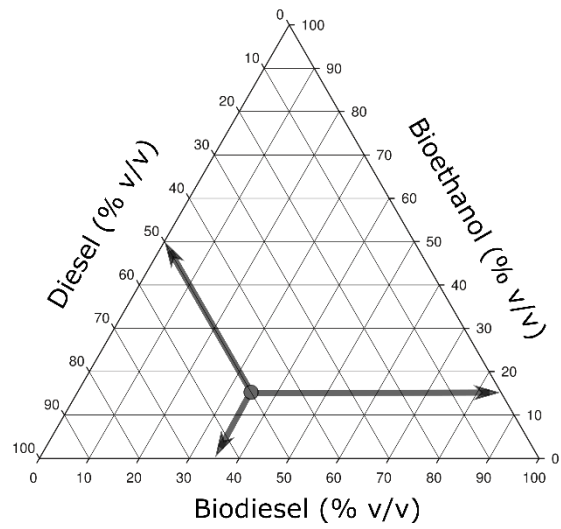
Figure 18. Ternary diagrams representing the tested blends (a) Fischer-Tropsch 50%, Ethanol 15%, and Biodiesel 35% (E15FTD) and (b) Diesel 50%, Ethanol 15%, and Biodiesel 35% (E15)

Table 15. Physical and chemical properties of the fuels.

Abbreviation	% volumetric make-up
Diesel	100 diesel
D50E15B35	15 ethanol + 35 biodiesel + 50 diesel
FTD50E15B35	15 ethanol + 35 biodiesel + 50 F-T diesel

Properties	Diesel	Ethanol	Biodiesel	F-T diesel	D50E15B35	FTD50E15B35
Representative chemical formula	$C_{14}H_{26.1}$	C_2H_5OH	$C_{19}H_{35.3}O_2$	$C_{16.89}H_{35.77}$	$C_{14.13}H_{26.88}O_{1.21}$	$C_{15.52}H_{31.53}O_{1.24}$
Cetane number	53.9	8	54.7	79	47.7 [a]	59.6 [a]
Heat of vaporization [kJ/kg]	243	858	216	339 (SOLOIU *et al.*, 2019)	n/a	n/a
Lower heating value [MJ/kg]	43.11	26.83	37.8	43.90	38.86 [a]	39.13 [a]
Density at 15 °C [kg/m³]	827.1	789.4	883.7	784.6	841.26 [b]	820.01 [b]
Aromatics [wt %]	24.4	0	~0	0.3	n/a	n/a
Theoretical A-F ratio	14.56 : 1	10.33 : 1	11.77 : 1	14.91 : 1	12.92 : 1	13.20 : 1
C/H ratio	6.41	3.97	6.43	5.67	6.02	5.65
Carbon content [wt %]	86.47	52.14	77.15	84.91	78.06	77.28
Hydrogen content [wt %]	13.53	13.13	12.03	15.09	12.94	13.72
Oxygen content [wt %]	0	34.73	10.82	0	9.0	9.0
Kinematic viscosity at 40 °C [mm²/s]	2.467	3.497	1.13	4.478	-	-
Lubricity at 60 °C [μm]	312	560	656	233	-	-

n/a: not available
[a] Estimated based on the mass fraction for each component (HERREROS *et al.*, 2015).
[b] Estimated based on the volumetric fraction for each component (HERREROS *et al.*, 2015).

4.3 Emissions instruments and particulate measurements

4.3.1 Exhaust gas analyzers

The oxygen (O_2) emissions were measured using Testo 340 gas analyzer. Also, a Fourier Transform Infrared (FTIR) spectrometry gas analyzer, MKS MultiGas 2030 (MKS INSTRUMENTS, 2017), was used to measure gaseous exhaust emissions such as carbon monoxide (CO), carbon dioxide (CO_2), nitrogen oxide (NO and NO_2), nitrous oxide (N_2O), ammonia (NH_3), formaldehyde (CH_2O), isocyanic acid (HNCO), total HC (sum of heavy and other unburned hydrocarbons), and individual light hydrocarbons species including methane (CH_4), ethane (C_2H_6), acetylene (C_2H_2), ethylene (C_2H_4), and propylene (C_3H_6). For the calculation of the total hydrocarbons species, the corresponding flame ionization detector (FID) response factors were contained from the FTIR raw file and implemented for each individual HC reading as shown in Equation (23) (SERHAN *et al.*, 2019). The exhaust gas sampling system of the emission analyzer was maintained at a constant temperature of 191 °C by using a heated sampling line to prevent moisture and condensation during the sampling

$$\text{THC} = (1.1 \times \text{methane}) + (2.4 \times \text{acetylene}) + (1.9 \times \text{ethylene}) + (2 \times \text{ethane}) + \tag{23}$$

$$(2.85 \times \text{propylene}) + (1.35 \times \text{heavy HC})$$

The FTIR is equipped with a liquid-nitrogen-cooled detector (on the top of the equipment), which must be filled with liquid nitrogen each time the instrument is used (Figure 19). The main screen of the FTIR is shown in Figure 19, in which the gas measurements can be visualized online.

The FTIR principle of operation is based on the phenomenon of molecular IR absorption since each compound has a characteristic region of its IR spectrum. The FTIR measurement provides online monitoring of the exhaust emission gaseous and capable of sensitivity in a variety of applications, such as catalysis and combustion emissions monitoring, stack emissions monitoring, process monitoring, ambient air monitoring, purity monitoring. The measuring range, resolution, and accuracy of the equipment are listed in Table 16.

Figure 19. The FTIR equipment (top left), gas measurement screen (bottom left), and the assembling of the FTIR (right).

Table 16. Technical data for the MKS MultiGas 2030 FTIR.

Specification	Comments
Gas analyzer	MultiGas 2030 FTIR Continuous Gas Analyzer
Measurement technique	FT-IR Spectrometer
Measurement range	Concentration setting between 10ppb and 100% full scale
Spectral resolution	0.5 - 128 cm^{-1}
Scan speed	1 scan/s @ 0.5 cm^{-1}
Scan time	1 - 300 s
Detector	Infrared Analysis 0.25mm Liquid Nitrogen cooled MCT, digitally linearized

4.3.2 Particulate matter analyzer

A scanning mobility particle sizer (SMPS) was utilized to measure the particulate matter (PM) number concentration and size distribution discharged from the diesel engine exhaust. The equipment is composed of three parts, all manufactured by TSI: an electrostatic classifier model 3080 (TSI INCORPORATED, 2001), a differential mobility analyzer (DMA) model 3081, and a condensation particle counter (CPC) model 3775 (Figure 20). A rotating disk thermodiluter, TSI model 379020A, was utilized to sample and dilute a portion of the exhaust gas with air to control the dilution ratio.
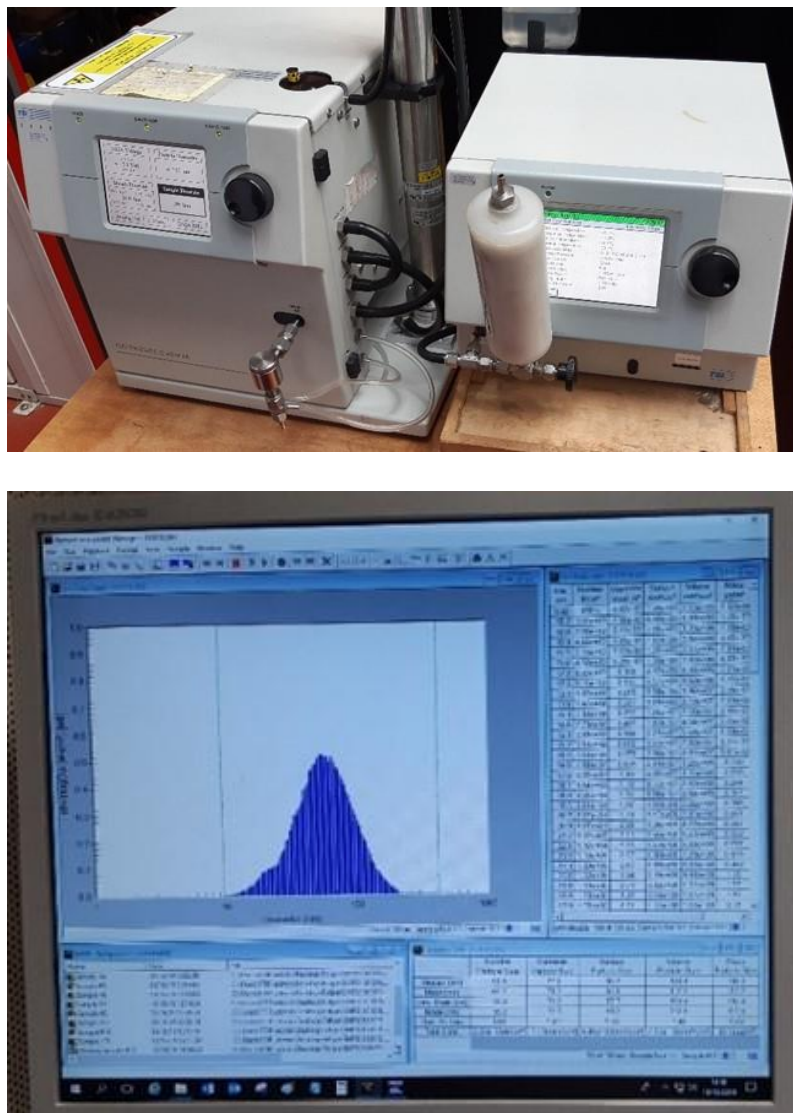
Figure 20. The assembling of the SMPS, DMA, and CPC (top) and the main screen of the SMPS online measurements (bottom).

Briefly, the operation of the SMPS is based on the principle of the mobility of a charged particle within an electrical field. After being diluted and entering the systems, the particles are neutralized (using a radioactive source). Then, they enter the DMA, in which they are classified according to electrical mobility, with only particles of a narrow range of mobility exiting through the output slit. Afterward, the particles enter the CPC, which determines the particle concentration.

The SMPS was connected downstream of the dilution system in order to extract a diluted sample for the particle size measurement (Figure 21). The temperature of dilution was 150 °C in order to prevent hydrocarbon condensation and nucleation, which may occur during the sampling of the exhaust gas, and the dilution ratio was set at 1:20. The technical data for the SMPS and parameters set to measure the PM distribution are shown in Table 17.
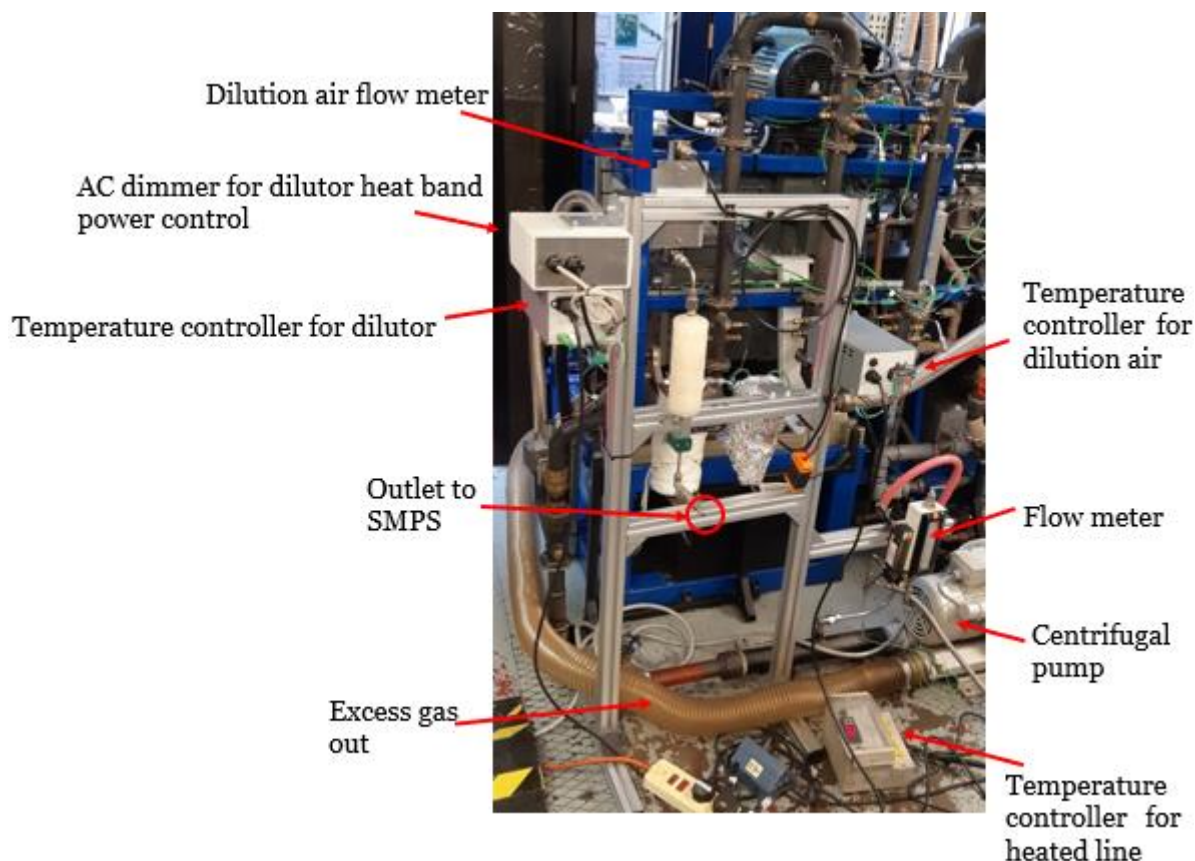
Figure 21. Overview of the dilution system.

The actual dilution ratio (DR) in this work was calculated according to the following Equation (24).

$$DR = \frac{[CO_2]_{exhaust} - [CO_2]_{background}}{[CO_2]_{diluted} - [CO_2]_{background}} \tag{24}$$

in which $[CO_2]_{exhaust}$ is the CO_2 concentration of the exhaust gas before dilution, $[CO_2]_{background}$ is the CO_2 concentration in the background, and $[CO_2]_{diluted}$ is the CO_2 concentration after dilution.

Table 17. SMPS technical data and parameters used to measure the particle size distribution

Specification	Corresponding value
Particle type	Solids and non-volatile liquids
Particle size range (nm)	10 – 1000
Maximum input concentration	10^8 particles/cm^3 @ 10 nm
Voltage (VDC)	10 - 10000
Sheath flow rate (L/min)	6.00
Aerosol flow rate (L/min)	0.60
Lower size (nm)	10.2
Upper size (nm)	414.2
Scan time (s)	120

The condensing particle counter (CPC 3775) had a particle count accuracy of $\pm 20\%$ for particle concentration larger than 5×10^4 particles/cm^3 while $\pm 10\%$ for particle concentration lower than 5×10^4 particles/cm^3 but smaller than 1×10^7 particles/cm^3. The particle number and size distribution were converted into particle mass distribution by multiplying the corresponding particle volume and apparent particle density (LAPUERTA, Magín; RODRÍGUEZ-FERNÁNDEZ; AGUDELO, 2008), calculated using an effective particle density function (LAPUERTA, Magín; ARMAS; GÓMEZ, 2003). Figure 22 shows the different types of particulates based on their size. The particulate matter emitted by the diesel engine exhaust is divided into three groups (i.e., small, medium, and large particulates).

In order to ensure the reliability of the tests, the FTIR measurements were recorded for 20 minutes, while the Testo values were an average of two readings. This product has been done for all tested fuels. Also, the SMPS measurements were an average of 5 readings for each of the fuels.
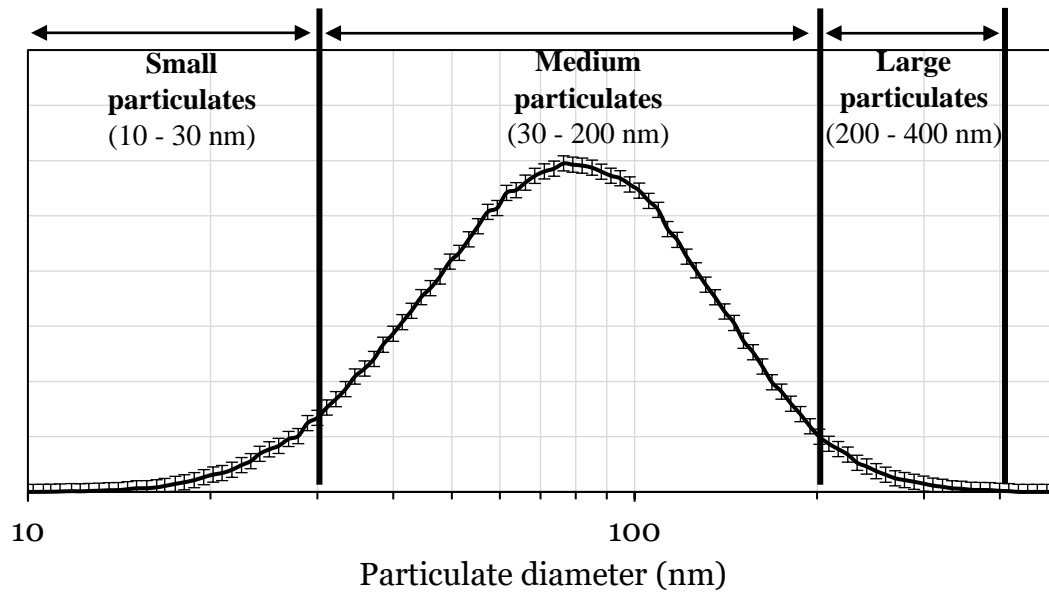
Figure 22. Typical particulate size distribution for the diesel engine used in this research.

4.4   Diesel Oxidation Catalyst

The gas hourly space velocity (GHSV) is an important parameter that is used to assess the exhaust gas residence time within the catalyst. The GHSV is calculated as the ratio of the volumetric flow rate on the catalyst volume and is expressed as h^{-1}. In other words, it is defined as the reactant's volumetric flow rate per hour over the total volume of the catalyst. The higher the volume of exhaust gas treated, the lower the contact time between the catalyst's active sites and the engine-out exhaust species. The GHSV can be influenced either by the exhaust gas flow rate (based on engine operating conditions) or by the catalyst volume.

$$\text{GHSV} = \frac{\text{gas flow rate over catalyst } \left(\text{m}^3/_\text{h} \right)}{\text{catalyst volume (m}^3)} \tag{25}$$

The diesel oxidation catalyst (DOC) studies were carried out using a monolith catalyst with 24.3 mm in diameter, 101.5 mm in length, 0.10922 mm wall thickness, and 0.258 cells/m^2, supplied by Johnson Matthey Plc. The catalyst was placed in a reactor inside a tubular furnace where K-type thermocouples (with a range of 0–1250 °C and an accuracy of ±2.2 °C) and a TC-08 Thermocouple Data Logger (Pico Technology) were used to measure the engine exhaust temperature. A flow meter was responsible for controlling the exhaust gas flow (see Figure 16). The details of the catalyst used in this work were a 4.237 kg/m^3 platinum:palladium (weight ratio 1:1) with alumina and zeolite washcoat (158.66 kg/m^3 loading). The effects of exhaust temperature and composition on the engine were investigated while the engine exhaust was

104

maintained at a gas hourly space velocity (GHSV) of 35,000 h^{-1} and a heating temperature of about 5 °C/min. The DOC catalyst utilized in this research was supplied by Johnson Matthey Plc. More details regarding the catalyst are previously discussed in section 3.3.1.
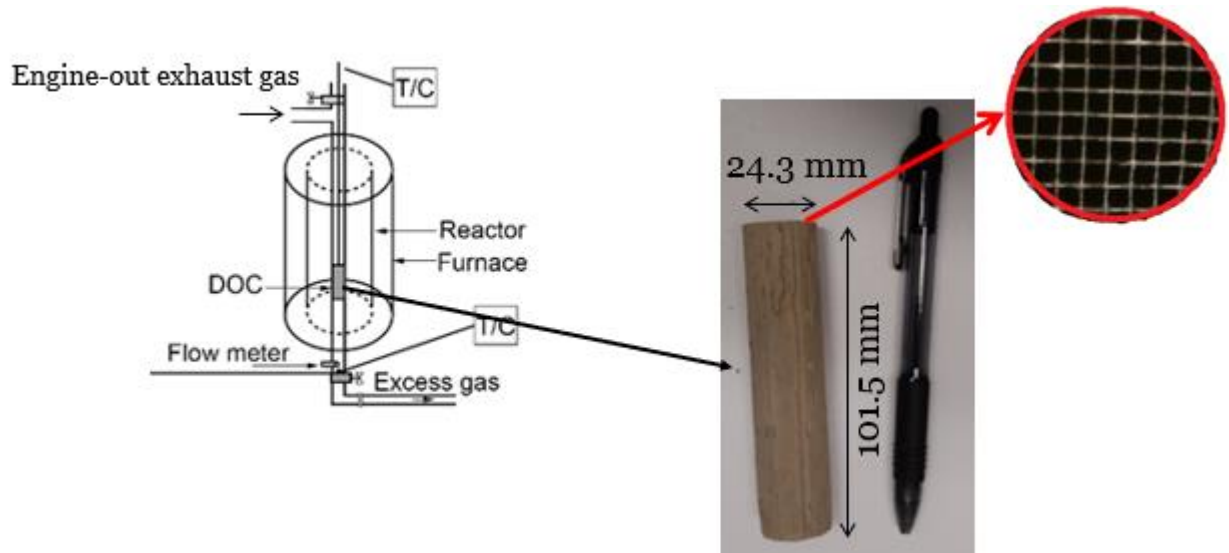
Figure 23. The assembly of the DOC catalyst and the main components of the systems (left) and a picture of the catalyst (right).

4.5 Thermodynamic analysis

The control volume of the thermodynamic system is given in Figure 24, including the inlet and outlet terms. The equations used to calculate the inlet and outlet energy and exergy rates follow the literature (DINCER; BICER, 2013; KOTAS, 1985; MORAN, MICHAEL J. ; SHAPIRO, HOWARD N. ; BOETTNER, DAISIE D. ; BAILEY, 2018; SZARGUT, 2005). The first and second laws of thermodynamics were applied to this system with the following assumptions:

- The engine operation is studied at the steady-state condition;

- The intake air and the outlet exhaust gases were considered as mixtures of ideal gases;

- The environment (reference state) was considered at $T_0 = 25$ °C, $P_0 = 101.325$ kPa, and did not vary with time;

- The kinetic and potential energy effects of incoming fluid streams and outgoing fluid streams were neglected (KARAGOZ *et al.*, 2020).
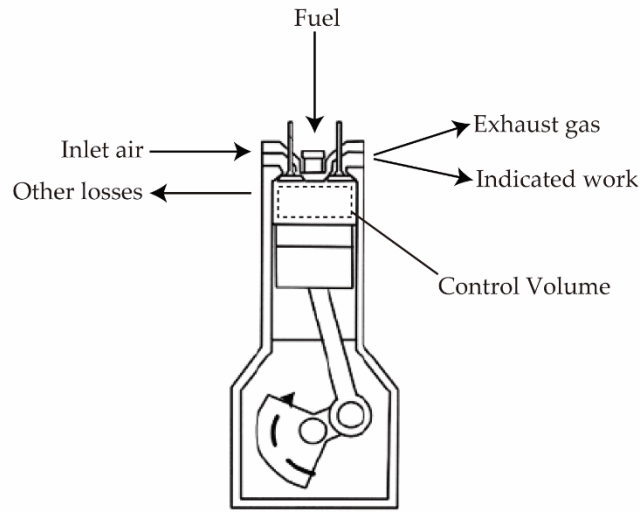
Figure 24. Control volume of the engine.

4.5.1 Energy analysis

Based on the assumptions made, the mass and energy balances of the control volume are given by Equations (26)-(28) below

$$\sum \dot{m}_{in} = \sum \dot{m}_{out} \tag{26}$$

$$\sum \dot{En}_{in} = \sum \dot{En}_{out} \tag{27}$$

$$\dot{En}_{air} + \dot{En}_{fuel} = \dot{En}_W + \dot{En}_{exh} + \dot{En}_{loss} \tag{28}$$

in which $\dot{m}_{in}$ and $\dot{m}_{out}$ are respectively the inlet and outlet mass flow rates, $\sum \dot{En}_{in}$ and $\sum \dot{En}_{out}$ represents the total energy inlet and outlet rates of the control volume, respectively, $\dot{En}_{air}$ is the inlet energy rate of air, $\dot{En}_{fuel}$ is the inlet energy rate of the fuel, $\dot{En}_W$ is the energy rate by work, $\dot{En}_{exh}$ is the energy outlet rate by the exhaust, and $\dot{En}_{loss}$ is the energy loss rate of the control volume. Because the intake air stream is at the same temperature as the reference state, the amount of energy inlet into the control volume can be neglected (SAYIN, C. *et al.*, 2007).

The rate of energy inlet from the fuel ($\dot{E}n_{fuel}$) to the control volume is calculated using the fuel mass flow ($\dot{m}_{fuel}$) and the fuel lower heating value (LHV) as shown in Equation (29) below, where the subscript i represents the different fuels that composed the blend.

$$\dot{E}n_{fuel} = \sum_{i=1}^{3} \dot{m}_{fuel_i} \cdot LHV_{fuel_i} \tag{29}$$

The work rate ($\dot{E}n_W$) was considered as the indicated power of the engine, which is expressed by Equation (30)

$$\dot{E}n_W = \frac{IMEP \cdot V_d \cdot N}{n_R \cdot 60 \cdot 10^3} \tag{30}$$

in which N (rpm) is the engine speed, V_d (m3) represents the displaced volume, IMEP is the indicated mean effective pressure and n_R is the number of crank revolutions for each power stroke per cylinder (e.g. n_R is 2 for a four-stroke engine). The IMEP is calculated only from the cylinder pressure to represent the average pressure over a cycle of the engine.

The outlet exhaust energy rate ($\dot{E}n_{exh}$) of the control volume is determined as in Equation (31)

$$\dot{E}n_{exh} = \sum_{i} \dot{m}_i \cdot h_i \tag{31}$$

in which $\dot{m}_i$ is the mass flow rate and h_i is the enthalpy of each gaseous species in the engine exhaust, respectively.

Then, the energy loss rate ($\dot{E}n_{loss}$) of the control volume consists of all energy heat losses involved, which includes the heat transfers from cylinder walls (combustion chamber and piston), by coolant, and by the oil, except for the exhaust losses. $\dot{E}n_{loss}$ is calculated as the difference between the energy inlet rate and the energy outlet rate (work and exhaust gases) from the control volume as shown in Equation (32) below:

$$\dot{E}n_{loss} = \dot{E}n_{fuel} - \dot{E}n_W + \dot{E}n_{exh} \tag{32}$$

Finally, the energy efficiency (η) of the control volume, based on the First Law of Thermodynamics (i.e., thermal efficiency), is defined as the work outlet ratio to the fuel energy inlet is shown in Equation (33).

$$\eta = \frac{\dot{E}n_W}{\dot{E}n_{fuel}} \tag{33}$$

4.5.2 Exergy analysis

Similar to the case of the energy analysis, the same assumptions were valid for the exergy analysis of the control volume. The exergy balance can be expressed as Equations (34) and (35) as follows

$$\sum \dot{E}x_{in} = \sum \dot{E}x_{out} + \dot{E}x_{dest} \tag{34}$$

$$\dot{E}x_{air} + \dot{E}x_{fuel} = \dot{E}x_W + \dot{E}x_{exh} + \dot{E}x_{loss} + \dot{E}x_{dest} \tag{35}$$

in which $\sum \dot{E}x_{in}$, $\sum \dot{E}x_{out}$ and $\dot{E}x_{dest}$ represents respectively, the total exergy inlet and outlet rates and the exergy destruction (irreversibility) rate of the control volume. $\dot{E}x_{air}$ is the inlet exergy rate of air, $\dot{E}x_{fuel}$ is the inlet exergy rate from the fuel, $\dot{E}x_W$ is the exergy rate by work, $\dot{E}x_{exh}$ is the exergy outlet rate by the exhaust, and $\dot{E}x_{loss}$ is the exergy loss rate of the control volume. An equivalent assumption was considered for the air inlet rate, and by considering the environmental atmosphere as a reference state, so the exergy associated with naturally aspirated air into the engine control volume is zero (VERMA *et al.*, 2018).

The inlet exergy rate from the fuel ($\dot{E}x_{fuel}$) to the control volume can be determined as follows in Equation (36), where the subscript *i* represents the different fuels that composed the blend.

$$\dot{E}x_{fuel} = \sum_{i=1}^{3} \dot{m}_{fuel_i} \cdot ex_{fuel_i} = \dot{m}_{fuel_i} \cdot LHV_{fuel_i} \cdot \varphi_{fuel_i} \tag{36}$$

in which ex_{fuel} is the fuel-specific exergy of the fuel, which can be obtained by multiplying the fuel lower heating value by the chemical exergy factor (φ) of each fuel, which can be obtained through Equation (37) as in (KOTAS, 1985; SZARGUT, 2005) for liquid fuels. The accuracy of this expression is estimated to be ±0.38%.

$$\varphi = 1.0401 + 0.1728\frac{h}{c} + 0.0432\frac{o}{c} + 0.2169\frac{s}{c}\left(1 - 2.0628\frac{h}{c}\right) \qquad (37)$$

in which h, c, o, and s are respectively the mass fractions of hydrogen, oxygen, carbon, and sulfur of the fuel (KOTAS, 1985; SZARGUT, 2005).

The exergy work rate ($\dot{E}x_W$) is equal to the energy work rate of the control volume, as shown in Equation (38).

$$\dot{E}x_W = \dot{E}n_W \qquad (38)$$

The exergy rate of exhaust gases ($\dot{E}x_{exh}$) is composed of two components that are the physical (thermomechanical) and chemical exergies, which is expressed in Equation (39).

$$\dot{E}x_{exh} = \sum_i \dot{n}_i\left(ex_{ph,i} + ex_{ch,i}\right) \qquad (39)$$

in which $\dot{n}_i$ is the molar flow rate of each exhaust gas species, $ex_{ph,i}$ and $ex_{ch,i}$ are the specific physical and chemical exergies of each exhaust gas species, respectively.

For a mass flow that goes through the volume control, the specific physical exergy rate ($ex_{ph,i}$) of the exhaust gas species is obtained by Equation (40) below

$$ex_{ph,i} = (h_i - h_0) - T_0 \cdot (s_i - s_0) \qquad (40)$$

in which s_i is the entropy of each gaseous species in the engine exhaust.

For a gas mixture, the chemical exergy rate ($ex_{ch,i}$) of the exhaust gas species can be calculated using Equation (41) as following

$$ex_{ch,i} = \sum_i x_i \cdot \varepsilon_{ch,i} + R \cdot T_0 \cdot \sum_i (x_i \cdot \ln\gamma_i \cdot x_i) \qquad (41)$$

in which x_i is the molar fraction of each species of the exhaust gas, $\varepsilon_{ch,i}$ is the standard chemical exergy (KOTAS, 1985; SZARGUT, 2005), R is the universal gas constant (8.314 kJ/kmol.K) and γ_i is the activity coefficient ($\gamma_i = 1$ for ideal gases).

The exergy loss rate ($\dot{E}x_{loss}$) shown in Equation (42) is considered to be the amount of exergy loss from the control volume, and the lost-exergy rate was assumed to be all heat losses occurring from the measured coolant temperature (Tcool = 353.15 K) to the environment at reference state temperature, as in (KHOOBBAKHT; AKRAM; *et al.*, 2016; TAT, 2011).

$$\dot{E}x_{loss} = \sum \left(1 - \frac{T_o}{T_{cool}}\right) \dot{E}n_{loss} \tag{42}$$

Hence, the exergy destruction ($\dot{E}x_{dest}$) is obtained from the exergy balance by Equation (43).

$$\dot{E}x_{dest} = \dot{E}x_{fuel} - \dot{E}x_W - \dot{E}x_{exh} - \dot{E}x_{loss} \tag{43}$$

Finally, the exergy efficiency (ψ) of the control volume is presented in Equation (44) as follows.

$$\psi = \frac{\dot{E}x_W}{\dot{E}x_{fuel}} \tag{44}$$

The entropy generation rate ($\dot{S}_{gen}$) is determined from the equation for the exergy destruction and is represented in Equation (45).

$$\dot{S}_{gen} = \frac{\dot{E}x_{dest}}{T_0} \tag{45}$$

4.6 Error analysis and uncertainty analysis

Experimental evaluations usually have associated intrinsic uncertainties, as they are dependent on experimental conditions, instrument selection, and calibration, observation, data input, setup assembly, among other factors. Thus, an analysis of uncertainty is essential to validate results obtained from experimental results. The uncertainties have been calculated by the root-sum-square combination of the fixed errors introduced from different sources, with methods further described in (MOFFAT, 1988), as shown in Equation (46)

$$X_i = \bar{X}_i \pm U_x \tag{46}$$

in which X_i is the actual value, $\bar{X}_i$ is the measured value and U_x is the total uncertainty of the measurement, which may be calculated using equation (47)

$$U_x = \sqrt{(E_s)^2 \pm (E_r)^2} \tag{47}$$

in which E_s and E_r are respectively the systematic and random errors. In general, those errors are provided by the instrument manufacturer specifications. As for the uncertainty associated when multiple measurements are obtained (e.g., exhaust emissions), it may be estimated by a statistical average, calculated as shown in equation (48) below

$$X_{average} = \frac{(X_1 + X_2 + \ldots + X_n)}{n} \tag{48}$$

in which $X_{average}$ is the reported value, X_1 to X_n are values measured within intervals, and finally, n is the total number of values. Moreover, the standard deviation (SD) of data is obtained using equation (49).

$$SD_{mean/average} = \frac{\sqrt{\sum_{i=1}^{n}(X_i - X_{average})^2}}{1 - n} \tag{49}$$

The experimental uncertainty has been calculated, and error bars have been added to graphs. Moreover, the main technical characteristics and measurement accuracies of the equipment used in this work are shown in Table 18.

Table 18. Accuracy of the equipment used in this work.

Measure	Instrument	Range	Accuracy of the measurement range
Exhaust gas (CO, CO_2, NO_x, THC)	Multigas 2030 FTIR	10ppb-100% full scale	± 5%
Exhaust gas (O_2)	Testo 340	0-25%	± 0.2%
Crank angle, engine speed	Digital shaft encoder	-	± 1 rev/min
In-cylinder pressure	AVL GH13P pressure sensor	0-250 bar	± 1%
Temperature	K-type thermocouples	of 0-1250 °C	± 2.2 °C

5 RESULTS AND DISCUSSION

This chapter presents the results of this investigation. The combustion and performance, exhaust emissions, energy and exergy analysis, PM characterization, and the aftertreatment performance results are referred to and discussed.

5.1 Performance characteristics

In order to obtain the same IMEP output for every test, the blends have shown increased indicated specific fuel consumption (ISFC) of about 11.8% and 10.8%, respectively, in comparison with diesel (Figure 25). Higher ISFC can be associated with the LHV of the fuels, as pointed out by several studies with ethanol fuel blends (ÇELEBI; AYDIN, 2019; PRADELLE *et al.*, 2019).
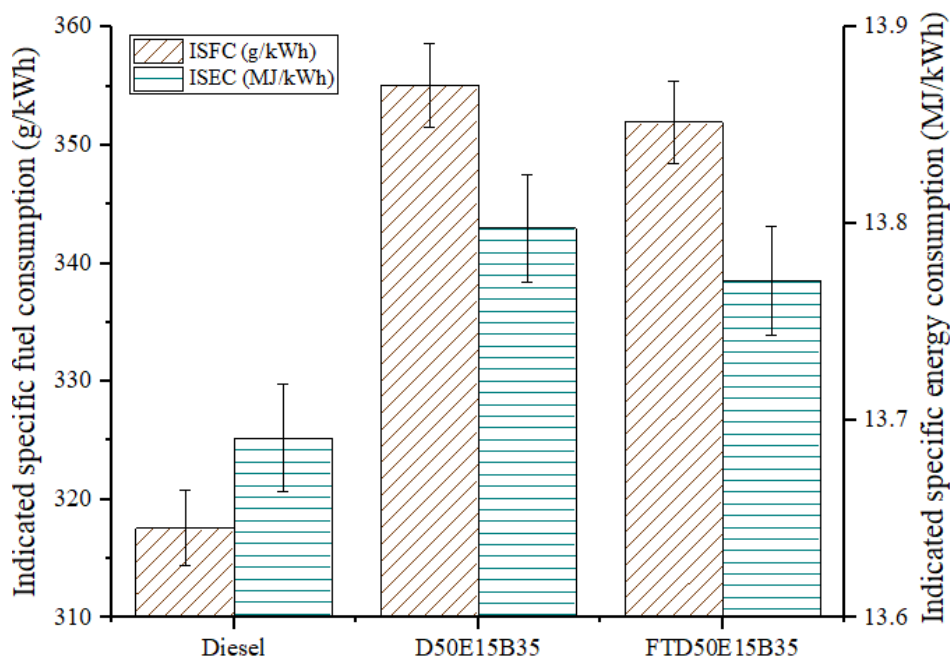
Figure 25. Indicated specific fuel consumption (ISFC) and indicated specific energy consumption (ISEC) for diesel, D50E15B35, and FTD50E15B35.

On the other hand, indicated specific energy consumption (ISEC) is a more adequate parameter than ISFC to compare different fuels and for evaluating the potential of fueling the engine with ethanol blends. ISEC indicates the amount of energy that is consumed to produce one unit of indicated work in one hour, and it can be defined as the specific fuel consumption times the fuel LHV. Figure 2 shows the variation of ISEC for the engine fueled with diesel, D50E15B35, and FTD50E15B35. The blend of FTD50E15B35 showed a slightly higher ISEC

(approximately 1.1%) than diesel, whilst D50E15B35 has shown a 0.8% increase in value over diesel. Overall, the increase in ISFC for FTD50E15B35 is compensated by its LHV, which results in a percentually lower increase in ISEC. Other researchers have obtained similar results with other oxygenated fuels (CHACKO; JEYASEELAN, 2020; GUARIEIRO *et al.*, 2014).

5.2 Combustion characteristics

Figure 26 shows the in-cylinder pressure and HRR versus the crank angle degree for the combustion of diesel, D50E15B35, and FTD50E15B35 at 2 bar IMEP and 1500 rpm. A significant increase in HRR, but later in the cycle, was obtained from the combustion of both alternative fuel blends, which may also explain the changes in emissions later to be discussed. As it may be seen, ethanol's higher heat of vaporization has a direct effect on HRR peak, and this seems to be following the literature (JAMUWA; SHARMA; SONI, 2016). Additionally, ethanol parameters such as heat of vaporization increase ID, and hence more fuel undergoes premixed combustion phase, promoting an increase in later HRR.

The start of combustion was defined by the literature as the variation in inclination of the HRR curve, obtained from the cylinder pressure data (JAMUWA; SHARMA; SONI, 2016). The duration of combustion was characterized as the difference between CA10 (crank angle when 10% accumulated HRR has occurred) and CA90 (crank angle when 90% accumulated HRR has occurred). As for the duration of premixed combustion, it was assumed as the difference between CA10 and CA50 (crank angle when 50% accumulated HRR has occurred).

The peak in-cylinder pressures for diesel, D50E15B35, and FTD50E15B35 at 2 bar IMEP and 1500 rpm are presented in Figure 27 for the three fuels. It was noticed that the ethanol addition to F-T resulted in a blended fuel with the highest peak pressure in comparison with the diesel fuel and the D50E15B35. In comparison with FTD50E15B35, the D50E15B35 blend had a slight reduction in peak pressure, in addition to the aforementioned increase in the main injection duration. Moreover, both blends had a lower CN in comparison with diesel (see Table 15), which extended the ID period and boosted the maximum pressure. Additionally, the heating value of FTD50E15B35 had a significant effect on the increased pressure. This trend was recently reported by a similar work (JIAO; LIU; ZHANG; YANG; *et al.*, 2019).
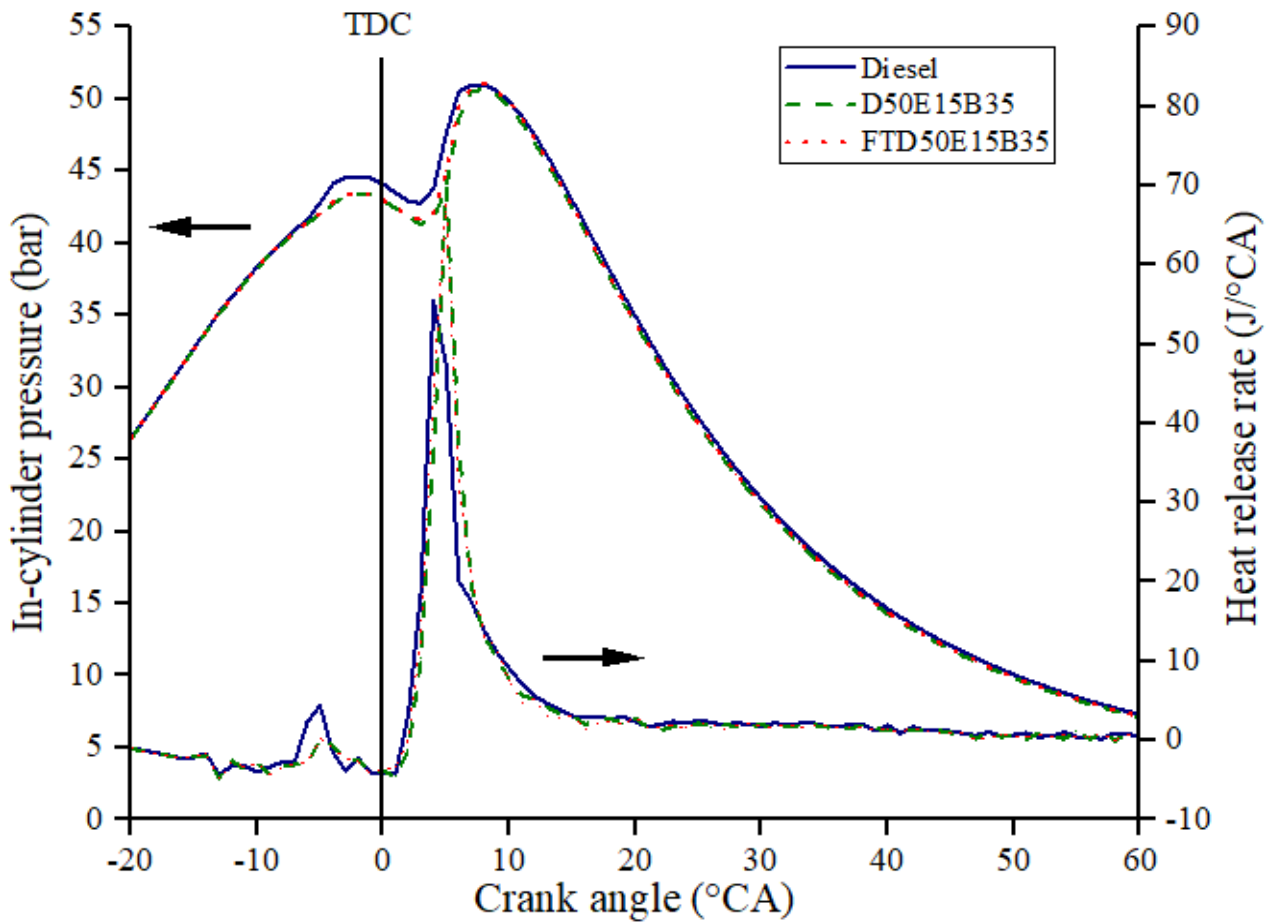
Figure 26. Effect of different fuel combustion on in-cylinder and heat release rate with a crank angle at 2 bar indicated mean effective pressure (IMEP) and 1500 rpm.

As for the peak HRR, both fuel blends had higher energy release in the premixed combustion phase compared to diesel. Furthermore, D50E15B35 presented the higher peak HRR among the fuels and a slight increase of 2.85% in peak HRR as related to FTD50E15B35. Again, the longer ID due to ethanol addition leads to a longer F/A mixture time and thus more fuel burnt in the premixed combustion phase, which results in a higher peak of HRR compared to diesel combustion, although at a slightly later time.
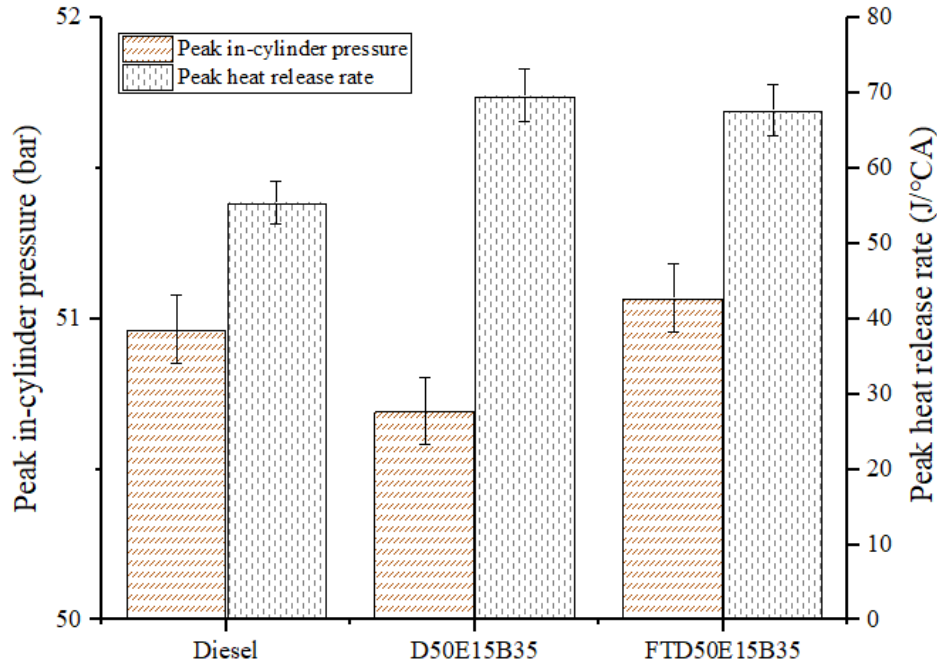
Figure 27. Peak in-cylinder pressure and peak heat release for diesel, D50E15B35, and FTD50E15B35 at 2 bar IMEP and 1500 rpm.

The variation of ID and the duration of combustion are presented in Figure 28. The ID is a parameter that has a direct influence on engine performance and that is affected by many parameters (e.g., CN, F/A ratio, injection timing, in-cylinder temperature). Similarly, the duration of combustion relies on parameters such as equivalence ratio, compression ratio, engine operational conditions, and fuel. A higher ID is observed for both blends D50E15B35 and FTD50E15B35. Longer ID could be explained by the lower CN (as seen in Table 15) and the high latent heat of vaporization of ethanol, thus leading to longer air and fuel mixing time and lower temperatures during compression. Hence, more fuel is burned in the premixed phase, which results in a higher maximum HRR (see Figure 27).

Various discussions of ID for ethanol/diesel/biodiesel blends are found in the literature (SHAHIR *et al.*, 2015; TSE; LEUNG; CHEUNG, 2015). Furthermore, in comparison with D50E15B35, the F-T diesel blend had a similar, although slightly lower ID. The reason for this is due to the higher CN of F-T diesel in comparison with pure diesel fuel, hence lowering the ID of the blend (GILL *et al.*, 2011b). With the addition of ethanol, the duration of combustion decreased for both D50E15B35 and FTD50E15B35 due to the increase in the ID, probably as a result of the higher latent heat of vaporization of the ethanol.
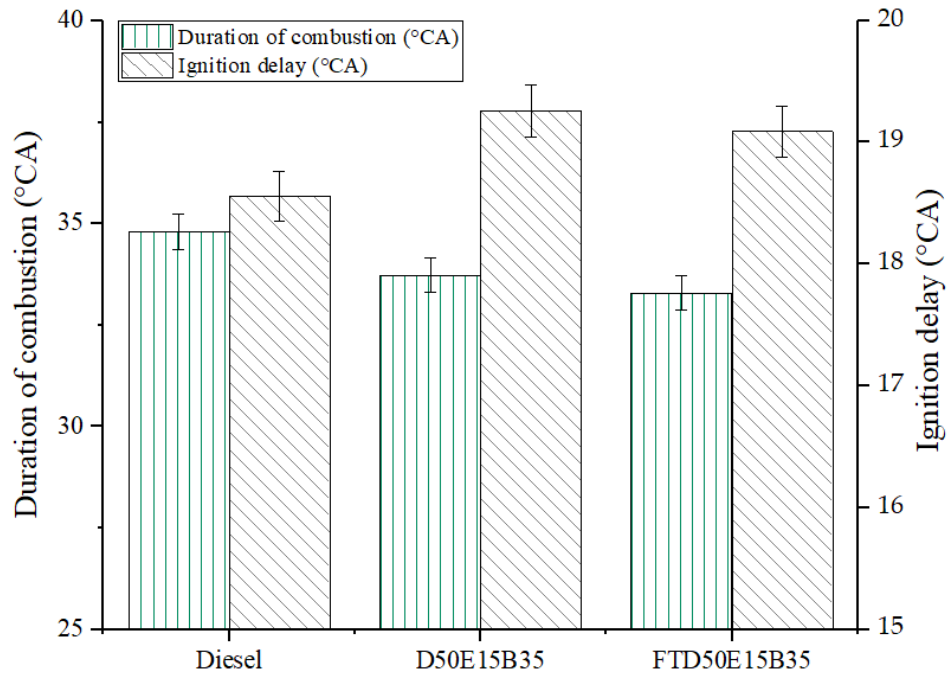
Figure 28. Duration of combustion and ignition delay for different fuels at 2 bar IMEP and 1500 rpm.

5.3 Engine exhaust emissions

5.3.1 CO and CO_2 emissions

Figure 29 shows the effects of fuel blends on exhaust emissions in comparison to diesel fuel. The overall lambda (i.e., actual air/fuel ratio over the stoichiometric air/fuel ratio) was found to be similar for the tested fuels as 2.9, 2.84, and 2.82 for diesel, D50E15B35, and FTD50E15B35, respectively. This is an indication that the difference between the fuels was the direct result of the fuel composition.

The oxygenated fuels are expected to reduce carbonaceous exhaust emissions as the presence of oxygen in fuel molecules eases hydrocarbon oxidation. However, as discussed by Herreros et al. (HERREROS; JONES; *et al.*, 2014), the lower cetane number (because of ethanol) may conceivably increase exhaust emissions as a result of less time for the oxidation to occur and thus favoring incomplete combustion. Additionally, the high latent heat of vaporization of ethanol could reduce the in-cylinder gas temperature, which decreases the oxidation reaction rate and thus increase CO emission under lower engine loads (RIBEIRO *et al.*, 2007; ZHU *et al.*, 2011) as is the case for this work (Figure 29). Furthermore, the comparatively higher viscosity of biodiesel creates poor fuel atomization, which also contributes to incomplete combustion (MOFIJUR *et al.*, 2016), and consequently increasing CO levels (GÜLÜM; BILGIN, 2018).

A recent investigation by Choi et al. (CHOI *et al.*, 2019) reported that blends of F-T diesel and biodiesel resulted in slightly higher CO emission and the researchers attributed this to the insufficient evaporation and short mixing time of the blend during premixed combustion. The application of a diesel oxidation catalyst could effectively reduce these CO levels from the combustion of these alternative fuels, as shown by Torres et al. (ANDRADE TORRES *et al.*, 2021). D50E15B35 and FTD50E15B35 have shown higher CO emissions than diesel fuel. This can also be attributed to lower local in-cylinder temperature due to the ethanol cooling effect, as explained in Jamrozik et al. (JAMROZIK *et al.*, 2019).

A slight decrease in CO_2 emissions was observed when the engine was fueled with D50E15B35, while CO_2 emissions for FTD50E15B35 are slightly higher than in the case of diesel fuel. This is in line with the carbon content of the estimated chemical formula of the fuel blends, though it has to be noted that the differences are within the confidence interval of the results. CO_2 is a common product of the combustion of hydrocarbon fuels, so the lower carbon content of ethanol molecules leads to lower CO_2 formation, even on an energy basis (g_{CO_2}/MJ_{fuel}). In addition, to combustion stoichiometry, previous studies reported that an increase in CO_2 emission with the addition of biofuels (ethanol and biodiesel) is attributed to the higher oxygen content of the oxygenated, which favors the combustion process and hence increases CO_2 formation (GUARIEIRO *et al.*, 2009; MOFIJUR *et al.*, 2016).
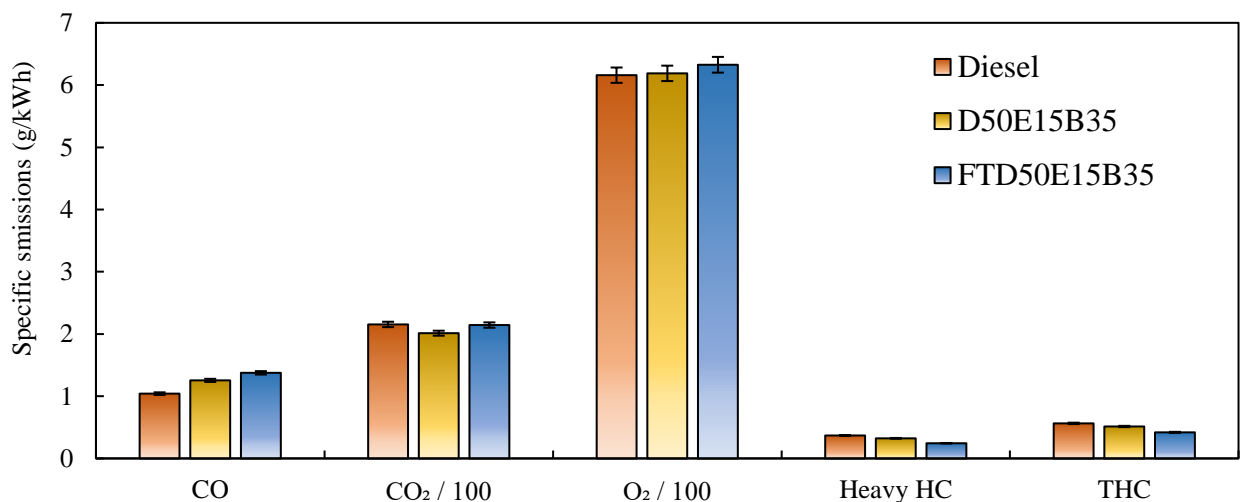
Figure 29. Effect of diesel, D50E15B35, and FTD50E15B35 on CO, CO_2, O_2, and HCs emissions at 2 bar IMEP and 1500 rpm.

5.3.2 Hydrocarbon emissions

The lack of oxygen in the chemical molecule of the fuel explains the higher THC emission for the conventional diesel, as shown in the previous Figure 29. The combustion of D50E15B35 and FTD50E15B35 have reduced the THC emissions (mostly comprised of heavy unburned hydrocarbons) by 9% and 26%, respectively when compared to diesel fuel. Previous researchers have discussed the role of ethanol/biodiesel addition to diesel fuel as either increase (AYDIN; ÖĞÜT, 2017) or decrease (BARABÁS; TODORUȚ; BĂLDEAN, 2010; ROY *et al.*, 2016) HC emissions. The total and the heavy hydrocarbons presented in the THC have decreased between 18%-33% for FTD50E15B35 in comparison with diesel or D50E15B35. This might be associated with the higher cetane number and the absence of aromatics of F-T diesel, contributing to the reduction in THC.

When comparing the FTD50E15B35 fuel with the D50E15B35, the absence of aromatic hydrocarbons of the Fischer-Tropsch diesel, as well as his higher cetane number, further reduces THC exhaust emissions. The combustion of FTD50E15B35 produced the lowest THC emissions, which was 26% lower than the reference fuel and 19% lower than the D50E15B35 blend. Khan et al. (KHAN *et al.*, 2016) discussed that a higher cetane number and lower aromatic content are the main reasons for the occurrence of a shorter ignition delay time. In other words, it has good auto-ignition qualities and a high cetane number, thus proving higher combustion efficiencies. Also, the virtually zero sulfur, as well as the absence of aromatics, have been mentioned by Gill et al. (GILL *et al.*, 2011a) to result in a reduction in the engine-out exhaust emissions (i.e., reduce HC development and lowering PM). It has been previously reported by Soriano (SORIANO *et al.*, 2018) et al. that F-T diesel reduces hydrocarbons emissions in comparison with diesel fuel. In this work, the addition of the oxygenated biofuels (ethanol and biodiesel) further reduced the unburned hydrocarbons emissions (Figure 29).

The light-saturated HC (methane and ethane) and the unsaturated HC (acetylene, ethylene, and propylene) species, shown in Figure 30, have been separately analyzed from the heavy HC in order to provide an in-depth analysis of the THC. The heavy hydrocarbons solely correspond to approximately 88%, 85%, and 78% of THC for diesel, D50E15B35, and FTD50E15B35, respectively. The decrease in the heavy HC (seen in Figure 29) follows the same trend for the blends as with the THC. On the other hand, higher emissions of the light HC species (saturated and unsaturated) were measured for the FTD50E15B35 and D50E15B35 as compared to diesel fuel. This result could be attributed to the thermal decomposition of the alcohol component of the blends into shorter molecules of HC (i.e., light HC species) and CO,

as discussed by Fayad et al.(FAYAD, M. A. *et al.*, 2018). Nevertheless, the combustion of diesel is likely to produce heavier HC, which supports the reduction of the THC for the blends. As the literature review indicated, the few previous works that considered blending F-T diesel/ethanol/biodiesel have not reported the heavy- or light-hydrocarbons in their investigations. Therefore, the present work also contributes to this aspect.

Also, formaldehyde is the intermediate product of incomplete combustion of alcohol fuel, being another unregulated emission. It is a member of the carbonyl compound and is related as a strong pollutant to the atmosphere once it behaves as a basis of free radicals for tropospheric photochemistry, as discussed in Tira et al. (TIRA *et al.*, 2014). The equations of formation and oxidation rates of CH_2O are described in Zhou and Qiu (ZHOU; QIU, 2019). Also, it may affect human health through eyes and lung irritation (EL MORABET, 2018). The measured emissions of CH_2O increased respectively 45% and 52% for FTD50E15B35 and D50E15B35 in comparison with diesel fuel.
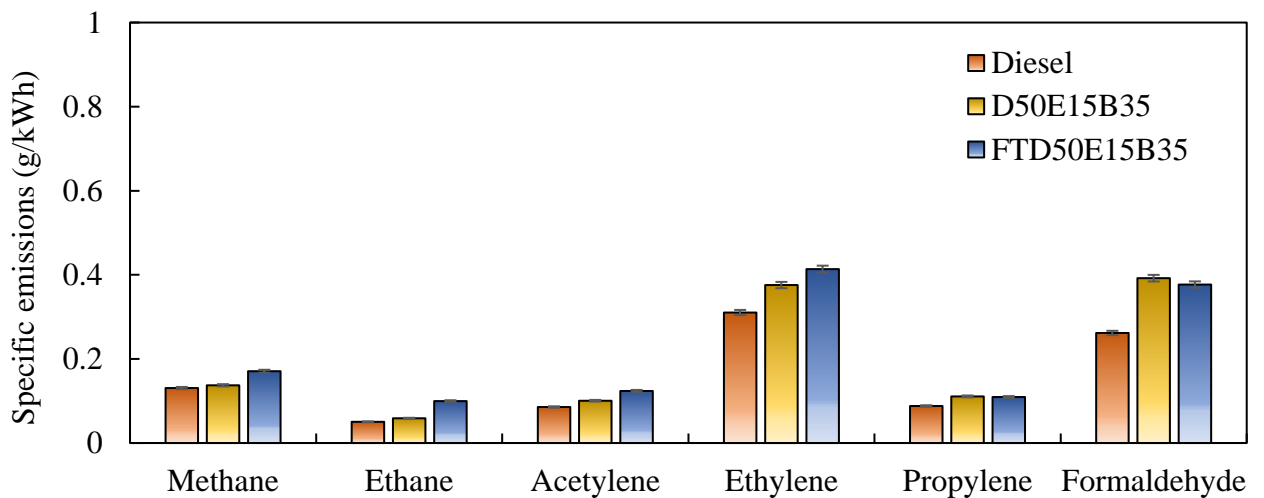
Figure 30. HC speciation for diesel, D50E15B35, and FTD50E15B35 at 2 bar IMEP and 1500 rpm.

5.3.3 Nitrogen species

Figure 31 shows the results of NO_x exhaust emission for diesel, FTD50E15B35, and D50E15B35 at 2 bar IMEP and 1500 rpm. The NO_x emission from diesel engines mainly consists of NO and NO_2, in about 90% and 5%, respectively, and also includes N_2O, N_2O_3, and N_2O_4. Hence, the NO_x emissions can mainly be referred to as NO. Previous works have discussed oxygenate fuel blends to mainly increase NO_x emissions, e.g., (ARMAS; GARCÍA-CONTRERAS; RAMOS, 2014; YILMAZ, Nadir; VIGIL; BENALIL; *et al.*, 2014), with some studies

have reported a slight reduction (CARVALHO, Márcio *et al.*, 2020). Additionally, it has been reported that the presence of aromatics may increase NO_x emissions, so the engine operating conditions must be considered (REIJNDERS; BOOT; DE GOEY, 2016). Moreover, the lower cetane number of the ethanol leads to an increase in the ignition delay, which increases the heat release rate during the combustion process because of the higher fuel amount in the combustion chamber, as discussed in Yilmaz et al. (YILMAZ, Nadir; VIGIL; BENALIL; *et al.*, 2014) and Gnanamoorthi and Devaradjane (GNANAMOORTHI; DEVARADJANE, 2015).
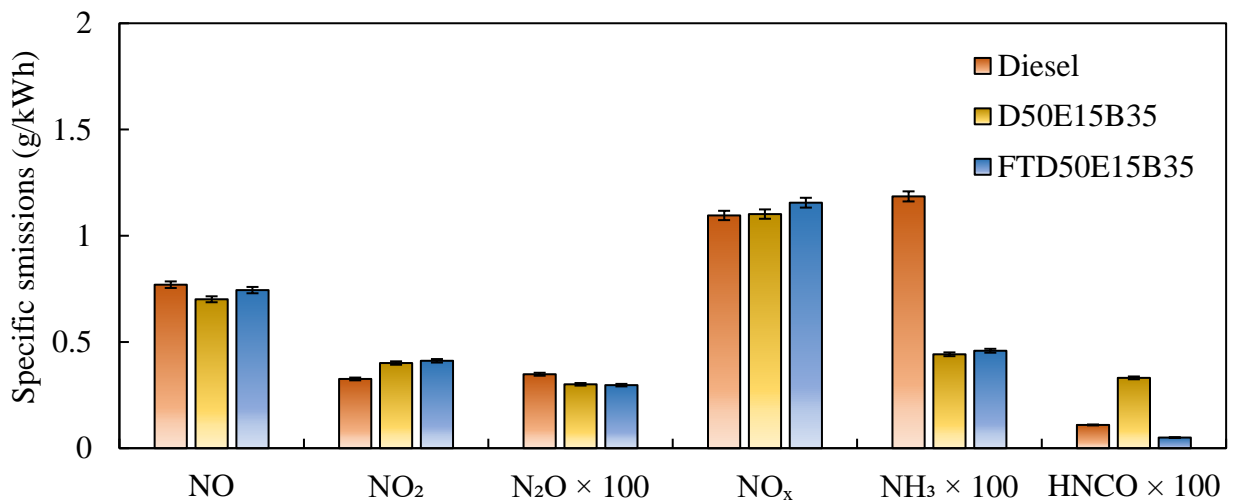
Figure 31. Effect of diesel, D50E15B35, and FTD50E15B35 on NO, NO_2, N_2O, NO_x, NH_3, and HNCO emissions at 2 bar IMEP and 1500 rpm.

Besides, it has been previously reported by Ye et al. (YE, Lihua *et al.*, 2020) that F-T diesel decreases NO_x emissions in comparison with diesel fuel. However, it was observed that the NO emissions had decreased around 2% and 8%, respectively, for FTD50E15B35 and D50E15B35 blends in comparison to diesel fuel. Also, the NO_2 emissions increased for these blends, which resulted in a similar or slight increase in the NO_x. In general, the NO_x results have shown a slight increase in nitrogen oxides emissions (4-5%) with the use of the FTD50E15B35 blend in comparison with diesel and D50E15B35 blend (Figure 31). This is probably due to the biodiesel addition, which increased the oxygen content of the blend and may contribute to increasing the combustion temperature and thereby providing additional oxygen for NOx formation. Similar results with oxygenated biofuels (ethanol and biodiesel) have been reported in the literature (DE OLIVEIRA; VALENTE; SODRÉ, 2017; MARTINS *et al.*, 2013). The higher oxygen content led to modified combustion patterns (Figure 26) and increased ignition delay.

The NO$_x$ emissions are directly dependent on high combustion temperatures, and thus ethanol could reduce the NO$_x$ formation as a result of its high heat of evaporation that reduces the in-cylinder temperatures. The temperature is one of the major influences on NO$_x$; however, the emissions depend on other parameters such as pressure, droplet sizes, type of combustion chamber, and others. For further details, please refer to the available literature (AHMED *et al.*, 2021; GLARBORG *et al.*, 2018).

The N$_2$O, which is not usually taken into account in the NO$_x$ emissions, was also measured. The emissions of N$_2$O have decreased around 13% for both FTD50E15B35 and D50E15B35 blends when compared to diesel fuel. Moreover, Herreros et al. (HERREROS; GILL; *et al.*, 2014) have referred to N$_2$O as a harmful greenhouse gas promoter and also one of the responsible for ozone destruction. Detailed reaction and formation equations of N$_2$O may be consulted in Glarborg et al. (GLARBORG *et al.*, 2018).

Also, the exhaust emissions results included other unregulated emissions, as in the case of the light fuel-nitrogen species NH$_3$ and HNCO. NH$_3$, another important nitrogen compound. It was observed that the NH$_3$ emissions reduced nearly 60% in the combustion of E15B35FTD60 and D50E15B35 concerning diesel. NH$_3$ is a precursor to secondary inorganic PM formation and secondary inorganic aerosol (i.e., NH$_4$NO$_3$, ammonium nitrate, and (NH$_4$)$_2$SO$_4$, ammonia sulfate) (SUAREZ-BERTOA *et al.*, 2017).

Moreover, as discussed in Kumar et al. (KUMAR, Vikram; SINGH; AGARWAL, 2020), HNCO emission is a key critical unregulated species. It can be formed at large levels when NO, CO, and either H$_2$ or NH$_3$ react in the presence of precious metals (e.g., platinum, palladium, or rhodium) (BRADY *et al.*, 2014). Also, as paraphrased by Brady et al. (BRADY *et al.*, 2014), exposure to the gas-phase HNCO is related to human health issues. The formation mechanisms and reactions of HNCO are described in Glarborg et al. (GLARBORG *et al.*, 2018). It was observed that the lowest values of HNCO occurred for the combustion of FTD50E15B35, diesel, and D50E15B35, respectively. In comparison with diesel fuel, FTD50E15B35 reduced the HNCO emissions by about 54%, whilst reduced nearly 85% as compared to D50E15B35.

5.4   Particle Size Distribution

Figure 32 shows the particle size distributions (PSD) resulting from the combustion of diesel, D50E15B35, and FTD50E15B35. According to the results, for most of the particle sizes, the concentration from diesel combustion is significantly higher than that obtained from the combustion of D50E15B35 and FTD50E15B35. The lower particulate number concentration

resulting from the combustion of ethanol/diesel/biodiesel blend when compared to diesel fuel has been previously reported in the literature (GHADIKOLAEI *et al.*, 2020; TSE; LEUNG; CHEUNG, 2015).
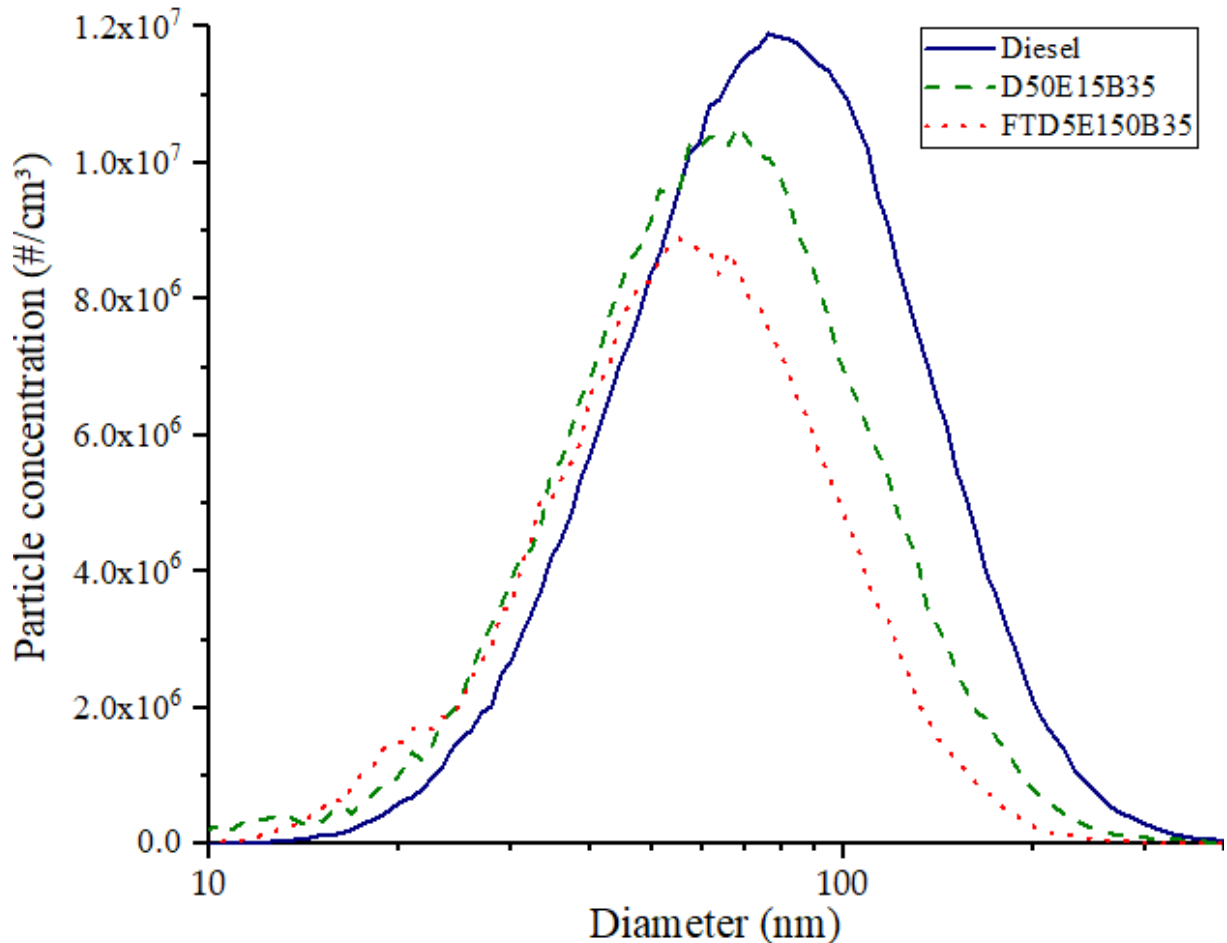
Figure 32. Effects of diesel, D50E15B35, and FTD50E15B35 on particle size distribution at 2 bar IMEP and 1500 rpm.

In addition, it may be noticed that the PM concentration of the FTD50E15B35 blend is lower than the D50E15B35 blend (Figure 32). The oxygen present in the hydroxyl group of ethanol and the ester group of biodiesel, the lower content of aromatics with respect to diesel fuel, and the longer proportion of premixed combustion leading to a lower number of rich in fuel regions are the main responsible for reducing particle precursors and particles themselves (SUKJIT *et al.*, 2014).

Despite FTD50E15B35 and D50E15B35 having the same oxygen content (9.0 wt %), the Fischer–Tropsch diesel composition does not have aromatics (DI; CHEUNG; HUANG, 2009), which further contributes to reducing the particulate number emitted during the

combustion process. Furthermore, Figure 33 shows that the reduction in total particle number was 14 ± 1.7% and 31 ± 1.6%, respectively, for D50E15B35 and FTD50E15B35 blend in comparison with conventional diesel.
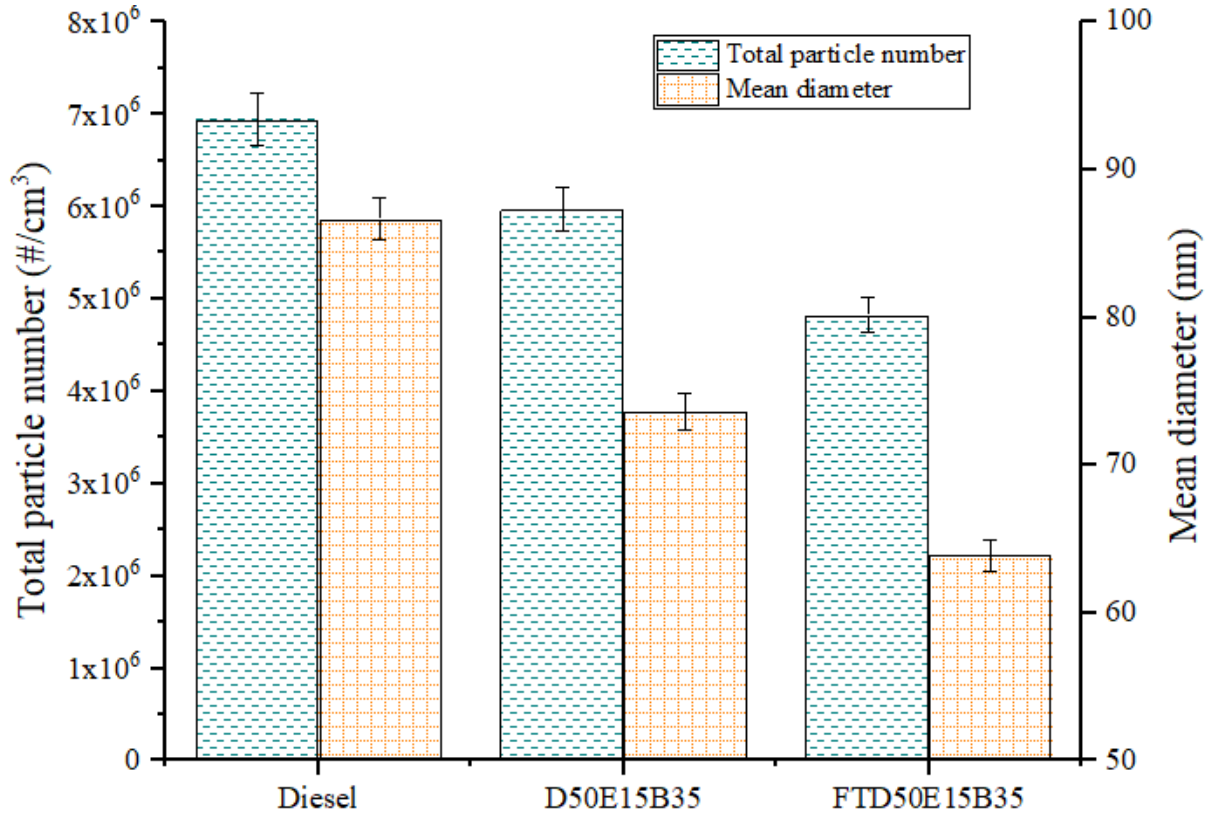
Figure 33. Effects of diesel, D50E15B35, and FTD50E15B35 on total particle number and mean diameter at 2 bar IMEP and 1500 rpm.

Figure 34 shows an estimative of the total particle mass concentration for diesel, D50E15B35, and E15FTD based on the number of particle size distribution particles. A practical particle density function enabled the calculation of an apparent particle density (LAPUERTA, Magín; ARMAS; GÓMEZ, 2003). The particle mass result indicates that both blends had reduced the PM emissions in comparison with diesel fuel by 68 ± 1.6% and 86 ± 1.6%, respectively, for D50E15B35 and FTD50E15B35. Furthermore, FTD50E15B35 is an advantageous fuel for lowering particulate matter emissions in comparison with diesel.
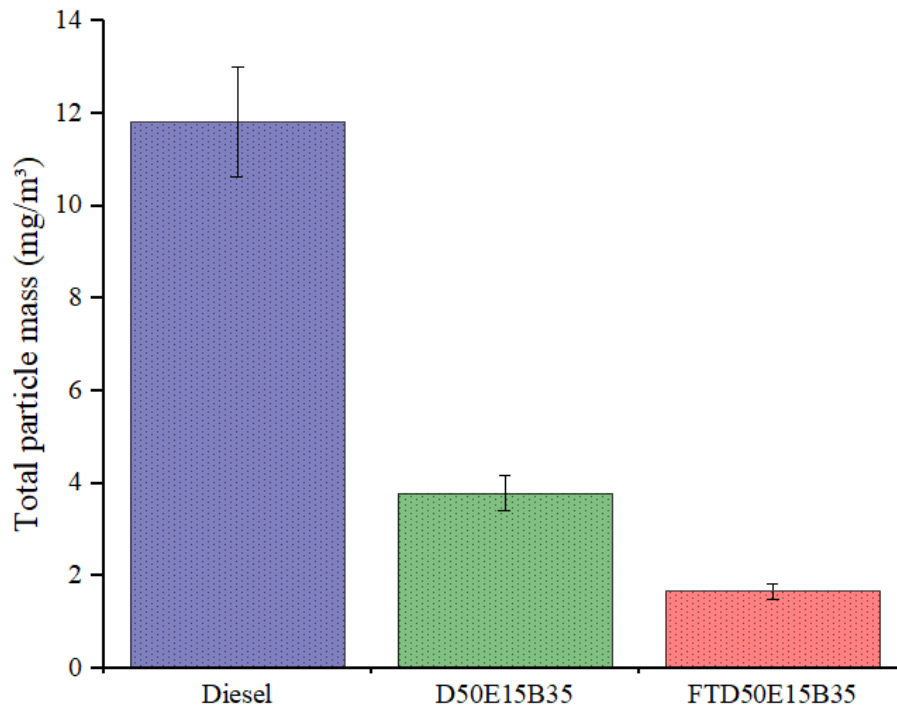
Figure 34. Effects of diesel, D50E15B35, and FTD50E15B35 on total particle mass at 2 bar IMEP and 1500 rpm.

Regarding the mean particle diameter, the results suggest that both FTD50E15B35 and D50E15B35 produce a reduction of the particle mean diameter in comparison with diesel of approximately $15 \pm 1.7\%$ and 26 ± 1.6, respectively. The reduction in the mean particle size can be mainly explained by a significant reduction in the number of large particles. This was possibly a result of a lower likelihood of particle collision and the formation of larger particulate matter agglomerates (HERREROS *et al.*, 2015; LAPUERTA, Magín *et al.*, 2010) rather than by an increase in the number of small size particle concentrations, which are more difficult to trap and are commonly associated with human health issues (ZHANG, Zhi Hui; BALASUBRAMANIAN, 2018).

Table 19. Properties of particle matter for diesel, D50E15B35, and FTD50E15B35.

Fuel	Total number (10^6 #/cm^3)	Mean diameter (nm)	Total mass[1] (10^{-9} g/cm³)
Diesel	6.95	86.67 ± 2.1	11.81
D50E15B35	5.97	73.60 ± 1.9	3.79
FTD50E15B35	4.82	63.85 ± 0.3	1.67

[1] Estimated using an agglomerate particle density function (LAPUERTA, Magín; ARMAS; GÓMEZ, 2003).

In conclusion, the use of both bio blends resulted in the slight shifting of the particle concentration curve to lower particles due to the use of oxygenated fuels (i.e., ethanol and biodiesel) (TSE; LEUNG; CHEUNG, 2016), as is indicated in Figure 24. Table 19 shows the summary of the exhaust particle number and size distribution.

Figure 35 depicts the particle size distribution of diesel, D50E15B35, and FTD50E15B35, which is obtained by arranging the particle number concentration (Figure 24) in different particle sizes. Through the addition of ethanol and biodiesel to diesel (D50E15B35), the share of nanoparticles increased considerably as the share of fine particles reduces progressively in comparison with diesel fuel. Likewise, the replacement of diesel for F-T diesel (FTD50E15B35) further increased the proportion of nanoparticles simultaneously as the fine particles also decreased. The increase in nano and ultra-fine particles number as the size of the fine particles decreased could be explained due to oxygenated fuels being able to boost atomization characteristics and promoting better vaporization (ZHANG, Wugao *et al.*, 2014). The higher oxygen content entering the combustion chamber boosts the particles' oxidation rate, and the particles were gradually oxidized (XU, Zhengxin *et al.*, 2020). The oxygen content presented in the blends promotes fine particles to be oxidized into ultra-fine particles and thus decreasing the share of fine particles.

It is also shown in Figure 35 that the D50E15B35 blend has a higher share of nanoparticles (approximately 11% more particles), a similar share of ultra-fine particles (0.6% less), and fewer share of fine particles (roughly 12% less) in comparison with diesel fuel. Also, the FTD50E15B35 blend has a higher share of nanoparticles (about 83%), shows no variation in ultra-fine particles, and a reduction in the share of fine particles (-59%) in comparison with diesel fuel. Moreover, when comparing both blends, the FTD50E15B35 has a higher share of nanoparticles (20%), a decrease in the share of ultra-fine particles (-1%), and fine particles (-32%) as compared to the D50E15B35 blend.
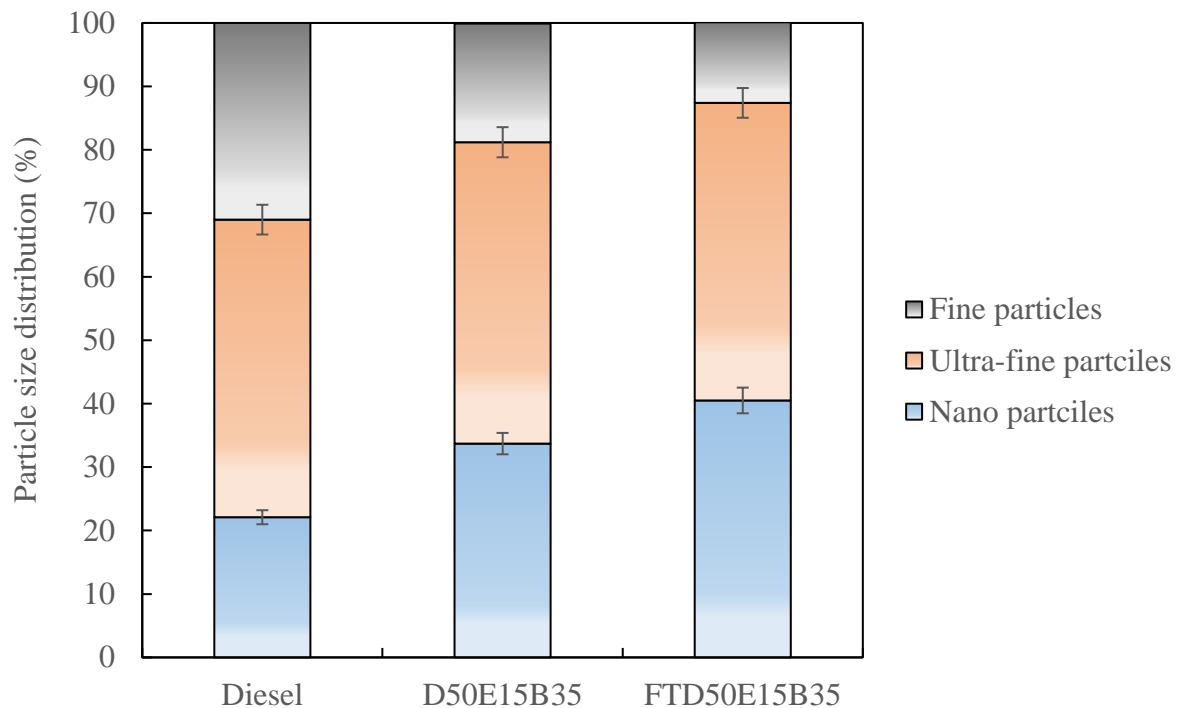
Figure 35. Effects of fuels (diesel, D50E15B35, FTD50E15B35) on particle size distribution under 2 bar IMEP and 1500 rpm.

5.5   Impact of Biofuels on a Diesel Oxidation Catalyst (DOC)

5.5.1   CO Oxidation over a Diesel Oxidation Catalyst

Figure 36 shows the catalyst CO light-off curves for all fuels. The engine exhaust emissions levels of CO from the combustion of conventional diesel are lower compared to the biofuel blends (as seen in Figure 6). Moreover, the THC emissions decreased for FTD50E15B35 and D50E15B35 in comparison with conventional diesel fuel (as seen in Figure 6). The high levels of CO in the engine-out emissions have slightly delayed the catalyst light-off activity. This is shown in Figure 36, as the temperature to reach is 50% of conversion efficiency is shifted to the right (i.e., higher temperatures than for the diesel fuel). This may be explained because CO can be adsorbed strongly in the catalyst and hence be the dominant species on the catalyst surface, which has been previously reported in the literature (WATLING *et al.*, 2012).
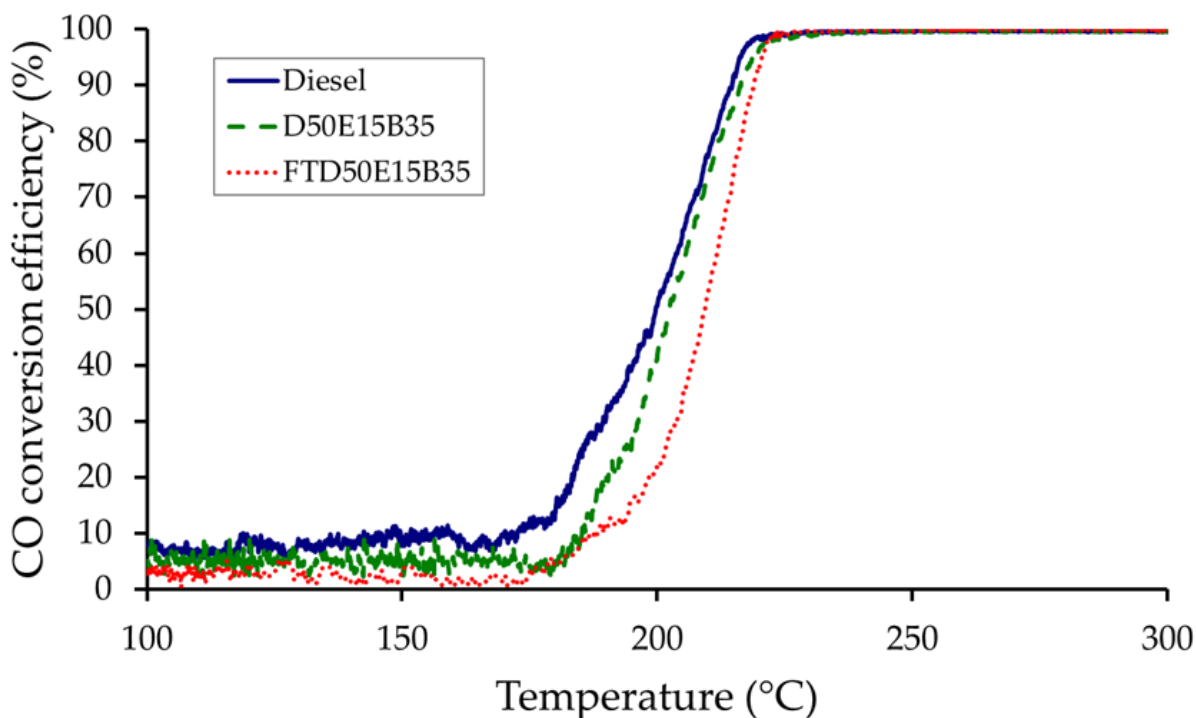
Figure 36. CO light-off curves from the exhaust gas produced for diesel, D50E15B35, and FTD50E15B35 at 2 bar IMEP and 1500 rpm.

Moreover, Pt-group metals only show sufficiently high activity for CO oxidation above ~150 °C, which suggests that catalytic oxidation of CO may be kinetically limited at low temperatures (KIM *et al.*, 2017). Therefore, CO could self-inhibit the start of CO oxidation on the DOC catalyst, thus shifting the light-off into higher temperatures (Figure 37). It has been previously explained in the literature that at lower temperatures, higher concentrations of CO inhibit the rate of reaction in the catalyst. Although, as the reactant is oxidized at higher temperatures, the rate of reaction is increased (YE, Shifei *et al.*, 2012). A similar trend was previously reported for butanol/biodiesel/diesel blend and pure biodiesel when compared to conventional diesel, as the latter had earlier catalyst light-off than the oxygenated fuel blends (FAYAD, Mohammed A. *et al.*, 2015).

Furthermore, competitive adsorption on the same active sites by hydrocarbons (see Figure **38**) and nitrogen oxide (see Figure 39) promotes reciprocal inhibition by each other and thus affecting CO oxidation (AL-HARBI *et al.*, 2012; OH; LUO; EPLING, 2011). Previous reports have discussed that both NO and NO_2 can quickly adsorb and dissociate towards Pt and Pd active sites. This may generate a high coverage of adsorbed nitrogen species and oxygen atoms on the active sites, which limits CO adsorption. As a result, adsorption competition may

difficult CO access to the catalyst's active sites limiting the oxidation of CO (LEFORT; HERREROS; TSOLAKIS, 2014; WATLING *et al.*, 2012).
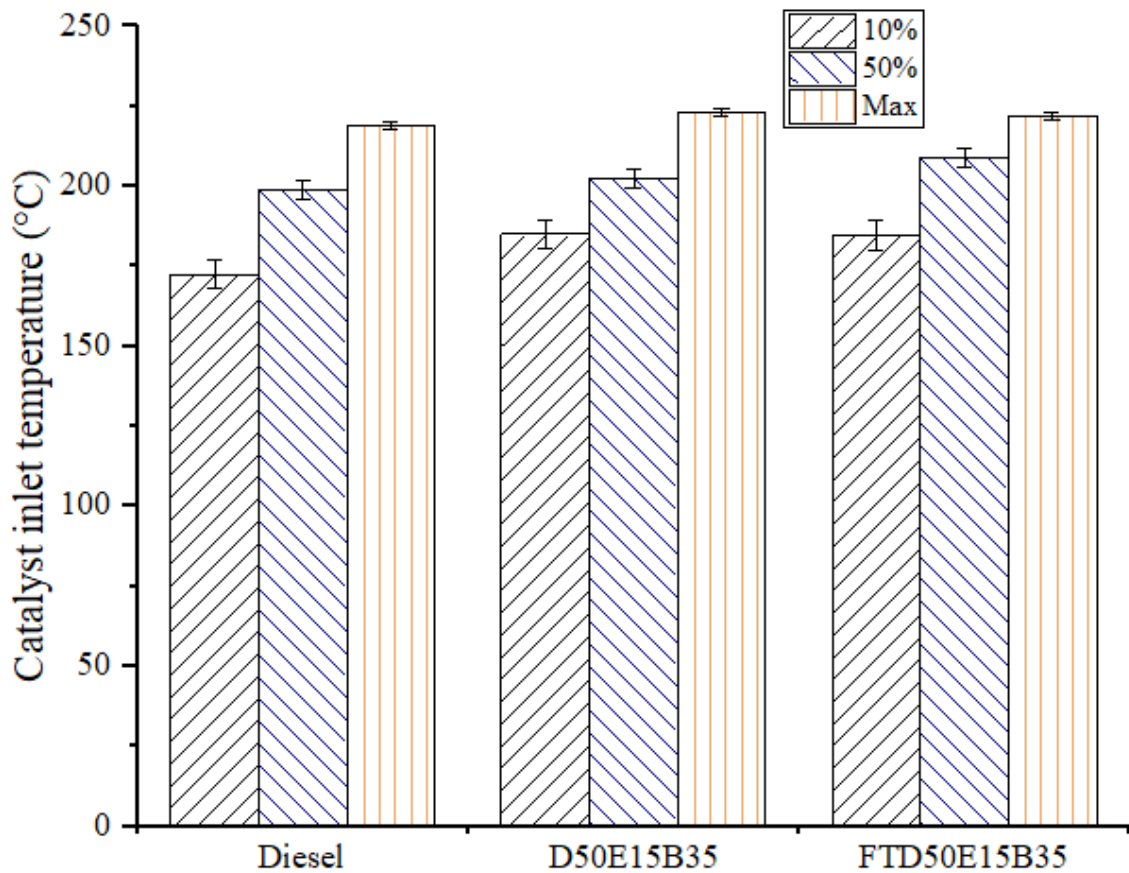
Figure 37. Diesel oxidation catalyst (DOC) inlet temperature that was required to reach 10%, 50%, and maximum CO conversion for diesel, D50E15B35, and FTD50E15B35 at 2 bar IMEP and 1500 rpm.

As observed in the emission results, the combustion of FTD50E15B35 produced higher CO exhaust emissions in comparison with diesel fuel and D50E15B35. Hence, as soon as oxidation starts, it increases the local catalyst's temperature and activity and therefore increases the CO oxidation reaction rate. Consequently, although this synthetic alternative fuel blend presented later light-off, it reached the maximum conversion efficiency in a lower temperature difference than the other tested fuels, as seen in Figure 37.

5.5.2 THC Oxidation over a Diesel Oxidation Catalyst

Figure 38 shows the total hydrocarbon conversion efficiency from the combustion of different fuels. Hydrocarbon conversion at low catalyst temperatures over the diesel oxidation catalyst should be considered a "virtual conversion" because it is a result of the trapping effect

by catalyst zeolites, once the hydrocarbons are not exactly oxidized but just temporarily kept over the catalyst zeolites (FAYAD, Mohammed A. *et al.*, 2015; LEFORT; HERREROS; TSOLAKIS, 2014). It has been previously discussed that CO is considered as an inhibitor for itself and the oxidation of other species.
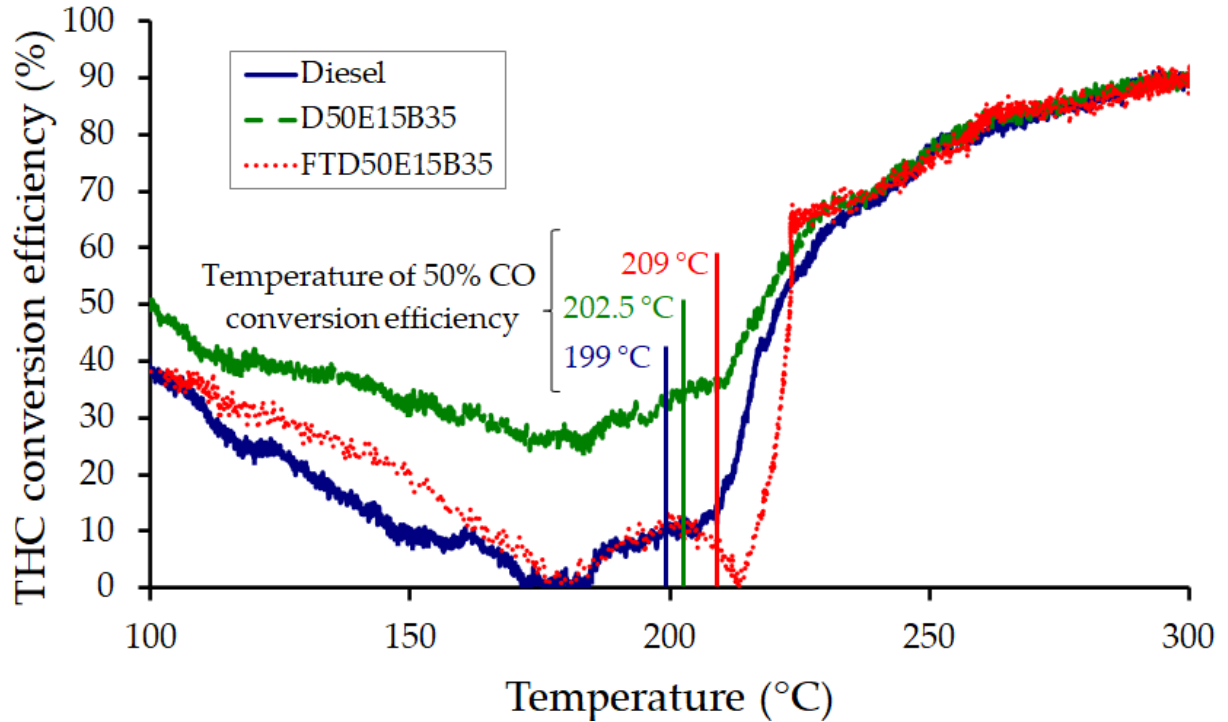
Figure 38. Total hydrocarbons (THC) light-off curves from diesel, D50E15B35, and FTD50E15B35 combustion at 2 bar IMEP and 1500 rpm.

It is possible to observe in Figure 36, and Figure 38 that hydrocarbon oxidation is promoted after the maximum rate of oxidation is reached for CO. As CO oxidation over the DOC catalyst increases due to a rise in reaction temperature, hydrocarbon adsorption starts onto catalyst active sites. Further, it seems that, for all fuels, the start of hydrocarbon oxidation only occurs when at least 50% of the CO has been oxidized. The THC light-off curves seem to show that between 170 °C to 230 °C, there is a plateau in conversion efficiency for the D50E15B35. Moreover, the graph illustrates that there was no conversion efficiency around 180 °C for diesel and FTD50E15B35. At this temperature interval (170-230 °C), the rate of conversion efficiency decreased to a minimum value, as there were fluctuations in the oxidation reactions in the DOC catalyst. It should be noticed that this specific temperature interval is correlated with CO oxidation interval from the required temperature to reach 10% conversion efficiency to its maximum conversion, previously shown in Figure 37.

Furthermore, the higher conversion efficiency of THC was noticed for the D50E15B35 in comparison with the diesel fuel. This may be explained, as the blend is expected to have lower aromatic hydrocarbons than pure diesel, which have been reported to be more difficult to be adsorbed and oxidized (AYDIN; ILKILIÇ, 2010; DEMIDYUK *et al.*, 2011; PATTERSON; ANGOVE; CANT, 2000). Additionally, it has been formerly discussed that NO could compete with HC for adsorption over the catalyst, thus limiting hydrocarbon oxidation (IRANI; EPLING; BLINT, 2009; LEFORT; HERREROS; TSOLAKIS, 2014). Moreover, the hydrocarbons from FTD50E15B35 exhaust combustion gas had been limited to start their oxidation only when CO has reached nearly maximum conversion efficiency. On the other hand, the conversion of HC for FTD50E15B35 increases and reaches a higher level of conversion efficiency immediately after CO has fully oxidized over the catalyst's active sites.

5.5.3 NO to NO_2 Oxidation over DOC Catalyst

Figure 39 shows the oxidation of NO to NO_2 in the DOC catalyst. This reaction is directly affected by the concentration of CO, THC, and NO in the exhaust. The results have shown that at low temperatures, NO_2 is reacting with CO and HC in the catalyst since the concentration of NO_2 is lower than the engine-out exhaust emission (see Figure 31).

Once O_2 has oxidized CO, it was observed an increase in NO_2 concentration for all fuels at nearly the same temperature, around 220 °C. It should be noticed that the higher NO_2 production at low temperatures is possibly due to the oxygenated components of the FTD50E15B35 and the D50E15B35 fuels, which could enhance the formation of active oxygenated components to produce NO_2 (JOHNSON; FISHER; TOOPS, 2012).

The NO_2 concentration starts to increase downstream of the DOC oxidation catalyst at around the same temperature of approximately 290 °C for all fuels, once the CO and THC have been completely oxidized in the catalyst active sites. Therefore, it is clear that the inhibition of carbonaceous emission on NO_2 production occupying the catalyst active sites and consequently the consumption of any NO_2 resulted from the combustion reaction with CO and THC to form CO_2 (FAYAD, Mohammed A. *et al.*, 2015).
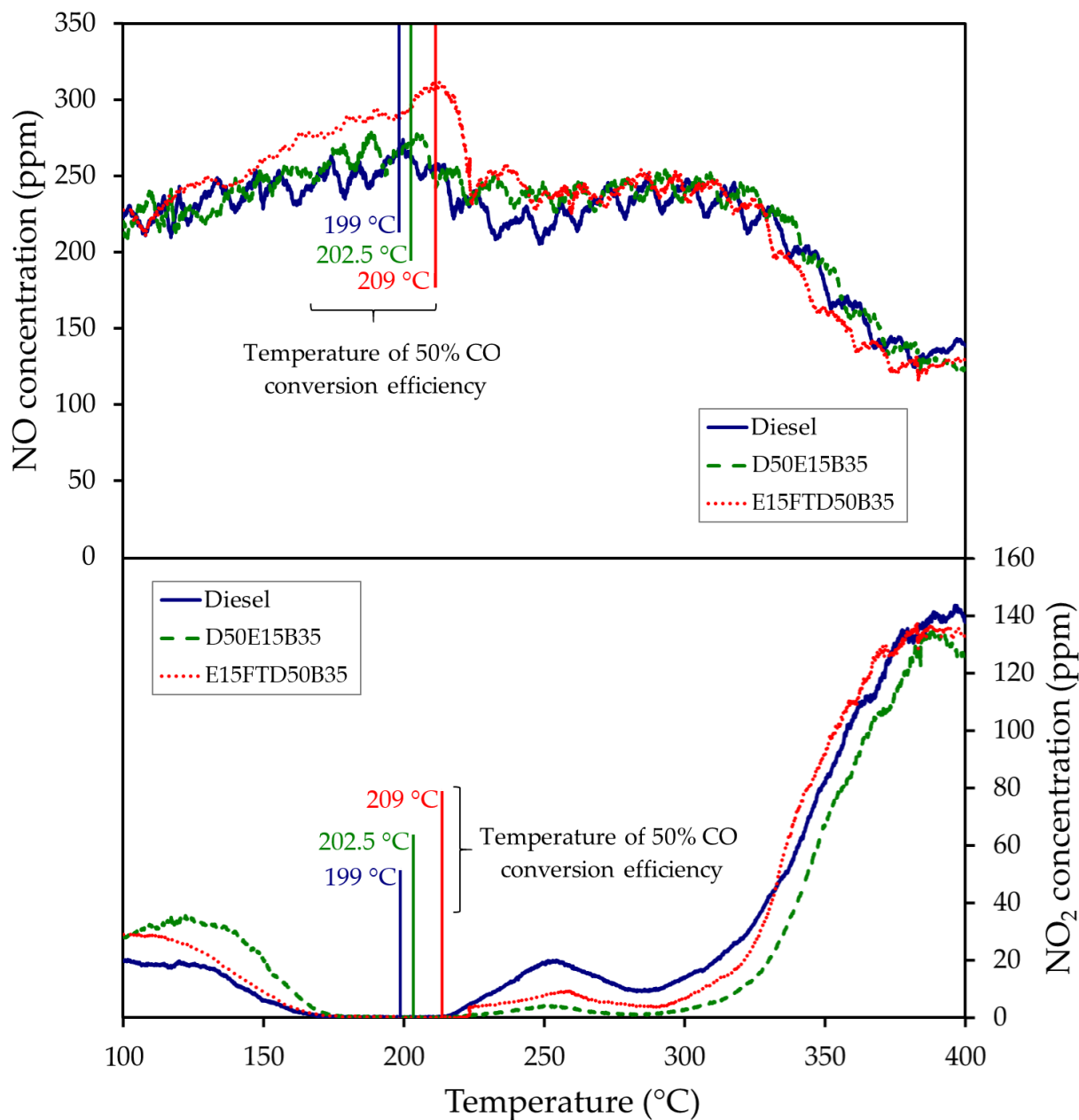
Figure 39. NO and NO_2 downstream DOC catalyst at 2 bar IMEP and 1500 rpm.

5.6   Energy analysis

In order to evaluate the effects of the fuel type on the energetic performance of the engine, the inlet and outlet energy fractions (work energy flow rate, exhaust gases energy flow rate, and energy losses flow rate) were calculated by dividing each energy component by the energy of the fuel, as shown in Table 20. During the tests, the IMEP was kept constant, whereas the fuel flow variated.

The rate of energy inlet from the fuel is mainly related to the LHV and the combustion efficiency of the fuel. The inlet fuel energy increased when the engine was fueled with the FTD50E15B35 blend compared with diesel. In order to maintain the same IMEP, when the engine was fueled with different fuels, more fuel was consumed for FTD50E15B35 (10.8% in mass) mainly due to the lower LHV (9.8%) of the blend in comparison with diesel fuel, as shown in Table 20. As for the D50E15B35 blend, the mass fuel consumption was increased by 11.8%, and the LHV decreased by 8.7% when compared with diesel. In comparison with the D50E15B35 blend, the blend of ethanol and F-T diesel (FTD50E15B35) presented a slight difference in the LHV value of approximately 1%. Previous researchers had reported similar results and found an increase in the fuel energy rate whilst the energy efficiency decreased (SARIKOÇ; ÖRS; ÜNALAN, 2020; YESILYURT, 2020) because of the difference in the LHV of the tested fuels compared to the baseline diesel.

The small variation in the energy outlet rate by exhaust gases for the evaluated fuels could be explained due to the differences in the engine-outlet exhaust gas temperature and emissions. The measured exhaust gas temperature ranged around 234-240 °C for diesel, 230-234 °C for D50E15B35, and 232-235 °C for FTD50E15B35. The addition of ethanol to F-T diesel and biodiesel (FTD50E15B35) caused a decrease in the exhaust temperature of the engine, probably due to the alcohol cooling effect related to the higher heat of evaporation. Previous works have reported similar results of combustion temperature decrease by adding ethanol to diesel or biodiesel (TUTAK *et al.*, 2017).

Table 20. Energy distribution in the engine control volume.

Fuel	Fuel energy rate (kW)	Work rate (kW)	Exhaust gas energy rate (kW)	Heat losses rate (kW)
Diesel	4.70	1.25	1.58	1.87
D50E15B35	4.74	1.25	1.45	2.04
FTD50E15B35	4.75	1.25	1.59	1.92

In addition, as the exhaust energy is directly related to the engine output emissions, the slightly higher emissions for FTD50E15B35 of some measured species have influenced the exhaust energy rate. Although, for the blend D50E15B35, the exhaust energy rate of the blend was mainly affected by the lower CO_2 amount in the exhaust and presented the lowest value among the tested fuels. Nevertheless, the released amount of energy rate in the exhaust might be partially recovered and thus enhance the energy efficiency (BOURHIS; LEDUC, 2010).

Moreover, other losses such as the heat transfers from the cylinder walls and by the coolant were merged to simplify the control volume.

Figure 40 shows the energy balance of diesel, D50E15B35, and FTD50E15B35. The graph shows that 26.6% of the inlet fuel energy of diesel fuel was converted to outlet engine work, 33.6% was discharged in the exhaust gases, whereas the remaining (39.8%) was computed as energy losses. Similarly, for the combustion of FTD50E15B35, the energy distribution has revealed that 26.2% of the inlet energy was transformed into outlet work, 33.4% was lost through exhaust gases, and it can be deduced that 40.3% of the inlet energy is lost through heat transfer. Similar results were reported by previous works (HOSEINPOUR *et al.*, 2017; JENA; MISRA, 2014).
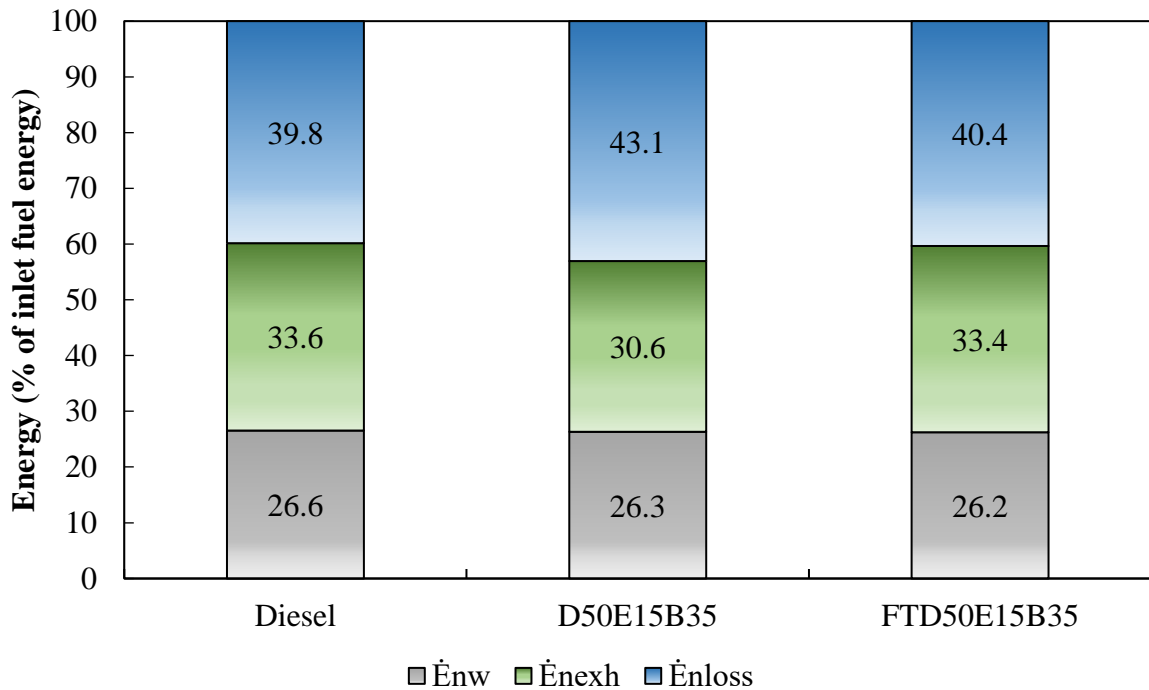
Figure 40. Energy balance of the engine for each tested fuel.

Sarıkoç et al. (SARIKOÇ; ÖRS; ÜNALAN, 2020) found that the mixture of butanol (5-20% v/v), biodiesel (20% v/v), and diesel (60-75% v/v) resulted in lower outlet work energy and energy efficiency than when using diesel fuel. The researchers stated that the addition of biodiesel and butanol resulted in a reduction in the LHV of the blends, which caused a decrease in energy efficiency. In the present work, the energy balance analysis resulted in the lower energy efficiency of the engine when fueled with FTD50E15B35 as a result of the higher fuel energy rate of the blend concerning the diesel fuel.

5.7   Exergy analysis

An energy analysis of the engine does not provide enough data enabling the determination of the overall losses and the efficiency regarding the engine operation when it is fueled with different fuels. Hence, the exergy analysis complements the thermodynamic analysis of the diesel engine.

The exergy analysis was calculated through the experimental data of the diesel engine based on the used fuel and blends. The inlet fuel exergy rate and the outlet exergy (work outlet exergy, exhaust exergy, exergy loss, and exergy destruction) values were determined by dividing each exergy component by the exergy of the fuel, as given in Table 21.

The results for the fuel energy and for the fuel exergy rates shown a similar trend for diesel fuel, D50E15B35, and FTD50E15B35, as both are functions of the fuel mass flow rate and their LHV. There was an increase in the fuel exergy when the diesel engine was fueled with the FTD50E15B35 blend in comparison with diesel. Moreover, the inlet exergy rates of the evaluated fuels were increased in comparison with the inlet energy rates. The results have shown that the inlet exergy of the tested fuels ranged from 6.7-7.4% higher in comparison with its respective inlet energy. This is attributed to the chemical exergy factor of FTD50E15B35 and D50E15B35. At the respective engine operational condition, the fuel exergy rates for diesel, D50E15B35, and FTD50E15B35 were found to be in the range of 5.01-5.10 kW, respectively. The higher value for the FTD50E15B35 blend is attributed to the increased fuel consumption compared to the engine fueled with diesel fuel, which was required to maintain the same indicated power. These findings are in agreement with previous works in the literature using blends of biofuels (KHOOBBAKHT; AKRAM; *et al.*, 2016). Paul et al. (PAUL; PANUA; DEBROY, 2017) reported that this behavior is attributed to the increase in fuel consumption as a result of the decrease in the LHV and an opposite relation between the fuel inlet exergy and the exergy efficiency.

The exergy outlet rate within the exhaust gases had slightly decreased when the engine was fueled with the biofuels in the blends. This is because the higher the exhaust gas temperature, the higher is the exhaust gas exergy rate (VERMA *et al.*, 2018). In the present work, the exhaust gas temperature decreased for the combustion of the D50E15B35 and FTD50E15B35 blends compared to diesel. A similar result was reported by Kul and Kahraman (SAYIN KUL; KAHRAMAN, 2016). Their research reported that the exhaust exergy was affected by the exhaust gas temperature and that the latter was slightly higher for diesel fuel

than for the tested blends of diesel/biodiesel/ethanol. The lost exergy rate through the exhaust gases has decreased by 3.8% for D50E15B35 and 1.9% FTD50E15B35 blends, respectively. Moreover, the exergy loss rates of the tested fuels were determined as 0.29-0.32 kW. The other exergy losses have shown a similar trend with the energy losses, whereas the FTD50E15B35 blend presented a higher value than diesel fuel.

The exergy destruction rate or irreversibility rate indicates the rate of the available work, which is destroyed due to irreversible processes that occur in the control volume (DA SILVA *et al.*, 2018). It is observed that the exergy destruction of the FTD50E15B35 and D50E15B35 blends were found to be respectively 2.4% and 1.8% higher than for the diesel fuel. Previous investigations have reported that the addition of biodiesel to diesel increases the exergy destruction rate of the blends in comparison with pure diesel (KARAGOZ *et al.*, 2021). Sarıkoç et al. (SARIKOÇ; ÖRS; ÜNALAN, 2020) obtained lower values of exergy destruction rate with diesel/biodiesel/butanol blends rather than with diesel fuel. The researchers have attributed this result to the decrease in the combustion temperature promoted by the alcohol addition, although the pure biodiesel fuel and the diesel/biodiesel blend had lower values than the ternary blends.

Table 21. Exergy distribution in the engine control volume.

Fuel	Fuel exergy rate (kW)	Work rate (kW)	Exhaust gas exergy rate (kW)	Heat losses rate (kW)	Exergy destruction rate (kW)
Diesel	5.01	1.25	0.28	0.29	3.20
D50E15B35	5.08	1.25	0.26	0.32	3.25
FTD50E15B35	5.10	1.25	0.27	0.30	3.29

The entropy generation assists in comprehending the system's irreversibilities. It supports the evaluation of the thermal performance of combustion engines (YESILYURT, 2020). The irreversibility in a system results in entropy generation, which is directly related to the exergy destruction rate. At the evaluated engine condition, the entropy generation of diesel, D50E15B35, and FTD50E15B35 were respectively 0.0107, 0.0109, and 0.0110 kW/K. This could be partially explained by the higher mechanical friction at lower engine loads, as previously reported in (HOSEINPOUR *et al.*, 2017), which is the major thermodynamic

irreversibility of combustion engines. However, the friction losses were not covered within this work.

Moreover, it has been reported that higher fuel consumption, as well as the combustion process itself, lead to more irreversibilities (SARIKOÇ; ÖRS; ÜNALAN, 2020). Kavitha et al. (KAVITHA; JAYAPRABAKAR; PRABHU, 2019) have reported that the exergy destruction rate was higher with diesel fuel than with diesel/biodiesel/ethanol blends, and thus the entropy generated increased. However, Kul and Kahraman (SAYIN KUL; KAHRAMAN, 2016) have found higher exergy destruction rates for 8-25% (v/v) of biofuels (biodiesel/ethanol) blended with a diesel under the same experimental engine operating condition when compared to reference diesel. This can be explained by the difference between the injection systems (common-rail or conventional injection system) used in these researches, which affects the timing that the fuel is injected, as it varies with the compressibility of the fuel, and the ignition time, which varies with the cetane number of the fuel blend. Also, as shown in Equations (36) and (37), the term φ is directly proportional to the loss (i.e., higher φ leads to higher losses) and φ is higher in the blends, because of the increased fuel mass fractions of c, h, and o.

Similar to the energy analysis, the exergy balance of each tested fuel was determined based on the inlet fuel exergy. Thus, the exergy balance of diesel, D50E15B35, and FTD50E15B35 are shown in Figure 41. The graph shows that 24.4% of the available inlet fuel exergy of FTD50E15B35 was used in the form of work, 5.3% was discharged within the exhaust gases, 5.8% was computed as energy losses, while 63.8% was destroyed. The exergy destruction rate represents the major fraction of the exergetic balance in the combustion engine, which is due to the irreversibilities. However, it is possible to use part of the exergy from the exhaust gases. It has been previously recognized in the literature that combustion is the major source of irreversibility inside the ICE cylinder (ÖZCAN, 2019; VERMA *et al.*, 2018).

Hoseinpour et al. (HOSEINPOUR *et al.*, 2017) stated that the fuel type does not show an apparent effect on the exergy losses or irreversibilities in the engine. The researchers argued that this could be due to the many variables that affect the irreversibilities. Moreover, Şanli and Uludamar (ŞANLI, Bengi Gözmen; ULUDAMAR, 2020) have reported that only a slight difference was observed among the destruction exergy rate of the different biodiesels with respect to diesel fuel and also concluded that the fuel type was not effective on the irreversibilities fraction.
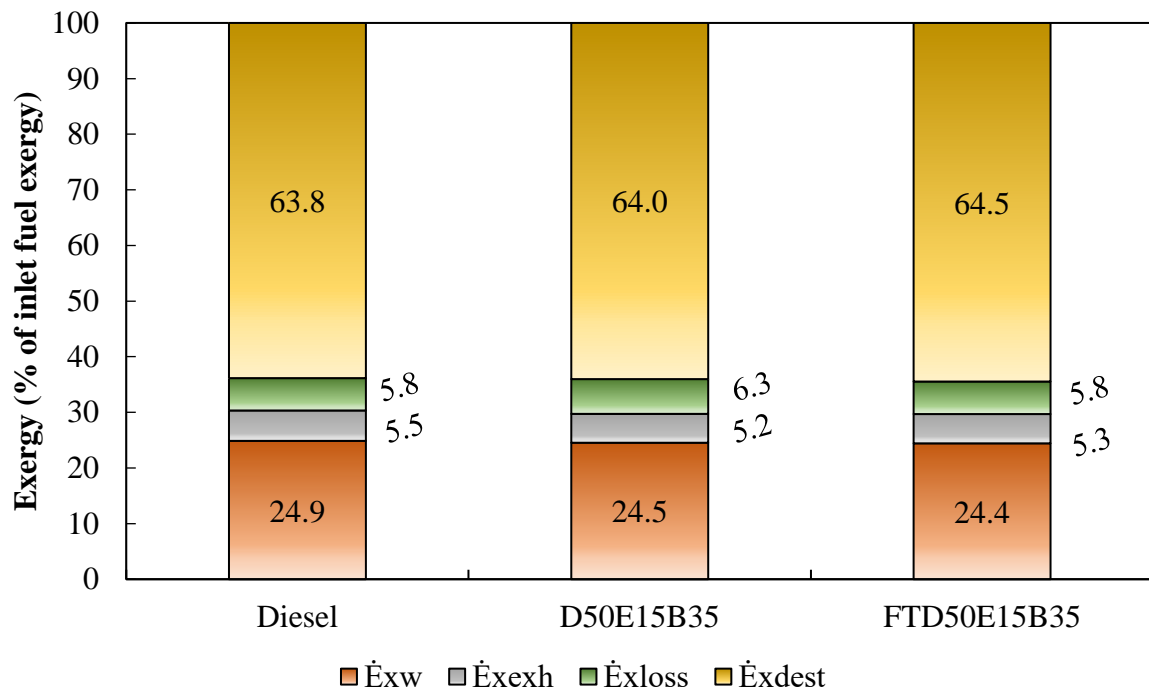
Figure 41. Exergy balance of the engine for each tested fuel.

The comparison between the energy and exergy efficiency (i.e., energy and exergy outlet work) shown in Figure 42(a)-(e) demonstrates that both efficiencies had similar findings, approximately 26% and 24%, respectively, with a small variation between them. The exergy efficiencies were slightly lower than the corresponding energy efficiency. This is a consequence of the different chemical exergy of the tested fuels (φ), as shown in Equations (36) and (37). The specific chemical exergy is higher than the LHV of the tested fuels. Thus, the total inlet exergy is always greater than the total inlet fuel energy, which relies on the volumetric fractions of the fuel (i.e., fuel blend proportions). As a result, the exergy efficiency is always slightly lower for fuel than the corresponding energy efficiency (VERMA *et al.*, 2018).

Moreover, Hoseinpour et al. (HOSEINPOUR *et al.*, 2017) stated that this decrease in the exergy efficiency is because of the exergy destruction during the combustion of the fuel. It was observed that the addition of the biofuels (ethanol and biodiesel) to diesel fuel reduced both energy and exergy efficiencies, while the substitution to F-T diesel has also slightly reduced both efficiencies. This result is in agreement with the findings of Kul and Kahraman (SAYIN KUL; KAHRAMAN, 2016) utilizing blends of diesel/biodiesel/ethanol and Sarıkoç et al. (SARIKOÇ; ÖRS; ÜNALAN, 2020) with diesel/biodiesel/butanol, as compared with results using diesel fuel.
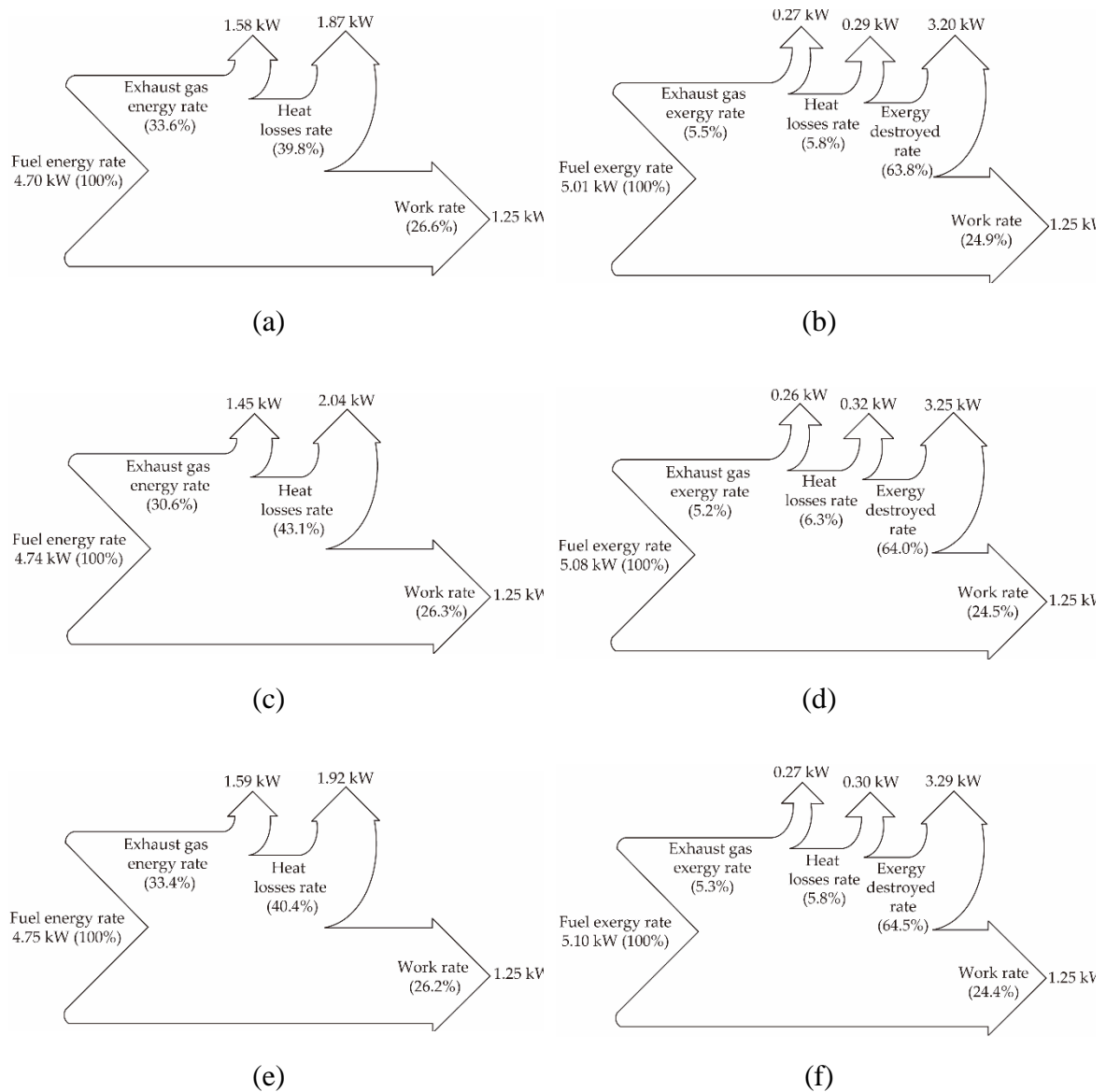
Figure 42. Energy flow (Sankey) diagrams on the left side and exergy flow (Grossman) diagrams on the right side showing the comparison of energy and exergy efficiencies of the engine fueled with (a) and (b) diesel; (c) and (d) D50E15B35; (e) and (f) FTD50E15B35.

Table 22 shows the summary of the energy and exergy efficiencies of the current work. The comparison of the present results with those by previous researchers, presented in Table 7, for different fuel types and engine operating conditions were either lower, nearly the same, or higher than that of the current work. The main reasons for the difference in these results are the fuel type, blend composition, and properties (e.g., cetane number, heating value, and others) and the experimental conditions at which the diesel engines were evaluated.

Table 22. Summary of the energy and exergy results of this work.

Engine characteristics	Operating conditions	Fuel type	Energy efficiency (%)	Exergy efficiency (%)	
1-cylinder 4 stroke	1500 rpm 2 bar IMEP (30% load)	Diesel D50E15B35 FTD50E15B35	26.2-26.6	24.4-24.9	$\eta_{diesel} >$ η_{blends} $\psi_{diesel} >$ ψ_{blends}

D: diesel fuel, B: biodiesel fuel, E: ethanol fuel, FTD: Fischer-Tropsch diesel fuel

6   CONCLUSIONS

This chapter presents the summary of the main research results in an attempt to understand the effect of alternative fuels (ethanol and Fischer-Tropsch diesel) on exhaust emissions, particulate matter (PM) characteristics, and the performance of an aftertreatment system, as well as the energy and exergy analysis. Moreover, the implications of this investigation are also presented as suggestions for future work.

The contribution of this thesis answers, at least partially, the lack of information regarding the utilization of synthetic diesel-like fuels and biofuels (ethanol and biodiesel) on the engine`s exhaust emissions, PM characteristics, and aftertreatment system. In order to partially substitute the increasing demand for fossil diesel fuel, to meet with fuel specifications, and also with sustainable policies, it is clear that alternative fuels, such as F-T diesel, could be considered. Besides, to reduce the final cost of the fuel, blending F-T diesel with others biofuels was shown to be a feasible option. Although limited literature is available, there are still aspects to be further investigated, such as those covered in this thesis.

In order to compare the effects of the proposed blend of alternative fuels, a second blend which included the conventional diesel fuel has also been tested under the same oxygen ratio and engine operation condition.

6.1   Concluding remarks

In this thesis, the results of the experimental investigation of the combustion of alternative fuels into the reduction of exhaust emissions and PM characteristics from the engine-out exhaust have been demonstrated and discussed. Different types of fuels (diesel, diesel/ethanol/biodiesel, and F-T diesel/ethanol/biodiesel blend) were employed in this experimental investigation. The volumetric fraction of ethanol and biodiesel were kept constant, at respectively 15% and 35%, for both blends, while either F-T diesel or conventional diesel fraction was 50%. Thus, the effect of substitution of diesel fuel per F-T diesel could also be evaluated.

It was found that the F-T diesel and ethanol blend can be combined to conform with the current diesel fuel standards, provided that biodiesel is added to the mixture to overcome miscibility problems and to improve the lubricity of the fuel blend. Also, the blend of diesel/ethanol/biodiesel can effectively meet the criteria. However, the energy consumption has

shown that the blend of F-T diesel/ethanol/biodiesel has similar energy consumption than the diesel fuel and the diesel/ethanol/biodiesel. Still, a higher peak HRR was observed for the F-T diesel/ethanol/biodiesel fuel blend.

The renewable fuels were effective in reducing the regulated emissions of THC, NO, and PM. However, the lower cetane number and higher latent heat of vaporization of ethanol possibly created an undesired increase in CO emissions compared to the reference fuel. Regarding FTD50E15B35, it was demonstrated that the oxygenated fuels and the also the absence of aromatics from the synthetic diesel-like fuel had a positive effect on THC reduction and also promoted a synergetic effect on the PM reduction. Moreover, the heavy-hydrocarbons have decreased as they represent the major components in the THC. On the other hand, the light-hydrocarbons, both saturated and unsaturated species, presented higher emissions than those of diesel fuel.

Nevertheless, the combustion of the diesel fuel resulted in more heavy-hydrocarbons, which endorses the overall reduction in THC for the blends. Also, it was observed that the unregulated emissions, such as N_2O, NH_3, and HNCO, decreased with the blends, more evident with F-T diesel/ethanol/biodiesel, although CH_2O slightly increased. Overall, the utilization of synthetic F-T diesel and biofuels such as ethanol and biodiesel can effectively mitigate the engine-out emissions, resulting in a similar efficiency of the engine. Only minimal literature evaluated the effects of the utilization of F-T diesel/ethanol/biodiesel on the engine emissions without in-depth engine calibration. Furthermore, none included the light hydrocarbons speciation and unregulated emissions, such as NO_2, NH_3, N_2O, CH_4, and formaldehyde.

The diesel oxidation catalyst has effectively reduced the levels of CO and THC in the exhaust, as well as NO emissions. It was found that the DOC catalyst temperatures light-off of the blended fuels have shifted to higher values due to the increased CO emissions present in the engine exhaust gases.

The combustion of the alternative fuels reduced PM number and mass concentrations, particularly the blend containing ethanol and F-T diesel. The total particle number and mass concentrations emitted from F-T diesel/ethanol/biodiesel combustion were lower than the diesel/ethanol/biodiesel blend and much lower than the diesel fuel. It may be inferred that the oxygen content of ethanol promotes positive effects on reducing the emissions of PM. Besides, the blend of ethanol, biodiesel with the incorporation of F-T diesel was demonstrated to be

more effective than the blend of diesel/ ethanol/biodiesel in providing substantial benefit to engine combustion and particle emission levels. By keeping the same oxygen content in the fuel blends, it was possible to observe the benefit of the higher cetane number and the absence of aromatic of the synthetic (F-T) fuel concerning conventional diesel. This thesis contributed to the selection of alternative fuels in the CI engines system, aiming to improve combustion characteristics, reduce exhaust pollutants, and particulate emissions.

This work also extended the understanding regarding the energetic and exergetic performance of synthesized diesel-like fuels and biofuels (ethanol and biodiesel). The energy and the exergy efficiencies were found to be similar, around 26% and 24%, respectively, with a bit of difference. The energy efficiency and exergy efficiency of the diesel engine fueled with F-T diesel and ethanol/biodiesel (FTD50E15B35) was slightly lower than for the diesel fuel due to the higher inlet fuel energy and higher fuel chemical exergy of the blend, respectively. The primary cause of the inefficiency of the engine was the destroyed exergy caused by the irreversibilities of the system, especially by the combustion process. The exergy losses from exhaust gases and from the sum of the other losses also contributed to a decrease in the efficiency of the engine.

Among the conclusions of this work, it became clear that ethanol, biodiesel, and Fischer–Tropsch diesel fuels have individual properties that, when combined, have a potential for particulate emission-reducing along with aftertreatment systems and injection strategies promoting benefits for the engine combustion, as future emissions legislation standards are foreseen to be more stringent. These findings will be beneficial for biofuel and diesel vehicle synergies to achieve emission regulations by 2050. Thus, it can be concluded that the use of alternative and sustainable fuels such as biofuels to attend the transport sector contributes to the effort to minimizing the pollution and the fossil-based CO_2 emitted by ICE. Consequently, these alternative fuels that may be used without requiring modifications to the engine can also mitigate fossil diesel utilization.

6.2   Suggestions for future work

This present investigation provided an overview of F-T diesel and ethanol blends' potential regarding engine performance and combustion, exhaust emissions (regulated, unregulated, and PM characteristics), and the impact over a diesel oxidation catalyst. Nevertheless, there are still some potential topics for further work that can be carried out.

- Some fuel properties (cetane number, heating value, density) were estimated, whereas lubricity and viscosity were not measured due to technical issues, still analyzing these properties is suggested.

- The tests were conducted with a fixed volumetric concentration of the blends (15% ethanol; 35% biodiesel; 50% diesel, and F-T diesel). An optimized model to determine the most suitable F-T diesel/ethanol/biodiesel fractions is recommended.

- An additive is indicated to enhance the miscibility problems associated with F-T diesel and ethanol blends. Cetane improvers, such as f DGE (diethylene glycol diethyl ether), cyclic peroxide, cyclohexanol, DTBP (di-tert-butyl peroxide), and others, could be considered.

- Due to the compatibility of advanced combustion strategies (i.e., RCCI and GCI) in diesel engines, it is suggested that future research investigate the performance of ethanol and FT-diesel and higher chain alcohols (i.e., butanol and pentanol). Butanol and pentanol provide better miscibility as blended with FT-diesel.

- The effect of the blends on others aftertreatment devices' efficiency (i.e., DPF and SCR catalysts) is advised to be considered.

- It is also suggested that the physical properties of PM morphology, such as (radius of gyration, number of primary particles, and fractal dimension; micro- and nano-structures) must be studied to extend the investigation on PM characteristics.

- In this investigation the effects of engine condition (speed and IMEP) were not extended. A single operating condition was used to evaluate the combustion, performance, and exhaust emissions. However, for the physicochemical properties of PM, more conditions shall be considered to comprehend the impact of the engine speed and IMEP on the PM characteristics. In addition,, it is suggested to include engine tests under transient conditions.

- To extend the thermodynamic analysis by considering the thermoeconomic, exergoeconomic, environmental, and enviroeconomic analyses.

- Also, the tested engine was equipped with a common rail fuel injection system that allowed the control of the injection parameters (injection pressures, timings, and duration). However, the influence of these parameters on the PM's morphology may be investigated.

- Finally, it is advised that for future exergy analysis, the sources' irreversibilities should be calculated and included.

LIST OF PUBLICATIONS

TORRES, Felipe Andrade; DOUSTDAR, Omid; HERREROS, Jose Martin; LI, Runzhao; POKU, Robert; TSOLAKIS, Athanasios; MARTINS, Jorge; VIEIRA DE MELO, Silvio A. B. Fischer-Tropsch Diesel and Biofuels Exergy and Energy Analysis for Low Emissions Vehicles. Applied Sciences, vol. 11, no. 13, p. 5958, 2021. DOI 10.3390/app11135958. Available at: https://www.mdpi.com/2076-3417/11/13/5958

ANDRADE TORRES, Felipe; DOUSTDAR, Omid; HERREROS, Jose Martin; LI, Runzhao; POKU, Robert; TSOLAKIS, Athanasios; MARTINS, Jorge; VIEIRA DE MELO, Silvio A. B. A Comparative Study of Biofuels and Fischer–Tropsch Diesel Blends on the Engine Combustion Performance for Reducing Exhaust Gaseous and Particulate Emissions. Energies, vol. 14, no. 6, p. 1538, 2021. DOI 10.3390/en14061538. Available at: https://www.mdpi.com/1996-1073/14/6/1538.

CARVALHO, Márcio; TORRES, Felipe; FERREIRA, Vitor; SILVA, Júlio; MARTINS, Jorge; TORRES, Ednildo. Effects of Diethyl Ether Introduction in Emissions and Performance of a Diesel Engine Fueled with Biodiesel-Ethanol Blends. Energies, vol. 13, no. 15, p. 3787, 2020. DOI 10.3390/en13153787. Available at: https://www.mdpi.com/1996-1073/13/15/3787

Conference papers:

MUNIZ, Pedro Bancillon Ventin; TORRES, Felipe Andrade; PEREIRA, Clara Rodrigues; CÂMARA, Júlio César Chaves; TORRES, Ednildo Andrade; GUARIEIRO, Lílian Lefol Nani Evaluation of Particles Size During the Combustion of Biodiesel and Optimizer Additive in a Compression Ignition Engine, Proceedings of the VI International Symposium of Innovation and Technology, Blucher Engineering Proceedings, Volume 7, 2020, p. 122-129, DOI 10.1016/siintec2020-EVALUATIONOFPARTICLES. Available at: https://www.proceedings.blucher.com.br/article-details/35606

MUNIZ, Pedro Bancillon Ventin; TORRES, Felipe Andrade; PEREIRA, Clara Rodrigues; TEIXEIRA, João Felipe; TORRES, Ednildo Andrade; GUARIEIRO, Lílian Lefol Nani Performance Evaluation, Emissions and Particle Size Distribution on A Diesel Engine Using Performance Optimizing Additive, Proceedings of the XXVIII International Symposium of Automotive Engineering, Blucher Engineering Proceedings, vol. 8, 2021, p. 228-234, DOI 10.1016/simea2021-PAP53. Available at: https://www.proceedings.blucher.com.br/article-details/36243

REFERENCES

ABU-QUDAIS, M.; HADDAD, O.; QUDAISAT, M. The effect of alcohol fumigation on diesel engine performance and emissions. **Energy Conversion and Management**, vol. 41, no. 4, p. 389–399, 1 Mar. 2000. https://doi.org/10.1016/S0196-8904(99)00099-0.

ADITIYA, H. B.; MAHLIA, T. M.I.; CHONG, W. T.; NUR, Hadi; SEBAYANG, A. H. Second generation bioethanol production: A critical review. **Renewable and Sustainable Energy Reviews**, vol. 66, p. 631–653, 2016. https://doi.org/10.1016/j.rser.2016.07.015.

AGARWAL, Avinash Kumar. Biofuels (alcohols and biodiesel) applications as fuels for internal combustion engines. **Progress in Energy and Combustion Science**, vol. 33, no. 3, p. 233–271, 1 Jun. 2007. https://doi.org/10.1016/J.PECS.2006.08.003.

AGÊNCIA NACIONAL DO PETRÓLEO GÁS NATURAL E BIOCOMBUSTÍVEIS (ANP). RenovaBio. 2021. Available at: https://www.gov.br/anp/pt-br/assuntos/renovabio. Accessed on: 7 Dec. 2020.

AGÊNCIA NACIONAL DO PETRÓLEO GÁS NATURAL E BIOCOMBUSTÍVEIS (ANP). **Resolução ANP n° 30/2016**. [*S. l.: s. n.*], 2016. Available at: http://legislacao.anp.gov.br/?path=legislacao-anp/resol-anp/2016/junho&item=ranp-30-2016 [In Portuguese]. Accessed on: 19 Sep. 2019.

AHMED, Sheikh F.; AGHDAM, Ali Charchi; DRYER, Frederick L.; FAROUK, Tanvir I. Multidimensional simulations of Mckenna-driven flow tube configuration: Investigating non-ideality in NOx formation flow tube experiments. **Combustion and Flame**, vol. 223, p. 511–524, Jan. 2021. https://doi.org/10.1016/j.combustflame.2020.10.011.

AIL, Snehesh Shivananda; DASAPPA, S. Biomass to liquid transportation fuel via Fischer Tropsch synthesis – Technology review and current scenario. **Renewable and Sustainable Energy Reviews**, vol. 58, p. 267–286, 1 May 2016. DOI 10.1016/j.rser.2015.12.143. Available at: https://linkinghub.elsevier.com/retrieve/pii/S1364032115015269. Accessed on: 23 May 2021.

AL-HARBI, Meshari; HAYES, Robert; VOTSMEIER, Martin; EPLING, William S. Competitive no, co and hydrocarbon oxidation reactions over a diesel oxidation catalyst. **Canadian Journal of Chemical Engineering**, vol. 90, no. 6, p. 1527–1538, 2012. https://doi.org/10.1002/cjce.20659.

ALKIDAS, A.C. Combustion-chamber crevices: the major source of engine-out hydrocarbon emissions under fully warmed conditions. **Progress in Energy and Combustion Science**, vol. 25, no. 3, p. 253–273, Jun. 1999. https://doi.org/10.1016/S0360-1285(98)00026-4.

ALLEMAN, Teresa L.; MCCORMICK, Robert L. Fischer-Tropsch Diesel Fuels - Properties and Exhaust Emissions: A Literature Review. 3 Mar. 2003. **SAE Technical Papers** [...]. [*S. l.: s. n.*], 3 Mar. 2003. https://doi.org/10.4271/2003-01-0763.

ANDRADE TORRES, Felipe; DOUSTDAR, Omid; HERREROS, Jose Martin; LI, Runzhao; POKU, Robert; TSOLAKIS, Athanasios; MARTINS, Jorge; VIEIRA DE MELO, Silvio A. B.

A Comparative Study of Biofuels and Fischer–Tropsch Diesel Blends on the Engine Combustion Performance for Reducing Exhaust Gaseous and Particulate Emissions. **Energies**, vol. 14, no. 6, p. 1538, 2021. DOI 10.3390/en14061538. Available at: https://www.mdpi.com/1996-1073/14/6/1538.

ARMAS, Octavio; GARCÍA-CONTRERAS, Reyes; RAMOS, Ángel. Pollutant emissions from New European Driving Cycle with ethanol and butanol diesel blends. **Fuel Processing Technology**, vol. 122, p. 64–71, 1 Jun. 2014. https://doi.org/10.1016/j.fuproc.2014.01.023.

AUGUSTO HORTA NOGUEIRA, Luiz; SILVA CAPAZ, Rafael. Biofuels in Brazil: Evolution, achievements and perspectives on food security. **Global Food Security**, vol. 2, no. 2, p. 117–125, 2013. https://doi.org/10.1016/j.gfs.2013.04.001.

AVL. MicroIFEM Piezo 4th Generation - Piezo Amplifier. 2013. Available at: https://www.avl.com/documents/10138/2699442/MicroIFEM+4P4+Piezo. Accessed on: 27 Aug. 2019.

AVL. Pressure sensor for combustion analysis. 2011. Available at: https://www.avl.com/documents/10138/885983/AT3368E_GH13P.pdf. Accessed on: 27 Aug. 2019.

AWAD, Omar I.; MAMAT, R.; ALI, Obed M.; SIDIK, N. A.C.; YUSAF, T.; KADIRGAMA, K.; KETTNER, Maurice. Alcohol and ether as alternative fuels in spark ignition engine: A review. **Renewable and Sustainable Energy Reviews**, vol. 82, no. May 2017, p. 2586–2605, 2018. https://doi.org/10.1016/j.rser.2017.09.074.

AYDIN, F.; ÖĞÜT, H. Effects of using ethanol-biodiesel-diesel fuel in single cylinder diesel engine to engine performance and emissions. **Renewable Energy**, vol. 103, p. 688–694, 1 Apr. 2017. https://doi.org/10.1016/J.RENENE.2016.10.083.

AYDIN, Hüseyin; ILKILIÇ, Cumali. Effect of ethanol blending with biodiesel on engine performance and exhaust emissions in a CI engine. **Applied Thermal Engineering**, vol. 30, no. 10, p. 1199–1204, 1 Jul. 2010. https://doi.org/10.1016/j.applthermaleng.2010.01.037.

AYODELE, Bamidele Victor; ALSAFFAR, May Ali; MUSTAPA, Siti Indati. An overview of integration opportunities for sustainable bioethanol production from first- and second-generation sugar-based feedstocks. **Journal of Cleaner Production**, vol. 245, p. 118857, 2020. https://doi.org/https://doi.org/10.1016/j.jclepro.2019.118857.

AZAD, A. K.; RASUL, M. G.; KHAN, M. M.K.; SHARMA, Subhash C.; HAZRAT, M. A. Prospect of biofuels as an alternative transport fuel in Australia. **Renewable and Sustainable Energy Reviews**, vol. 43, p. 331–351, 2015. https://doi.org/10.1016/j.rser.2014.11.047.

BALAT, Mustafa; BALAT, Havva. Recent trends in global production and utilization of bio-ethanol fuel. **Applied Energy**, vol. 86, p. 2273–2282, 2009. https://doi.org/10.1016/j.apenergy.2009.03.015.

BARABÁS, István; TODORUŢ, Adrian; BĂLDEAN, Doru. Performance and emission characteristics of an CI engine fueled with diesel–biodiesel–bioethanol blends. **Fuel**, vol. 89, no. 12, p. 3827–3832, 1 Dec. 2010. https://doi.org/10.1016/j.fuel.2010.07.011.

BEATRICE, Carlo; DENBRATT, Ingemar; DI BLASIO, Gabriele; DI LUCA, Giuseppe; IANNIELLO, Roberto; SACCULLO, Michael. Experimental Assessment on Exploiting Low Carbon Ethanol Fuel in a Light-Duty Dual-Fuel Compression Ignition Engine. **Applied Sciences**, vol. 10, no. 20, p. 7182, 15 Oct. 2020. https://doi.org/10.3390/app10207182.

BHUIYA, M. M.K.; RASUL, M. G.; KHAN, M. M.K.; ASHWATH, N.; AZAD, A. K.; HAZRAT, M. A. Second generation biodiesel: Potential alternative to-edible oil-derived biodiesel. **Energy Procedia**, vol. 61, p. 1969–1972, 2014. https://doi.org/10.1016/j.egypro.2014.12.054.

BORUGADDA, Venu Babu; KAMATH, Girish; DALAI, Ajay K. Techno-economic and life-cycle assessment of integrated Fischer-Tropsch process in ethanol industry for bio-diesel and bio-gasoline production. **Energy**, vol. 195, p. 116985, Mar. 2020. DOI 10.1016/j.energy.2020.116985. Available at: http://www.sciencedirect.com/science/article/pii/S036054422030092X.

BOURHIS, G.; LEDUC, P. Energy and Exergy Balances for Modern Diesel and Gasoline Engines. **Oil & Gas Science and Technology – Revue de l'Institut Français du Pétrole**, vol. 65, no. 1, p. 39–46, 10 Jan. 2010. https://doi.org/10.2516/ogst/2009051.

BOWMAN, Craig T. Kinetics of pollutant formation and destruction in combustion. **Progress in Energy and Combustion Science**, vol. 1, no. 1, p. 33–45, Jan. 1975. https://doi.org/10.1016/0360-1285(75)90005-2.

BP. **Statistical Review of World Energy 2019**. [*S. l.*: *s. n.*], 2019.

BP. **Statistical Review of World Energy 2020**. [*S. l.*: *s. n.*], 2020. Available at: https://www.bp.com/content/dam/bp/business-sites/en/global/corporate/pdfs/energy-economics/statistical-review/bp-stats-review-2020-full-report.pdf.

BRADY, James M.; CRISP, Timia A.; COLLIER, Sonya; KUWAYAMA, Toshihiro; FORESTIERI, Sara D.; PERRAUD, Véronique; ZHANG, Qi; KLEEMAN, Michael J.; CAPPA, Christopher D.; BERTRAM, Timothy H. Real-Time Emission Factor Measurements of Isocyanic Acid from Light Duty Gasoline Vehicles. **Environmental Science & Technology**, vol. 48, no. 19, p. 11405–11412, 7 Oct. 2014. DOI 10.1021/es504354p. Available at: https://pubs.acs.org/doi/10.1021/es504354p.

BRESSANIN, Jéssica Marcon; KLEIN, Bruno Colling; CHAGAS, Mateus Ferreira; WATANABE, Marcos Djun Barbosa; SAMPAIO, Isabelle Lobo de Mesquita; BONOMI, Antonio; MORAIS, Edvaldo Rodrigo de; CAVALETT, Otávio. Techno-Economic and Environmental Assessment of Biomass Gasification and Fischer–Tropsch Synthesis Integrated to Sugarcane Biorefineries. **Energies**, vol. 13, no. 17, p. 4576, 3 Sep. 2020. DOI 10.3390/en13174576. Available at: www.mdpi.com/journal/energies. Accessed on: 24 May 2021.

CAO, Y.-S.; WANG, T.; YANG, T.-T.; WU, Z.-F.; YANG, L.-J.; JIANG, Q.-J. Effects of methanol/biodiesel/F-T diesel coal-based multi-fuels on engine performance. **Chinese Internal Combustion Engine Engineering**, vol. 37, no. 5, p. 21–26, 2016. .

CARVALHO, Márcio; TORRES, Felipe; FERREIRA, Vitor; SILVA, Júlio; MARTINS, Jorge; TORRES, Ednildo. Effects of Diethyl Ether Introduction in Emissions and Performance of a

Diesel Engine Fueled with Biodiesel-Ethanol Blends. **Energies**, vol. 13, no. 15, p. 3787, 2020. DOI 10.3390/en13153787. Available at: https://www.mdpi.com/1996-1073/13/15/3787.

ÇELEBI, Yahya; AYDIN, Hüseyin. An overview on the light alcohol fuels in diesel engines. **Fuel**, vol. 236, p. 890–911, 15 Jan. 2019. DOI 10.1016/J.FUEL.2018.08.138. Available at: https://www.sciencedirect.com/science/article/pii/S0016236118315102. Accessed on: 30 Apr. 2019.

CHACKO, Nivin; JEYASEELAN, Thangaraja. Comparative evaluation of graphene oxide and graphene nanoplatelets as fuel additives on the combustion and emission characteristics of a diesel engine fuelled with diesel and biodiesel blend. **Fuel Processing Technology**, vol. 204, no. January, p. 106406, Jul. 2020. https://doi.org/10.1016/j.fuproc.2020.106406.

CHANSAURIA, Prakhar; MANDLOI, R. K. Effects of Ethanol Blends on Performance of Spark Ignition Engine-A Review. **Materials Today: Proceedings**, vol. 5, no. 2, p. 4066–4077, 2018. https://doi.org/10.1016/j.matpr.2017.11.668.

CHOI, Kibong; PARK, Suhan; ROH, Hyun Gu; LEE, Chang Sik. Combustion and Emission Reduction Characteristics of GTL-Biodiesel Fuel in a Single-Cylinder Diesel Engine. **Energies**, vol. 12, no. 11, p. 2201, 10 Jun. 2019. DOI 10.3390/en12112201. Available at: https://www.mdpi.com/1996-1073/12/11/2201.

COMPACTGTL. Commercial Demonstration Plant. 2021. Available at: https://www.compactgtl.com/technology/petrobas/. Accessed on: 7 Feb. 2021.

CORREA, G.; MUÑOZ, P.M.; RODRIGUEZ, C.R. A comparative energy and environmental analysis of a diesel, hybrid, hydrogen and electric urban bus. **Energy**, vol. 187, p. 115906, 15 Nov. 2019. DOI 10.1016/j.energy.2019.115906. Available at: https://linkinghub.elsevier.com/retrieve/pii/S0360544219315841. Accessed on: 11 Apr. 2021.

DA SILVA CÉSAR, Aldara; CONEJERO, Marco Antonio; BARROS RIBEIRO, Eliene Cristina; BATALHA, Mário Otávio. Competitiveness analysis of "social soybeans" in biodiesel production in Brazil. **Renewable Energy**, vol. 133, p. 1147–1157, 1 Apr. 2019. https://doi.org/10.1016/J.RENENE.2018.08.108.

DA SILVA, Julio A.M.; SEIFERT, Vitor; DE MORAIS, Vinícius O.B.; TSOLAKIS, Athanasios; HERREROS, Jose; TORRES, Ednildo. Exergy evaluation and ORC use as an alternative for efficiency improvement in a CI-engine power plant. **Sustainable Energy Technologies and Assessments**, vol. 30, no. June, p. 216–223, 2018. DOI 10.1016/j.seta.2018.10.007. Available at: https://doi.org/10.1016/j.seta.2018.10.007.

DE CARVALHO, Márcio A. S.; ACHY, Acbal R. A.; JUNIOR, Luiz C. S. S.; FERREIRA, Vitor P.; DA SILVA, Julio A. M.; PEPE, Iuri M.; TORRES, Ednildo A. Mechanical and emissions performance of a diesel engine fueled with biodiesel, ethanol and diethyl ether blends. **Journal of the Brazilian Society of Mechanical Sciences and Engineering**, vol. 42, no. 4, p. 182, 19 Apr. 2020. DOI 10.1007/s40430-020-2269-7. Available at: https://doi.org/10.1007/s40430-020-2269-7.

DE MORAIS, André Marcelino; DE MORAIS HANRIOT, Sérgio; DE OLIVEIRA, Alex; JUSTINO, Marco Aurélio Mendes; VALENTE, Osmano Souza; SODRÉ, José Ricardo. An assessment of fuel consumption and emissions from a diesel power generator converted to

operate with ethanol. **Sustainable Energy Technologies and Assessments**, vol. 35, no. January, p. 291–297, 2019. DOI 10.1016/j.seta.2019.08.005. Available at: https://doi.org/10.1016/j.seta.2019.08.005.

DE OLIVEIRA, Alex; DE MORAIS, André Marcelino; VALENTE, Osmano Souza; SODRÉ, José Ricardo. Combustion characteristics, performance and emissions from a diesel power generator fuelled by B7-ethanol blends. **Fuel Processing Technology**, vol. 139, p. 67–72, 1 Nov. 2015. https://doi.org/10.1016/J.FUPROC.2015.08.010.

DE OLIVEIRA, Alex; DE MORAIS, André Marcelino; VALENTE, Osmano Souza; SODRÉ, José Ricardo. Combustion, performance and emissions of a diesel power generator with direct injection of B7 and port injection of ethanol. **Journal of the Brazilian Society of Mechanical Sciences and Engineering**, vol. 39, no. 4, p. 1087–1096, 31 Apr. 2017. DOI 10.1007/s40430-016-0667-7. Available at: http://link.springer.com/10.1007/s40430-016-0667-7. Accessed on: 15 Jan. 2019.

DE OLIVEIRA, Alex; VALENTE, Osmano Souza; SODRÉ, José Ricardo. Effects of ethanol addition to biodiesel-diesel oil blends (B7 and B20) on engine emissions and fuel consumption. **MRS Advances**, vol. 2, no. 64, p. 4005–4015, 18 Jan. 2017. https://doi.org/10.1557/adv.2017.617.

DE SOUZA, Nariê Rinke Dias; FRACAROLLI, Juliana Aparecida; JUNQUEIRA, Tassia L.; CHAGAS, Mateus F.; CARDOSO, Terezinha F.; WATANABE, Marcos D.B.; CAVALETT, Otavio; VENZKE FILHO, Solismar P.; DALE, Bruce E.; BONOMI, Antonio; CORTEZ, Luis Augusto Barbosa. Sugarcane ethanol and beef cattle integration in Brazil. **Biomass and Bioenergy**, vol. 120, p. 448–457, 1 Jan. 2019. https://doi.org/10.1016/j.biombioe.2018.12.012.

DEMIDYUK, Vladimir; HARDACRE, Christopher; BURCH, Robbie; MHADESHWAR, Ashish; NORTON, Daniel; HANCU, Dan. Aromatic hydrocarbons and sulfur based catalyst deactivation for selective catalytic reduction of NOx. 164., 30 Apr. 2011. **Catalysis Today** [...]. [*S. l.*]: Elsevier, 30 Apr. 2011. vol. 164, p. 515–519. https://doi.org/10.1016/j.cattod.2010.12.047.

DHARMA, S.; ONG, Hwai Chyuan; MASJUKI, H.H.; SEBAYANG, A.H.; SILITONGA, A.S. An overview of engine durability and compatibility using biodiesel–bioethanol–diesel blends in compression-ignition engines. **Energy Conversion and Management**, vol. 128, p. 66–81, 15 Nov. 2016. https://doi.org/10.1016/J.ENCONMAN.2016.08.072.

DI, Yage; CHEUNG, C. S.; HUANG, Zuohua. Comparison of the Effect of Biodiesel-Diesel and Ethanol-Diesel on the Particulate Emissions of a Direct Injection Diesel Engine. **Aerosol Science and Technology**, vol. 43, no. 5, p. 455–465, 20 Apr. 2009. https://doi.org/10.1080/02786820902718078.

DINCER, Ibrahim; BICER, Yusuf. **Exergy: Energy, Environment and Sustainable Development**. 2nd ed. Amsterdam, The Netherlands: Elsevier Science, 2013.

DOGAN, Battal; CAKMAK, Abdulvahap; KADIR YESILYURT, Murat; EROL, Dervis. Investigation on 1-heptanol as an oxygenated additive with diesel fuel for compression-ignition engine applications: An approach in terms of energy, exergy, exergoeconomic, enviroeconomic, and sustainability analyses. **Fuel**, vol. 275, p. 117973, 1 Sep. 2020. DOI

10.1016/j.fuel.2020.117973. Available at: https://linkinghub.elsevier.com/retrieve/pii/S0016236120309698. Accessed on: 24 Jan. 2021.

DRY, Mark E. The Fischer–Tropsch process: 1950–2000. **Catalysis Today**, vol. 71, no. 3–4, p. 227–241, Jan. 2002. https://doi.org/10.1016/S0920-5861(01)00453-9.

DU, Jiakun; SUN, Wanchen; WANG, Xiaodan; LI, Guoliang; TAN, Manzhi; FAN, Luyan. Experimental study on combustion and particle size distribution of a common rail diesel engine fueled with GTL/diesel blends. **Applied Thermal Engineering**, vol. 70, no. 1, p. 430–440, 5 Sep. 2014. DOI 10.1016/j.applthermaleng.2014.05.037. Available at: https://linkinghub.elsevier.com/retrieve/pii/S1359431114003986. Accessed on: 13 Dec. 2020.

EL MORABET, Rachida. Effects of Outdoor Air Pollution on Human Health. **Reference Module in Earth Systems and Environmental Sciences**. 2nd ed. [*S. l.*]: Elsevier, 2018. p. 1–9. DOI 10.1016/B978-0-12-409548-9.11012-7. Available at: http://dx.doi.org/10.1016/B978-0-12-409548-9.11012-7.

EMIROĞLU, A. Osman; ŞEN, Mehmet. Combustion, performance and emission characteristics of various alcohol blends in a single cylinder diesel engine. **Fuel**, vol. 212, no. February 2017, p. 34–40, 2018a. https://doi.org/10.1016/j.fuel.2017.10.016.

EMIROĞLU, A. Osman; ŞEN, Mehmet. Combustion, performance and exhaust emission characterizations of a diesel engine operating with a ternary blend (alcohol-biodiesel-diesel fuel). **Applied Thermal Engineering**, vol. 133, no. March 2017, p. 371–380, Mar. 2018b. DOI 10.1016/j.applthermaleng.2018.01.069. Available at: https://linkinghub.elsevier.com/retrieve/pii/S1359431117320069.

EMPRESA DE PESQUISA ENERGÉTICA (EPE). **Balanço energético nacional 2020: Ano base 2019 - Relatório Síntese**. Brasília: [*s. n.*], 2020a. Available at: https://www.epe.gov.br/sites-pt/publicacoes-dados-abertos/publicacoes/PublicacoesArquivos/publicacao-479/topico-521/Relatório Síntese BEN 2020-ab 2019_Final.pdf.

EMPRESA DE PESQUISA ENERGÉTICA (EPE). **Balanço energético nacional 2021: Ano base 2020 - Relatório Síntese**. Brasília: [*s. n.*], 2021. Available at: https://www.epe.gov.br/pt/publicacoes-dados-abertos/publicacoes/balanco-energetico-nacional-2021.

EMPRESA DE PESQUISA ENERGÉTICA (EPE). **Plano Nacional de Energia 2050**. Brasília: [*s. n.*], 2020b. Available at: https://www.epe.gov.br/sites-pt/publicacoes-dados-abertos/publicacoes/PublicacoesArquivos/publicacao-227/topico-563/Relatorio Final do PNE 2050.pdf.

ETIP BIOENERGY. FT-Liquids & Biomass to Liquids (BtL). 2021. Available at: https://www.etipbioenergy.eu/value-chains/products-end-use/products/ft-liquids. Accessed on: 20 May 2021.

EXXONMOBIL. **2019 Outlook for Energy: A Perspective to 2040**. Irving, TX, USA: [*s. n.*], 2019. Available at: https://corporate.exxonmobil.com/Energy-and-innovation/Outlook-for-Energy.

FAYAD, M. A.; FERNÀNDEZ-RODRÍGUEZ, D.; HERREROS, J. M.; LAPUERTA, M.; TSOLAKIS, A. Interactions between aftertreatment systems architecture and combustion of oxygenated fuels for improved low temperature catalysts activity. **Fuel**, vol. 229, p. 189–197, 1 Oct. 2018. https://doi.org/10.1016/j.fuel.2018.05.002.

FAYAD, Mohammed A.; HERREROS, Jose M.; MARTOS, Francisco J.; TSOLAKIS, Athanasios. Role of Alternative Fuels on Particulate Matter (PM) Characteristics and Influence of the Diesel Oxidation Catalyst. **Environmental Science and Technology**, vol. 49, no. 19, p. 11967–11973, 2015. https://doi.org/10.1021/acs.est.5b02447.

FAYAD, Mohammed A.; TSOLAKIS, Athanasios; MARTOS, Francisco J. Influence of alternative fuels on combustion and characteristics of particulate matter morphology in a compression ignition diesel engine. **Renewable Energy**, vol. 149, p. 962–969, 1 Apr. 2020. https://doi.org/10.1016/j.renene.2019.10.079.

FERREIRA, Vitor Pinheiro; TORRES, Ednildo Andrade; DA SILVA, Julio Augusto Mendes; SILVA, Leonard Fernandes. Evaluation of ethanol as additive for NOx and PM reduction in CI engines fueled with diesel–biodiesel blends using a pump assembly. **Journal of the Brazilian Society of Mechanical Sciences and Engineering**, vol. 42, no. 8, p. 408, 15 Aug. 2020. https://doi.org/10.1007/s40430-020-02494-0.

FILIP, Ondrej; JANDA, Karel; KRISTOUFEK, Ladislav; ZILBERMAN, David. Food versus fuel: An updated and expanded evidence. **Energy Economics**, vol. 82, p. 152–166, 2019. https://doi.org/https://doi.org/10.1016/j.eneco.2017.10.033.

FISCHER, Franz. **The Conversion of Coal into Oils**. Authorised. London: Ernest Benn, Ltd., 1925.

FISCHER, Franz; TROPSCH, Hans. Über die direkte Synthese von Erdöl-Kohlenwasserstoffen bei gewöhnlichem Druck. (Erste Mitteilung). **Berichte der deutschen chemischen Gesellschaft (A and B Series)**, vol. 59, no. 4, p. 830–831, 14 Apr. 1926a. DOI 10.1002/cber.19260590442. Available at: https://chemistry-europe.onlinelibrary.wiley.com/doi/full/10.1002/cber.19260590442. Accessed on: 18 May 2021.

FISCHER, Franz; TROPSCH, Hans. Über die direkte Synthese von Erdöl-Kohlenwasserstoffen bei gewöhnlichem Druck. (Zweite Mitteilung.). **Berichte der deutschen chemischen Gesellschaft (A and B Series)**, vol. 59, no. 4, p. 832–836, 14 Apr. 1926b. DOI 10.1002/cber.19260590443. Available at: https://chemistry-europe.onlinelibrary.wiley.com/doi/full/10.1002/cber.19260590443. Accessed on: 18 May 2021.

FISCHER, Franz; TROPSCH, Hans. Über die Synthese hochmolekularer Paraffin-Kohlenwasserstoffe aus Kohlenoxyd. (Nach Versuchen von Walther Ter-Nedden). **Berichte der deutschen chemischen Gesellschaft (A and B Series)**, vol. 60, no. 6, p. 1330–1334, 15 Jun. 1927. DOI 10.1002/cber.19270600610. Available at: https://chemistry-europe.onlinelibrary.wiley.com/doi/full/10.1002/cber.19270600610. Accessed on: 18 May 2021.

FISCHER, Franz; TROPSCH, Hans. Über einige Eigenschaften der aus Kohlenoxyd bei gewöhnlichem Druck hergestellten synthetischen Erdöl-Kohlenwasserstoffe. **Berichte der**

deutschen chemischen Gesellschaft (A and B Series), vol. 59, no. 5, p. 923–925, 5 May 1926c. DOI 10.1002/cber.19260590513. Available at: https://chemistry-europe.onlinelibrary.wiley.com/doi/full/10.1002/cber.19260590513. Accessed on: 18 May 2021.

FOREST, Coryne A.; MUZZELL, Patsy A. Fischer-tropsch fuels: Why are they of interest to the united states military? **SAE Technical Papers**, no. 724, 2005. https://doi.org/10.4271/2005-01-1807.

FURTADO JÚNIOR, Juarez Corrêa; PALACIO, José Carlos Escobar; LEME, Rafael Coradi; LORA, Electo Eduardo Silva; DA COSTA, José Eduardo Loureiro; REYES, Arnaldo Martín Martínez; DEL OLMO, Oscar Almazán. Biorefineries productive alternatives optimization in the brazilian sugar and alcohol industry. **Applied Energy**, vol. 259, p. 113092, 1 Feb. 2020. DOI 10.1016/j.apenergy.2019.04.088. Available at: https://linkinghub.elsevier.com/retrieve/pii/S0306261919307329. Accessed on: 24 May 2021.

GARCÍA, Antonio; MONSALVE-SERRANO, Javier. Analysis of a series hybrid vehicle concept that combines low temperature combustion and biofuels as power source. **Results in Engineering**, vol. 1, p. 100001, Mar. 2019. DOI 10.1016/j.rineng.2019.01.001. Available at: https://doi.org/10.1016/j.rineng.2019.01.001.

GARCÍA, Antonio; MONSALVE-SERRANO, Javier; MARTÍNEZ-BOGGIO, Santiago; RÜCKERT ROSO, Vinícius; DUARTE SOUZA ALVARENGA SANTOS, Nathália. Potential of bio-ethanol in different advanced combustion modes for hybrid passenger vehicles. **Renewable Energy**, vol. 150, p. 58–77, May 2020. DOI 10.1016/j.renene.2019.12.102. Available at: https://linkinghub.elsevier.com/retrieve/pii/S0960148119319743.

GARDNER, N.; MANLEY, B.J.W.; PEARSON, J.M. Gas emissions from landfills and their contributions to global warming. **Applied Energy**, vol. 44, no. 2, p. 165–174, Jan. 1993. https://doi.org/10.1016/0306-2619(93)90059-X.

GAS PROCESSING & LNG. Smaller-scale and modular technologies drive GTL industry forward. 2017. Available at: http://www.gasprocessingnews.com/features/201706/smaller-scale-and-modular-technologies-drive-gtl-industry-forward.aspx. Accessed on: 6 Feb. 2021.

GERDES, K. R.; SUPPES, G. J. Miscibility of Ethanol in Diesel Fuels. **Industrial & Engineering Chemistry Research**, vol. 40, no. 3, p. 949–956, Feb. 2001. https://doi.org/10.1021/ie000566w.

GHADIKOLAEI, Meisam Ahmadi. Effect of alcohol blend and fumigation on regulated and unregulated emissions of IC engines—A review. **Renewable and Sustainable Energy Reviews**, vol. 57, p. 1440–1495, 1 May 2016. https://doi.org/10.1016/J.RSER.2015.12.128.

GHADIKOLAEI, Meisam Ahmadi; CHEUNG, Chun Shun; YUNG, Ka-Fu. Study of combustion, performance and emissions of a diesel engine fueled with ternary fuel in blended and fumigation modes. **Fuel**, vol. 235, p. 288–300, 1 Jan. 2019. https://doi.org/10.1016/J.FUEL.2018.07.089.

GHADIKOLAEI, Meisam Ahmadi; WEI, Long; CHEUNG, Chun Shun; YUNG, Ka Fu; NING, Zhi. Particulate emission and physical properties of particulate matter emitted from a diesel engine fueled with ternary fuel (diesel-biodiesel-ethanol) in blended and fumigation

modes. **Fuel**, vol. 263, no. August 2019, p. 116665, 2020. https://doi.org/10.1016/j.fuel.2019.116665.

GILL, S.S.; TSOLAKIS, A.; DEARN, K.D.; RODRÍGUEZ-FERNÁNDEZ, J. Combustion characteristics and emissions of Fischer–Tropsch diesel fuels in IC engines. **Progress in Energy and Combustion Science**, vol. 37, no. 4, p. 503–523, 1 Aug. 2011a. DOI 10.1016/j.pecs.2010.09.001. Available at: https://www.sciencedirect.com/science/article/pii/S036012851000064X?via%3Dihub. Accessed on: 6 May 2019.

GILL, S.S.; TSOLAKIS, A.; DEARN, K.D.; RODRÍGUEZ-FERNÁNDEZ, J. Combustion characteristics and emissions of Fischer–Tropsch diesel fuels in IC engines. **Progress in Energy and Combustion Science**, vol. 37, no. 4, p. 503–523, 1 Aug. 2011b. https://doi.org/10.1016/J.PECS.2010.09.001.

GLARBORG, Peter; MILLER, James A.; RUSCIC, Branko; KLIPPENSTEIN, Stephen J. Modeling nitrogen chemistry in combustion. **Progress in Energy and Combustion Science**, vol. 67, p. 31–68, Jul. 2018. DOI 10.1016/j.pecs.2018.01.002. Available at: https://doi.org/10.1016/j.pecs.2018.01.002.

GLENSOR, Kain; MUÑOZ B., María Rosa. Life-Cycle Assessment of Brazilian Transport Biofuel and Electrification Pathways. **Sustainability**, vol. 11, no. 22, p. 6332, 11 Nov. 2019. DOI 10.3390/su11226332. Available at: https://www.mdpi.com/2071-1050/11/22/6332. Accessed on: 11 Apr. 2021.

GLOBAL SYNGAS TECHNOLOGIES COUNCIL (GSTC). Synthetic Fuels. 2020. Available at: https://www.globalsyngas.org/syngas-applications/synthetic-fuels/. Accessed on: 3 Nov. 2019.

GNANAMOORTHI, V.; DEVARADJANE, G. Effect of compression ratio on the performance, combustion and emission of DI diesel engine fueled with ethanol – Diesel blend. **Journal of the Energy Institute**, vol. 88, no. 1, p. 19–26, Feb. 2015. DOI 10.1016/j.joei.2014.06.001. Available at: http://dx.doi.org/10.1016/j.joei.2014.06.001.

GOLDEMBERG, Jose; MACEDO, Isaias C. Brazilian alcohol program: an overview. **Energy for Sustainable Development**, vol. 1, no. 1, p. 17–22, 1 May 1994. https://doi.org/10.1016/S0973-0826(08)60009-5.

GÓMEZ, A.; SORIANO, J.A.; ARMAS, O. Evaluation of sooting tendency of different oxygenated and paraffinic fuels blended with diesel fuel. **Fuel**, vol. 184, p. 536–543, 15 Nov. 2016. DOI 10.1016/J.FUEL.2016.07.049. Available at: https://www.sciencedirect.com/science/article/pii/S0016236116306524?via%3Dihub. Accessed on: 6 May 2019.

GOMEZ, José M A; LEGEY, Luiz F L. An analysis of the impact of Flex-Fuel vehicles on fuel consumption in Brazil, applying Cointegration and the Kalman Filter. **Energy**, vol. 81, p. 696–705, 2015. https://doi.org/https://doi.org/10.1016/j.energy.2015.01.015.

GUARIEIRO, Lílian Lefol Nani; DE SOUZA, Amanda Figueiredo; TORRES, Ednildo Andrade; DE ANDRADE, Jailson B. Emission profile of 18 carbonyl compounds, CO, CO2, and NOx emitted by a diesel engine fuelled with diesel and ternary blends containing diesel,

ethanol and biodiesel or vegetable oils. **Atmospheric Environment**, vol. 43, no. 17, p. 2754–2761, 1 Jun. 2009. https://doi.org/10.1016/J.ATMOSENV.2009.02.036.

GUARIEIRO, Lílian Lefol Nani; GUERREIRO, Egídio Teixeira de Almeida; AMPARO, Keize Katiane dos Santos; MANERA, Victor Bonfim; REGIS, Ana Carla D.; SANTOS, Aldenor Gomes; FERREIRA, Vitor P.; LEÃO, Danilo J.; TORRES, Ednildo A.; DE ANDRADE, Jailson B. Assessment of the use of oxygenated fuels on emissions and performance of a diesel engine. **Microchemical Journal**, vol. 117, no. x, p. 94–99, Nov. 2014. https://doi.org/10.1016/j.microc.2014.06.004.

GÜLÜM, Mert; BILGIN, Atilla. A comprehensive study on measurement and prediction of viscosity of biodiesel-diesel-alcohol ternary blends. **Energy**, vol. 148, p. 341–361, 1 Apr. 2018. https://doi.org/10.1016/J.ENERGY.2018.01.123.

GUO, Meiyu; XU, Yuan. Coal-to-liquids projects in China under water and carbon constraints. **Energy Policy**, vol. 117, no. February, p. 58–65, Jun. 2018. DOI 10.1016/j.enpol.2018.02.038. Available at: https://doi.org/10.1016/j.enpol.2018.02.038.

HAN, Jinlin; SOMERS, L. M.T.; CRACKNELL, Roger; JOEDICKE, Arndt; WARDLE, Robert; MOHAN, Vivek Raja Raj. Experimental investigation of ethanol/diesel dual-fuel combustion in a heavy-duty diesel engine. **Fuel**, vol. 275, no. April, p. 117867, 2020. https://doi.org/10.1016/j.fuel.2020.117867.

HANSDAH, Dulari; MURUGAN, S. Bioethanol fumigation in a DI diesel engine. **Fuel**, vol. 130, p. 324–333, 15 Aug. 2014. https://doi.org/10.1016/J.FUEL.2014.04.047.

HANSEN, Alan C.; ZHANG, Qin; LYNE, Peter W.L. Ethanol–diesel fuel blends — a review. **Bioresource Technology**, vol. 96, no. 3, p. 277–285, 1 Feb. 2005. https://doi.org/10.1016/J.BIORTECH.2004.04.007.

HERREROS, J. M.; GILL, S. S.; LEFORT, I.; TSOLAKIS, A.; MILLINGTON, P.; MOSS, E. Enhancing the low temperature oxidation performance over a Pt and a Pt-Pd diesel oxidation catalyst. **Applied Catalysis B: Environmental**, vol. 147, p. 835–841, 2014. https://doi.org/10.1016/j.apcatb.2013.10.013.

HERREROS, J.M.; GEORGE, P.; UMAR, M.; TSOLAKIS, A. Enhancing selective catalytic reduction of NOx with alternative reactants/promoters. **Chemical Engineering Journal**, vol. 252, p. 47–54, 15 Sep. 2014. https://doi.org/10.1016/J.CEJ.2014.04.095.

HERREROS, J.M.; JONES, A.; SUKJIT, E.; TSOLAKIS, A. Blending lignin-derived oxygenate in enhanced multi-component diesel fuel for improved emissions. **Applied Energy**, vol. 116, p. 58–65, 1 Mar. 2014. https://doi.org/10.1016/j.apenergy.2013.11.022.

HERREROS, J.M.; SCHROER, K.; SUKJIT, E.; TSOLAKIS, A. Extending the environmental benefits of ethanol–diesel blends through DGE incorporation. **Applied Energy**, vol. 146, p. 335–343, 15 May 2015. https://doi.org/10.1016/J.APENERGY.2015.02.075.

HEYWOOD, J.B. **Internal Combustion Engine Fundamentals**. 2nd ed. New York: McGraw-Hill Education, 2018.

HÖÖK, Mikael; ALEKLETT, Kjell. A review on coal-to-liquid fuels and its coal consumption. **International Journal of Energy Research**, vol. 34, no. 10, p. 848–864, Aug. 2010. DOI 10.1002/er.1596. Available at: http://doi.wiley.com/10.1002/er.1596.

HOSEINPOUR, Marziyeh; SADRNIA, Hassan; TABASIZADEH, Mohammad; GHOBADIAN, Barat. Energy and exergy analyses of a diesel engine fueled with diesel, biodiesel-diesel blend and gasoline fumigation. **Energy**, vol. 141, p. 2408–2420, 15 Dec. 2017. https://doi.org/10.1016/J.ENERGY.2017.11.131.

HOSSAIN, S.; MASJUKI, H. H.; VARMAN, M.; KALAM, M. A.; RAHMAN, S. M.Ashrafur. Comparative evaluation of the blends of gas-to-liquid (GTL) fuels and biodiesels with diesel at high idling conditions: An in-depth analysis on engine performance and environment pollutants. **RSC Advances**, vol. 5, no. 17, p. 13068–13077, 2015. https://doi.org/10.1039/c4ra16239k.

IMRAN, A.; VARMAN, M.; MASJUKI, H.H.; KALAM, M.A. Review on alcohol fumigation on diesel engine: A viable alternative dual fuel technology for satisfactory engine performance and reduction of environment concerning emission. **Renewable and Sustainable Energy Reviews**, vol. 26, p. 739–751, 1 Oct. 2013. https://doi.org/10.1016/J.RSER.2013.05.070.

INTERNATIONAL ENERGY AGENCY (IEA). **CO2 emisions from fuel combustion**. Paris: [*s. n.*], 2019.

INTERNATIONAL ENERGY AGENCY (IEA). **Germany 2020: Energy Policy Review**. [*S. l.*]: OECD, 2020a. https://doi.org/10.1787/cedb9b0a-en.

INTERNATIONAL ENERGY AGENCY (IEA). Global biofuel production 2010-2025 compared to consumption in the Sustainable Development Scenario. 2020b. Available at: https://www.iea.org/data-and-statistics/charts/global-biofuel-production-2010-2025-compared-to-consumption-in-the-sustainable-development-scenario. Accessed on: 15 Jun. 2020.

INTERNATIONAL ENERGY AGENCY (IEA). **Tracking Clean Energy Progress 2017**. Paris: [*s. n.*], 2017. Available at: https://www.iea.org/reports/tracking-clean-energy-progress-2017.

INTERNATIONAL ENERGY AGENCY (IEA). Tracking Transport 2020. 2020c. Available at: https://www.iea.org/reports/tracking-transport-2020. Accessed on: 10 Jun. 2020.

INTERNATIONAL ENERGY AGENCY (IEA). World oil final consumption by sector. 2020d. Available at: https://www.iea.org/reports/key-world-energy-statistics-2020/final-consumption. Accessed on: 21 Oct. 2020.

IRANI, Karishma; EPLING, William S.; BLINT, Richard. Effect of hydrocarbon species on no oxidation over diesel oxidation catalysts. **Applied Catalysis B: Environmental**, vol. 92, no. 3–4, p. 422–428, 2009. https://doi.org/10.1016/j.apcatb.2009.08.022.

JAMBO, Siti Azmah; ABDULLA, Rahmath; MOHD AZHAR, Siti Hajar; MARBAWI, Hartinie; GANSAU, Jualang Azlan; RAVINDRA, Pogaku. A review on third generation bioethanol feedstock. **Renewable and Sustainable Energy Reviews**, vol. 65, p. 756–769, 2016. https://doi.org/10.1016/j.rser.2016.07.064.

JAMROZIK, Arkadiusz. The effect of the alcohol content in the fuel mixture on the performance and emissions of a direct injection diesel engine fueled with diesel-methanol and diesel-ethanol blends. **Energy Conversion and Management**, vol. 148, p. 461–476, 15 Sep. 2017. https://doi.org/10.1016/J.ENCONMAN.2017.06.030.

JAMROZIK, Arkadiusz; TUTAK, Wojciech; GNATOWSKA, Renata; NOWAK, Łukasz. Comparative analysis of the combustion stability of diesel-methanol and diesel-ethanol in a dual fuel engine. **Energies**, vol. 12, no. 6, 2019. https://doi.org/10.3390/en12060971.

JAMUWA, D.K.; SHARMA, D.; SONI, S.L. Experimental investigation of performance, exhaust emission and combustion parameters of compression ignition engine with varying ethanol energy fractions. **Energy**, vol. 127, p. 544–557, 15 May 2017. https://doi.org/10.1016/J.ENERGY.2017.03.121.

JAMUWA, D.K.; SHARMA, D.; SONI, S.L. Experimental investigation of performance, exhaust emission and combustion parameters of stationary compression ignition engine using ethanol fumigation in dual fuel mode. **Energy Conversion and Management**, vol. 115, p. 221–231, 1 May 2016. https://doi.org/10.1016/J.ENCONMAN.2016.02.055.

JANSSEN, R.; RUTZ, D.; HOFER, A.; MOREIRA, J.; SANTOS, S.; COELHO, S.T.; VELAZQUEZ, S.; CAPACCIOLI, S.; LANDAHL, G.; ERICSON, J. Bioethanol as Sustainable Bus Transport Fuel in Brazil and Europe. 2010. **18th European Biomass Conference and Exhibition** [...]. [*S. l.: s. n.*], 2010. p. 1975–1981. https://doi.org/10.5071/18thEUBCE2010-VP2.8.7.

JENA, Jibanananda; MISRA, Rahul Dev. Effect of fuel oxygen on the energetic and exergetic efficiency of a compression ignition engine fuelled separately with palm and karanja biodiesels. **Energy**, vol. 68, p. 411–419, 15 Apr. 2014. DOI 10.1016/j.energy.2014.02.079. Available at: http://dx.doi.org/10.1016/j.energy.2014.02.079. Accessed on: 5 Jan. 2021.

JIAO, Yufei; LIU, Ruilin; ZHANG, Zhongjie; DONG, Surong; YANG, Chunhao; REN, Lu. Review on the physicochemical, spray characteristics and chemical reaction mechanism of F-T diesel-methanol-diesel-biodiesel blended alternative fuels. **IOP Conference Series: Earth and Environmental Science**, vol. 227, no. 2, p. 022006, 2 Mar. 2019. DOI 10.1088/1755-1315/227/2/022006. Available at: https://iopscience.iop.org/article/10.1088/1755-1315/227/2/022006. Accessed on: 2 Jun. 2021.

JIAO, Yufei; LIU, Ruilin; ZHANG, Zhongjie; YANG, Chunhao; ZHOU, Guangmeng; DONG, Surong; LIU, Wuquan. Comparison of combustion and emission characteristics of a diesel engine fueled with diesel and methanol-Fischer-Tropsch diesel-biodiesel-diesel blends at various altitudes. **Fuel**, vol. 243, p. 52–59, 1 May 2019. DOI 10.1016/j.fuel.2019.01.107. Available at: https://www.sciencedirect.com/science/article/pii/S0016236119301073#f0010. Accessed on: 6 May 2019.

JOHNSON, William L.; FISHER, Galen B.; TOOPS, Todd J. Mechanistic investigation of ethanol SCR of NO x over Ag/Al 2O 3. 184., 30 Apr. 2012. **Catalysis Today** [...]. [*S. l.*]: Elsevier, 30 Apr. 2012. vol. 184, p. 166–177. https://doi.org/10.1016/j.cattod.2011.12.002.

KALGHATGI, Gautam. Is it really the end of internal combustion engines and petroleum in transport? **Applied Energy**, vol. 225, no. February, p. 965–974, 2018. https://doi.org/10.1016/j.apenergy.2018.05.076.

KARAGOZ, Mustafa; UYSAL, Cuneyt; AGBULUT, Umit; SARIDEMIR, Suat. Energy, exergy, economic and sustainability assessments of a compression ignition diesel engine fueled with tire pyrolytic oil − diesel blends. **Journal of Cleaner Production**, vol. 264, p. 121724, Aug. 2020. https://doi.org/10.1016/j.jclepro.2020.121724.

KARAGOZ, Mustafa; UYSAL, Cuneyt; AGBULUT, Umit; SARIDEMIR, Suat. Exergetic and exergoeconomic analyses of a CI engine fueled with diesel-biodiesel blends containing various metal-oxide nanoparticles. **Energy**, vol. 214, p. 118830, 2021. DOI 10.1016/j.energy.2020.118830. Available at: https://doi.org/10.1016/j.energy.2020.118830.

KARLSRUHE INSTITUTE OF TECHNOLOGY. bioliq - The bioliq® Pilot Project - The bioliq® Project. 2020. Available at: https://www.bioliq.de/english/177.php. Accessed on: 23 May 2020.

KAVITHA, K. R.; JAYAPRABAKAR, J.; PRABHU, A. Exergy and energy analyses on biodiesel–diesel-ethanol blends in a diesel engine. **International Journal of Ambient Energy**, vol. 0750, p. 1–5, 1 Oct. 2019. DOI 10.1080/01430750.2019.1670261. Available at: https://doi.org/10.1080/01430750.2019.1670261.

KHAN, Muzammil; TAFRESHI, Reza; MOKAHAL, Ahmad J.; MOHAMED, Mohamed Tarek; HANBAL, Mohab Yasser; ELTURK, Jayson. Single Cylinder GTL ENGINE: An Experimental Comparison between Traditional Diesel and GTL Diesel on Single Cylinder Engine. 5 Apr. 2016. **SAE Technical Papers** [...]. [*S. l.: s. n.*], 5 Apr. 2016. https://doi.org/10.4271/2016-01-1262.

KHOOBBAKHT, Golmohammad; AKRAM, A.; KARIMI, Mahmoud; NAJAFI, G. Exergy and Energy Analysis of Combustion of Blended Levels of Biodiesel, Ethanol and Diesel Fuel in a DI Diesel Engine. **Applied Thermal Engineering**, vol. 99, p. 720–729, 25 Apr. 2016. https://doi.org/10.1016/j.applthermaleng.2016.01.022.

KHOOBBAKHT, Golmohammad; NAJAFI, G.; KARIMI, Mahmoud; AKRAM, A. Optimization of operating factors and blended levels of diesel, biodiesel and ethanol fuels to minimize exhaust emissions of diesel engine using response surface methodology. **Applied Thermal Engineering**, vol. 99, p. 1006–1017, 25 Apr. 2016. https://doi.org/10.1016/j.applthermaleng.2015.12.143.

KIM, Il Hee; SEO, Hyun Ook; PARK, Eun Ji; HAN, Sang Wook; KIM, Young Dok. Low temperature CO oxidation over iron oxide nanoparticles decorating internal structures of a mesoporous alumina. **Scientific Reports**, vol. 7, p. 1–11, 2017. https://doi.org/10.1038/srep40497.

KITTELSON, David B. Engines and nanoparticles. **Journal of Aerosol Science**, vol. 29, no. 5–6, p. 575–588, Jun. 1998. https://doi.org/10.1016/S0021-8502(97)10037-4.

KOTAS, Tadeusz Jozef. **The Exergy Method of Thermal Plant Analysis**. Amsterdam, The Netherlands: Elsevier, 1985.

KRISHNA, Sachin Muralee; ABDUL SALAM, P.; TONGROON, Manida; CHOLLACOOP, Nuwong. Performance and emission assessment of optimally blended biodiesel-diesel-ethanol in diesel engine generator. **Applied Thermal Engineering**, vol. 155, p. 525–533, 5 Jun. 2019. https://doi.org/10.1016/j.applthermaleng.2019.04.012.

KUMAR, Satish; CHO, Jae Hyun; PARK, Jaedeuk; MOON, Il. Advances in diesel-alcohol blends and their effects on the performance and emissions of diesel engines. **Renewable and Sustainable Energy Reviews**, vol. 22, p. 46–72, 2013. https://doi.org/10.1016/j.rser.2013.01.017.

KUMAR, Vikram; SINGH, Akhilendra Pratap; AGARWAL, Avinash Kumar. Gaseous emissions (regulated and unregulated) and particulate characteristics of a medium-duty CRDI transportation diesel engine fueled with diesel-alcohol blends. **Fuel**, vol. 278, p. 118269, 15 Oct. 2020. DOI 10.1016/j.fuel.2020.118269. Available at: https://linkinghub.elsevier.com/retrieve/pii/S0016236120312655. Accessed on: 21 Jun. 2021.

KWANCHAREON, Prommes; LUENGNARUEMITCHAI, Apanee; JAI-IN, Samai. Solubility of a diesel–biodiesel–ethanol blend, its fuel properties, and its emission characteristics from diesel engine. **Fuel**, vol. 86, no. 7–8, p. 1053–1061, 1 May 2007. https://doi.org/10.1016/J.FUEL.2006.09.034.

KYRIAKIDES, Alexios; DIMAS, Vasilis; LYMPEROPOULOU, Eleni; KARONIS, Dimitris; LOIS, Evripidis. Evaluation of gasoline-ethanol-water ternary mixtures used as a fuel for an Otto engine. **Fuel**, vol. 108, p. 208–215, 2013. https://doi.org/10.1016/j.fuel.2013.02.035.

LAPUERTA, Magín; ARMAS, Octavio; GARCÍA-CONTRERAS, Reyes. Effect of Ethanol on Blending Stability and Diesel Engine Emissions. **Energy & Fuels**, vol. 23, no. 9, p. 4343–4354, 17 Sep. 2009. DOI 10.1021/ef900448m. Available at: https://pubs.acs.org/doi/10.1021/ef900448m.

LAPUERTA, Magín; ARMAS, Octavio; GÓMEZ, Arántzazu. Diesel particle size distribution estimation from digital image analysis. **Aerosol Science and Technology**, vol. 37, no. 4, p. 369–381, 2003. https://doi.org/10.1080/02786820300970.

LAPUERTA, Magín; ARMAS, Octavio; HERNÁNDEZ, Juan José; TSOLAKIS, Athanasios. Potential for reducing emissions in a diesel engine by fuelling with conventional biodiesel and Fischer–Tropsch diesel. **Fuel**, vol. 89, no. 10, p. 3106–3113, 1 Oct. 2010. DOI 10.1016/j.fuel.2010.05.013. Available at: https://www.sciencedirect.com/science/article/pii/S001623611000222X. Accessed on: 10 Jun. 2019.

LAPUERTA, Magín; ARMAS, Octavio; HERREROS, José M. Emissions from a diesel–bioethanol blend in an automotive diesel engine. **Fuel**, vol. 87, no. 1, p. 25–31, 1 Jan. 2008. DOI 10.1016/j.fuel.2007.04.007. Available at: https://www.sciencedirect.com/science/article/pii/S0016236107001901. Accessed on: 3 Mar. 2020.

LAPUERTA, Magín; GARCÍA-CONTRERAS, Reyes; CAMPOS-FERNÁNDEZ, Javier; DORADO, M. Pilar. Stability, Lubricity, Viscosity, and Cold-Flow Properties of Alcohol−Diesel Blends. **Energy & Fuels**, vol. 24, no. 8, p. 4497–4502, 19 Aug. 2010. DOI 10.1021/ef100498u. Available at: http://pubs.acs.org/doi/abs/10.1021/ef100498u. Accessed on: 9 Jan. 2019.

LAPUERTA, Magín; RODRÍGUEZ-FERNÁNDEZ, José; AGUDELO, John R. Diesel particulate emissions from used cooking oil biodiesel. **Bioresource Technology**, vol. 99, no. 4, p. 731–740, 1 Mar. 2008. https://doi.org/10.1016/J.BIORTECH.2007.01.033.

LAPUERTA, Magín; RODRÍGUEZ-FERNANDEZ, José; GARCÍA-CONTRERAS, Reyes; BOGARRA, María. Molecular interactions in blends of alcohols with diesel fuels: Effect on stability and distillation. **Fuel**, vol. 139, p. 171–179, 1 Jan. 2015. DOI 10.1016/j.fuel.2014.08.055. Available at: https://www.sciencedirect.com/science/article/pii/S0016236114008333?via%3Dihub#b0090. Accessed on: 10 Jun. 2019.

LECKEL, Dieter. Diesel Production from Fischer−Tropsch: The Past, the Present, and New Concepts. **Energy & Fuels**, vol. 23, no. 5, p. 2342–2358, 21 May 2009. https://doi.org/10.1021/ef900064c.

LEE, Jeongwoo; LEE, Sunyoup; LEE, Seokhwan. Experimental investigation on the performance and emissions characteristics of ethanol/diesel dual-fuel combustion. **Fuel**, vol. 220, no. December 2017, p. 72–79, 2018. https://doi.org/10.1016/j.fuel.2018.02.002.

LEFORT, I.; HERREROS, J. M.; TSOLAKIS, A. Reduction of low temperature engine pollutants by understanding the exhaust species interactions in a diesel oxidation catalyst. **Environmental Science and Technology**, vol. 48, no. 4, p. 2361–2367, 2014. https://doi.org/10.1021/es4051499.

LEI, Jilin; SHEN, Lizhong; BI, Yuhua; CHEN, Hong. A novel emulsifier for ethanol-diesel blends and its effect on performance and emissions of diesel engine. **Fuel**, vol. 93, p. 305–311, 2012. https://doi.org/10.1016/j.fuel.2011.06.013.

LI, De Gang; ZHEN, Huang; XINGCAI, Lǔ; WU-GAO, Zhang; JIAN-GUANG, Yang. Physico-chemical properties of ethanol-diesel blend fuel and its effect on performance and emissions of diesel engines. **Renewable Energy**, vol. 30, no. 6, p. 967–976, 2005. https://doi.org/10.1016/j.renene.2004.07.010.

LIU, Haifeng; HU, Bin; JIN, Chao. Effects of different alcohols additives on solubility of hydrous ethanol/diesel fuel blends. **Fuel**, vol. 184, p. 440–448, 15 Nov. 2016. https://doi.org/10.1016/J.FUEL.2016.07.037.

MA, Qixin; ZHANG, Quanchang; LIANG, Jichao; YANG, Chao. The performance and emissions characteristics of diesel/biodiesel/alcohol blends in a diesel engine. **Energy Reports**, vol. 7, p. 1016–1024, Nov. 2021. DOI 10.1016/j.egyr.2021.02.027. Available at: https://doi.org/10.1016/j.egyr.2021.02.027.

MAGAND, S; PIDOL, L; CHAUDOYE, F; SINOQUET, D; WAHL, F; CASTAGNE, M; LECOINTE, B. Use of Ethanol / Diesel Blend and Advanced Calibration Methods to Satisfy Euro 5 Emission Standards without DPF. **Oil Gas Sci. Technol. – Rev. IFP Energies**, vol. 66, no. 5, p. 855–875, 2011. DOI 10.2516/ogst/2011136. Available at: https://ogst.ifpenergiesnouvelles.fr/articles/ogst/abs/2011/05/ogst100088/ogst100088.html.

MAHMOUDI, Hamid; JAHANGIRI, Hessam; DOUSTDAR, Omid; AKBARI, Nazanin; WOOD, Joe; TSOLAKIS, Athanasios; WYSZYNSKI, Miroslaw Lech. Maximizing paraffin to olefin ratio employing simulated nitrogen-rich syngas via Fischer-Tropsch process over Co3O4/SiO2 catalysts. **Fuel Processing Technology**, vol. 208, no. July, p. 106477, 2020. https://doi.org/10.1016/j.fuproc.2020.106477.

MAJEWSKI, W.A.; KHAIR, M. K. **Diesel Emissions and Their Control**. [*S. l.*]: SAE International, 2006.

MALAQUIAS, Augusto César Teixeira; NETTO, Nilton Antônio Diniz; DA COSTA, Roberto Berlini Rodrigues; BAÊTA, José Guilherme Coelho. Combined effects of internal exhaust gas recirculation and tumble motion generation in a flex-fuel direct injection engine. **Energy Conversion and Management**, vol. 217, no. March, p. 113007, 2020. https://doi.org/10.1016/j.enconman.2020.113007.

MARTINS, Jorge; BRITO, F. P. Alternative fuels for internal combustion engines. **Energies**, vol. 13, no. 15, 2020. https://doi.org/10.3390/en13164086.

MARTINS, Jorge; TORRES, Felipe; TORRES, Ednildo; PIMENTA, Helcio; FERREIRA, Vitor. The Use of Biodiesel on the Performance and Emission Characteristics of Diesel Engined Vehicles. 3., 2013. **SAE Technical Papers** [...]. [*S. l.*]: SAE International: Warrendale, PA, USA, 2013. vol. 3, p. 1–8. DOI 10.4271/2013-01-1698. Available at: http://www.sae.org/technical/papers/2013-01-1698.

MAY-CARLE, J.-B.; PIDOL, L.; NICOLLE, A.; ANDERLOHR, J. M.; TOGBÉ, C.; DAGAUT, P. Experimental and Numerical Study of F-T/Biodiesel/Bioethanol Surrogate Fuel Oxidation in Jet-Stirred Reactor. **Combustion Science and Technology**, vol. 184, no. 7–8, p. 901–915, Jul. 2012. https://doi.org/10.1080/00102202.2012.663982.

MENDES GUEDES, Andrew David; LEAL BRAGA, Sergio; PRADELLE, Florian. Performance and combustion characteristics of a compression ignition engine running on diesel-biodiesel-ethanol (DBE) blends – Part 2: Optimization of injection timing. **Fuel**, vol. 225, p. 174–183, 1 Aug. 2018. https://doi.org/10.1016/j.fuel.2018.02.120.

MINISTÉRIO DA ECONOMIA. Rota 2030 - Mobilidade e Logística. Jan. 2021. Available at: https://www.gov.br/produtividade-e-comercio-exterior/pt-br/assuntos/competitividade-industrial/setor-automotivo/rota-2030-mobilidade-e-logistica. Accessed on: 27 May 2021.

MKS INSTRUMENTS. MultiGas^{TM} 2030 on-line gas analysis. 2017. Available at: https://www.mksinst.com/mam/celum/celum_assets/resources/onlinemultigas2030ds.pdf?1. Accessed on: 7 Sep. 2019.

MOFFAT, Robert J. Describing the uncertainties in experimental results. **Experimental Thermal and Fluid Science**, vol. 1, no. 1, p. 3–17, 1988. https://doi.org/10.1016/0894-1777(88)90043-X.

MOFIJUR, M.; RASUL, M. G.; HYDE, J.; AZAD, A. K.; MAMAT, R.; BHUIYA, M. M.K. Role of biofuel and their binary (diesel-biodiesel) and ternary (ethanol-biodiesel-diesel) blends on internal combustion engines emission reduction. **Renewable and Sustainable Energy Reviews**, vol. 53, p. 265–278, 2016. https://doi.org/10.1016/j.rser.2015.08.046.

MOON, Gunfeel; LEE, Yonggyu; CHOI, Kyonam; JEONG, Dongsoo. Emission characteristics of diesel, gas to liquid, and biodiesel-blended fuels in a diesel engine for passenger cars. **Fuel**, vol. 89, no. 12, p. 3840–3846, 1 Dec. 2010. DOI 10.1016/j.fuel.2010.07.009. Available at: https://linkinghub.elsevier.com/retrieve/pii/S001623611000356X. Accessed on: 27 May 2021.

MOON, Gunfeel; LEE, Yonggyu; CHOI, Kyonam; JEONG, Dongsoo. Experimental study on characteristics of diesel particulate emissions with diesel, GTL, and blended fuels. **SAE Technical Papers**, 2009. https://doi.org/10.4271/2009-24-0098.

MORAN, MICHAEL J. ; SHAPIRO, HOWARD N. ; BOETTNER, DAISIE D. ; BAILEY, Margaret B. **Fundamentals of Engineering Thermodynamics**. 9th ed. Hoboken, NJ, USA: Wiley, 2018. Available at: https://www.wiley.com/en-us/Fundamentals+of+Engineering+Thermodynamics%2C+9th+Edition-p-ES81119391388.

MUINOS, Martin; SOLOIU, Valentin; MONCADA, Jose; GAUBERT, Remi; MOLINA, Gustavo; WILLIAMS, Johnnie. Experimental Investigation on the Combustion and Emissions Characteristics of n-Butanol / GTL and n-Butanol/Diesel Blends in a Single-Cylinder MD-CI Engine. 2017-March., 28 Mar. 2017. **SAE Technical Papers** [...]. [*S. l.: s. n.*], 28 Mar. 2017. vol. 2017-March, . DOI 10.4271/2017-01-0719. Available at: https://www.sae.org/content/2017-01-0719/.

MUSSATTO, Solange I.; DRAGONE, Giuliano; GUIMARÃES, Pedro M.R.; SILVA, João Paulo A.; CARNEIRO, Lívia M.; ROBERTO, Inês C.; VICENTE, António; DOMINGUES, Lucília; TEIXEIRA, José A. Technological trends, global market, and challenges of bio-ethanol production. **Biotechnology Advances**, vol. 28, no. 6, p. 817–830, 2010. https://doi.org/10.1016/j.biotechadv.2010.07.001.

NABI, Md Nurun; HUSTAD, Johan Einar; AREFIN, Md Arman. The influence of Fischer–Tropsch-biodiesel–diesel blends on energy and exergy parameters in a six-cylinder turbocharged diesel engine. **Energy Reports**, vol. 6, p. 832–840, Nov. 2020. DOI 10.1016/j.egyr.2020.04.011. Available at: https://doi.org/10.1016/j.egyr.2020.04.011.

NETT TECHNOLOGIES. Diesel Oxidation Catalyst. 2019. Available at: https://www.nettinc.com. Accessed on: 6 Dec. 2019.

NEVES, Renato Cruz; KLEIN, Bruno Colling; DA SILVA, Ricardo Justino; REZENDE, Mylene Cristina Alves Ferreira; FUNKE, Axel; OLIVAREZ-GÓMEZ, Edgardo; BONOMI, Antonio; MACIEL-FILHO, Rubens. A vision on biomass-to-liquids (BTL) thermochemical routes in integrated sugarcane biorefineries for biojet fuel production. **Renewable and Sustainable Energy Reviews**, vol. 119, p. 109607, 1 Mar. 2020. DOI 10.1016/j.rser.2019.109607. Available at: https://linkinghub.elsevier.com/retrieve/pii/S1364032119308159. Accessed on: 24 May 2021.

NO, Soo Young. Application of bioethanol to advanced CI engines; dual fuel and RCCI combustion modes–a review. **International Journal of Green Energy**, vol. 16, no. 14, p. 1105–1130, 2019. https://doi.org/10.1080/15435075.2019.1653878.

NOUR, Mohamed; KOSAKA, Hidenori; BADY, Mahmoud; SATO, Susumu; ABDEL-RAHMAN, Ali K. Combustion and emission characteristics of DI diesel engine fuelled by ethanol injected into the exhaust manifold. **Fuel Processing Technology**, vol. 164, p. 33–50, 1 Sep. 2017. https://doi.org/10.1016/J.FUPROC.2017.04.018.

ODZIEMKOWSKA, Małgorzata; MATUSZEWSKA, Anna; CZARNOCKA, Joanna. Diesel oil with bioethanol as a fuel for compression-ignition engines. **Applied Energy**, vol. 184, p. 1264–1272, 2016. https://doi.org/https://doi.org/10.1016/j.apenergy.2016.07.069.

OECD/FAO. **OECD-FAO Agricultural Outlook 2019-2028**. [*S. l.: s. n.*], 2019. DOI https://doi.org/10.1787/agr_outlook-2019-en. Available at: https://www.oecd-ilibrary.org/agriculture-and-food/oecd-fao-agricultural-outlook-2019-2028_agr_outlook-2019-en.

OH, Harry; LUO, Jinyong; EPLING, William S. NO oxidation inhibition by hydrocarbons over a diesel oxidation catalyst: Reaction between surface nitrates and hydrocarbons. **Catalysis Letters**, vol. 141, no. 12, p. 1746–1751, 2011. https://doi.org/10.1007/s10562-011-0714-z.

OKEKE, Ikenna J; SAHOO, Kamalakanta; KALIYAN, Nalladurai; MANI, Sudhagar. Life cycle assessment of renewable diesel production via anaerobic digestion and Fischer-Tropsch synthesis from miscanthus grown in strip-mined soils. **Journal of Cleaner Production**, vol. 249, p. 119358, Mar. 2020. DOI 10.1016/j.jclepro.2019.119358. Available at: http://www.sciencedirect.com/science/article/pii/S0959652619342283.

OKUBO, Masaaki; KUWAHARA, Takuya. Emission regulations. **New Technologies for Emission Control in Marine Diesel Engines**. [*S. l.*]: Elsevier, 2020. p. 25–51. https://doi.org/10.1016/b978-0-12-812307-2.00002-x. Accessed on: 7 Jun. 2021.

ÖZCAN, Hakan. Energy and exergy analyses of Al2O3-diesel-biodiesel blends in a diesel engine. **International Journal of Exergy**, vol. 28, no. 1, p. 29, 2019. https://doi.org/10.1504/IJEX.2019.097270.

PAREDES ROJAS, Juan Carlos; TORRES SAN MIGUEL, Christopher Rene; VÁZQUEZ MEDINA, Rubén; LEAL NARANJO, José Alfredo; ORTIZ HERNÀNDEZ, Fernando Elí; COSTA CASTELLÓ, Ramón. Pollutant Emissions and Combustion Efficiency Assessment of Engines Using Biodiesel. **Applied Sciences**, vol. 10, no. 23, p. 8646, 3 Dec. 2020. https://doi.org/10.3390/app10238646.

PARRAVICINI, Matteo; BARRO, Christophe; BOULOUCHOS, Konstantinos. Experimental characterization of GTL, HVO, and OME based alternative fuels for diesel engines. **Fuel**, vol. 292, p. 120177, 15 May 2021. DOI 10.1016/j.fuel.2021.120177. Available at: https://linkinghub.elsevier.com/retrieve/pii/S0016236121000533. Accessed on: 27 May 2021.

PATTERSON, Michael J.; ANGOVE, Dennys E.; CANT, Noel W. The effect of carbon monoxide on the oxidation of four C6 to C8 hydrocarbons over platinum, palladium and rhodium. **Applied Catalysis B: Environmental**, vol. 26, no. 1, p. 47–57, 10 Apr. 2000. https://doi.org/10.1016/S0926-3373(00)00110-7.

PAUL, Abhishek; PANUA, Rajsekhar; DEBROY, Durbadal. An experimental study of combustion, performance, exergy and emission characteristics of a CI engine fueled by Diesel-ethanol-biodiesel blends. **Energy**, vol. 141, p. 839–852, 15 Dec. 2017. DOI 10.1016/j.energy.2017.09.137. Available at: https://www.sciencedirect.com/science/article/pii/S0360544217316596?via%3Dihub. Accessed on: 7 Jan. 2019.

PAYUS, C.M.; VASU THEVAN, A.T.; SENTIAN, J. Impact of school traffic on outdoor carbon monoxide levels. **City and Environment Interactions**, vol. 4, no. 2019, p. 100032, Dec. 2019. https://doi.org/10.1016/j.cacint.2020.100032.

PEDROZO, Vinícius B.; MAY, Ian; GUAN, Wei; ZHAO, Hua. High efficiency ethanol-diesel dual-fuel combustion: A comparison against conventional diesel combustion from low to full engine load. **Fuel**, vol. 230, p. 440–451, 15 Oct. 2018. https://doi.org/10.1016/J.FUEL.2018.05.034.

PETROBRAS. Petrobras - Fatos e Dados - Iniciamos produção de Libra. 2017. Available at: https://petrobras.com.br/fatos-e-dados/iniciamos-producao-de-libra.htm. Accessed on: 16 Mar. 2021.

PETROSA. GTL Technology. 2021. Available at: http://www.petrosa.co.za/innovation_in_action/Pages/GTL-TECHNOLOGY.aspx. Accessed on: 17 Feb. 2021.

PIDOL, Ludivine; LECOINTE, Bertrand; JEULAND, Nicolas. Ethanol as a Diesel Base Fuel: Managing the Flash Point Issue - Consequences on Engine Behavior. 4970., 15 Jun. 2009. **SAE Technical Papers** [...]. [*S. l.*: *s. n.*], 15 Jun. 2009. vol. 4970, . DOI 10.4271/2009-01-1807. Available at: https://www.sae.org/content/2009-01-1807/.

PIDOL, Ludivine; LECOINTE, Bertrand; PESANT, Laurie; JEULAND, Nicolas. Ethanol as a Diesel Base Fuel - Potential in HCCI Mode. 6 Oct. 2008. **SAE Technical Papers** [...]. [*S. l.*: *s. n.*], 6 Oct. 2008. DOI 10.4271/2008-01-2506. Available at: https://www.sae.org/content/2008-01-2506/.

PIDOL, Ludivine; LECOINTE, Bertrand; STARCK, Laurie; JEULAND, Nicolas. Ethanol–biodiesel–Diesel fuel blends: Performances and emissions in conventional Diesel and advanced Low Temperature Combustions. **Fuel**, vol. 93, p. 329–338, 1 Mar. 2012. DOI 10.1016/j.fuel.2011.09.008. Available at: https://www.sciencedirect.com/science/article/pii/S0016236111005485#b0135. Accessed on: 4 Mar. 2020.

PINTO, Angelo C.; GUARIEIRO, Lilian L. N.; REZENDE, Michelle J. C.; RIBEIRO, Núbia M.; TORRES, Ednildo A.; LOPES, Wilson A.; PEREIRA, Pedro A. de P.; ANDRADE, Jailson B. de. Biodiesel: an overview. **Journal of the Brazilian Chemical Society**, vol. 16, no. 6b, p. 1313–1330, Nov. 2005. https://doi.org/10.1590/S0103-50532005000800003.

POLICARPO, N. A.; FRUTUOSO, F. S.; CASSIANO, D. R.; CAVALCANTE, F. S.A.; ARAÚJO, R. S.; BERTONCINI, B. V.; OLIVEIRA, M. L.M. Emission estimates for an on-road flex-fuel vehicles operated by ethanol-gasoline blends in an urban region, Brazil. **Urban Climate**, vol. 24, no. July 2017, p. 111–120, 2018. https://doi.org/10.1016/j.uclim.2018.01.005.

PRADELLE, Florian; LEAL BRAGA, Sergio; FONSECA DE AGUIAR MARTINS, Ana Rosa; TURKOVICS, Franck; NOHRA CHAAR PRADELLE, Renata. Performance and combustion characteristics of a compression ignition engine running on diesel-biodiesel-ethanol (DBE) blends – Potential as diesel fuel substitute on an Euro III engine. **Renewable Energy**, vol. 136, p. 586–598, 1 Jun. 2019. https://doi.org/10.1016/J.RENENE.2019.01.025.

PRAPTIJANTO, Achmad; MUHARAM, Aam; NUR, Arifin; PUTRASARI, Yanuandri. Effect of ethanol percentage for diesel engine performance using virtual engine simulation tool. **Energy Procedia**, vol. 68, p. 345–354, 2015. https://doi.org/10.1016/j.egypro.2015.03.265.

PUŠKÁR, Michal; KOPAS, Melichar. System based on thermal control of the HCCI technology developed for reduction of the vehicle NOX emissions in order to fulfil the future standard Euro 7. **Science of The Total Environment**, vol. 643, p. 674–680, 1 Dec. 2018. https://doi.org/10.1016/J.SCITOTENV.2018.06.082.

RAELE, Ricardo; BOAVENTURA, João Mauricio Gama; FISCHMANN, Adalberto Américo; SARTURI, Greici. Scenarios for the second generation ethanol in Brazil. **Technological Forecasting and Social Change**, vol. 87, p. 205–223, 2014. https://doi.org/10.1016/j.techfore.2013.12.010.

RAMOS, André Luis Dantas; MARQUES, José Jailton; SANTOS, Vagner dos; FREITAS, Lisiane dos Santos; SANTOS, Rosanne Graziele Vieira de Melo; SOUZA, Mariana de Mattos Vieira Mello. Current stage of development of GTL technology and perspectives for Brazil. **Química Nova**, vol. 34, no. 10, p. 1704–1716, 2011. DOI 10.1590/S0100-40422011001000004. Available at: http://www.scielo.br/scielo.php?script=sci_arttext&pid=S0100-40422011001000004&lng=en&nrm=iso&tlng=pt. Accessed on: 24 May 2021.

RASTOGI, Meenal; SHRIVASTAVA, Smriti. Recent advances in second generation bioethanol production: An insight to pretreatment, saccharification and fermentation processes. **Renewable and Sustainable Energy Reviews**, vol. 80, no. January, p. 330–340, 2017. https://doi.org/10.1016/j.rser.2017.05.225.

RASUL, Ijaz; AZEEM, Farrukh; SIDDIQUE, Muhammad H; MUZAMMIL, Saima; RASUL, Azhar; MUNAWAR, Anam; AFZAL, Muhammad; ALI, Muhammad A; NADEEM, Habibullah. Chapter 8 - Algae Biotechnology: A Green Light for Engineered Algae. *In*: ZIA, Khalid Mahmood; ZUBER, Mohammad; ALI BLENDS, AND COMPOSITES, Muhammad B T - Algae Based Polymers (eds.). [*S. l.*]: Elsevier, 2017. p. 301–334. https://doi.org/https://doi.org/10.1016/B978-0-12-812360-7.00008-2.

REIJNDERS, Jos; BOOT, Michael; DE GOEY, Philip. Impact of aromaticity and cetane number on the soot-NOx trade-off in conventional and low temperature combustion. **Fuel**, vol. 186, p. 24–34, Dec. 2016. https://doi.org/10.1016/j.fuel.2016.08.009.

REN21. **Renewables 2020 Global Status Report**. Paris: [*s. n.*], 2020. Available at: http://www.ren21.net/resources/publications/.

RENEWABLE FUELS ASSOCIATION (RFA). Annual World Fuel Ethanol Production 2015-2019. 2020. Available at: https://ethanolrfa.org/statistics/annual-ethanol-production/. Accessed on: 10 Jun. 2020.

REŞITOĞLU, İbrahim Aslan; ALTINIŞIK, Kemal; KESKIN, Ali. The pollutant emissions from diesel-engine vehicles and exhaust aftertreatment systems. **Clean Technologies and Environmental Policy**, vol. 17, no. 1, p. 15–27, 11 Jan. 2015. DOI 10.1007/s10098-014-0793-9. Available at: http://link.springer.com/10.1007/s10098-014-0793-9.

RIBEIRO, Núbia; PINTO, Angelo C .; QUINTELLA, Cristina M.; DA ROCHA, Gisele O.; TEIXEIRA, Leonardo S.G.; GUARIEIRO, Lílian L.N.; RANGEL, Maria do Carmo; VELOSO, Márcia C.C.; REZENDE, Michelle J.C.; DA CRUZ, Rosenira Serpa; DE OLIVEIRA, Ana Maria; TORRES, Ednildo A.; DE ANDRADE, Jailson B. The role of additives for diesel and

diesel blended (ethanol or biodiesel) fuels: A review. **Energy and Fuels**, vol. 21, no. 4, p. 2433–2445, 2007. https://doi.org/10.1021/ef070060r.

ROBERTS, L G; PATTERSON, T J. Biofuels. *In*: WEXLER, Philip B T - Encyclopedia of Toxicology (Third Edition) (ed.). Oxford: Academic Press, 2014. p. 469–475. https://doi.org/https://doi.org/10.1016/B978-0-12-386454-3.01054-X.

ROCKY MOUNTAIN GTL. Carseland Alberta Facility. 2021. Available at: http://rockymountaingtl.com/projects/. Accessed on: 5 Mar. 2021.

RODRÍGUEZ-FERNÁNDEZ, J.; TSOLAKIS, A.; AHMADINEJAD, M.; SITSHEBO, S. Investigation of the deactivation of a NOx-reducing hydrocarbon-selective catalytic reduction (HC-SCR) catalyst by thermogravimetric analysis: Effect of the fuel and prototype catalyst. **Energy and Fuels**, vol. 24, no. 2, p. 992–1000, 2010. https://doi.org/10.1021/ef900996f.

RODRÍGUEZ-FERNÁNDEZ, J.; TSOLAKIS, A.; THEINNOI, K.; SNOWBALL, J.; SAWTELL, A.; YORK, A.P.E. Engine Performance and Emissions from Dual Fuelled Engine with In-Cylinder Injected Diesel Fuels and In-Port Injected Bioethanol. 15 Jun. 2009. **SAE Technical Papers** [...]. [*S. l.*: *s. n.*], 15 Jun. 2009. https://doi.org/10.4271/2009-01-1853.

RODRÍGUEZ-FERNÁNDEZ, José; HERNÁNDEZ, Juan José; SÁNCHEZ-VALDEPEÑAS, Jesús. Effect of oxygenated and paraffinic alternative diesel fuels on soot reactivity and implications on DPF regeneration. **Fuel**, vol. 185, p. 460–467, 1 Dec. 2016. https://doi.org/10.1016/J.FUEL.2016.08.016.

ROSA, Josimar Souza; TELLI, Giovani Dambros; ALTAFINI, Carlos Roberto; WANDER, Paulo Roberto; OLIVEIRA ROCHA, Luiz Alberto. Dual fuel ethanol port injection in a compression ignition diesel engine: Technical analysis, environmental behavior, and economic viability. **Journal of Cleaner Production**, vol. 308, p. 127396, 25 Jul. 2021. DOI 10.1016/j.jclepro.2021.127396. Available at: https://linkinghub.elsevier.com/retrieve/pii/S0959652621016152. Accessed on: 16 May 2021.

ROSEN, Marc A.; DINCER, Ibrahim; KANOGLU, Mehmet. Role of exergy in increasing efficiency and sustainability and reducing environmental impact. **Energy Policy**, vol. 36, no. 1, p. 128–137, 2008. https://doi.org/10.1016/j.enpol.2007.09.006.

ROSLI, Mohd A.F.; AZIZ, A. Rashid A.; ISMAEL, Mhadi A.; ELBASHIR, Nimir O.; ZAINAL A., Ezrann Z.; BAHAROM, Masri; MOHAMMED, Salah E. Experimental study of micro-explosion and puffing of gas-to-liquid (GTL) fuel blends by suspended droplet method. **Energy**, vol. 218, p. 119462, 1 Mar. 2021. DOI 10.1016/j.energy.2020.119462. Available at: https://linkinghub.elsevier.com/retrieve/pii/S036054422032569X. Accessed on: 16 Dec. 2020.

ROSO, Vinícius Rückert; SANTOS, Nathália Duarte Souza Alvarenga; ALVAREZ, Carlos Eduardo Castilla; RODRIGUES FILHO, Fernando Antonio; PUJATTI, Fabricio José Pacheco; VALLE, Ramon Molina. Effects of mixture enleanment in combustion and emission parameters using a flex-fuel engine with ethanol and gasoline. **Applied Thermal Engineering**, vol. 153, no. March, p. 463–472, 2019. https://doi.org/10.1016/j.applthermaleng.2019.03.012.

ROUNCE, P.; TSOLAKIS, A.; RODRÍGUEZ-FERNÁNDEZ, J.; YORK, A. P.E.; CRACKNELL, R. F.; CLARK, R. H. Diesel engine performance and emissions when first

generation meets next generation biodiesel. **SAE Technical Papers**, vol. 4970, p. 1–10, 2009. https://doi.org/10.4271/2009-01-1935.

ROY, Murari Mohon; CALDER, Jorge; WANG, Wilson; MANGAD, Arvind; DINIZ, Fernando Cezar Mariano. Cold start idle emissions from a modern Tier-4 turbo-charged diesel engine fueled with diesel-biodiesel, diesel-biodiesel-ethanol, and diesel-biodiesel-diethyl ether blends. **Applied Energy**, vol. 180, p. 52–65, 15 Oct. 2016. https://doi.org/10.1016/j.apenergy.2016.07.090.

RULLI, Maria Cristina; BELLOMI, Davide; CAZZOLI, Andrea; DE CAROLIS, Giulia; D'ODORICO, Paolo. The water-land-food nexus of first-generation biofuels. **Scientific Reports**, vol. 6, no. February, p. 1–10, 2016. https://doi.org/10.1038/srep22521.

RUSSELL, April; EPLING, William S. Diesel oxidation catalysts. **Catalysis Reviews - Science and Engineering**, vol. 53, no. 4, p. 337–423, 2011. https://doi.org/10.1080/01614940.2011.596429.

SADEQ, A.M.; BASSIONY, M.A.; ELBASHIR, A.M.; AHMED, S.F.; KHRAISHEH, M. Combustion and emissions of a diesel engine utilizing novel intake manifold designs and running on alternative fuels. **Fuel**, vol. 255, p. 115769, 1 Nov. 2019. DOI 10.1016/j.fuel.2019.115769. Available at: https://linkinghub.elsevier.com/retrieve/pii/S0016236119311214. Accessed on: 27 May 2021.

SAJJAD, H.; MASJUKI, H.H.; VARMAN, M.; KALAM, M.A.; ARBAB, M.I.; IMTENAN, S.; ASHRAFUL, A.M. Influence of gas-to-liquid (GTL) fuel in the blends of Calophyllum inophyllum biodiesel and diesel: An analysis of combustion–performance–emission characteristics. **Energy Conversion and Management**, vol. 97, p. 42–52, 1 Jun. 2015. https://doi.org/10.1016/J.ENCONMAN.2015.02.037.

SAJJAD, H.; MASJUKI, H.H.; VARMAN, M.; KHAN, Mohammad Mahmudur Rahman; ARBAB, M.I.; IMTENAN, S.; SANJID, A. Comparative Study of Biodiesel, GTL Fuel and Their Blends in Context of Engine Performance and Exhaust Emission. **Procedia Engineering**, vol. 90, p. 466–471, 1 Jan. 2014. https://doi.org/10.1016/J.PROENG.2014.11.758.

SAMAVATI, Mahrokh; SANTARELLI, Massimo; MARTIN, Andrew; NEMANOVA, Vera. Production of Synthetic Fischer–Tropsch Diesel from Renewables: Thermoeconomic and Environmental Analysis. **Energy & Fuels**, vol. 32, no. 2, p. 1744–1753, 15 Feb. 2018. DOI 10.1021/acs.energyfuels.7b02465. Available at: https://pubs.acs.org/doi/10.1021/acs.energyfuels.7b02465.

ŞANLI, Bengi Gozmen. Energetic and exergetic performance of a diesel engine fueled with diesel and microalgae biodiesel. **Energy Sources, Part A: Recovery, Utilization, and Environmental Effects**, vol. 41, no. 20, p. 2519–2533, 18 Oct. 2019. DOI 10.1080/15567036.2019.1587097. Available at: https://www.tandfonline.com/doi/full/10.1080/15567036.2019.1587097. Accessed on: 30 Jul. 2019.

ŞANLI, Bengi Gözmen; ULUDAMAR, Erinç. Energy and exergy analysis of a diesel engine fuelled with diesel and biodiesel fuels at various engine speeds. **Energy Sources, Part A: Recovery, Utilization, and Environmental Effects**, vol. 42, no. 11, p. 1299–1313, 2 Jun. 2020. https://doi.org/10.1080/15567036.2019.1635229.

SANTOS, Ronaldo Gonçalves dos; ALENCAR, Andre Cardoso. Biomass-derived syngas production via gasification process and its catalytic conversion into fuels by Fischer Tropsch synthesis: A review. **International Journal of Hydrogen Energy**, vol. 45, no. 36, p. 18114–18132, 13 Jul. 2020. DOI 10.1016/j.ijhydene.2019.07.133. Available at: https://www.sciencedirect.com/science/article/pii/S0360319919327090. Accessed on: 23 Sep. 2019.

SANTOS, Tito B.; FERREIRA, Vitor P.; TORRES, Ednildo A.; DA SILVA, Julio A. M.; ORDONEZ, Juan C. Energy analysis and exhaust emissions of a stationary engine fueled with diesel–biodiesel blends at variable loads. **Journal of the Brazilian Society of Mechanical Sciences and Engineering**, vol. 39, no. 8, p. 3237–3247, 1 Aug. 2017. DOI 10.1007/s40430-017-0847-0. Available at: http://link.springer.com/10.1007/s40430-017-0847-0. Accessed on: 17 Apr. 2019.

SARAVANAN, P.; KUMAR, Nallapaneni Manoj; ETTAPPAN, M.; DHANAGOPAL, R.; VISHNUPRIYAN, J. Effect of exhaust gas re-circulation on performance, emission and combustion characteristics of ethanol-fueled diesel engine. **Case Studies in Thermal Engineering**, vol. 20, no. April, p. 100643, Aug. 2020. https://doi.org/10.1016/j.csite.2020.100643.

SARIKOÇ, Selçuk; ÖRS, İlker; ÜNALAN, Sebahattin. An experimental study on energy-exergy analysis and sustainability index in a diesel engine with direct injection diesel-biodiesel-butanol fuel blends. **Fuel**, vol. 268, p. 117321, 15 May 2020. DOI 10.1016/j.fuel.2020.117321. Available at: https://www.sciencedirect.com/science/article/pii/S0016236120303161. Accessed on: 4 Mar. 2020.

SASOL. Gas-to-Liquids: Overview. 2021. Available at: https://www.sasol.com/innovation/gas-liquids/overview. Accessed on: 4 Feb. 2021.

SAYIN, C.; HOSOZ, M.; CANAKCI, M.; KILICASLAN, I. Energy and exergy analyses of a gasoline engine. **International Journal of Energy Research**, vol. 31, no. 3, p. 259–273, 10 Mar. 2007. https://doi.org/10.1002/er.1246.

SAYIN, Cenk; USLU, Kadir; CANAKCI, Mustafa. Influence of injection timing on the exhaust emissions of a dual-fuel CI engine. **Renewable Energy**, vol. 33, no. 6, p. 1314–1323, 1 Jun. 2008. https://doi.org/10.1016/J.RENENE.2007.07.007.

SAYIN KUL, Bahar; KAHRAMAN, Ali. Energy and Exergy Analyses of a Diesel Engine Fuelled with Biodiesel-Diesel Blends Containing 5% Bioethanol. **Entropy**, vol. 18, no. 11, p. 387, 31 Oct. 2016. DOI 10.3390/e18110387. Available at: http://www.mdpi.com/1099-4300/18/11/387.

SERHAN, N.; TSOLAKIS, A.; WAHBI, A.; MARTOS, F.J.; GOLUNSKI, S. Modifying catalytically the soot morphology and nanostructure in diesel exhaust: Influence of silver De-NOx catalyst (Ag/Al2O3). **Applied Catalysis B: Environmental**, vol. 241, p. 471–482, 1 Feb. 2019. https://doi.org/10.1016/j.apcatb.2018.09.068.

SERRANO, José Ramón; NOVELLA, Ricardo; PIQUERAS, Pedro. Why the Development of Internal Combustion Engines Is Still Necessary to Fight against Global Climate Change from the Perspective of Transportation. **Applied Sciences**, vol. 9, no. 21, p. 4597, 29 Oct. 2019. https://doi.org/10.3390/app9214597.

SHAHIR, S. A.; MASJUKI, H. H.; KALAM, M. A.; IMRAN, A.; ASHRAFUL, A. M. Performance and emission assessment of diesel-biodiesel-ethanol/bioethanol blend as a fuel in diesel engines: A review. **Renewable and Sustainable Energy Reviews**, vol. 48, p. 62–78, 2015. https://doi.org/10.1016/j.rser.2015.03.049.

SHAHIR, S.A.; MASJUKI, H.H.; KALAM, M.A.; IMRAN, A.; FATTAH, I.M. Rizwanul; SANJID, A. Feasibility of diesel–biodiesel–ethanol/bioethanol blend as existing CI engine fuel: An assessment of properties, material compatibility, safety and combustion. **Renewable and Sustainable Energy Reviews**, vol. 32, p. 379–395, 1 Apr. 2014. https://doi.org/10.1016/j.rser.2014.01.029.

SHELL. Gas-to-liquids. 2021. Available at: https://www.shell.com/energy-and-innovation/natural-gas/gas-to-liquids.html. Accessed on: 31 Jan. 2021.

SHI, Jinhong; WANG, Tie; ZHAO, Zhen; WU, Zhifei; ZHANG, Zhengwu. Cycle-to-Cycle Variation of a Diesel Engine Fueled with Fischer–Tropsch Fuel Synthesized from Coal. **Applied Sciences**, vol. 9, no. 10, p. 2032, 17 May 2019. DOI 10.3390/app9102032. Available at: https://www.mdpi.com/2076-3417/9/10/2032.

SOLOIU, Valentin; GAUBERT, Remi; MONCADA, Jose; WILEY, Justin; WILLIAMS, Johnnie; HARP, Spencer; ILIE, Marcel; MOLINA, Gustavo; MOTHERSHED, David. Reactivity controlled compression ignition and low temperature combustion of Fischer-Tropsch Fuel Blended with n-butanol. **Renewable Energy**, vol. 134, p. 1173–1189, 1 Apr. 2019. DOI 10.1016/j.renene.2018.09.047. Available at: https://www.sciencedirect.com/science/article/pii/S0960148118311108#fig2. Accessed on: 6 May 2019.

SOLOMON, Barry D.; BARNES, Justin R.; HALVORSEN, Kathleen E. Grain and cellulosic ethanol: History, economics, and energy policy. **Biomass and Bioenergy**, vol. 31, no. 6, p. 416–425, 2007. https://doi.org/10.1016/j.biombioe.2007.01.023.

SORIANO, José Antonio; GARCÍA-CONTRERAS, Reyes; LEIVA-CANDIA, David; SOTO, Felipe. Influence on Performance and Emissions of an Automotive Diesel Engine Fueled with Biodiesel and Paraffinic Fuels: GTL and Biojet Fuel Farnesane. **Energy & Fuels**, vol. 32, no. 4, p. 5125–5133, 19 Apr. 2018. https://doi.org/10.1021/acs.energyfuels.7b03779.

SRIKANTH, H.V.; G, Sharanappa; MANNE, Bhaskar; KUMAR, S. Bharath. Niger seed oil biodiesel as an emulsifier in diesel-ethanol blends for compression ignition engine. **Renewable Energy**, vol. 163, p. 1467–1478, 1 Jan. 2021. DOI 10.1016/j.renene.2020.07.010. Available at: https://linkinghub.elsevier.com/retrieve/pii/S0960148120310867. Accessed on: 17 May 2021.

STRANGES, Anthony N. A History of the Fischer-Tropsch Synthesis in Germany 1926–45. **Studies in Surface Science and Catalysis**. [*S. l.*: *s. n.*], 2007. vol. 163, p. 1–27. DOI 10.1016/S0167-2991(07)80469-1. Available at: https://linkinghub.elsevier.com/retrieve/pii/S0167299107804691.

SUAREZ-BERTOA, Ricardo; MENDOZA-VILLAFUERTE, Pablo; RICCOBONO, Francesco; VOJTISEK, Michal; PECHOUT, Martin; PERUJO, Adolfo; ASTORGA, Covadonga. On-road measurement of NH 3 emissions from gasoline and diesel passenger cars during real world driving conditions. **Atmospheric Environment**, vol. 166, p. 488–497, Oct.

2017. DOI 10.1016/j.atmosenv.2017.07.056. Available at: http://dx.doi.org/10.1016/j.atmosenv.2017.07.056.

SUKJIT, Ekarong; HERREROS, Jose M.; DEARN, Karl; TSOLAKIS, Athanasios. Improving Ethanol-Diesel Blend Through the Use of Hydroxylated Biodiesel. 13 Oct. 2014. **SAE Technical Papers** [...]. [*S. l.*: *s. n.*], 13 Oct. 2014. https://doi.org/10.4271/2014-01-2776.

SUN, Dandan; WANG, Tie; CAO, Yisen; YANG, Tiatian; JIANG, Quanjun; FAN, Bo. The Influence of F-T Diesel/Methanol Micro-Emulsified Fuels on Emission Characteristics of a Diesel Engine. **Chinese Internal Combustion Engine Engineering**, vol. 38, no. 3, p. 41–51, 2017. https://doi.org/10.13949/j.cnki.nrjgc.2017.03.007.

SUN, Wenxu; LIU, Zhan. Parametric Assessment on the Advanced Exergy Performance of a CO2 Energy Storage Based Trigeneration System. **Applied Sciences**, vol. 10, no. 23, p. 8341, 24 Nov. 2020. DOI 10.3390/app10238341. Available at: https://www.mdpi.com/2076-3417/10/23/8341.

SUTJIONO, Raymond; TAYAL, Prateek; ZHOU, Keqin; MECKL, Peter. Real-Time On-Board Indirect Light-Off Temperature Estimation as a Detection Technique of Diesel Oxidation Catalyst Effectiveness Level. 2., 8 Apr. 2013. **SAE Technical Papers** [...]. [*S. l.*: *s. n.*], 8 Apr. 2013. vol. 2, . https://doi.org/10.4271/2013-01-1517.

SZARGUT, Jan. **Exergy Method: Technical and Ecological Applications**. Southampton, UK: WIT Press, 2005.

TAGHIZADEH-ALISARAEI, Ahmad; REZAEI-ASL, Abbas. The effect of added ethanol to diesel fuel on performance, vibration, combustion and knocking of a CI engine. **Fuel**, vol. 185, p. 718–733, 1 Dec. 2016. https://doi.org/10.1016/J.FUEL.2016.08.041.

TAGOMORI, Isabela S.; ROCHEDO, Pedro R.R.; SZKLO, Alexandre. Techno-economic and georeferenced analysis of forestry residues-based Fischer-Tropsch diesel with carbon capture in Brazil. **Biomass and Bioenergy**, vol. 123, p. 134–148, 1 Apr. 2019. DOI 10.1016/j.biombioe.2019.02.018. Available at: https://www.sciencedirect.com/science/article/pii/S0961953419300881. Accessed on: 10 Jun. 2019.

TAT, Mustafa Ertunc. Cetane number effect on the energetic and exergetic efficiency of a diesel engine fuelled with biodiesel. **Fuel Processing Technology**, vol. 92, no. 7, p. 1311–1321, 2011. https://doi.org/10.1016/j.fuproc.2011.02.006.

TELLI, Giovani Dambros; ALTAFINI, Carlos Roberto; ROSA, Josimar Souza; COSTA, Carlos Alberto. Experimental investigation of a compression ignition engine operating on B7 direct injected and hydrous ethanol fumigation. **Energy**, vol. 165, p. 106–117, 15 Dec. 2018. https://doi.org/10.1016/j.energy.2018.09.171.

THAKUR, Amit Kumar; KAVITI, Ajay Kumar; MEHRA, Roopesh; MER, K. K.S. Progress in performance analysis of ethanol-gasoline blends on SI engine. **Renewable and Sustainable Energy Reviews**, vol. 69, no. July 2016, p. 324–340, 2017. https://doi.org/10.1016/j.rser.2016.11.056.

TIRA, Hendry S.; HERREROS, José M.; TSOLAKIS, Athanasios; WYSZYNSKI, Miroslaw L. Influence of the addition of LPG-reformate and H2 on an engine dually fuelled with LPG–

diesel, –RME and –GTL Fuels. **Fuel**, vol. 118, p. 73–82, 15 Feb. 2014. DOI 10.1016/j.fuel.2013.10.065. Available at: https://www.sciencedirect.com/science/article/pii/S0016236113010065. Accessed on: 1 Oct. 2019.

TOTAL GROUP. BioTfueL: developing Second-Generation Biofuels | Total.com. 2021a. Available at: https://www.total.com/energy-expertise/projects/bioenergies/biotfuel-converting-plant-wastes-into-fuel. Accessed on: 23 May 2021.

TOTAL GROUP. La Mède: A Multipurpose Facility for the Energies of Tomorrow | Total.com. 2021b. Available at: https://www.total.com/energy-expertise/projects/bioenergies/la-mede-a-forward-looking-facility. Accessed on: 23 May 2021.

TSE, H.; LEUNG, C. W.; CHEUNG, C. S. Investigation on the combustion characteristics and particulate emissions from a diesel engine fueled with diesel-biodiesel-ethanol blends. **Energy**, vol. 83, p. 343–350, 1 Apr. 2015. https://doi.org/10.1016/j.energy.2015.02.030.

TSE, H.; LEUNG, C.W.; CHEUNG, C.S. Performances, Emissions and Soot Properties from a Diesel-Biodiesel- Ethanol Blend Fuelled Engine. **Advances in Automobile Engineering**, vol. 01, no. S1, p. 1–7, 2016. https://doi.org/10.4172/2167-7670.s1-005.

TSI INCORPORATED. Model 3080-Series Electrostatic Classifiers. 2001. Available at: www.tsi.com. Accessed on: 1 Aug. 2019.

TÜRKMENGAZ. Gasoline production plant from natural gas. 2021. Available at: https://turkmengaz.gov.tm/en/projects/1. Accessed on: 3 Mar. 2021.

TUTAK, Wojciech; JAMROZIK, Arkadiusz; PYRC, Michał; SOBIEPAŃSKI, Michał. A comparative study of co-combustion process of diesel-ethanol and biodiesel-ethanol blends in the direct injection diesel engine. **Applied Thermal Engineering**, vol. 117, p. 155–163, 5 May 2017. https://doi.org/10.1016/j.applthermaleng.2017.02.029.

TWIGG, By Martyn V.; PHILLIPS, Paul R. Cleaning the Air We Breathe - Controlling Diesel Particulate Emissions from Passenger Cars. **Platinum Metals Review**, vol. 53, no. 1, p. 27–34, 1 Jan. 2009. https://doi.org/10.1595/147106709X390977.

UNGLERT, Martin; BOCKEY, Dieter; BOFINGER, Christine; BUCHHOLZ, Bert; FISCH, Georg; LUTHER, Rolf; MÜLLER, Martin; SCHAPER, Kevin; SCHMITT, Jennifer; SCHRÖDER, Olaf; SCHÜMANN, Ulrike; TSCHÖKE, Helmut; REMMELE, Edgar; WICHT, Richard; WINKLER, Markus; KRAHL, Jürgen. Action areas and the need for research in biofuels. **Fuel**, vol. 268, no. January, p. 117227, May 2020. https://doi.org/10.1016/j.fuel.2020.117227.

UNITED NATIONS. **World Population Prospects 2019: Highlights**. [*S. l.*: *s. n.*], 2019. Available at: https://www.un.org/en/desa/world-population-prospects-2019-highlights.

U.S. ENERGY INFORMATION ADMINISTRATION (EIA). **International Energy Outlook 2017**. [*S. l.*: *s. n.*], 2017. Available at: https://www.eia.gov/outlooks/ieo/pdf/0484(2017).pdf.

VALENCIA OCHOA, Guillermo; ACEVEDO PEÑALOZA, Carlos; DUARTE FORERO, Jorge. Combustion and Performance Study of Low-Displacement Compression Ignition Engines Operating with Diesel–Biodiesel Blends. **Applied Sciences**, vol. 10, no. 3, p. 907, 30

Jan. 2020. DOI 10.3390/app10030907. Available at: https://www.mdpi.com/2076-3417/10/3/907.

VELOCYS. Bringing sustainable fuels to life. 2021a. Available at: https://www.velocys.com/projects/. Accessed on: 7 Mar. 2021.

VELOCYS. Technical validation: key milestones. 2021b. Available at: https://www.velocys.com/technology/. Accessed on: 7 Mar. 2021.

VENU, Harish; RAJU, V. Dhana; LINGESAN, S.; ELAHI M SOUDAGAR, Manzoore. Influence of Al2O3nano additives in ternary fuel (diesel-biodiesel-ethanol) blends operated in a single cylinder diesel engine: Performance, combustion and emission characteristics. **Energy**, vol. 215, p. 119091, 15 Jan. 2021. DOI 10.1016/j.energy.2020.119091. Available at: https://doi.org/10.1016/j.energy.2020.119091. Accessed on: 7 Dec. 2020.

VERMA, Saket; DAS, L. M.; KAUSHIK, S. C.; TYAGI, S. K. An experimental investigation of exergetic performance and emission characteristics of hydrogen supplemented biogas-diesel dual fuel engine. **International Journal of Hydrogen Energy**, vol. 43, no. 4, p. 2452–2468, 2018. https://doi.org/10.1016/j.ijhydene.2017.12.032.

WANG, Chongming; CHAHAL, Jasprit; JANSSEN, Andreas; CRACKNELL, Roger; XU, Hongming. Investigation of gasoline containing GTL naphtha in a spark ignition engine at full load conditions. **Fuel**, vol. 194, p. 436–447, 15 Apr. 2017. https://doi.org/10.1016/J.FUEL.2017.01.042.

WATLING, Timothy C.; AHMADINEJAD, Mehrdad; ȚUȚUIANU, Monica; JOHANSSON, Åsa; PATERSON, Michael A.J. Development and Validation of a Pt-Pd Diesel Oxidation Catalyst Model. **SAE International Journal of Engines**, vol. 5, no. 3, p. 1420–1442, 2012. https://doi.org/10.4271/2012-01-1286.

WEBB, A.H.; HUNTER, G.C. Power-station contributions to local concentrations of NO2 at ground level. **Environmental Pollution**, vol. 102, no. 1, p. 283–288, 1998. https://doi.org/10.1016/S0269-7491(98)80045-6.

WOOD, David A.; NWAOHA, Chikezie; TOWLER, Brian F. Gas-to-liquids (GTL): A review of an industry offering several routes for monetizing natural gas. **Journal of Natural Gas Science and Engineering**, vol. 9, p. 196–208, 1 Nov. 2012. https://doi.org/10.1016/j.jngse.2012.07.001. Accessed on: 19 May 2021.

XU, Min; CHENG, Wei; LI, Zhi; ZHANG, Hongfei; AN, Tao; MENG, Zhaokang. Pre-injection strategy for pilot diesel compression ignition natural gas engine. **Applied Energy**, vol. 179, p. 1185–1193, 2016. https://doi.org/10.1016/j.apenergy.2016.07.024.

XU, Min; CHENG, Wei; ZHANG, Hongfei; AN, Tao; ZHANG, Shaohua. Effect of diesel pre-injection timing on combustion and emission characteristics of compression ignited natural gas engine. **Energy Conversion and Management**, vol. 117, p. 86–94, 1 Jun. 2016. https://doi.org/10.1016/J.ENCONMAN.2016.02.054.

XU, Zhengxin; DUAN, Xiongbo; LIU, Yiqun; DENG, Banglin; LIU, Jingping. Spray combustion and soot formation characteristics of the acetone-butanol-ethanol/diesel blends under diesel engine-relevant conditions. **Fuel**, vol. 280, p. 118483, 15 Nov. 2020. https://doi.org/10.1016/j.fuel.2020.118483.

YANG, Tiantian; WANG, Tie; QIAO, Jing; GAO, Ji; FENG, Yizhuo; SUN, Dandan. Influence of the Methanol Proportion on the Combustion Characteristics of Methanol-Biodiesel -F-T Diesel Blended Fuel. 1., 8 Oct. 2017. **SAE Technical Paper Series** [...]. [*S. l.: s. n.*], 8 Oct. 2017. vol. 1, . DOI 10.4271/2017-01-2335. Available at: https://www.sae.org/content/2017-01-2335/.

YE, Lihua; SHI, Yefan; LIU, Tianyu; ZHENG, Qingming; ASHFAQ, Muhammad Muzamal; SUN, Chengwei; SHI, Aiping; AJMAL, Muhammad. Study on emission and particulate matter characteristics from diesel engine fueled with n-pentanol/Fischer–Tropsch diesel. **Energy Sources, Part A: Recovery, Utilization, and Environmental Effects**, , p. 1–17, 21 Jul. 2020. DOI 10.1080/15567036.2020.1791286. Available at: https://www.tandfonline.com/doi/full/10.1080/15567036.2020.1791286. Accessed on: 15 Dec. 2020.

YE, Shifei; YAP, Yeow H.; KOLACZKOWSKI, Stan T.; ROBINSON, Kevin; LUKYANOV, Dmitry. Catalyst 'light-off' experiments on a diesel oxidation catalyst connected to a diesel engine—Methodology and techniques. **Chemical Engineering Research and Design**, vol. 90, no. 6, p. 834–845, Jun. 2012. https://doi.org/10.1016/j.cherd.2011.10.003.

YESILYURT, Murat Kadir. The examination of a compression-ignition engine powered by peanut oil biodiesel and diesel fuel in terms of energetic and exergetic performance parameters. **Fuel**, vol. 278, p. 118319, 15 Oct. 2020. https://doi.org/10.1016/j.fuel.2020.118319.

YESILYURT, Murat Kadir; ARSLAN, Mevlüt. Analysis of the fuel injection pressure effects on energy and exergy efficiencies of a diesel engine operating with biodiesel. **Biofuels**, vol. 10, no. 5, p. 643–655, 3 Sep. 2019. DOI 10.1080/17597269.2018.1489674. Available at: https://doi.org/10.1080/17597269.2018.1489674.

YILMAZ, I. T.; GUMUS, M. Effects of hydrogen addition to the intake air on performance and emissions of common rail diesel engine. **Energy**, vol. 142, p. 1104–1113, 2018. https://doi.org/10.1016/j.energy.2017.10.018.

YILMAZ, Nadir; VIGIL, Francisco M.; BENALIL, Kyle; DAVIS, Stephen M.; CALVA, Antonio. Effect of biodiesel–butanol fuel blends on emissions and performance characteristics of a diesel engine. **Fuel**, vol. 135, p. 46–50, 1 Nov. 2014. https://doi.org/10.1016/j.fuel.2014.06.022.

YILMAZ, Nadir; VIGIL, Francisco M.; BURL DONALDSON, A.; DARABSEH, Tariq. Investigation of CI engine emissions in biodiesel–ethanol–diesel blends as a function of ethanol concentration. **Fuel**, vol. 115, p. 790–793, 1 Jan. 2014. https://doi.org/10.1016/j.fuel.2013.08.012.

ZHANG, Wugao; CHEN, Xiaoling; GU, Genxiang; HU, Huaili; LIU, Taotao; HUANG, Zhen. Experimental study of the spray characteristics of USLD, methanol and DME on the swirl nozzle of a Stirling engine. **Fuel Processing Technology**, vol. 119, p. 1–9, 1 Mar. 2014. https://doi.org/10.1016/j.fuproc.2013.10.006.

ZHANG, Zhi Hui; BALASUBRAMANIAN, Rajasekhar. Effects of oxygenated fuel blends on the composition of size-segregated engine-out diesel particulate emissions and on the toxicity of quasi-ultrafine particles. **Fuel**, vol. 215, no. May 2017, p. 161–170, 2018. https://doi.org/10.1016/j.fuel.2017.10.097.

ZHOU, Dianfeng; QIU, Chengqun. Experimental Study on Unregulated Emissions Characteristics of Alcohol-Diesel Dual-Fuel Combustion with Diesel Oxidation Catalyst. **Journal of Energy Engineering**, vol. 145, no. 2, p. 04018075, Apr. 2019. DOI 10.1061/(ASCE)EY.1943-7897.0000596. Available at: http://ascelibrary.org/doi/10.1061/%28ASCE%29EY.1943-7897.0000596.

ZHU, Lei; CHEUNG, C.S.; ZHANG, W.G.; HUANG, Zhen. Combustion, performance and emission characteristics of a DI diesel engine fueled with ethanol–biodiesel blends. **Fuel**, vol. 90, no. 5, p. 1743–1750, 1 May 2011. https://doi.org/10.1016/J.FUEL.2011.01.024.

ZIOLKOWSKA, Jadwiga R. Chapter 1 - Biofuels technologies: An overview of feedstocks, processes, and technologies. *In*: REN, Jingzheng; SCIPIONI, Antonio; MANZARDO, Alessandro; LIANG, Hanwei B T - Biofuels for a More Sustainable Future (eds.). **Biofuels for a More Sustainable Future: Life Cycle Sustainability Assessment and Multi-Criteria Decision Making**. [*S. l.*]: Elsevier, 2020. p. 1–19. https://doi.org/https://doi.org/10.1016/B978-0-12-815581-3.00001-4.
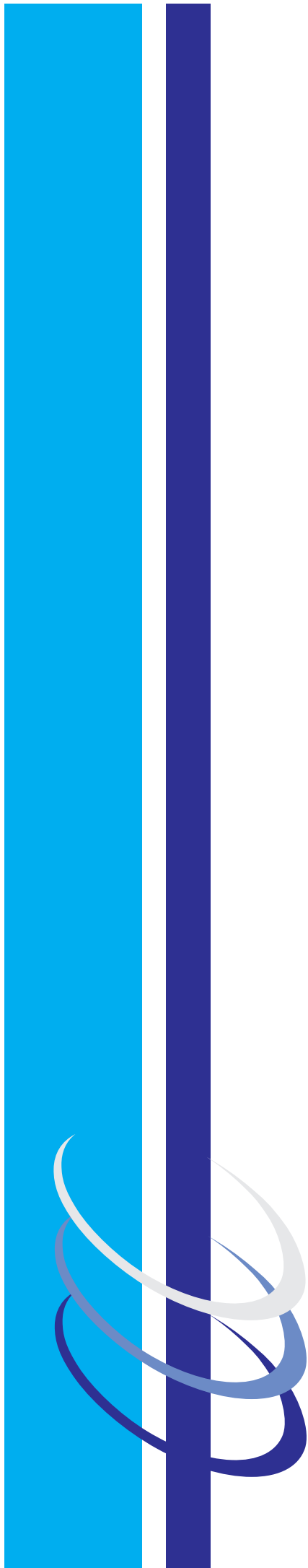
UFBA

UNIVERSIDADE FEDERAL DA BAHIA
ESCOLA POLITÉCNICA
PROGRAMA DE PÓS-GRADUAÇÃO
EM ENGENHARIA INDUSTRIAL - PEI

Rua Aristides Novis, 02, 6º andar, Federação, Salvador BA
CEP: 40.210-630
Telefone: (71) 3283-9800
E-mail: pei@ufba.br
Home page: http://www.pei.ufba.br